

JUL 13 1964

MASTER

UNCLASSIFIED

AD 428882

DEFENSE DOCUMENTATION CENTER

FOR

SCIENTIFIC AND TECHNICAL INFORMATION

CAMERON STATION, ALEXANDRIA, VIRGINIA



UNCLASSIFIED

DISCLAIMER

This report was prepared as an account of work sponsored by an agency of the United States Government. Neither the United States Government nor any agency Thereof, nor any of their employees, makes any warranty, express or implied, or assumes any legal liability or responsibility for the accuracy, completeness, or usefulness of any information, apparatus, product, or process disclosed, or represents that its use would not infringe privately owned rights. Reference herein to any specific commercial product, process, or service by trade name, trademark, manufacturer, or otherwise does not necessarily constitute or imply its endorsement, recommendation, or favoring by the United States Government or any agency thereof. The views and opinions of authors expressed herein do not necessarily state or reflect those of the United States Government or any agency thereof.

DISCLAIMER

Portions of this document may be illegible in electronic image products. Images are produced from the best available original document.

NOTICE: When government or other drawings, specifications or other data are used for any purpose other than in connection with a definitely related government procurement operation, the U. S. Government thereby incurs no responsibility, nor any obligation whatsoever; and the fact that the Government may have formulated, furnished, or in any way supplied the said drawings, specifications, or other data is not to be regarded by implication or otherwise as in any manner licensing the holder or any other person or corporation, or conveying any rights or permission to manufacture, use or sell any patented invention that may in any way be related thereto.



B&W

BAF-1267
Ca-7

AD No. 428882

DEC FILE COPY

SUMMARY REPORT OF THERMIONIC
CONVERTER INPILE EXPERIMENTS
March 1963

428882

THE BABCOCK & WILCOX COMPANY
ATOMIC ENERGY DIVISION

712.50

SUMMARY REPORT OF THERMIONIC
CONVERTER INPILE EXPERIMENTS

March 1963

By
W. L. Orr,
Application Development Department
and
H. J. Worsham
R. M. Ball
Critical Experiment Laboratory

Approved by G. K. Wicks
Project Manager

Prepared for
RADIO CORPORATION OF AMERICA
under
Bureau of Ships Contract No. NObS-84823
by
THE BABCOCK & WILCOX COMPANY
Atomic Energy Division
Lynchburg, Virginia

RCA Contract No. G9-137924-H18 B&W Contract No. 59-3077

The authors acknowledge the contributions
of A. C. Bitten, B&W, and W. E. Harbaugh,
RCA, to the program.

4
ABSTRACT

As part of the program for the development of a reliable vapor-filled thermionic converter for use with a nuclear heat source, a series of inpile experiments was conducted. The inpile experimental program consisted of two phases.

The first phase was a series of inpile heat transfer experiments in which a nuclear-fueled emitter was operated at the temperatures and heat flux required by the thermionic converter. Emitter temperature distribution data with electrical and nuclear heat sources were similar. No adverse temperature perturbations were introduced by the nuclear fuel.

The second phase was the successful inpile operation of the RCA Converter, Type A-1197A, for 300 hours in the Lynchburg Pool Reactor. A maximum electrical power output of 155 watts (2.58 watts/cm²) was produced at a computed efficiency of 10.3%.

4

PAGE BLANK

CONTENTS

	Page
1. INTRODUCTION AND SUMMARY	1-1
1.1. Introduction	1-1
1.1.1. Purpose	1-1
1.1.2. Program Description	1-1
1.1.3. Inpile Experiment Chronology	1-2
1.2. Summary	1-4
1.2.1. Heat Transfer Experiment	1-4
1.2.2. Thermionic Converter Experiment	1-6
2. NUCLEAR MEASUREMENTS	2-1
2.1. Introduction	2-1
2.1.1. Purpose	2-1
2.1.2. Scope	2-1
2.2. Reactor Core Configuration	2-1
2.3. Mock-Up Experiments	2-2
2.3.1. Preliminary Measurements	2-2
2.3.2. Converter Mock-Up Experiments	2-3
2.3.3. Diameter Variation Experiments	2-4
2.3.4. Heat Transfer Mock-Up Experiments	2-5
3. HEAT TRANSFER EXPERIMENT	3-1
3.1. Introduction	3-1
3.1.1. Purpose	3-1
3.1.2. Scope	3-1
3.2. Experiment Design	3-2
3.2.1. Design Considerations	3-2
3.2.2. Design Description	3-4
3.3. Electrical Calibration Experiment	3-5
3.3.1. Introduction	3-5
3.3.2. Experiment Description	3-5
3.3.3. Experimental Results	3-6
3.4. Inpile Heat Transfer Experiment Series 1	3-7
3.4.1. Experiment Description	3-7
3.4.2. Experimental Results	3-7
3.4.3. Conclusions	3-9
3.5. Inpile Heat Transfer Experiment Series 2	3-10
3.5.1. Experiment Description	3-10
3.5.2. Experimental Results	3-11
3.5.3. Conclusions	3-13

CONTENTS (Cont'd)

	Page
3.6. Dynamic Measurements of Nuclear Heating	3-14
3.6.1. Introduction	3-14
3.6.2. Experimental Setup	3-14
3.6.3. Theoretical Expectations	3-14
3.6.4. Static Measurements	3-17
3.6.5. Kinetic Measurement of Temperature	3-17
3.6.6. Conclusions	3-18
4. THERMIONIC CONVERTER EXPERIMENT	4-1
4.1. Introduction	4-1
4.1.1. Purpose	4-1
4.1.2. Scope	4-1
4.2. Design Description	4-1
4.2.1. Converter	4-1
4.2.2. Inpile Experiment Design	4-4
4.2.3. Assembly	4-6
4.2.4. Instrumentation	4-7
4.2.5. Coolant Circuit	4-7
4.2.6. Helium Circuit	4-8
4.3. Inpile Experiment Operation	4-8
4.3.1. Prestartup Phase	4-8
4.3.2. Summary of Operation, Startup and Shutdown	4-9
4.3.3. Startup Phase (Reactor Power 0-430 KW)	4-10
4.3.4. Intermediate Phase	4-10
4.3.5. Steady-State Phase	4-11
4.3.6. Device Parameters	4-11
4.3.7. Device-Power Reduction Phase	4-14
4.3.8. Shutdown Phase	4-15
4.4. Postoperation Analysis	4-15
 APPENDIXES	
A. Heat Transfer Experiment	A-1
B. Thermionic Converter Experiment	B-1

List of Tables

Table	
2-1. Summary of Axial Flux Measurements	2-6
3-1. Static Heat Transfer Determination	3-19
3-2. Dynamic Data on Heat Transfer Experiments	3-19
A-1. Synopsis, Experiment 73-19	A-6
A-2. Synopsis, Experiment 73-20	A-7
A-3. Synopsis, Experiment 73-21	A-8
A-4. Synopsis, Experiment 73-23	A-9
A-5. Synopsis, Experiment 73-24	A-11

Tables (Cont'd)

Table	Page
A-6. Synopsis, Experiments 73-25, 73-26, 73-27, 73-28	A-12
A-7. Synopsis, Electrical Calibration Experiment 4	A-13
A-8. Heating Schedule for Outgassing Pellets	A-14
B-1. Heating Schedule for Outgassing Pellets	B-2
B-2. Dimension Charges During Outgassing Treatment	B-3
B-3. Quantity of Gas Evolved From a Single Pellet	B-4
B-4. Analyses of Evolved Gas	B-5
B-5. Converter Temperature During 300-Hour Run	B-9
B-6. Calorimetric and Voltage Measurements	B-15

List of Figures

Figure

The Following Figures Follow Page 1-7

- 1-1. Inpile Experiment Chronology
- 1-2. The RCA Type A-1197A Converter Inpile

The Following Figures Follow Page 2-6

- 2-1. Cross-Section of Core 143
- 2-2. Horizontal Neutron Flux Distribution
- 2-3. Vertical Neutron Flux Distribution
- 2-4. Mock-Up 1
- 2-5. Assembly of Converter Mock-Up Experiment
- 2-6. Components of the Converter Mock-Up Experiment
- 2-7. Axial Power Measurements
- 2-8. Axial Power Measurements
- 2-9. Reactivity Vs Experiment Diameter
- 2-10. LPR Power to Produce 1500 Watts in the Experiment
Vs Experiment Diameter
- 2-11. Cross-Section of Mock-Up 4 With Flux Measurements Shown
- 2-12. Radial Power Distribution in the Fuel

The Following Figures Follow Page 3-19

- 3-1. Special Emitter Assembly
- 3-2. Heat Transfer Device
- 3-3. Assembled Components of the Heat Transfer Device
- 3-4. Heat Transfer Experiment Assembly
- 3-5. Components of Heat Transfer Assembly
- 3-6. Installed Electric Heater
- 3-7. Device Input Power Vs Reactor Power for Inpile Heat Transfer
Experiment Series 1
- 3-8. Emitter Temperature Distribution—Experiment 73-23
- 3-9. Emitter Temperature and Reactor Power Vs Time (Experiment
73-23)
- 3-10. Device Input Power Vs Reactor Power for Inpile Heat Transfer
Experiment Series 2
- 3-11. Plot of Heat Loss by Radiation for the Heat Transfer Experiment
Assuming Perfect Emissivity ($\epsilon = 1$)

Figures (Cont'd)

Figure

- 3-12. Temperature Plot of Thermocouple 5. Run 28, Scram
From 350 KW

The Following Figures Follow Page 4-15

- 4-1 The RCA Converter, Type A-1197A, With Cesium Heater
Assembly
- 4-2. Sectional View of the Type A-1197A Converter
- 4-3 Converter Section Assembly
- 4-4. Thermionic Converter Experiment Assembly
- 4-5. Component Parts of Inpile Experiment
- 4-6 Inpile Load With Fiberglas Insulation
- 4-7. Fueling the Converter
- 4-8. Converter Inpile Assembly
- 4-9 Cooling-Water Circuit
- 4-10. Helium Flow Circuits
- 4-11. Startup Phase
- 4-12. Output Power and Input Power Vs Time
- 4-13 Reactor Power and Position of Shim Rods Vs Time
- 4-14. Intermediate Phase
- 4-15 Intermediate Phase
- 4-16. Intermediate and Steady-State Phases
- 4-17. Steady-State Phase
- 4-18 Computed Efficiency Vs Input Power
- 4-19. Cesium Vapor Pressure Vs Temperature
- 4-20. Cesium Heating Experiment, Steady-State Phase
- 4-21 Helium Flow Experiment, Steady-State Phase
- 4-22. Output Voltage Vs Cesium Reservoir Temperature
- 4-23. Output Voltage Vs Cesium Reservoir Temperature
- 4-24. Output Power Vs Load Resistance
- 4-25. Output Power Vs Load Resistance
- 4-26 Output Power Vs Load Resistance
- 4-27 Power Reduction Phase
- 4-28. Power Reduction Phase
- 4-29 Device-Power Reduction Phase
- 4-30 Shutdown Phase
- 4-31. Shutdown Phase
- 4-32 Output Voltage Vs Cesium Reservoir Temperature

The Following Figures are Found in Appendix A

- A-1. Base Plate Components
- A-2 Emitter Assembly and Base Plate Components
- A-3 Components of Heat Transfer Device
- A-4. Heat Transfer Assembly With Extension Tube
- A-5 Lower Base Plate
- A-6. Base Plate Ring and Split Clamp
- A-7. Outer Can
- A-8. Split Sleeve
- A-9. Cooling Jacket
- A-10. Top External Plate and Top Heat Sink
- A-11 Bottom External Tube and Bottom Heat Sink

Figures (Cont'd)

Figure

- A-12. Bottom External Plate and Thermocouple Support
- A-13. External Can
- A-14. Heat Transfer Experiment Thermocouple Patterns

The Following Figures are Found in Appendix B

- B-1. Materials and Fabrication of RCA Type A1197-A Converter, Device 36
- B-2. Converter, Fuel, and End Cap Assembly
- B-3. View of Vacuum System and Oven
- B-4. Converter Connected to Vacuum System
- B-5. Installation of Converter in Outgassing Can
- B-6. Sealed Outgassing Can in Oven
- B-7. Outgassing the Device in the Oven
- B-8. Calibration of Inpile Load Bar Resistance Vs Temperature Emf
- B-9. Summary of Voltage Measurements of the Inpile Load
- B-10. Voltage Measurements of the Out-of-Pool Load
- B-11. Water Flow Meter Calibration Curves

1 INTRODUCTION AND SUMMARY

1.1 Introduction

1.1.1 Purpose

As part of the program for the development of a reliable vapor-filled thermionic converter for use with a nuclear heat source, a series of inpile experiments has been conducted. The work was performed in conjunction with the Radio Corporation of America under Contract No. NObs 84823 from the U. S. Navy Bureau of Ships. The objectives of the inpile experimental program were:

1. To operate a nuclear-fueled emitter at the temperatures and heat flux required by the thermionic converters developed under the prime contract.

2. To operate a nuclear-fueled thermionic converter in the Lynchburg Pool Reactor (LPR) for a period of up to 100 hours.

The period of performance for the inpile experimental program was June 7, 1962 to January 30, 1963. After the successful completion of the 100-hour thermionic-converter experiment, approval was received for the continuation of the inpile test an additional 200 hours.

1.1.2 Program Description

The overall test program for the development of a nuclear-fueled thermionic device consists of three major parts:

1. Electrically heated converter tests.
2. Inpile heat transfer experiments.
3. Converter experiments.

The general approach has been to develop the converter and prove its performance by electrical test before initiating extensive reactor tests. Throughout the converter development program the requirements for ultimate use of the converter as a subcomponent of a nuclear reactor

were considered. The selection of materials and the geometry of the converter were tailored to the requirements of the nuclear reactor fuel element. As a result a prototype thermionic converter unit was manufactured by RCA for the inpile test operations. The description of the development of the converter design has been reported in a series of RCA Quarterly Technical Reports. This report describes the subsequent inpile experimental program for testing these devices.

The inpile experimental program was divided into two phases. The first of these was a series of inpile heat transfer experiments in which a nuclear-fueled emitter was operated at the heat flux and temperatures required for the thermionic converter operation. The second phase was a 300-hour life test of a nuclear-fueled thermionic converter in the Lynchburg Pool Reactor. The following paragraphs describe the conduct of the inpile experimental program.

1.3 Inpile Experiment Chronology

To carry out the planned program of inpile experiments, it was necessary to upgrade the power capability of the Lynchburg Pool Reactor to one megawatt. A forced circulation cooling system for the reactor and a cooling tower were added to the facility to provide for the increased power output. These modifications were made by The Babcock & Wilcox Company without cost to the contract and were carried out in two distinct steps. The first modification permitted operation at 450 KW for one hour, the second permitted continuous operation at one megawatt with forced circulation.

Before modifications to the pool were begun, a nuclear measurements program was conducted. One purpose of this program was to verify that the upgrading steps were consistent with the power and time requirements of the scheduled experiments. These measurements established that a power level of 450 KW was adequate for the heat transfer experiments, but a power level of one megawatt would be required to provide sufficient margin to meet the power requirements for the thermionic converter experiment. A second purpose of the nuclear measurements was to determine neutron flux distributions in the core and in the experiments. Accurate mock-ups were made of both the heat transfer and converter inpile configurations. Flux and reactivity measurements were made with these mock-ups.

While the nuclear measurements and modifications to the pool were in progress, the design and fabrication of the heat transfer experiments were carried out. Electrical calibration experiments were performed with the heat transfer device to provide a comparison with the temperature and power results later obtained in pile. The first series of in-pile heat transfer experiments was conducted from September 12 through September 20, 1962, and consisted of three separate power runs.

When the first series of in-pile experiments was completed, the second pool modification was initiated. Meanwhile the assembly of a second heat transfer device proceeded. Improvements based upon results from the first series of experiments were incorporated in the fuel preparations, the device assembly, and the experiment operation and procedure for the second series of in-pile tests.

In addition, the design of the in-pile converter experiment proceeded as a cooperative effort by RCA and B&W. During this period, RCA made a number of changes in the converter configuration, which made the device more readily adaptable for in-pile operation.

After modification of the reactor to permit continuous operation at one megawatt, the necessary checkout of equipment was made and the second series of heat transfer experiments was begun. This series of experiments took place between December 14, 1962, and December 31, 1962, and included six power runs. Also included were a number of dynamic experiments to study the heat transfer characteristics of the device.

The thermionic converter to be operated in the Lynchburg Pool Reactor was fabricated and tested by electrical heating of the emitter at the RCA plant in Lancaster, Pennsylvania. Subsequent to delivery on December 19, the uranium dioxide fuel pellets, which had been previously outgassed, were loaded in the emitter cavity and the closure weld was made. Final outgassing and sealing of the fuel cavity were accomplished prior to installing the fueled device in the test assembly.

This assembly was then installed in-pile on January 14, 1963, and final preparations and checks were completed on January 15. Electrical power first exceeded 100-watts output at 2006 on January 15. Upon completion of the scheduled 100-hour test, approval to continue the experiment an additional 200 hours was received. The 300-hour mark was successfully reached without interruption and the experiment was terminated at 1553 on

January 28, 1963. Figure 1-1 shows the key events that occurred during the inpile experimental program.

1.2 Summary

1.2.1 Heat Transfer Experiment

The heat transfer experimental program was carried out in three steps. The first step was a series of electrical calibration experiments in which emitter temperature and calorimetric measurements were made in an electrically heated device. The second and third steps consisted of a series of inpile heat transfer experiments.

For the inpile experiments the device consisted of a nuclear-fueled emitter within a stainless steel outer can. Heat was initially transferred by radiation from the emitter to an aluminum split sleeve and then by conduction to the outer can. An aluminum water cooled jacket was installed around the outer can and the entire assembly was contained in aluminum to provide dual-containment for the experiment inpile.

Thermocouples were located on the emitter to measure circumferential and axial temperature distributions. Inlet and outlet water temperature and flow measurements were made for calorimetric calibrations.

1.2.1.1 Inpile Heat Transfer Experiment Series 1

The first series of inpile experiments consisted of three reactor power runs. In the first experiment, emitter temperature measurements were made at eight reactor power levels from 20 to 350 KW. At the maximum reactor power of 350 KW, a maximum emitter temperature of 1433 C was reached at the mid-plane. The input power to the emitter at this reactor power was 1243 watts. Two additional power runs were made with this assembly. During these experiments the emitter temperatures reduced with time at a constant reactor power indicating improved heat transfer between the emitter and surrounding split sleeve. Since fission gasses could diffuse into this gap, the change in heat transfer characteristics was attributed to improved gaseous conduction.

The first series of heat transfer experiments was important in showing the equivalence of the nuclear and electric

heat sources. Also, the results led to a number of improvements in fuel and device outgassing, vacuum capability and experiment instrumentation and operation, which were incorporated before the second series of experiments was carried out.

1.2.1.2 Inpile Heat Transfer Experiment Series 2

The second series of inpile heat transfer experiments consisting of six power runs was carried out after the upgrading of the pool reactor to a one megawatt capability was completed. The device was of the same design as that of the first series. The thermocouple pattern was improved to provide more axial temperature measurements.

To insure meeting both the emitter temperature and heat flux objectives, the reactor power was increased in steps to 262 KW, where a maximum emitter temperature of 1358 C was reached. Temperatures remained constant at a constant reactor power of 262 KW for approximately two hours. Thereafter, it was necessary to increase the reactor power to hold the desired emitter temperature of 1350 C. A maximum reactor power of 390 KW, corresponding to a power input to the emitter of 1699 watts, was required to reach an emitter temperature of 1357 C approximately four hours after reaching 1358 C at the 262 KW reactor power level. The reactor power level was held at 390 KW as a limit on the maximum desired heat flux and the emitter temperatures continued to drop with time. Emitter temperatures were recorded continuously throughout the experiment.

Two additional power runs were made to further investigate the change in heat transfer evident in the first power run. In addition three experiments were performed to determine the dynamic behavior of the system with changes in heat input. These experiments involved bringing the system to equilibrium power and then making a rapid power change. Usually the change was made by slamming the reactor. Within the accuracy of the experiments, the dynamic and static measurements of the heat transfer characteristics of the emitter to-collector gap were in good agreement.

Based upon the results obtained in the second series of inpile heat transfer experiments, the following conclusions were reached:

1 The emitter temperature and heat flux objectives were successfully met. An emitter surface temperature of 1350 C was achieved with a maximum power input of approximately 1700 watts to the emitter.

2 Temperature distribution measurements indicate no adverse temperature perturbations are introduced through the use of the nuclear fuel pellets.

3 Although an analytic evaluation was made, a post-irradiation examination is required to establish an accurate value for the fission-gas release rate.

4 The dynamic behavior of the system was adequately described with a single lumped parameter time constant. Since a single time constant decay was used, the separate mechanisms of radiative and conductive heat transfer could not be independently evaluated. However, the method did indicate how analytic studies of the kinetics can be simplified.

The heat transfer experiments are reported with greater detail in Section 3 and Appendix A.

1.2.2 Thermionic Converter Experiment

The inpile thermionic converter assembly consisted of three sections. The converter section consisted of the RCA Converter Type A 1197A with cesium-beater assembly, device thermocouples and instrumentation leads, an aluminum cooling jacket with associated coolant tubes, and an outer aluminum can. The converter section was coupled to a load section that extended above the active core and contained the coolant lines and calibrated tubes that made up part of the electrical load. A portion of the total load was placed inpile to minimize the size of the conductors brought to the top of the pool. The out-of-pile portion of the load contained a variable resistance leg to permit variation of the load externally. Figure 1.2 is a cross section of the converter section of the assembly. The load section is shown schematically. The load section was connected to a dry pipe which extended approximately 13 feet from the reactor to the surface of the pool. The electrical leads, the inlet coolant line which was also part of the load

and the thermocouple and cesium heater leads were contained within this dry pipe. Helium gas lines were included for purging the assembly. On one occasion during the experiment, flow through the helium circuit was used to cool the cesium reservoir.

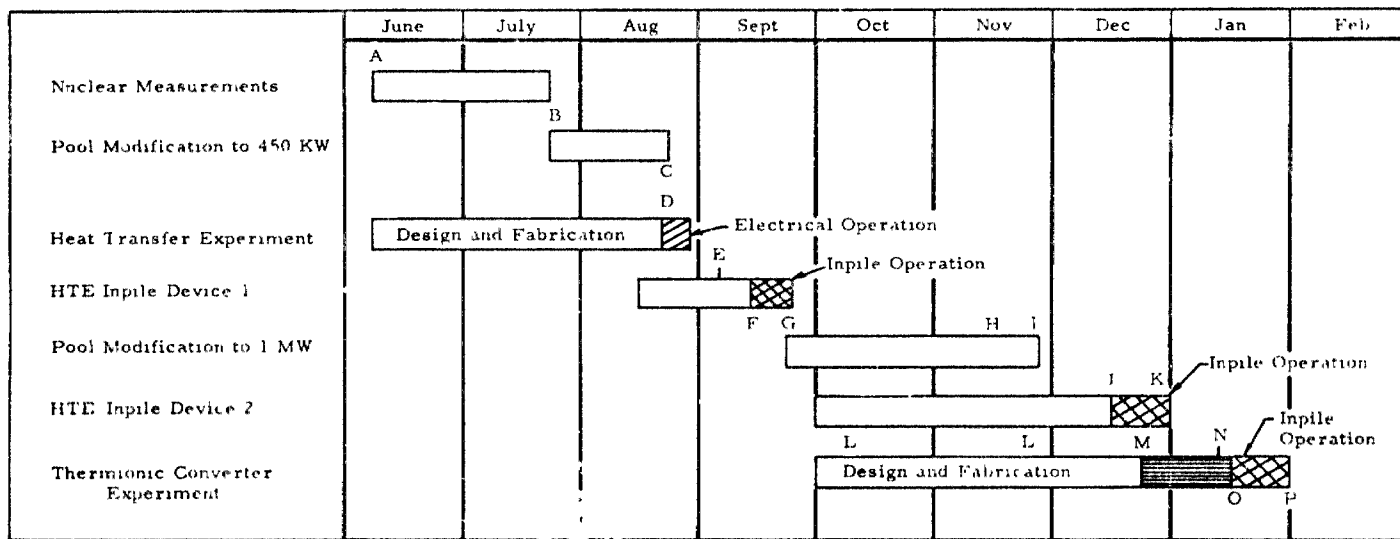
The thermionic converter experiment was conducted in two steps. The first step consisted of the electrical testing of the thermionic converter using the inpile converter section components. The second step was a 300-hour life test of the nuclear-fueled thermionic converter in the Lynchburg Pool Reactor.

The inpile operation of the thermionic converter met the experiment objectives. The device started smoothly and produced an average electrical power output of 132 watts for a major part of the test. With helium flow to cool the cesium reservoir, the device produced a maximum electrical output of 155 watts (2.58 watts/cm^2) at a computed efficiency of 10.3%. The device ran for a total of more than 300 hours, although the last 50 hours were at a somewhat reduced electrical power output. During the power run, the device produced approximately 38 kwhr of electrical energy.

A number of experiments were performed during the 300-hour life test to determine the converter characteristics. However, additional experiments are required to thoroughly investigate the thermionic converter performance in a near environment.

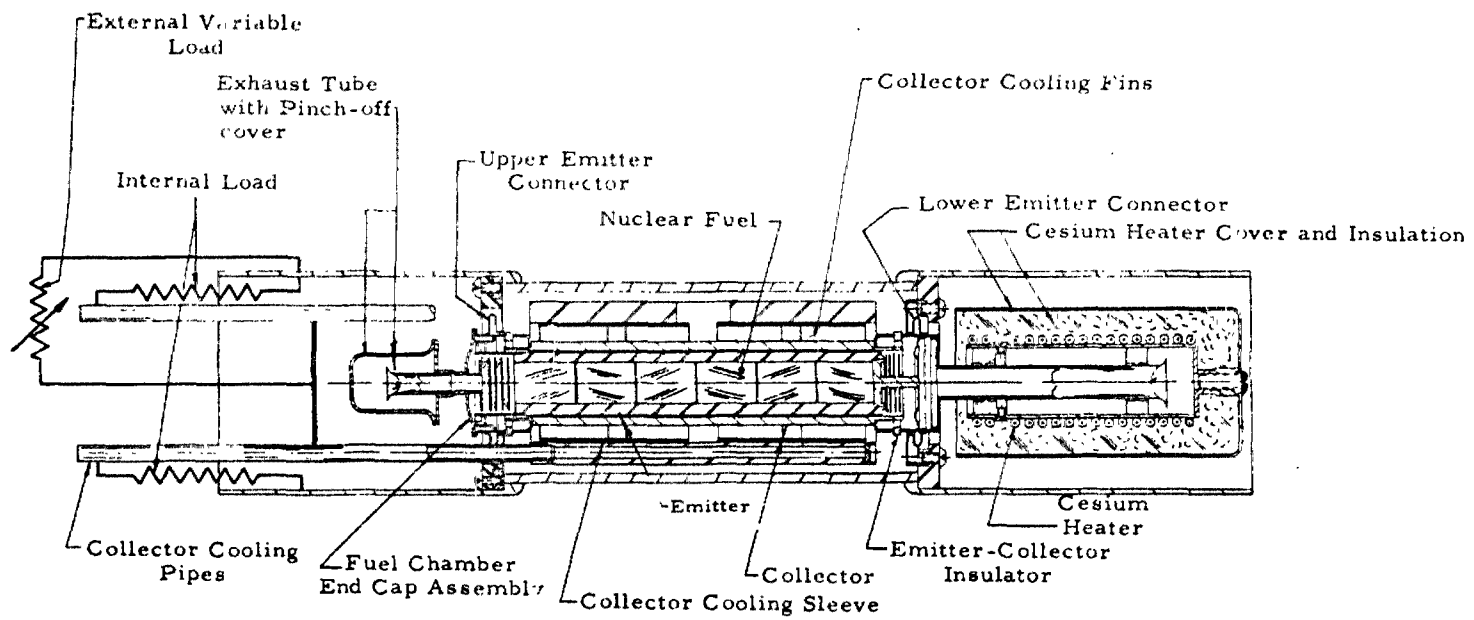
The thermionic converter experiment is reported with greater detail in Section 4 and Appendix B.

Figure 1-1. Inpile Experiment Chronology



- A Program began June 7, 1962.
- B Nuclear measurements were completed and pool modification to 450 KW began on July 23, 1962.
- C Modification was completed - Pool operated at 450 KW on August 24, 1962.
- D First electrical heat transfer experiment - August 23, 1962.
- E Electrically heated experiment of first inpile device - September 5, 1962.
- F First inpile heat transfer experiment - September 12, 1962.
- F-G Heat transfer Experiment Series 1 conducted September 12, 1962 - September 20, 1962.
- H AEC license for 1-MW operation received - November 15, 1962.
- I Reactor checkout and calibration completed - operated at 1 MW on November 26, 1962.
- J-K Heat Transfer Experiment Series 2 conducted December 14, 1962 - December 31, 1962.
- L Electrical operation of converter at RCA by RCA and B&W - October 8, 1962 and November 26, 1962.
- M Converter delivered to B&W - December 19, 1962.
- M-N Fueling, outgassing, and assembly of experiment by RCA and B&W - December 19, 1962 - January 14, 1963.
- N Installation and checkout of experiment inpile - January 14 and January 15, 1963.
- O Thermionic converter inpile experiment begun at 1135, January 15, 1963.
- P Thermionic converter inpile experiment completed at 1553, January 28, 1963.

Figure 1-2. The RCA Type A-1197A Converter Inpile



2. NUCLEAR MEASUREMENTS

2.1. Introduction

2.1.1. Purpose

A nuclear measurements program was carried out to establish a reactor core configuration suitable for conducting the inpile heat transfer and thermionic converter experiments, to determine the reactor power level required to supply the necessary input power to the experimental device, to measure the reactivity effects of the experiment components, and to determine the flux characteristics of both the core and the experiment.

2.1.2. Scope

A graphite reflected core with a center experiment hole was used for all inpile experiments. Vertical and horizontal thermal neutron flux measurements in the core were made. A series of mock-up experiments was carried out. The mock-ups began as simple devices and became more exact as the design of the inpile heat transfer and converter experiments progressed. Two mock-ups that closely simulated each experiment were constructed and were used for the measurement of flux distribution, reactivity effects, and the reactor power level required to provide sufficient input power to the device.

2.2. Reactor Core Configuration

To carry out the planned experimental program, a reactor core with a central hole equal in size to a fuel element (3 in. \times 3 in. cross-section) was loaded. This created a water-moderated flux trap in the most active region. To further increase the specific flux in the experiment, graphite reflector elements were used outside the active core, thus keeping the core size to a minimum.

The core used for the inpile heat transfer experiments, designated LPR Core 143, is shown in Figure 2-1. To insure that there would be

sufficient excess reactivity to compensate for the reactivity loss due to xenon in the 300-hour thermionic converter experiment. The core was changed to a configuration designated Core 144. The change consisted of replacing a partial fuel element (P-71, 95 grams of U^{235}) with a full fuel element (190 grams of U^{235}). This core had a cold clean excess reactivity of 2.69% $\delta k/k$.

A horizontal and vertical thermal neutron flux map was made in Core 143 by using one-quarter-inch dysprosium-aluminum foils. The results are shown in Figure 2-2 and Figure 2-3.

2.3. Mock-Up Experiments

2.3.1. Preliminary Measurements

To make a preliminary determination as to whether the planned upgrading of the pool reactor to a one-megawatt capability was adequate to carry out the experimental program using fuel enriched to 20% by weight of U^{235} , power sharing measurements were made in a simple mock-up of the emitter assembly. These experiments also provided a check-out of the measurement techniques to be used in later mock-ups.

2.3.1.1. Description of Mock-Up 1

Mock-up 1 was made of stainless steel, six and one-half inches long and one inch in outer diameter. A 0.5-inch hole was drilled through the length of the piece. The ends were threaded to allow them to be sealed by bolts and O-rings. The end plugs were fitted with spacers to center the device in the hole. Figure 2-4 illustrates the construction of Mock-up 1.

2.3.1.2. Experimental Results

Mock-up 1 without fuel had a reactivity worth of -40.5 ± 5.0 cents. The addition of the fuel stack resulted in a reactivity worth of $+21.6$ cents or a net increase of about 62 cents for the fuel. The reactivity measurements were made by comparing critical rod positions with and without the experiment in place. (The displacement of water from the test holes increases reactivity.)

Axial flux distribution measurements were made and are summarized in Table 2-1.

The power-sharing evaluation indicated the 20% -enriched fuel would probably provide sufficient input power to the device at power levels consistent with the planned upgrading schedule. However, because of the differences between the simple mock-up and the proposed experiments, these results were used primarily as a quick indication of a possible problem area.

2.3.2 Converter Mock-Up Experiments

2.3.2.1 Description of Mock-Up 2

Mock-up 2 consisted of an aluminum can of sufficient size to contain in a water tight environment a Type A-1197 thermionic converter with a single layer of collector cooling fins or only the emitter from the device. The aluminum can was 2.4 inches in diameter with a 200-mil wall and was designed to duplicate the size, water exclusion and metal volume of the thermionic converter experiment. (The outer diameter of the thermionic converter experiment used in the 300-hour run was 2.4 inches over the active fuel region.) Figures 2-5 and 2-6 are photographs of the assembly and component parts of Mock-up 2.

2.3.2.2. Experimental Results

Two reactivity experiments were conducted using Mock-up 2. In the first experiment the reactivity worth of the entire device (collector, emitter, fuel and aluminum can), was + 37.9 cents. In the second experiment the emitter, fuel, and can were worth \$1.02 in reactivity. Therefore the net reactivity worth of the collector and fins was - 66.3 cents.

Power-sharing measurements with Mock-up 2 indicated a reactor power level of 540 KW would be required to produce the desired 1500 watts power input to the thermionic device. This level is in good agreement with the 520-KW reactor power level at which a major portion of the 300-hour run was conducted.

Measurements with Mock-up 2 with emitter, fuel, and aluminum can indicated a reactor power level of 440 KW would be required for the heat transfer experiment. Since it was desired to conduct the heat transfer experiment before the reactor was upgraded to one-megawatt operation and while the reactor power was limited to a

maximum of 450 KW, this experiment showed the need for reducing the experiment diameter to insure sufficient input power would be available within the specified limitation. Section 2.3.3 describes power-sharing measurements in which the experiment diameter was varied.

Two methods were used to determine the power distribution axially along the fuel pellet stacks during the power-sharing experiments. The first method was a simple gamma counting of the gross fission products in each pellet on a scintillation counter. The pellets were counted approximately two days following the irradiation. The gross counts of the pellets were divided by the pellet weight, resulting in a specific activity which is proportional to the power generated in each pellet. These data appear in Table 2-1. There are no data for Pellet 3, since this pellet had been dissolved for Ba-140 measurements.

The second method employed thin U-Al alloy foils, irradiated between the pellets. The foils were 0.002 inch thick, 0.484 inch in diameter, and 18%-by-weight fully enriched uranium. Each foil was covered with 0.001-inch aluminum foil to protect against random fission-product contamination from the adjacent pellet surfaces. Figure 2-11 shows the foil position numbers with respect to the fuel pellet stack. All data have been summarized in Table 2-1. These data, except for that of Experiments 73-11, and 73-13, are shown in Figures 2-7 and 2-8. The data from these two experiments was not plotted because it was inconsistent with both the pellet data and the data from the other four experiments. Since no foils were placed at the ends of the fuel stack, the pellet data is believed to represent the most accurate axial power distribution.

2.3.3. Diameter Variation Experiments

2.3.3.1. Description of Mock-Up 3

Mock-up 3 consisted of a thick-walled aluminum cylinder, sealed at the ends by rubber gaskets and two plexi-glass spacers. The outer diameter of the can was two inches for the first experiment. Between successive runs, the aluminum can was machined to a smaller diameter, thus increasing the amount of the surrounding water moderator. The inner diameter was kept constant at 15/16-inch.

2.3.3.2. Experimental Results

Figure 2-9 summarizes the reactivity measurements as a function of diameter for Mock-up 3 containing the emitter and fuel. Figure 2-10 summarizes the power-sharing measurements. The axial power distribution measurements obtained with Mock-up 3 were described in Section 2.3.2.2.

2.3.4. Heat Transfer Mock-Up Experiments

2.3.4.1. Description of Mock-Up 4

Mock-up 4 was intended to closely simulate the heat transfer experiment design. It consisted of the Mock-up 2 aluminum can, the stainless steel outer can to be used in the heat transfer experiment, Kovar washers to simulate the end caps, and water filled aluminum tubes to simulate the heat sink. Figure 2-11 is a cross section of Mock-up 4.

2.3.4.2. Experimental Results

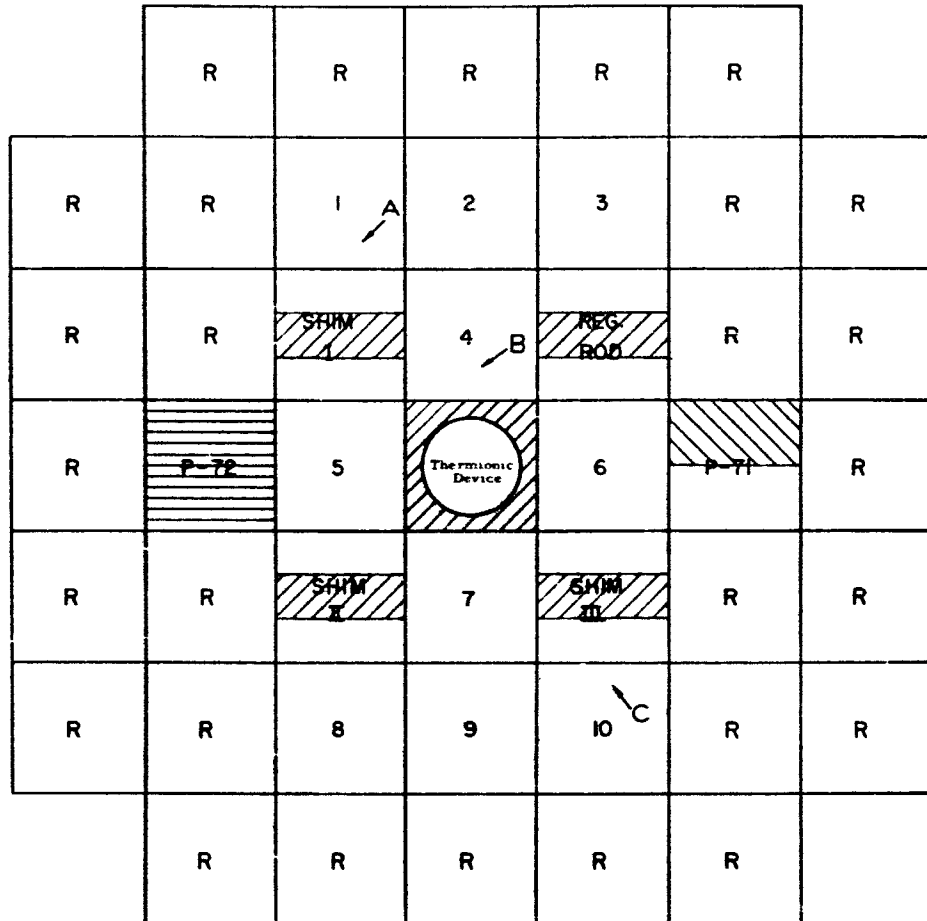
Power-sharing measurements with Mock-up 4 indicated a reactor power of 450 KW would be required for the heat transfer experiment. This value is consistent with the 440 KW determined with Mock-up 2. (Both experiments were at the same outer diameter.)

A complete flux map was made of Mock-up 4 using 0.004-inch by 0.259-inch-diameter copper foils. Figure 2-11 is a cross section showing the results of this measurement. One of the uranium-aluminum foils used in the axial flux distribution measurements (Section 2.3.2.2) was sectioned and the individual segments were counted. The results are shown in Figure 2-12.

Table 2-1. Summary of Axial Flux Measurements

U-Al foil data					
Mock-Up	Experiment no.	Foil position no.	Foil no.	Relative activity	Normalized position 1
1	73-3	1	1	1.0165	1.0000
		2	2	0.9932	0.9771
		3	3	0.9833	0.9673
		4	4	0.9783	0.9624
		5	5	0.9882	0.9722
2 with converter, fuel, no end caps	73-10	1	1	1.0053	1.0000
		2	2	0.9467	0.9417
		3	3	0.9384	0.9334
		4	4	0.9219	0.9170
		5	5	0.9314	0.9264
2 with emitter, fuel only	73-11	1	8	0.9958	1.0000
		2	9	1.0133	1.0176
		3	10	1.0470	1.0514
		4	11	1.0603	1.0648
		5	13	1.0380	1.0424
3 with can diameter = 2.0 inches	73-12	1	1	0.9904	1.0000
		2	2	0.9178	0.9267
		3	3	0.9147	0.9235
		4	4	0.8941	0.9027
		5	5	0.9071	0.9159
3 with can diameter = 1.75 inches	73-13	1	7	0.9686	1.0000
		2	8	1.0092	1.0420
		3	10	0.9665	0.9978
		4	11	1.0175	1.0505
		5	13	2.1025	2.1706
3 with can diameter = 1.5 inches	73-14	1	1	0.9954	1.0000
		2	2	0.9289	0.9332
		3	3	0.9097	0.9139
		4	4	0.9035	0.9077
		5	5	0.9180	0.9222
Fuel pellet data					
		Pellet no.			
1	73-2	1		2.283	1.0000
		2		1.955	0.8563
		4		1.887	0.8265
		5		1.895	0.8300
		6		2.176	0.9461

Figure 2-1. Cross Section of Core 143








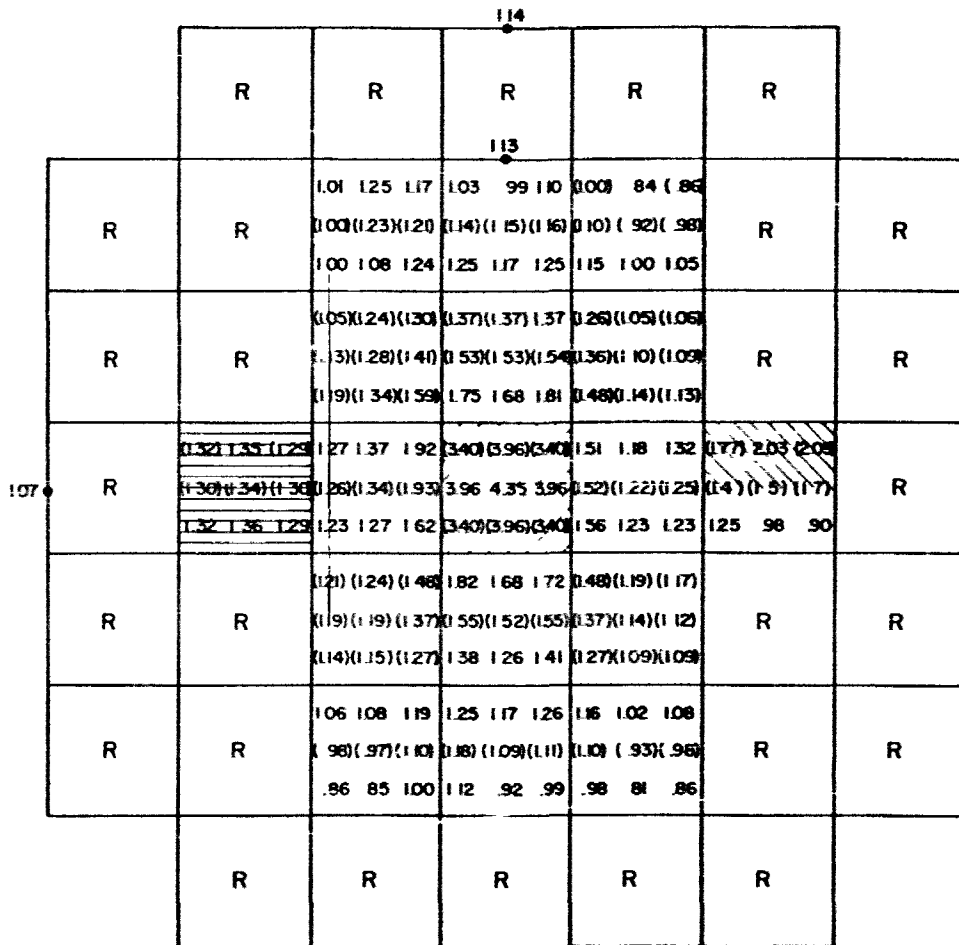
-  - WATER
-  - Al PLATE & WATER
-  - EVERYOTHER PLATE Al
-  - FUEL
-  - REFLECTOR

Figure 2-2. Horizontal Neutron Flux Distribution



- Water
- Al Plates & Water
- Reflector
- EVERY OTHER PLATE Al

NOTE:
 1 Units of $\phi_{2200} \times 10^7$ per watt in the water gaps.
 2 Values in Parenthesis are estimated.

Figure 2-3. Vertical Neutron Flux Distribution

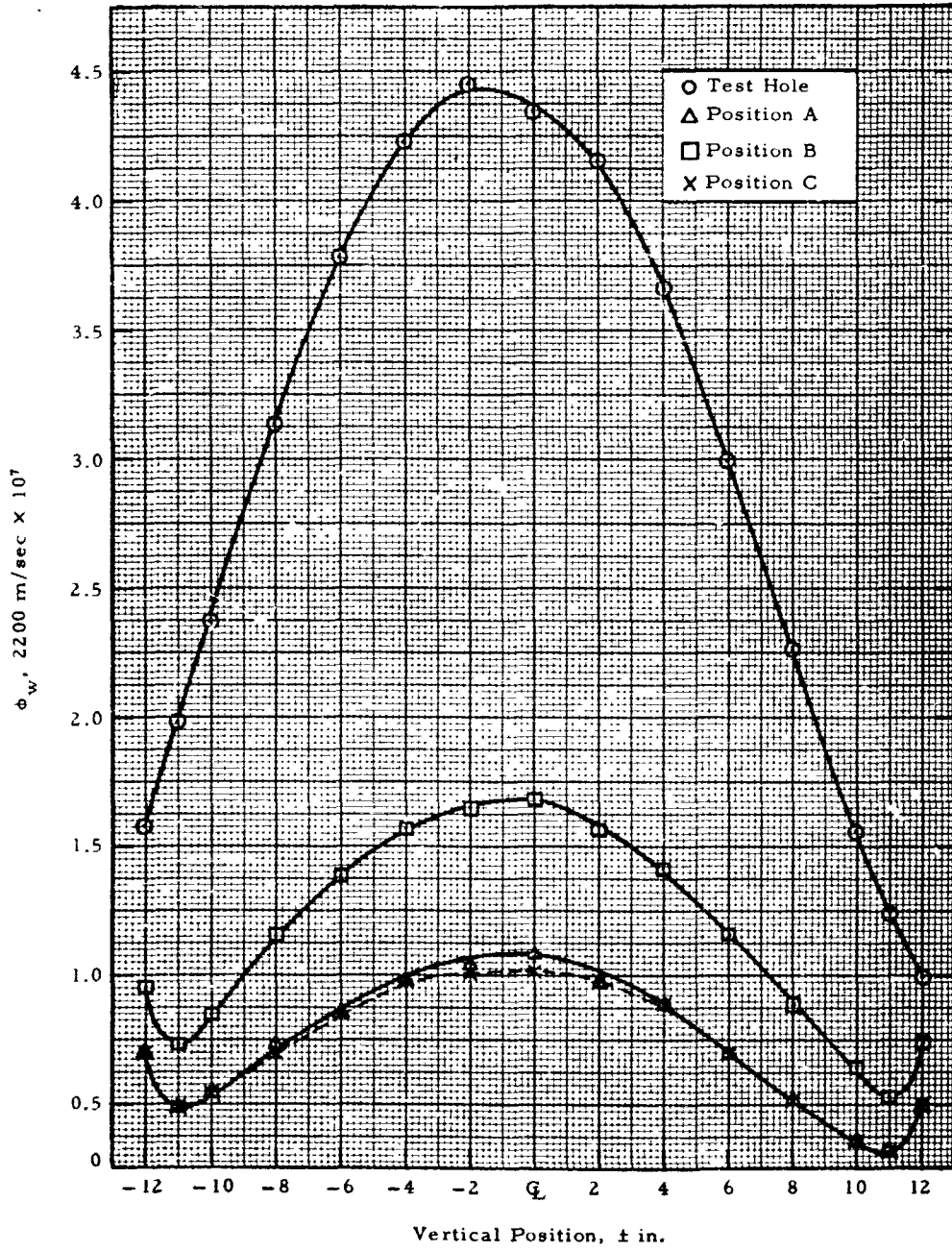


Figure 2-4. Mock-Up 1

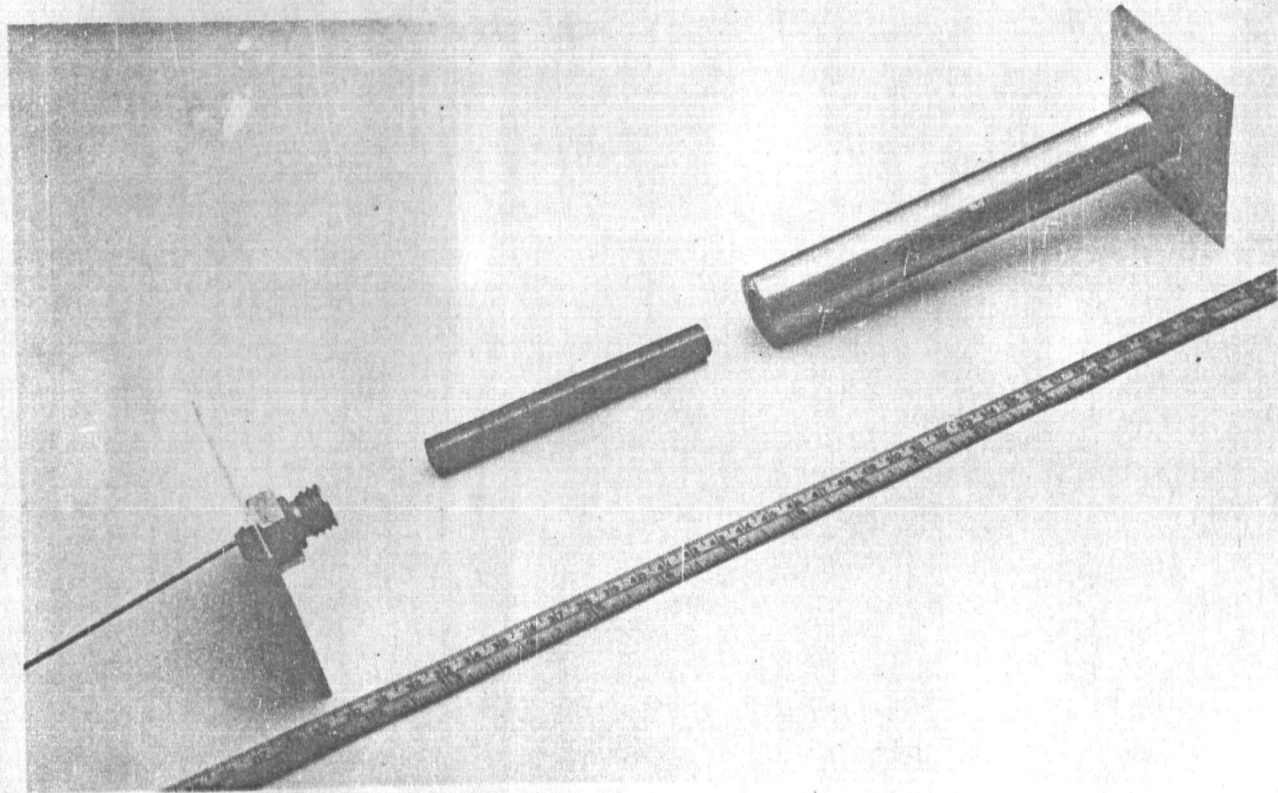


Figure 2-5. Assembly of Converter Mock-Up Experiment

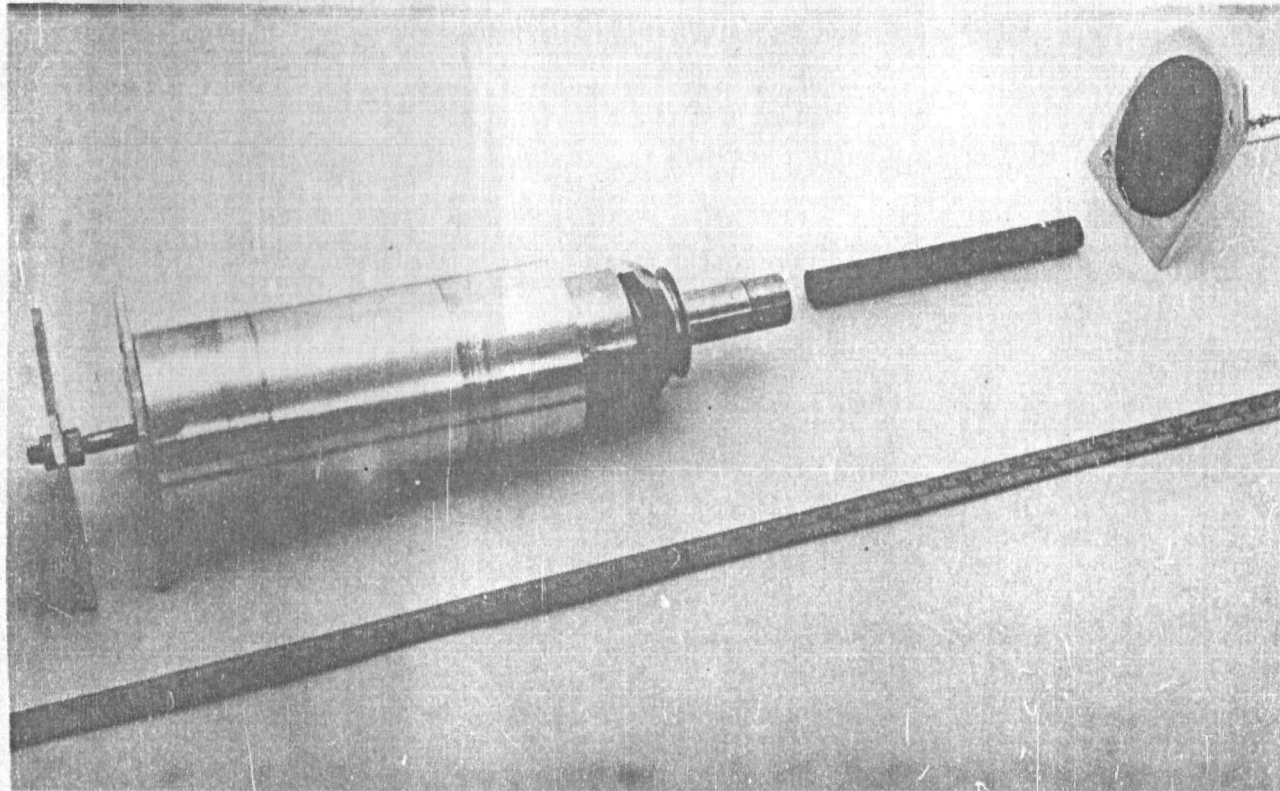


Figure 2-6. Components of the Converter Mock-Up Experiment

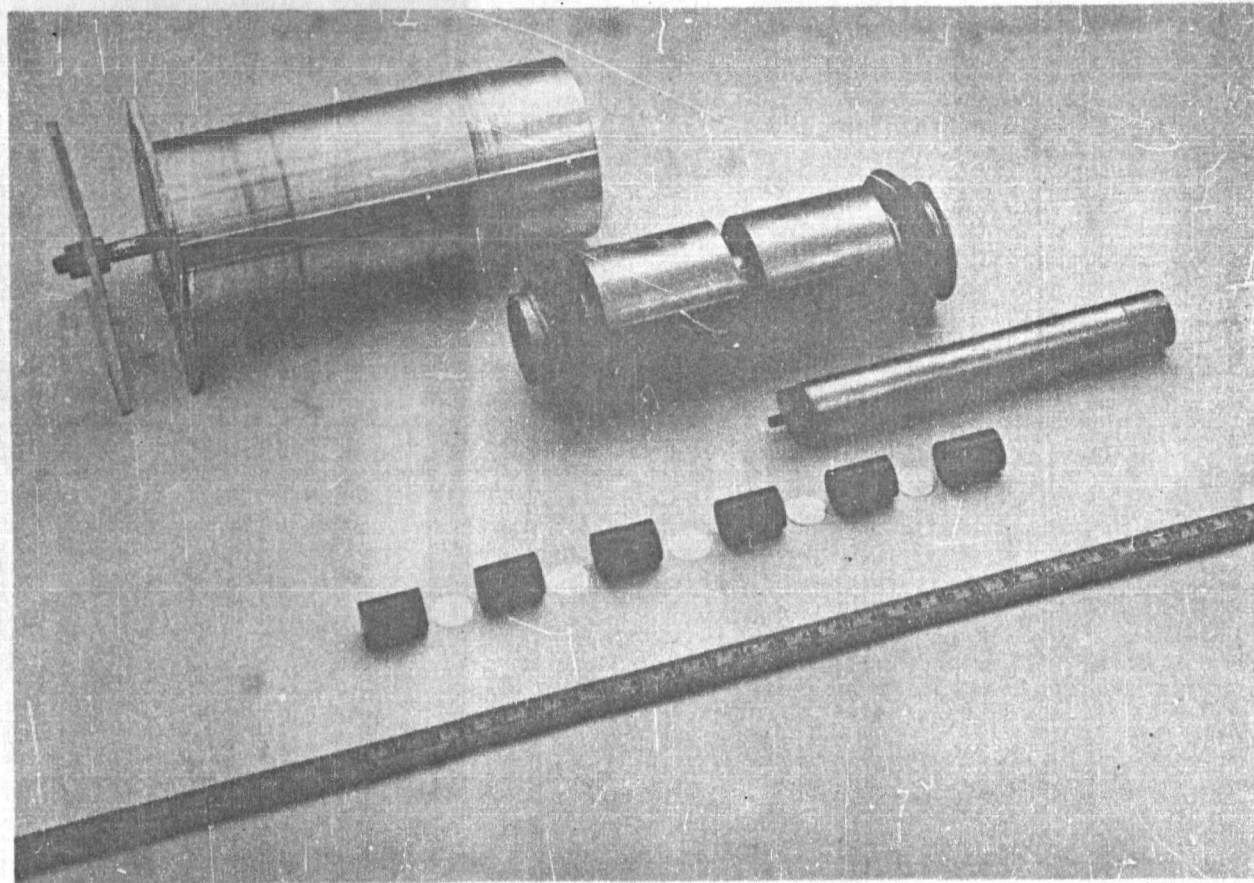


Figure 2-7. Axial Power Measurements

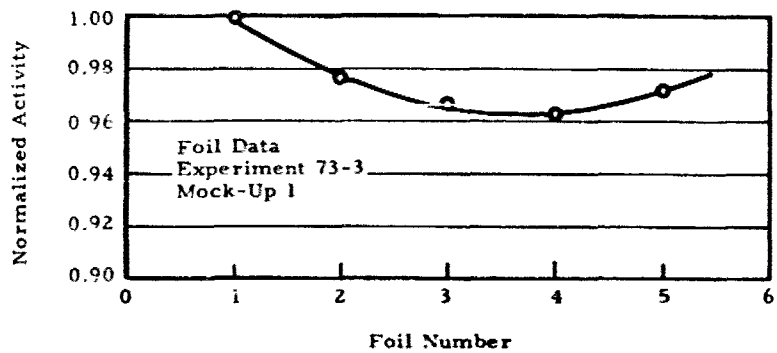
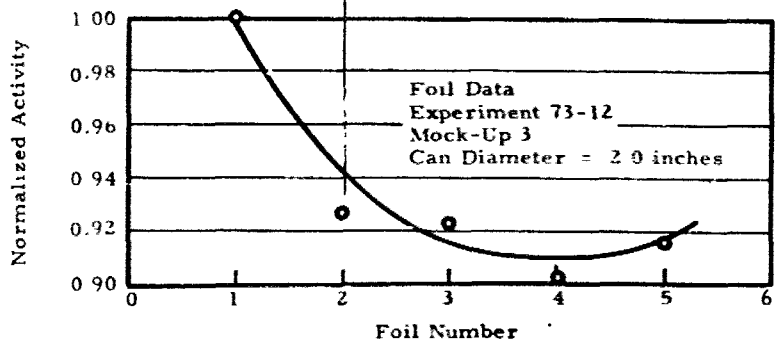
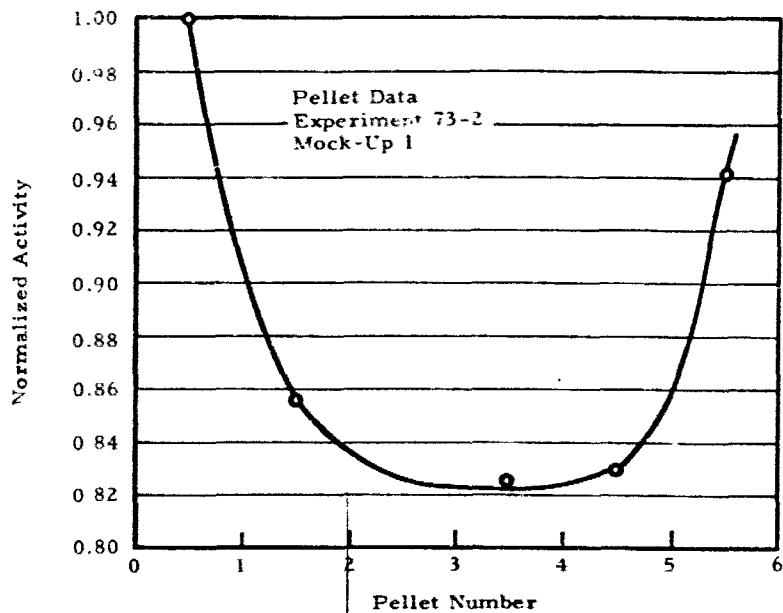


Figure 2-8. Axial Power Measurements

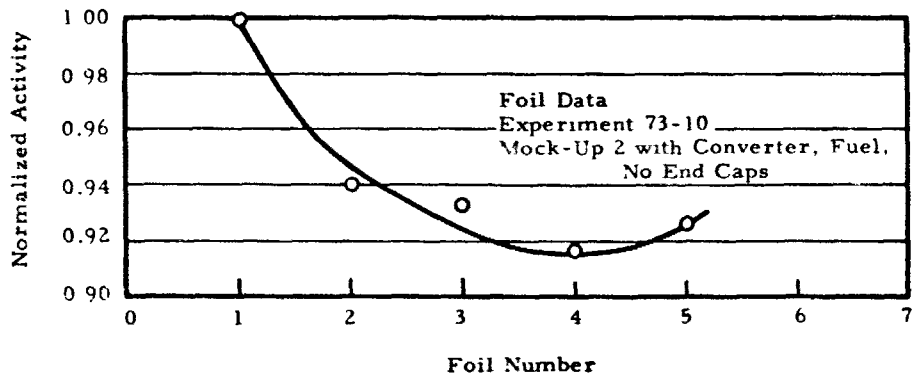
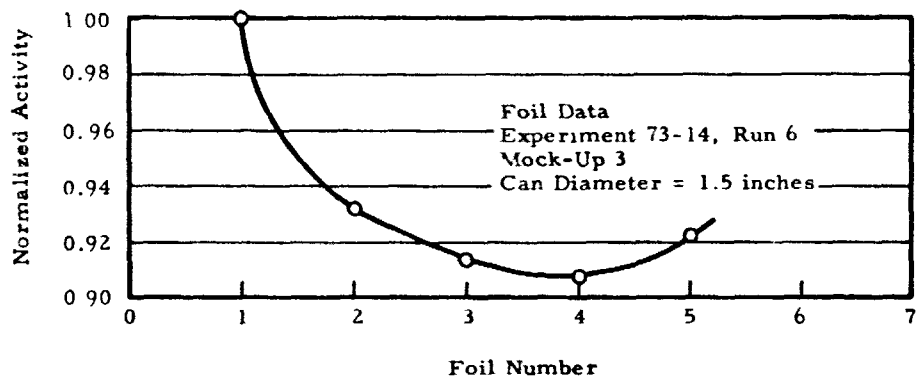


Figure 2-9. Reactivity Vs Mock-Up Container Diameter

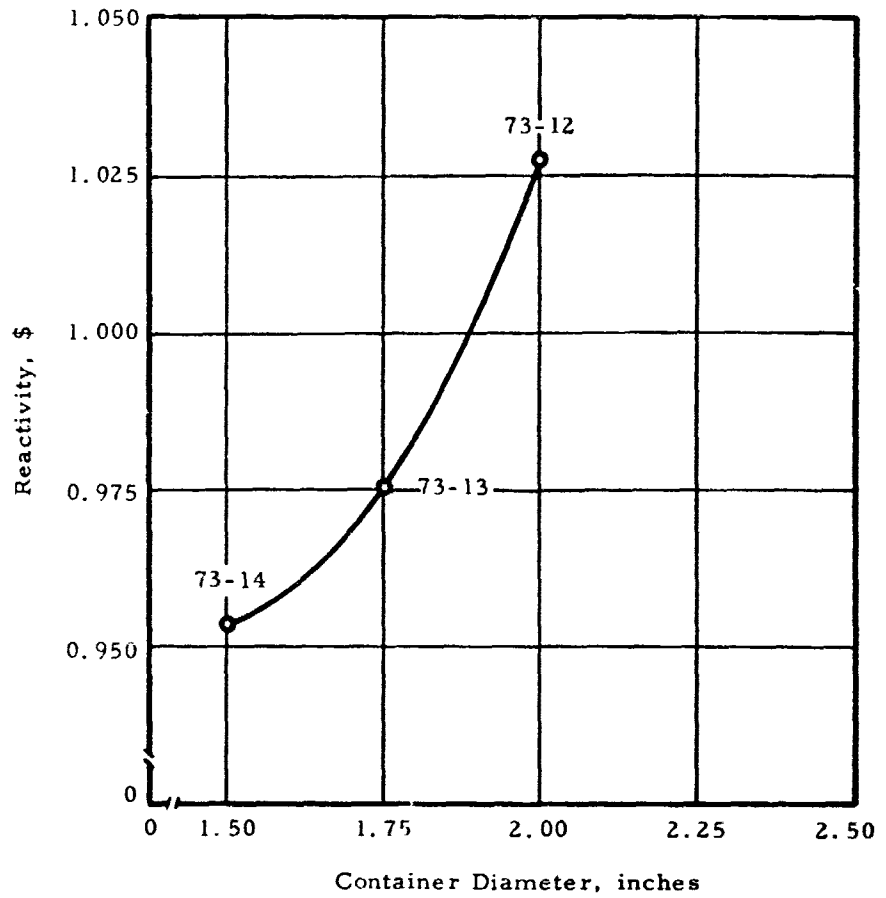


Figure 2-10. LPR Power to Produce 1500 Watts in the Experiment Vs Experiment Diameter

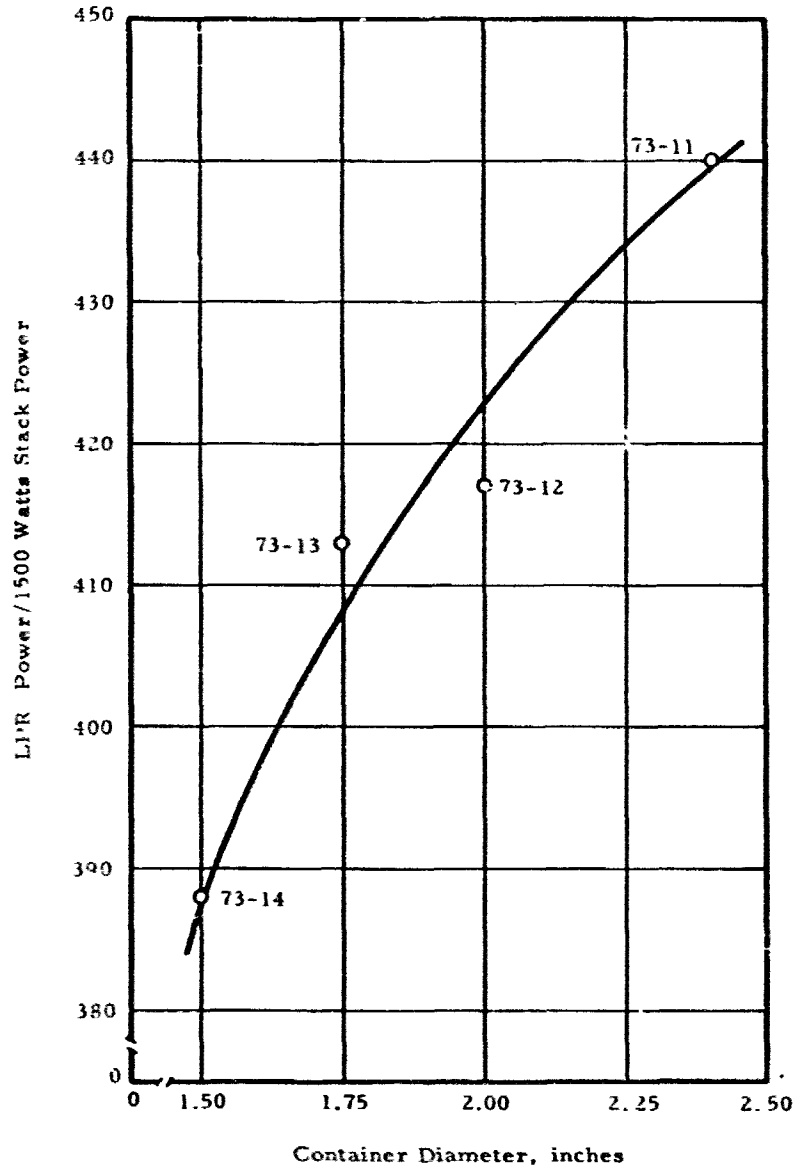
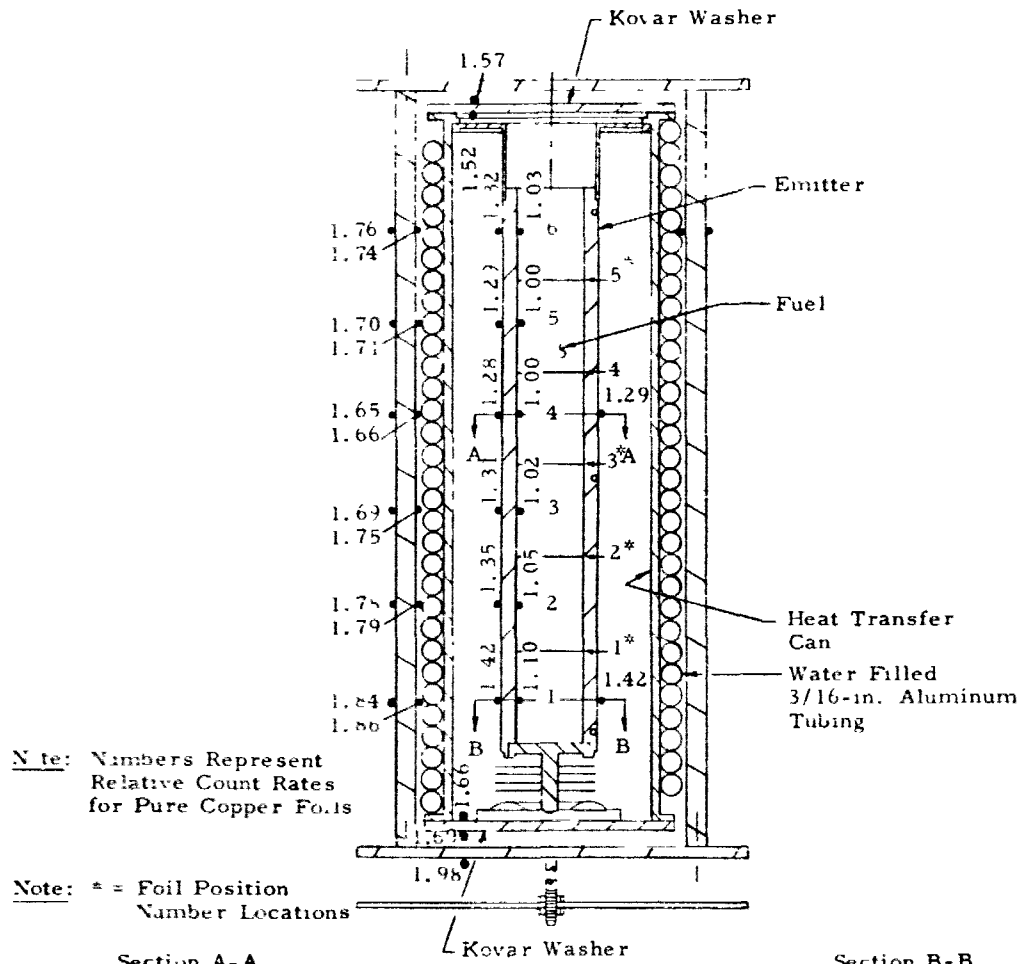


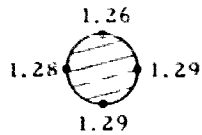
Figure 2-11. Cross-Section of Mock-Up 4 With Flux Measurements Shown



Note: Numbers Represent Relative Count Rates for Pure Copper Foils

Note: * = Foil Position Number Locations

Section A-A



Pellet No. 4

- 1.28
- 1.26
- 1.29
- 1.29

Pellet No. 1

- 1.42
- 1.40
- 1.42
- 1.47

Section B-B

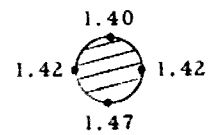
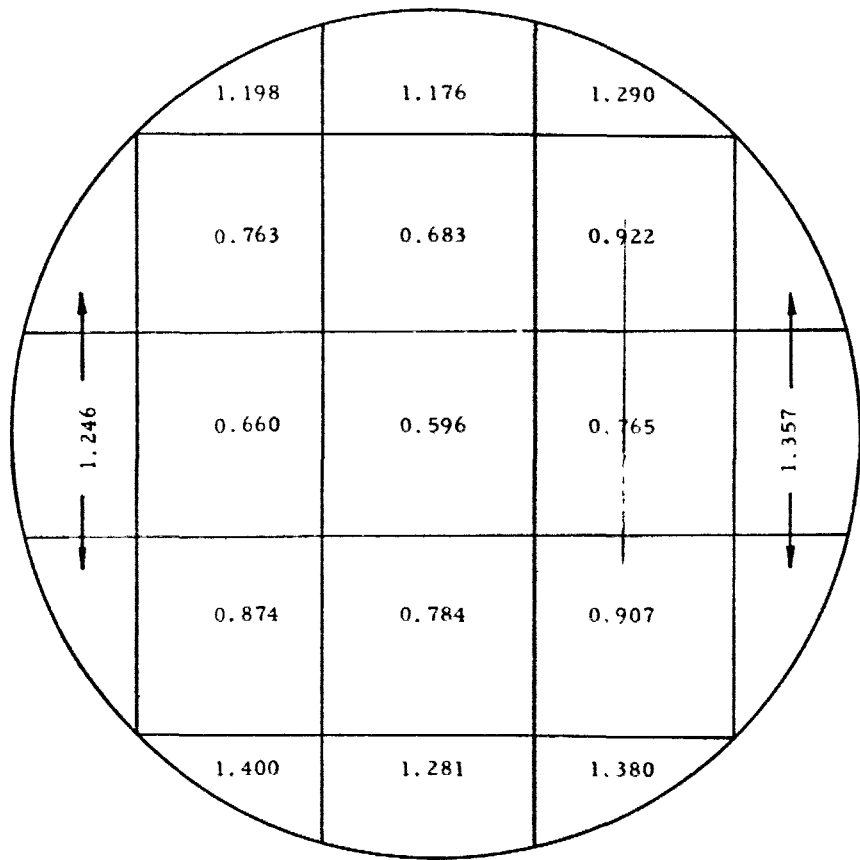


Figure 2-12. Radial Power Distribution in the Fuel



3 HEAT TRANSFER EXPERIMENT

3.1. Introduction

3.1.1. Purpose

The basic requirement for the heat transfer experiment was to operate a nuclear-fueled molybdenum emitter at the temperature and heat flux needed for the thermionic converter operation. These conditions were an emitter surface temperature of 1350 C and a heat flux at the fuel surface of 100,000 Btu/hr-ft². The heat flux condition corresponded to a power input to the device of 1500 watts. The purpose was to investigate the performance of the fuel and clad at design conditions. A second purpose, though not a specific requirement, was to measure the emitter circumferential and longitudinal temperature distributions. By comparing these measurements with those obtained using the same device heated electrically, it could be determined if the fuel pellets would introduce a temperature perturbation that would adversely affect the electrical performance of the converter in the subsequent inpile test.

3.1.2. Scope

The heat transfer experimental program was carried out in three steps. The first step was a series of electrical calibration experiments in which temperature and calorimetric measurements were made in an electrically heated device. Experiments were performed with an internal vacuum and with helium gas at low pressure. The second and third steps consisted of a series of inpile heat transfer experiments. Inpile Heat Transfer Experiment Series 1 was made up of three inpile power runs using the same device that was used previously in the electrical calibration experiments. This first series of inpile experiments was carried out before the upgrading of the LPR to a one megawatt capability was begun. Consequently, the time available at power for these experiments was limited. Inpile Heat Transfer Experiment Series 2 was

carried out in an assembly of nearly identical design to that used in the first two steps. However, since the upgrading of the reactor had been completed, the time available for the performance of these experiments was limited only by the objectives of the particular experiment. Six power runs were made with this assembly, including three power runs to test the dynamic characteristics of the device.

3.2. Experiment Design

3.2.1. Design Considerations

The design of the heat transfer experiment was influenced by the factors discussed in the following paragraphs.

3.2.1.1. Electron Cooling

In a thermionic converter producing electrical energy, a significant fraction of the energy transferred from emitter to collector is transferred by the electrons. Consequently, to duplicate both the desired temperature and heat flux in a device producing no electrical energy, an alternate heat transfer mechanism was needed to compensate for the electron cooling. Initial calculations showed that it was possible to transfer the entire 1500 watts input to the heat sink by a combination of the normal end-conduction losses and by radiation, provided the emissivity of the emitter surface could be increased to more than 0.5 and the emitter temperature was allowed to reach 1400 C, a temperature 50 C higher than design conditions. The emissivity of the emitter was increased by sandblasting the surface, and an experiment was performed at RCA to determine whether sufficient radiant heat transfer could be achieved. The results showed that a temperature considerably higher than 1400 C was needed if radiation alone were used. Therefore, it was decided to augment the radiant heat transfer by gaseous conduction between the emitter and a simulated collector. Gas pressure could then be used as a variable to achieve the desired temperature at the design heat flux. To permit varying the heat transfer rate from the emitter without changing the heat transfer characteristics of the fuel region, a two-compartment design was adopted. In this way the emitter temperature could be varied by changing the gas pressure in the outer compartment while beginning the experiment with a vacuum in the inner fuel compartment.

3.2.1.2. Longitudinal Temperature Distribution

To obtain the most meaningful longitudinal temperature information, it was necessary to establish the same heat conduction losses out of the ends of the heat transfer device as those of the converter. This goal and the decision to use a two-compartment design also made it desirable to use, with some modifications, the converter emitter support structure.

3.2.1.3. Thermal Design

A worthwhile simplification in the experiment thermal design was made by allowing the temperature of the stainless steel can containing the emitter to be the same as that of the water coolant. This was accomplished without an adverse effect upon the longitudinal temperature distribution by increasing the thermal resistance of the emitter support structure. Figure 3-1 is a drawing of the special emitter assembly supplied by RCA for the second series of inpile heat transfer experiments. The support structure was changed from that of the design converter by increasing the outer diameter and reducing the thickness of the Kovar support disc and by reducing the diameter of the molybdenum support pin. Also, increasing the diameter of the support disc provided sufficient space for the installation of thermocouple lead-throughs around the outside of the copper diaphragm. Because the outer can ran cool, low-temperature, small-size, dual-lead thermocouple lead-throughs could be used. With a large number of temperature measurements to be made, the size and type of lead-throughs were important from the standpoint of the effect upon the experiment diameter.

3.2.1.4. Experiment Diameter

Prior to upgrading to one megawatt, the reactor power was limited to a maximum of 450 KW. The preliminary nuclear measurements described in Section 2 showed the importance of minimizing the experiment diameter to insure producing 1500 watts in the device within the 450 KW limitation.

3.2.1.5. Safety

To insure the safety of both reactor and experiment, a dual-containment philosophy was followed. That is, it was

required that the fuel region be separated from the reactor water by two separate sealed containers.

3.2.2 Design Description

The component parts that make up the heat transfer assembly are shown in the photographs and drawings of Figures A-1 to A-13 in Appendix A. Also included is the assembly procedure that was followed. The description of the experiment is divided into two parts corresponding to the particular function of each part. The first part is designated the heat transfer device. It was a sealed unit containing the nuclear-fueled emitter. The second part is designated the heat transfer assembly. It contained the heat transfer device, the heat sinks, and the external can that was needed to provide dual-containment for the impile experiment.

3.2.2.1. Heat Transfer Device

The heat transfer device consisted of the components shown in Figure 3-2. The emitter assembly was supported by clamping the copper diaphragm between a split clamp and a base plate ring that was tack-welded to the lower base plate. The Pt-Pt, 13% Rd thermocouples were peened into the emitter surface. The thermocouple leads were fed through double-bore ceramic insulators, which passed through holes in an aluminum split sleeve surrounding the emitter. The insulated leads were then run in grooves in the outer surface of the split sleeves through insulated thermocouple lead-throughs in the lower base plate. The aluminum split sleeve served two purposes. First, by reducing the gap thickness between the emitter and a simulated collector, heat transfer by gaseous conduction was improved while the heat transfer by convection was limited. Second, the split sleeve provided an effective support for the insulated thermocouple leads. The inner surface of the split sleeve was painted with a carbon solution to improve its emissivity.

Figure 3-3 shows the insertion of the assembled components into the stainless steel outer can. The lower base plate was welded to the bottom flange of the outer can and the support disc was welded to an internal flange near the top of the can. This construction is illustrated by Figure 3-4, an assembly drawing of the impile experiment. This figure shows the separate compartments formed in the heat transfer device by the fuel chamber and the chamber between the emitter and split sleeve.

3.2.2.2. Heat Transfer Assembly

The heat transfer assembly was made up of the components shown in Figure 3-5. The heat transfer device was installed in a split aluminum cooling jacket. The jacket contained drilled channels that formed a parallel flow circuit when connected to the inlet and outlet water lines. Heat was transferred from the upper and lower base plates by conduction to the cooling jacket. The cooling jacket was insulated from the external can to permit calorimetric measurements, and metal-sheathed thermocouples were brazed into the inlet and outlet water tubes. Thermocouple extension wires and coolant tubes were run through the bottom external tube. Because the inpile heat transfer experiments were planned as comparatively short tests, it was possible to use an epoxy seal around the wires and tubes extending through the bottom tube. The heat transfer assembly was installed in an empty aluminum reflector element for insertion in the center hole in the LPR.

3.3. Electrical Calibration Experiment

3.3.1. Introduction

A series of five electrically heated experiments were performed using the heat device previously described. Experiments were carried out with a dynamic vacuum and with helium gas at a low pressure. The purposes of these experiments were to determine if the thermal design adequately established the desired temperature at the design heat flux and to provide a basis for comparison of the electrical and nuclear heat sources. The comparison was needed to show whether the nuclear fuel would introduce a temperature perturbation that would alter the converter performance in the subsequent inpile test.

3.3.2. Experiment Description

The heat transfer device was described in Paragraph 3.2.2.1. The electric heater, supplied by RCA, consisted of four tungsten rods which were inserted into the hollow emitter and which transferred energy to the emitter by radiation. The heater was attached to the experimental device by welding the top flange of the outer can to the flange on the heater as shown in an inverted view in Figure 3-6. Electric power was supplied to the heater through the water coolant leads.

Ten operable Pt-Pt, 13% Rd thermocouples were installed on the emitter and support structure in accordance with Thermocouple Pattern 1, shown in Figure A-14 in Appendix A. Inlet and outlet water temperatures were measured with precision thermometers for the following three flow paths:

1. Through the main cooling jacket installed around the stainless steel outer can.
2. Through the electric heater.
3. Through a series circuit consisting of a heat sink on the heater flange and a heat sink attached to the copper pinch-off tube on the lower base plate.

The coolant flow in each path was determined by timed volume measurements. The outer chamber, between the emitter and split sleeve, and the inner chamber, containing the tungsten rods, were not separately sealed because of a leak at the brazed joints between the tantalum heat dam and the Kovar support disc. Consequently, the device contained a single vacuum compartment.

Thermocouple voltages were read using a Type K-3 Universal Potentiometer (Leeds & Northrup Company). The voltages were also monitored using a Beckman/Berkeley Preset Universal E Put and Timer with a digital recorder. This instrumentation provided a digital print-out of the thermocouple readings on a paper tape.

3.3.3. Experimental Results

A synopsis of the electrically heated dynamic-vacuum test of the device that was later used in the first inpile heat transfer experiments is included in Appendix A. Table A-7 summarizes the temperature and power measurements. Also included in this table are the temperature measurements for the maximum power point reached in a later electrically heated experiment containing 7 microns (cold) of helium. The actual pressure in the device was not known at the time the temperature measurements were made. The measurements in helium are included solely to show the difference in temperature of the two thermocouples at the top of the emitter immediately before the first inpile experiment. Since approximately the same temperature difference was found in the

inpile measurements, it is unlikely that a real temperature perturbation exists. A comparison of these electrically heated and nuclear heated results is included in Section 3.4.2.1.

3.4. Inpile Heat Transfer Experiment Series 1

3.4.1. Experiment Description

The device used in the first series of inpile heat transfer experiments was the same as that used in the electrically heated test described in Section 3.3. After the device was removed from the heater, it was fueled and outgassed according to the schedule listed in Section 4 in Appendix A. The inpile assembly consisted of the components described in Section 3.2.2.2. Six operable thermocouples were attached to the emitter as shown in Figure A-14, Thermocouple Pattern 2. Two additional Pt-Pt, 13% Rd thermocouples were attached to the structure—one at the base of the molybdenum support pin and the other on the tantalum heat dam at the inner boundary of the upper Kovar support disc. Two copper-constantan thermocouples were attached to the upper and lower base plates and two metal-sheathed chromel-alumel thermocouples were installed in the inlet and outlet coolant lines. Thermocouple measurements were made using a Type K-3 potentiometer (L&N). The coolant flow was measured by a flowmeter and by timed volume measurements.

Three power runs were made with the first heat transfer assembly. A detailed synopsis of each of the three experiments is included in Appendix A. The following paragraphs describe the way the experiments were carried out and the experimental results that were obtained.

3.4.2. Experimental Results

3.4.2.1. Experiment 73-19

The first inpile heat transfer experiment was run on September 12, 1962. Temperature measurements were made at eight reactor power levels from 20 KW to 350 KW. At the maximum reactor power of 350 KW, an emitter temperature of 1433 C was reached at the midplane. A reactor power of 350 KW corresponds to a total power input to the device of 1383 watts. Part of the total device power is due to gamma heating of the heat sink and associated structure. Therefore, to

determine the energy input to the emitter it is necessary to subtract this gamma heating contribution. Table A-1 in Appendix A lists the temperature and flow measurements, the device power, structure gamma heating, and the net input power to the emitter. The gamma heating value is based upon a calculated midplane heating rate of 0.5 watts/gm/MW and a measured structure weight of about 800 grams.

The longitudinal temperature distribution from the nuclear heat source was similar to that obtained in the electrically heated test as shown in the following comparison of the same thermocouples:

<u>Heat source</u>	<u>Top of emitter, C</u>	<u>Midplane, C</u>	<u>Bottom of emitter, C</u>	<u>Emitter power, watts</u>
Electrical	1314	1450	1265	1285
Nuclear	1301	1433	1268	1243

Circumferential temperature variations were measured at planes near the top and bottom of the emitter. However, a circumferential temperature distribution at the midplane was lost due to the failure of two midplane thermocouples.

During the experiment, approximately 7.9×10^6 watt-seconds of fission energy were produced within the emitter.

3.4 2.2. Experiment 73-20

A second power run was made with the device on September 19, 1962, to investigate the effect of rod position on the longitudinal temperature distribution and to determine whether the data was reproducible after a thermal cycle and after a shutdown interval of one week. Temperature readings were duplicated at a reactor power level of 80 KW. However, at 200 KW, temperature readings were lower than in Experiment 73-19 and continued to drop with time at a constant reactor power. The reactor power was reduced to 80 KW and temperature readings were lower than those recorded at the 80 KW power level during the first part of the experiment. Table A-2 summarizes the temperature measurements.

3.4.2 3. Experiment 73-21

A third power run was made on September 20 to investigate the improved heat transfer noted in the previous experiment. Temperature and flow measurements were made at 10 reactor power levels from 20 KW to 400 KW. The initial emitter temperature readings at 80 KW were lower than those of Experiment 73-19 but higher than those at the end of Experiment 73-20. At the 80-KW reactor power level, the emitter temperatures were stable. When the reactor power was raised to 130 KW, the emitter temperatures reached a maximum, then dropped with time at constant reactor power. The reactor power was then raised in steps to 400 KW. At each power level, the temperatures dropped off as the reactor power level was held constant. The reactor power was then reduced in steps corresponding to three power levels reached on the way up to the maximum power point. At each of these power points, the temperature readings were lower than measured initially. Temperatures at the lower power levels did not decrease with time but showed a slight rise.

Table A-3 summarizes the measurements made during Experiment 73-21. At the maximum power of 400 KW, approximately 1700 watts were produced in the device and a maximum midplane emitter temperature of 1200 C was reached. For these conditions the input power to the emitter was 1593 watts.

The relationship of reactor power to device power that was determined in the first series of heat transfer experiments is shown in Figure 3-7. The change in heat transfer characteristics observed in Experiments 73-20 and 73-21 also occurred in the second series of experiments. The explanation for the change is included in the discussion of Experiment 73-23, Section 3.5.2.1.

3.4.3 Conclusions

The first series of heat transfer experiments was important in showing the equivalence of the nuclear and electric heat sources. Also, the results led to a number of improvements in fuel and device outgassing, vacuum capability, and experiment instrumentation and operation, which were incorporated before the second series of experiments was carried out. Thus, the first experiments proved of value in providing a basis for conducting a more meaningful second series.

3.5. Inpile Heat Transfer Experiment Series 2

3.5.1. Experiment Description

The heat transfer device used for the second series of inpile experiments was of the same design as that used in the first series with the following exceptions:

1. An improved emitter thermocouple pattern was used.
2. The fuel was outgassed at a higher temperature (about 1970 C) and there was an improved vacuum in the device at pinch off.
3. The center of the fuel was located one inch below the centerline of the core.
4. A longer pinch-off tube was left on the device requiring a change in the top external plate.
5. The aluminum cooling jacket was modified by replacing the drilled coolant channels with aluminum tubing. This modification required a change in the method of connecting the parallel flow paths through the jacket to the single inlet and outlet lines and resulted in a small increase in the structure weight. (A structure gamma heating rate of 0.48 watts/KW was used in determining the emitter input power for these experiments.)

In this device, as in the first, the inner chamber containing the fuel and the outer chamber between the emitter and split sleeve were not separately sealed.

Ten Pt-Pt, 13% Rd thermocouples were located on the emitter to measure the temperature distribution (Thermocouple Pattern 3, Figure A-14). Seven of these thermocouples were located in a vertical line. Three additional thermocouples were located at the longitudinal midplane, thus forming a circumferential pattern of four thermocouples displaced every 90 degrees. Inlet and outlet water temperatures and flow were measured for calorimetric calibrations. Temperatures were monitored throughout the experiment by using a multi-point recorder. More precise measurements were made at each power level by using a Type K-3 potentiometer (L&N). The coolant flow rate was determined from timed volume measurements.

3.5.2. Experimental Results

3.5.2.1. Experiment 73-23

To insure meeting both the emitter temperature and heat flux objectives, the experiment was carried out in the following way. The reactor power was increased in steps to 262 KW, where a maximum emitter temperature of 1358 C was reached. This reactor power corresponds to a power input to the emitter of 1187 watts. At each power step, temperature and flow measurements were made. Temperatures remained constant at a constant reactor power of 262 KW for approximately two hours. Thereafter, it was necessary to increase the reactor power level periodically to hold the desired emitter temperature of 1350 C. A maximum reactor power of 390 KW corresponding to a power input to the emitter of 1699 watts was required to reach an emitter temperature of 1357 C approximately four hours after reaching 1358 C at the 262-KW reactor power level. The reactor power level was held at 390 KW as a limit on the maximum desired heat flux and the emitter temperatures continued to drop with time.

The reactor power was then reduced in steps. Temperatures at the descending power steps were lower than those of identical ascending power steps. At reactor power levels of less than 130 KW, the emitter temperatures did not decrease with time at constant reactor power.

Table A-4 in Appendix A summarizes the measurements made during Experiment 73-23. Figure 3-8 summarizes the temperature measurements before the reduction of temperatures began. Also included is a temperature measurement for a comparable power point of Experiment 73-19. Figure 3-9 is a summary of the emitter temperatures (Thermocouple 5) as a function of time as determined from the recorder traces.

A synopsis of each experiment in this series is included in Appendix A. Figure 3-10 shows the relationship of reactor power to device power as determined from all the experiments in this series.

As shown in Figure 3-9 a change in heat transfer characteristics took place approximately two hours after reaching a steady-state power level of 262 KW. At this time the total fission energy produced within the emitter was approximately 1.71×10^7 watt-seconds.

Because of the length of the experiment and the decay time associated with chains which produce the noble gases, Xe and Kr, an equilibrium gas production rate per fission was not established before the change in heat transfer characteristics was noted. It was assumed that 0.1 gas atoms were produced per fission, which corresponds approximately to the direct yield of Xe¹³⁶ and Kr⁸⁶. With this assumption a total of approximately 5.58×10^{16} gas atoms was produced within the emitter at the time the temperature reduction began. Since the fuel compartment and the outer compartment were not separately sealed, a total void volume of about 41 cc was available for the diffusion of the gases. With free interchange between chambers and a 100% gas-release rate from the fuel, a fission gas density of 1.36×10^{15} atoms/cc results. Solving the following equation for pressure at an average gas temperature of 790 K results in a calculated pressure of 0.111 mm Hg.

$$n = 9.656 \times 10^{18} \frac{P_{\text{mm}}}{T}$$

where

n = number of molecules/cc

P = pressure in millimeters of Hg

T = gas temperature, K

A pressure of this magnitude would certainly have led to a temperature reduction much earlier than shown in Figure 3-9. Consequently, it seems reasonable to believe that the fission gas release rate was much less than 100%. Observations of the change in temperature with pressure during the electrically heated tests show the temperature changes observed in the impile experiment could have occurred at a release rate of less than 1%. Because of the assumptions that were made and because the rate of gas transfer from inner compartment to outer compartment is unknown, realistic values of gas release rate cannot be established until a postirradiation examination is completed.

3.5.2.2. Experiment 73-24

A second power run was made with the device on December 17, 1962, to further investigate the change in heat transfer characteristics, which is evident by the results of the first power run. The reactor power was increased in identical power steps to those of the

previous experiment, and the emitter temperatures were slightly higher (higher by approximately 20 C at 130 KW) than those recorded during the descending power steps of the first experiment.

The maximum power reached was 340 KW corresponding to a total input power to the device of 1630 watts and 1467 watts input to the emitter. At this power level the maximum midplane temperature was 1204 C. Temperatures continued to decrease with time at constant reactor power. Table A-5 summarizes the results of this experiment.

3.5.2.3. Experiment 73-25

During the third power run, the reactor power was raised immediately to 330 KW and the emitter temperatures were monitored at this power level for approximately 2 hours.

Temperature measurements for this experiment and the subsequent dynamic experiments are summarized in Table A-6.

3.5.2.4. Experiments 73-26, 73-27, and 73-28

Three dynamic experiments were performed to investigate the emitter temperature change associated with rapid changes in reactor power. These experiments are discussed in Section 3.6.

3.5.3. Conclusions

Based upon the results obtained in the second series of impile heat transfer experiments, the following conclusions were reached:

1. The emitter temperature and heat flux objectives were successfully met. An emitter surface temperature of 1350 C was achieved at a power input of 1500 watts to the emitter. The maximum power input was 1700 watts to the emitter.

2. Temperature distribution measurements indicate no adverse temperature perturbations are introduced through the use of the nuclear fuel pellets.

3. Although an analytic evaluation was made, a postirradiation examination is required to establish an accurate value for the fission-gas release rate.

3.6. Dynamic Measurements of Nuclear Heating

3.6.1. Introduction

As part of the second series of heat transfer experiments, several power runs were made to determine the dynamic behavior of the system with changes in heat input. It was anticipated that the parameters and mechanisms of heat transfer from the emitter to the collector and other materials would, in this way, be better understood. However, the analysis of the data has shown that the behavior of the system can be adequately described with a single lumped-parameter time constant.

3.6.2. Experimental Setup

The conditions of the experiment were those described for the second heat transfer experiment installation with the additional equipment necessary for fast recording of thermocouple outputs. A Keithley Model 310 voltage amplifier was used to feed a Sanborn recorder. The frequency response of the system was adequate to 100 cycles, although results indicated that no high frequency components were present and later work was done with a Model-G L&N multipoint recorder.

The experiments involved bringing the system up to equilibrium power and then making a rapid change in power, usually by scrambling the reactor so that input power was essentially removed as a step function. Plots were then made of the temperatures as indicated by the thermocouples on the emitter and other portions of the device.

3.6.3. Theoretical Expectations

The mechanisms of heat insertion and removal from the system were considered as

1. Fission heat created in the fuel itself from thermal neutron fissioning of the U^{235} .
2. Gamma and neutron heating in the structural materials, which heating is in turn directly related to the operating power of the driving reactor (the LPR).
3. Loss of heat by radiation from the surface of the emitter to the collector.

4. Loss of heat by conduction through the metal structure.
5. Loss of heat by gaseous conduction in the space between the emitter and collector.

In writing a kinetic equation of the temperature of the emitter as a function of system parameters, the model was simplified by assuming

1. The emitter sheath and the internal fuel were considered as one body and the specific heat was the sum of the two specific heats with the system assumed to be at the emitter temperature.

2. The conductive heat losses were simple first order conductions dependent on the material and the temperature differences, and a single conductivity parameter was used.

3. The radiative heat transfer obeyed the Stefan-Boltzmann law.

Thus the equation is

$$\dot{T} = \frac{Q_{in}}{C_p} - \frac{K_1 A}{C_p t} T - \frac{\sigma \epsilon A}{C_p} (T_e^4 - T_c^4) - \frac{K_2}{C_p} T \quad (1)$$

where

$$T = T_e - T_c$$

T_e = temperature of the emitter in K

T_c = temperature of the collector in K

Q_{in} = the heat from fuel fission and gamma neutron heating in watts

C_p = the total specific heat of the emitter structure and fuel in watt-seconds/C

K_1 = the conductivity in the emitter-collector gap (other conductivities are neglected) in watts/cm-C

K_2 = conductivity through metals

A = the area of the emitter surface = 60 cm²

t = the hot gap between emitter and collector = 0.24 cm

σ = the Stefan-Boltzmann constant = 5.67×10^{-12} watts/cm²-K⁴

ϵ = the total emissivity of the surfaces $\left(\frac{1}{\epsilon_e} + \frac{1}{\epsilon_c} - 1\right)^{-1}$

\dot{T} = the time derivative of the temperature difference.

3.6.3.1. Heat Capacity

The heat capacity of the system was determined from the sum of the individual heat capacities of the molybdenum emitter and the enclosed fuel (UO_2). Each of these materials exhibits an increase in specific heat with an increase in temperature. Information on the UO_2 ¹ and the molybdenum,² given in calories/gram-C, was converted to watt-second/C for the total 132 grams of UO_2 and the 141 grams of molybdenum. Near 100 C the total specific heat was 73 watt-seconds/C and near 1000 C the total specific heat was 90 watt-seconds/C.

3.6.3.2. Radiation Heat Losses

The radiative heat losses were increased by roughening the surfaces of the emitter and collector so that the emissivity would be increased. If the emissivity were perfect and the collector temperature were between 27 C (300 K), and 127 C (400 K) varying as a function of power to account for temperature drops, a calculation of the total watts radiated vs temperature of the emitter for the full 60 cm² would be as shown in Figure 3-11.

Electrical tests, which were performed on the experiment prior to inpile insertion, provide an indication of the emissivity. One such test on September 3, 1962, was operated with a near vacuum between collector and emitter (1.3×10^{-4} mm Hg). In this experiment the heat transferred by radiation was determined separately from the solid conduction end-losses by the use of separate heat sinks. A total of 1183 watts was transferred by radiation from an emitter with a weighted average temperature of 1420 C. This indicates a value for the radiative efficiency of 0.41. Thus, to determine the relative amount of heat transfer by radiation, the temperature of the emitter is determined by measurement. The perfect radiation loss is read from Figure 3-11, and the radiated watts are computed by multiplying by the radiative efficiency, 0.41.

3.6.3.3. Thermal Conductivity

The thermal conductivity of the gap, K_1 , between the emitter and the collector is a function of the type and quantity of material

in the gap. This value was subject to continual change during the experiment as gasses from fission products and residual gas diffused into the fuel-emitter gap and through the intercompartmental leak to the emitter-collector gap. This quantity is the subject of the measurements in Section 3.6.4. The conductivity through solids, represented by the K_2 constant in Equation 1, was evaluated from the material constants and the measurements of temperatures on the electrically heated experiments. The measured conduction loss at an average emitter temperature of 1370 C and for 1285 watts power input to the emitter was approximately 102 watts.

3.6.4. Static Measurements

For the static case, the time rate of change of the temperature is zero and all the numbers on the right side balance. The heat available for radiation and gap conduction loss (Q_{net}) is the heat measured from the calorimetric balance minus the solid conduction heat loss minus the gamma and neutron heating of the structure other than the emitter (0.48 watts/KW of reactor power). Thus the equation is

$$Q_{net} = K_1 \frac{A}{t} T + \sigma A \epsilon (T_e^4 - T_c^4) \quad (2)$$

Table 3-1 shows some of the results from static measurements. Note that the last determination was made by taking data after a sudden drop in reactor power from 200 to 100 KW. The change in power took about three minutes. Since the level at 100 KW came to equilibrium quickly, it is considered that the amount of gas in the gap remained constant. There was no calorimetric determination of the output power from the device, but the power is assumed to have dropped from 2A to A. Thus, there are two sets of conditions for Equation 2 with the unknowns A and K_1 . K_1 shown in Table 3-1 is the solution for this pair.

3.6.5. Kinetic Measurement of Temperature

Four sets of measurements were taken on the heat transfer system, which involved coming to an equilibrium temperature and then scrambling the reactor so that the heat input was essentially reduced to zero instantaneously. A plot of the temperature information from one of the thermocouples was put on semi-logarithmic paper shown typically

in Figure 3-12, and the slope of the temperature decrement was determined. The associated time constant is the time required for the temperature to drop one e-fold.

The information is not sufficiently precise to allow curve fitting on the following exact equation, which is based on lumping heat transfer conduction and assuming that the gamma and neutron heating went to zero when the reactor was scrammed.

$$\dot{\bar{T}} = -\frac{K_1 A}{C_p t} \bar{T} - \frac{\sigma \epsilon A}{C_p} (\bar{T}_e^4 - T_c^4) \quad (3)$$

At the low power inputs, the radiation loss can be considered negligible. Since the data appears to give a good exponential fit, the parameters are lumped into one time constant, C_p/K_3 , where K_3 equals $K_1 \times A/t$.

$$\dot{\bar{T}} = -\frac{K_3}{C_p} \bar{T} \quad (4)$$

Table 3-2 shows the results of the dynamic measurements.

3 6 6 Conclusions

The values of gap conduction determined from the static measurements show a significant increase occurred between the first and second experiments listed in Table 3-1. The direction of change was consistent with the change that was noted in the emitter temperatures. Within the accuracy of the experiment, the dynamic and static measurements of the heat transfer characteristics of the gap appear to be in good agreement. For comparison, a typical value of conductivity for helium at 320 C is 0.0022 watts/cm-C.³

The appearance of the single time constant decay did not permit evaluation of the separate mechanisms of radiative and conductive heat transfer, but it did indicate how studies of the kinetics can be greatly simplified by using first-order Equation 4. The time constant for emitter cooling as determined by the experimental results shown in Figure 3-12 was approximately 97 seconds.

Table 3-1. Static Heat Transfer Determination

Date	Time	Reactor power, KW	Calorimetric heat, watts	Q _{conduction} watts	T _e , C	T _c , C	Q _{ym} , watts 38.6 w/100 KW	Q _{radiation} watts	K ₁ , A/t (T _e - T _c) watts	K ₁ , watts/cm-C
December 14, 1962	2044	200	865	81	1121	85	96	615	84	0.0003
December 19, 1962	1648	200	827	64	905	82	96	291	376	0.0018
December 31, 1962	1345	200	2A	62	871	82	96	258	2A-416	0.0010
December 31, 1962	1550	100	A	42	587	55	48	82	A-174	

3-19

Table 3-2. Dynamic Data on Heat Transfer Experiments

Date	Time	Reactor power, KW	Time constant, τ sec	Total C _p , UO ₂ + MO, watt sec/C	K ₁ , C _p /τ watts/C	T _e avg (before) C	K K ₁ × t/A watts/cm-C
December 19, 1962	1648	200	114	90	0.82	320	--
December 31, 1962	1645	150	97	90	0.93	1110	-
January 2, 1963	1345	20	149	74	0.50	189	0.0019
January 4, 1963	0954	10	195	73	0.37	106	0.0014

Figure 3-1. Special Emitter Assembly

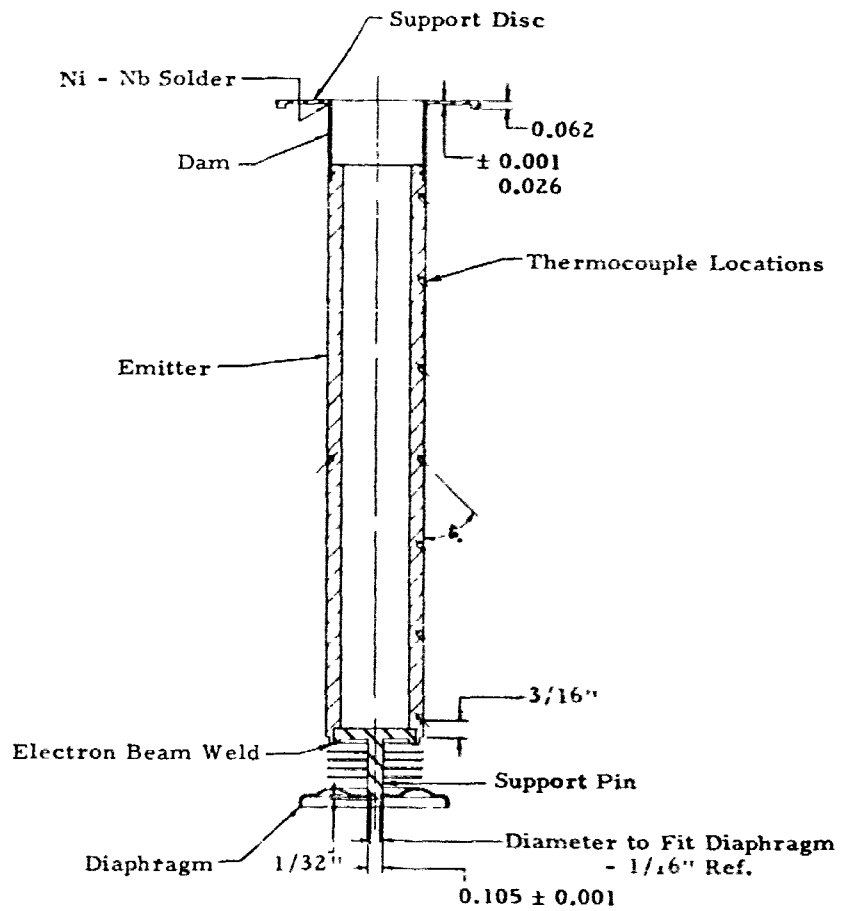


Figure 3-2. Heat Transfer Device

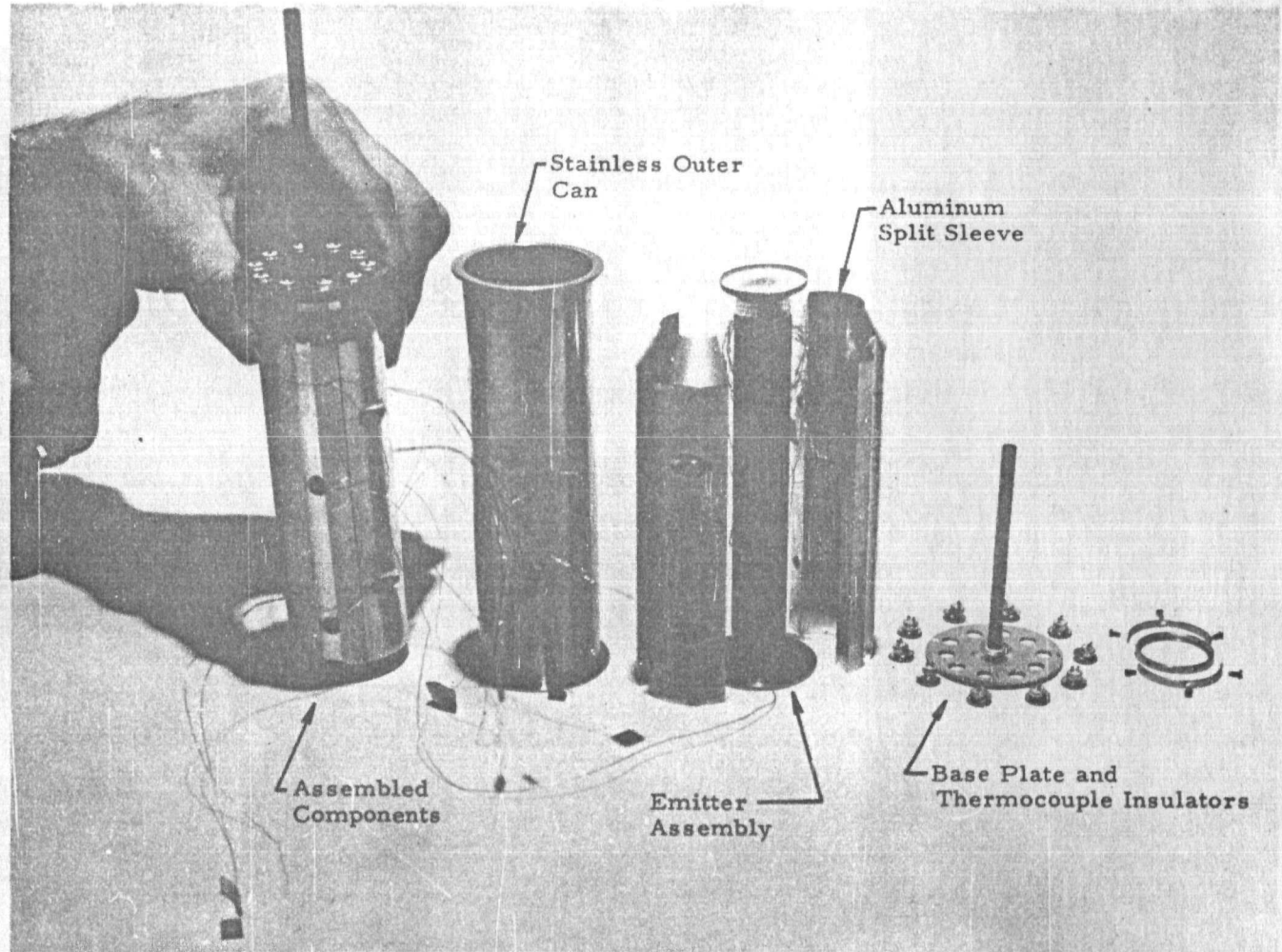


Figure 3-3. Assembled Components of the Heat Transfer Device

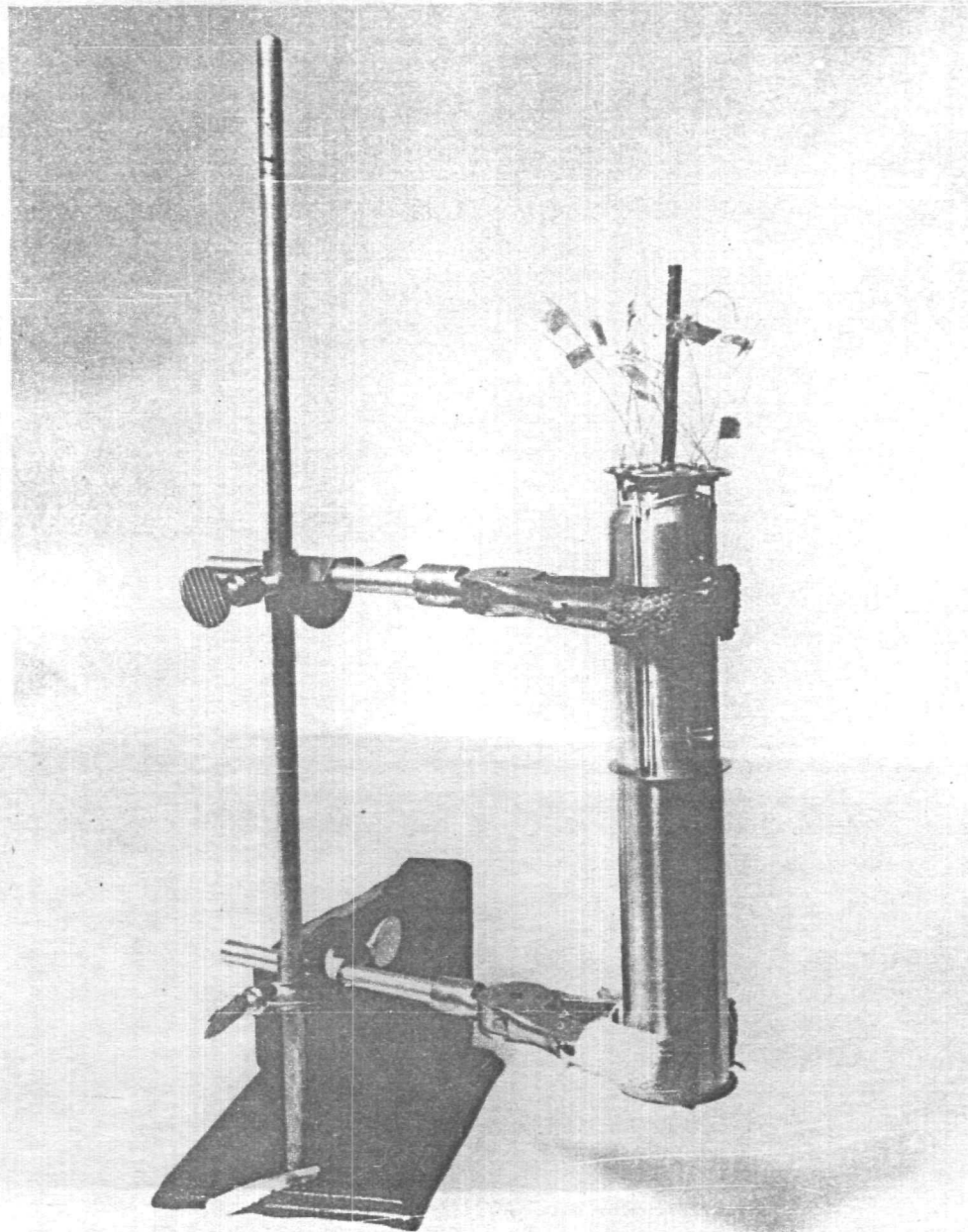
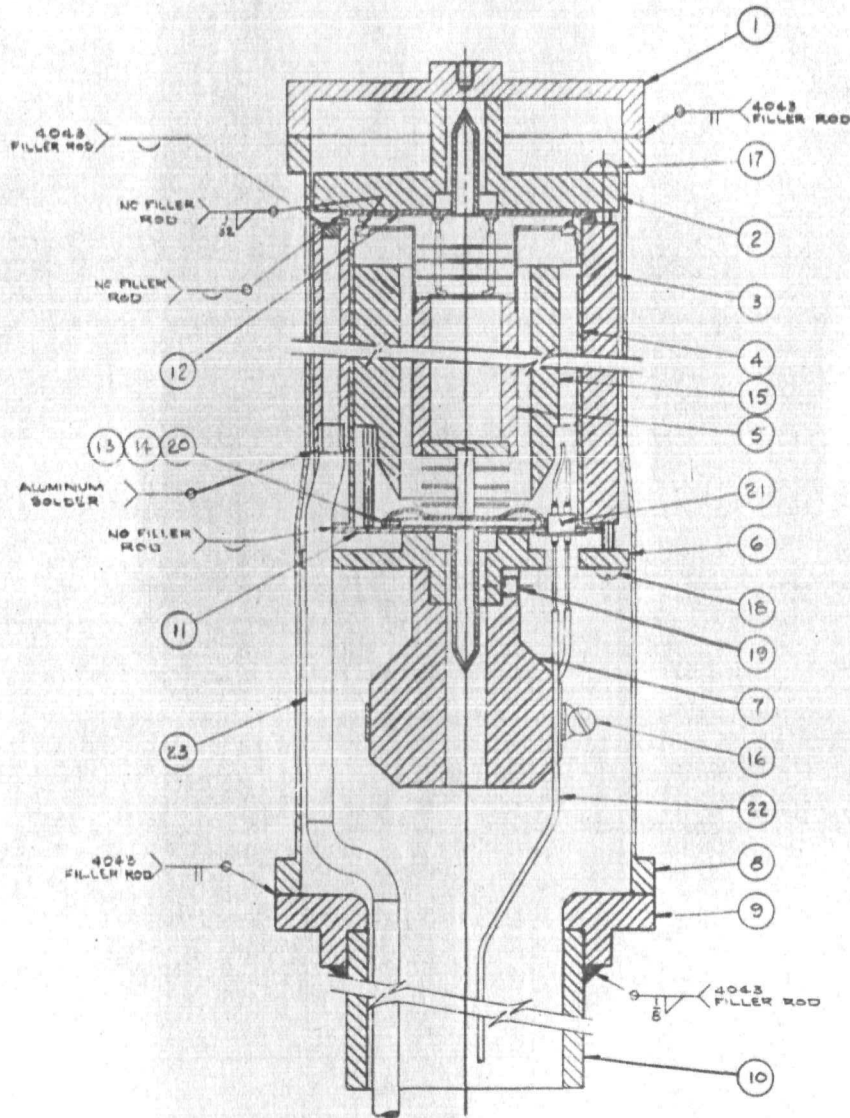


Figure 3-4. Heat Transfer Experiment Assembly



BILL OF MATERIAL			
PART NO	DWG. NO.	DESCRIPTION	QTY/MATERIAL
1	36135C	TOP EXTERNAL PLATE	1 AS NOTED
2	36135C	TOP HEAT SINK	1 AS NOTED
3	36225C	COOLING JACKET	1 AS NOTED
4	28227C	OUTER CAN	1 AS NOTED
5	34-7-F3	4 C.A. CATHODE ASSY.	1 BY P.C.A.
6	36136C	BOTTOM HEAT SINK	1 AS NOTED
7	36134C	THERMOCOUPLE SUPPORT	1 AS NOTED
8	36133C	EXTERNAL CAN	AS NOTED
9	36134C	BOTTOM EXTERNAL PLATE	1 AS NOTED
10	36136C	BOTTOM EXTERNAL TUBE	AS NOTED
11	28224C	LOWER BASE PLATE	1 AS NOTED
12	36126C	UPPER BASE PLATE	1 BY P.C.A.
13	36131C	BASE PLATE RING	1 AS NOTED
14	36131C	SPLIT CLAMP	1 AS NOTED
15	36126C	SPLIT SLEEVE	1 AS NOTED
16	36126C	HOSE CLAMP	1 304 S.S.
17	36126C	#4-40NC x 1/2 LG. RD. HD MACH. S.	4 BRASS
18	36126C	#3-48NC x 1/2 LG. RD. HD MACH. S.	6 BRASS
19	36126C	#5-40NC x 1/2 LG. LONG ZUP POINT SOCKET SET SCREW	3 304 S.S.
20	36126C	#0-80NF x 1/8 LG. RD. HD MACH. S.	6 304 S.S.
21	36126C	SPURKOFF DUAL LEAD TERMINAL # 95-5007	10 COMM'L.
22	36126C	#6WZPA EXTENSION WIRE (MINNEAPOLIS HONEYWELL)	10 COMM'L.
23	36126C	1/8 O.D. x .030 WALL TUBING	4 COPPER.

Figure 3-5. Components of Heat Transfer Assembly

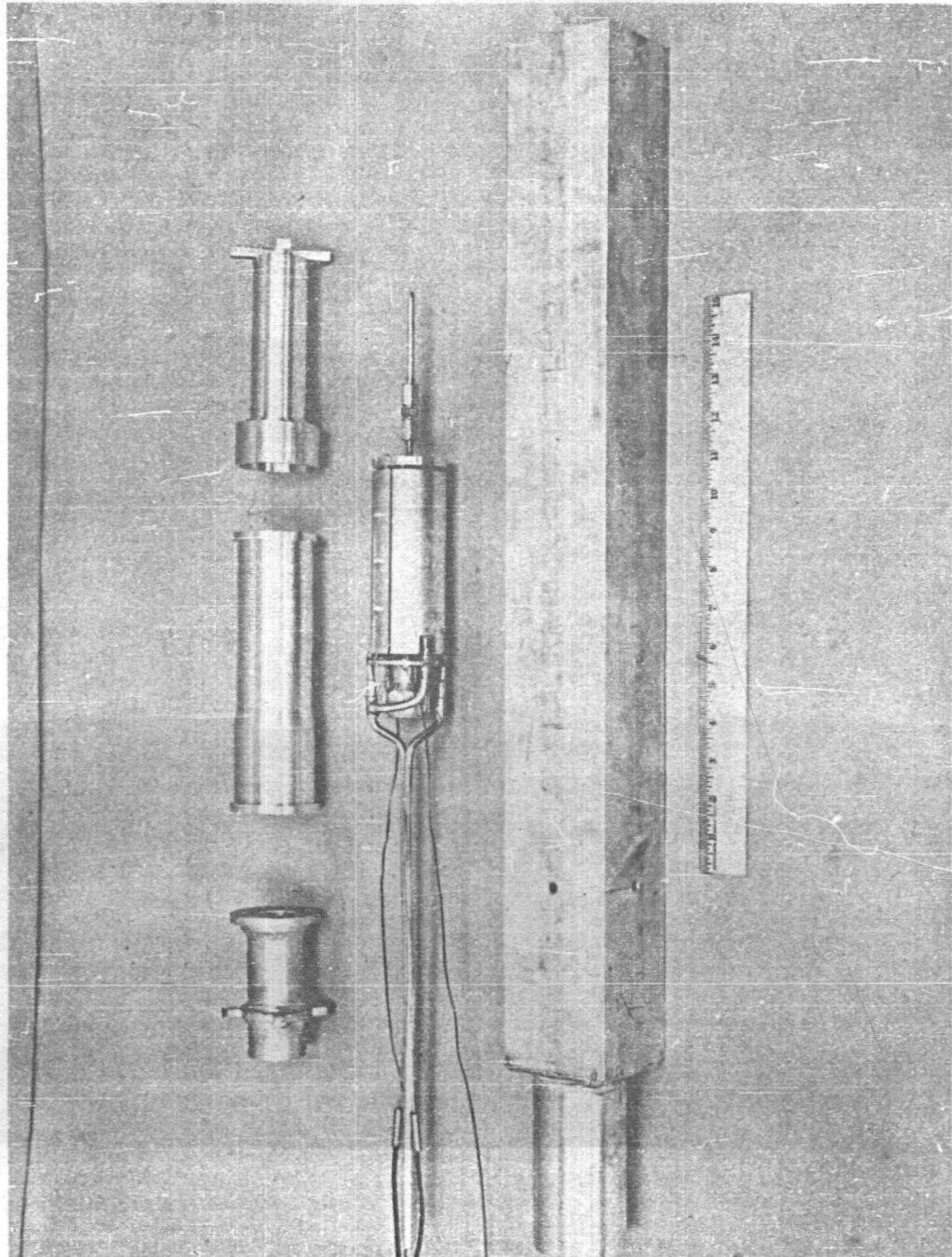


Figure 3-6. Installed Electric Heater

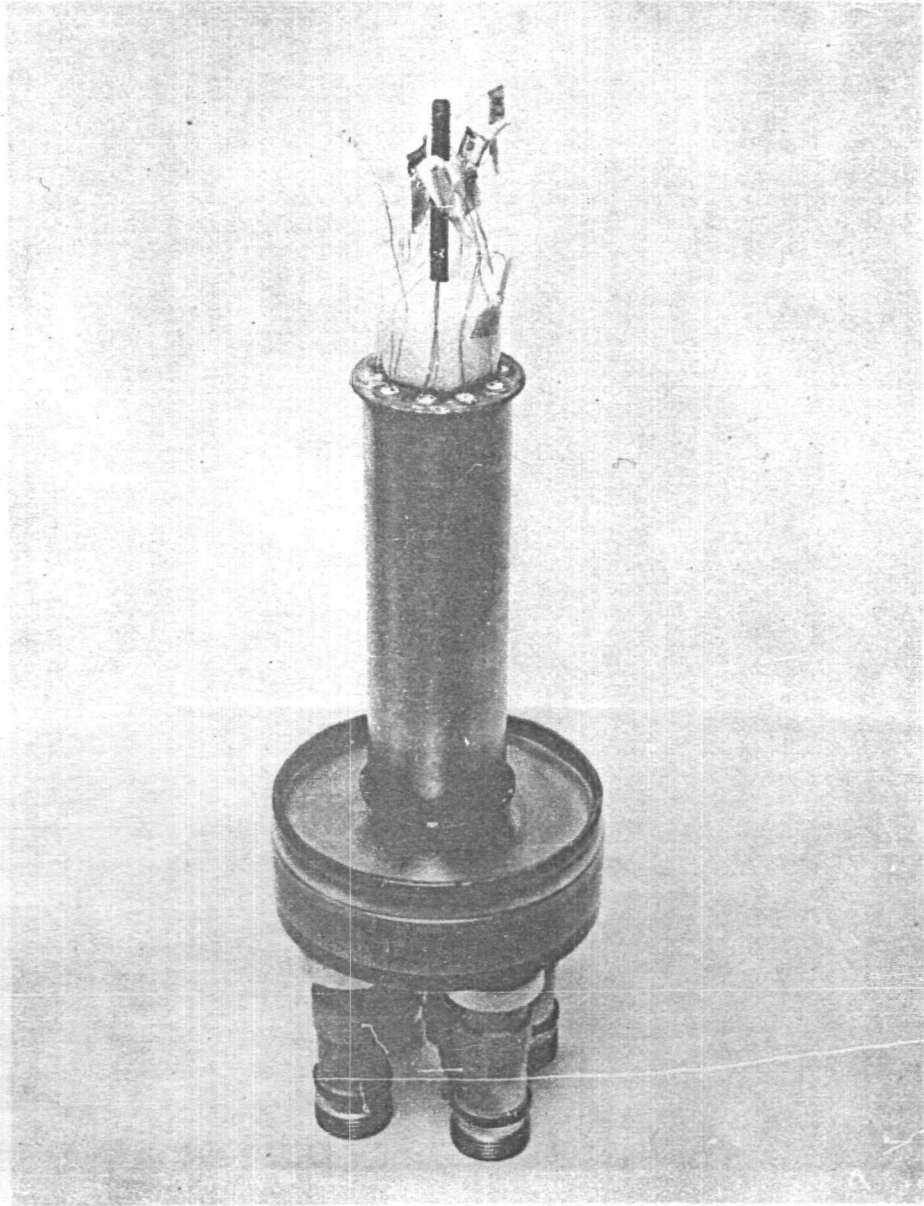


Figure 3-7. Device Input Power Vs Reactor Power for Inpile Heat Transfer Experiment Series 1

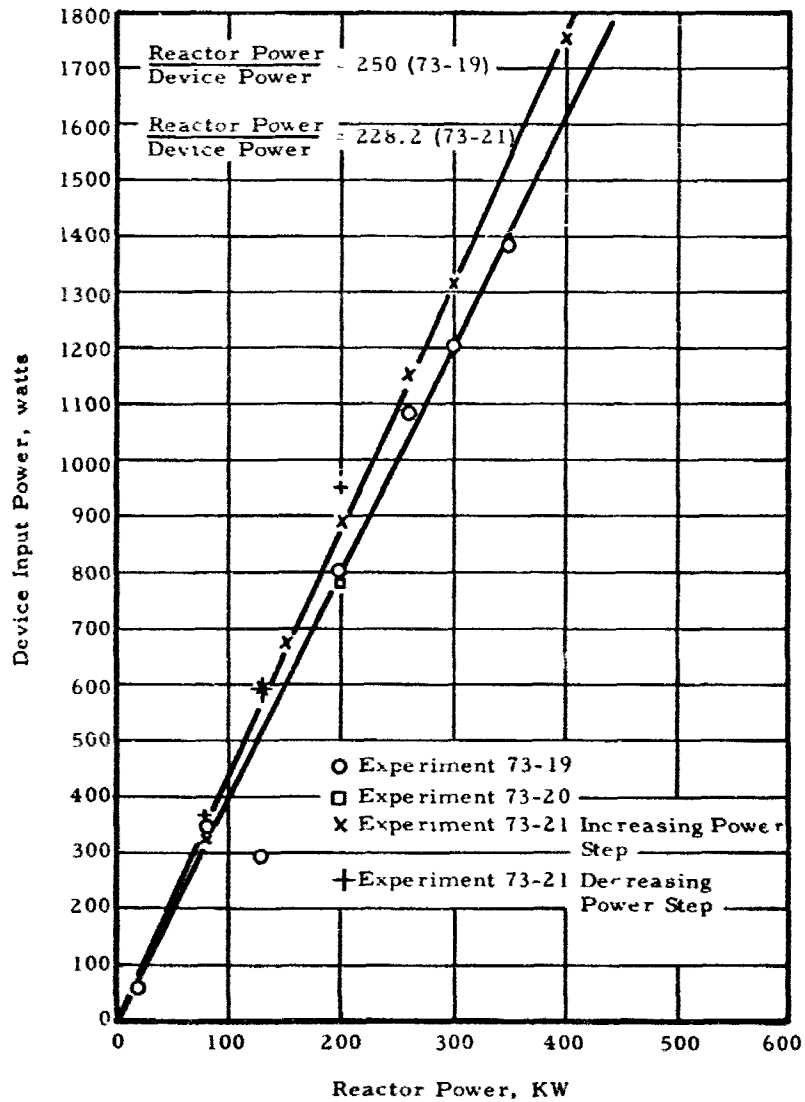


Figure 3-8. Emitter Temperature Distribution — Experiment 73-23

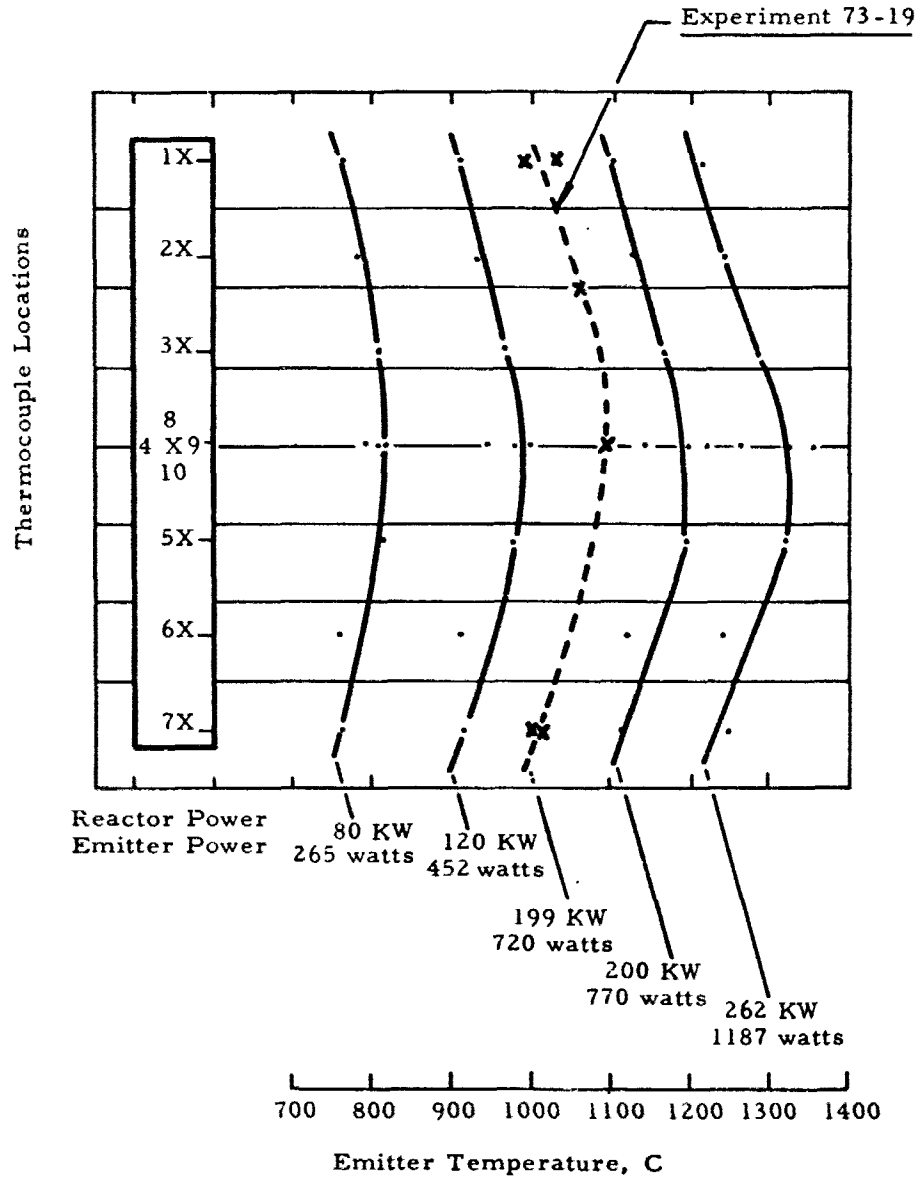


Figure 3-8 Emitter Temperature Distribution — Experiment 73-23

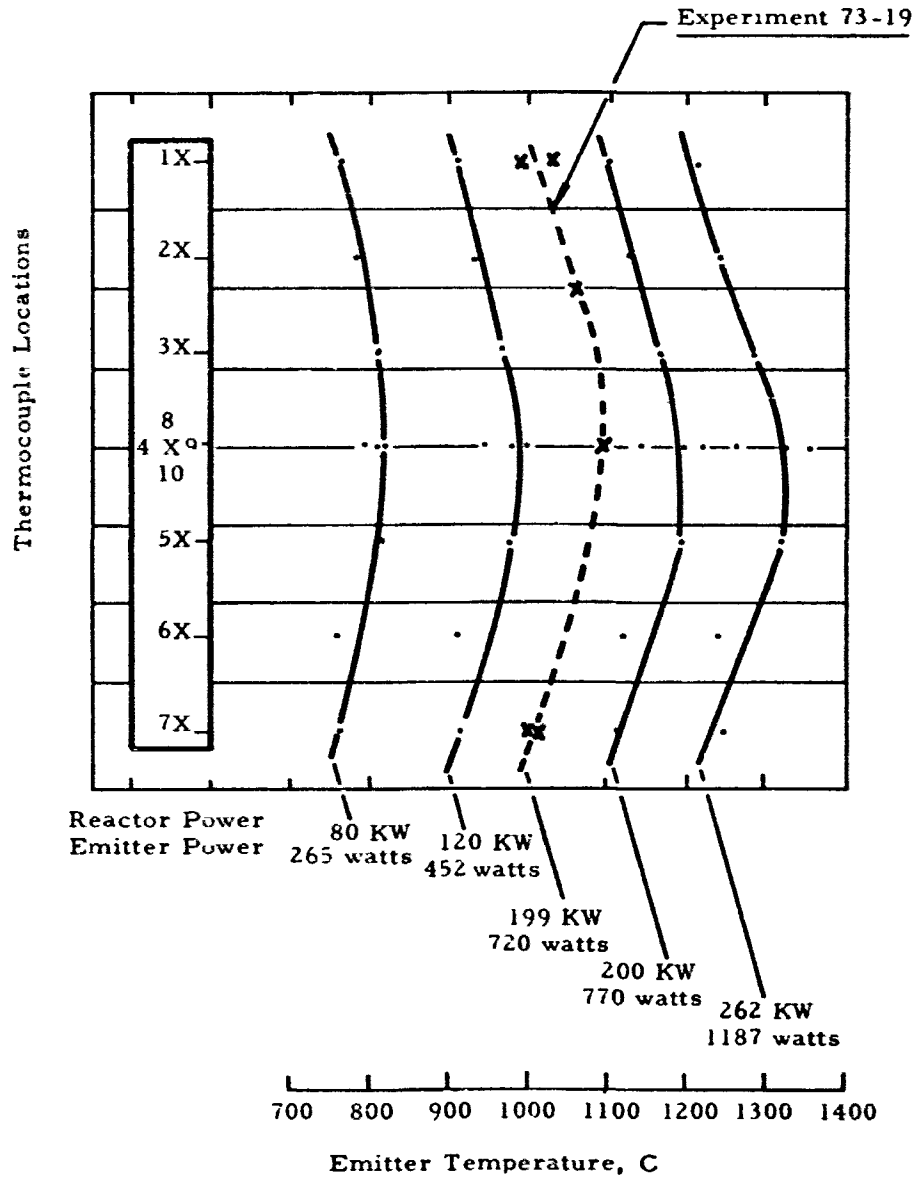


Figure 3-9. Emitter Temperature and Reactor Power Vs Time
(Experiment 73-23)

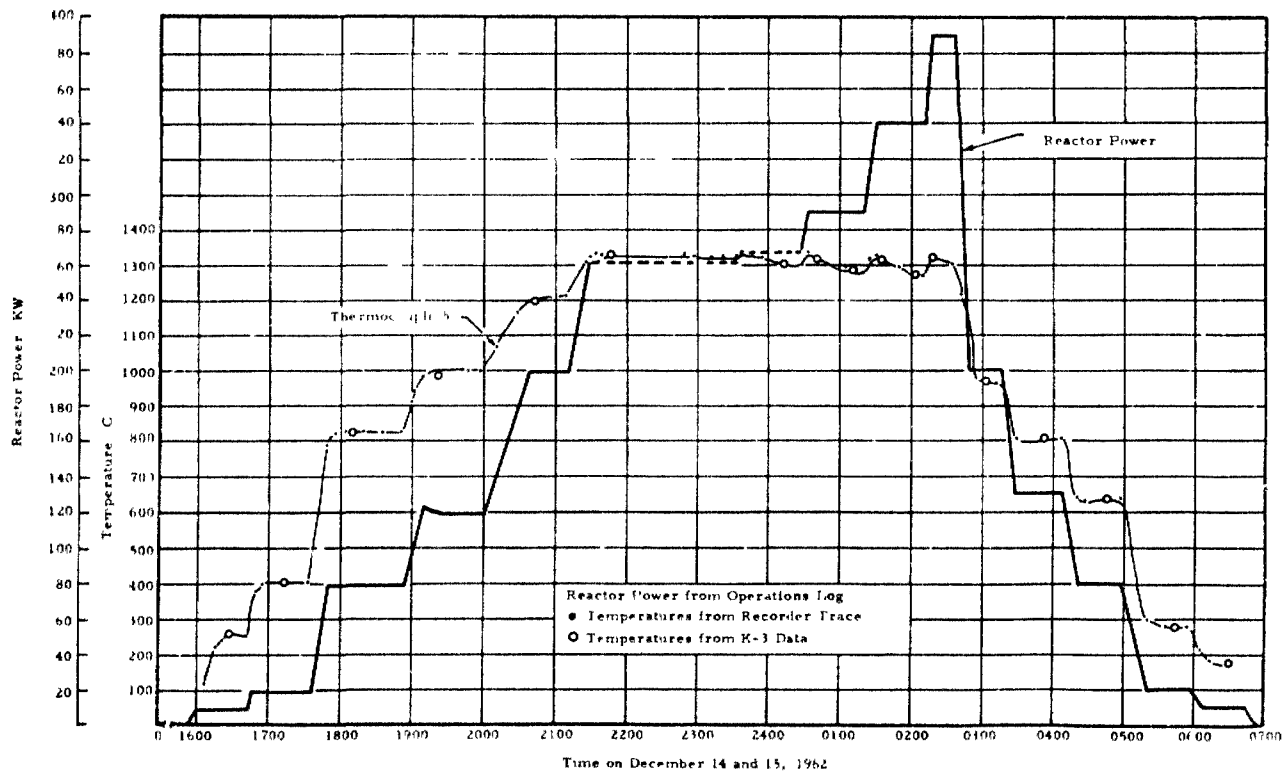


Figure 3-10. Device Input Power Vs Reactor Power for Inpile Heat Transfer Experiment Series 2

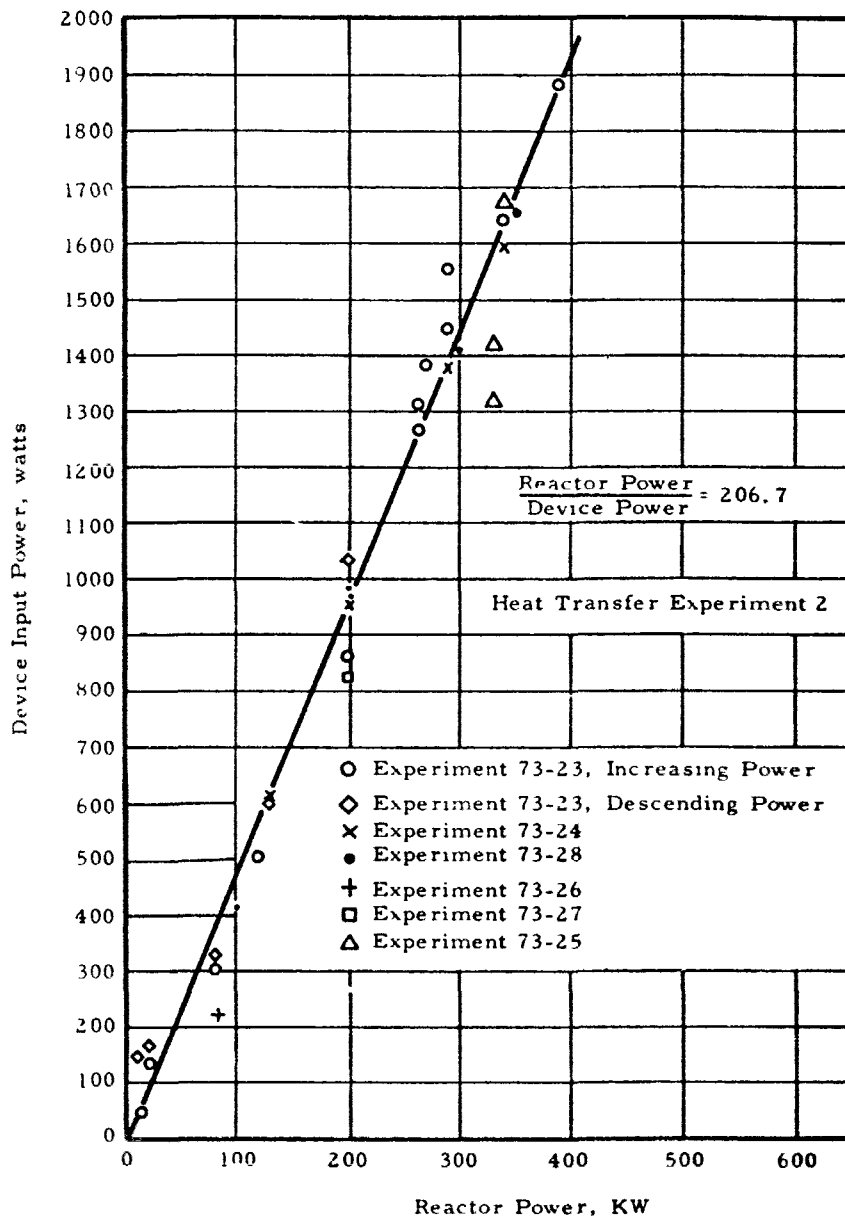


Figure 3-11. Plot of Heat Loss by Radiation for the Heat Transfer Experiment Assuming Perfect Emissivity ($e = 1$)

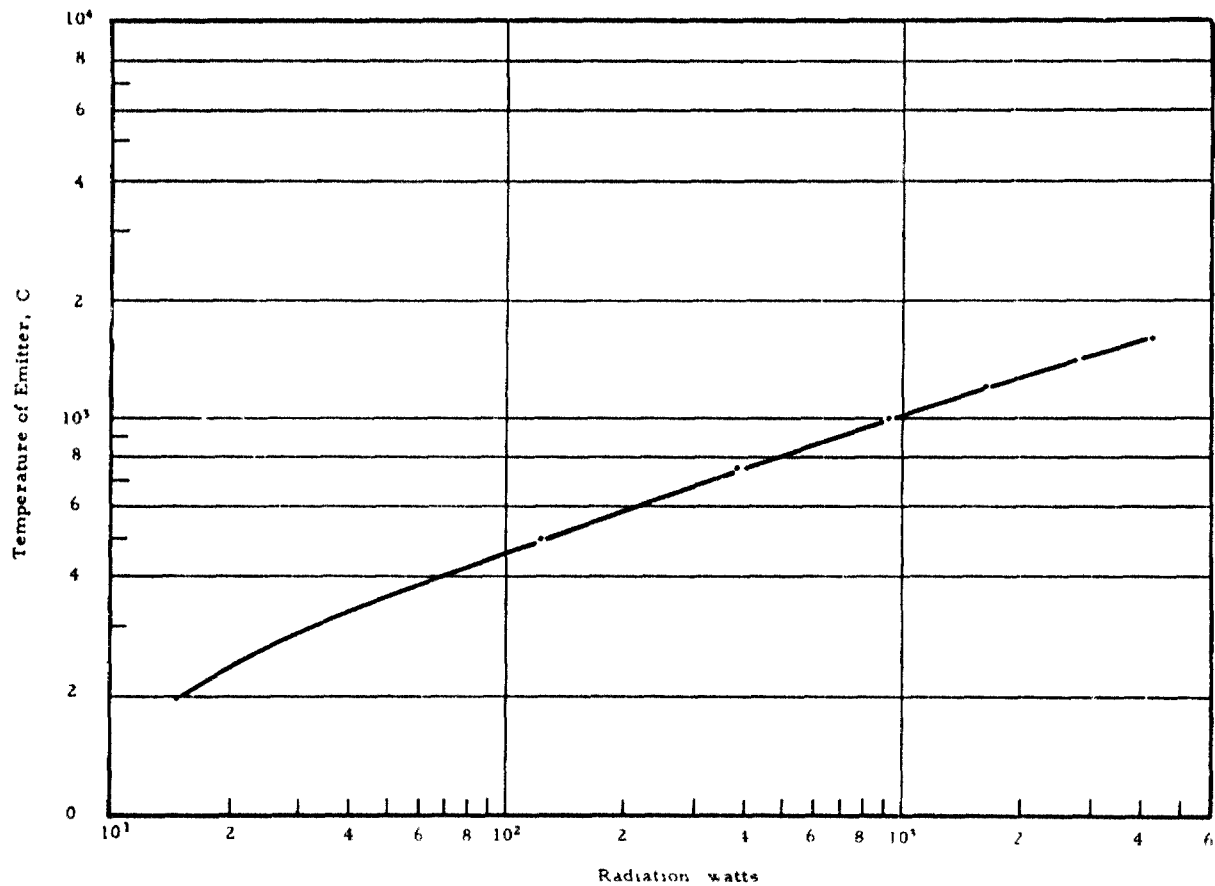
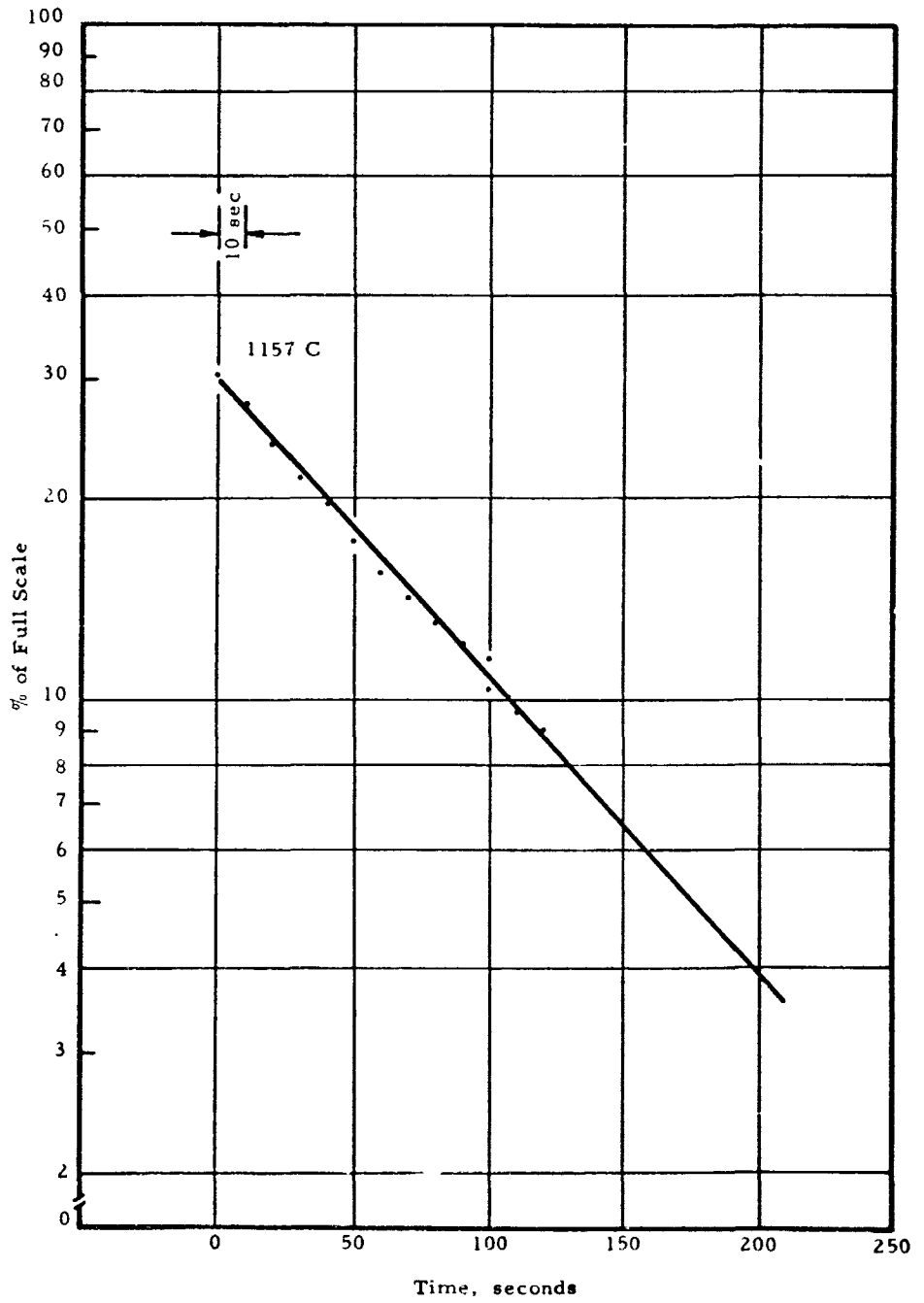


Figure 3-12. Temperature Plot of Thermocouple 5, Run 28, Scram from 350 KW



4. THERMIONIC CONVERTER EXPERIMENT

4.1. Introduction

4.1.1. Purpose

The purpose of the thermionic converter experiment was to operate a nuclear-fueled thermionic device in the Lynchburg Pool Reactor for a period of up to 100 hours. After successfully completing the required 100 hours operation, approval was received for continuing the inpile experiment an additional 200 hours. The additional 200-hour experimental period was also completed successfully.

4.1.2. Scope

The thermionic converter experiment was carried out in two steps. The first step consisted of the electrical testing of the converter using a heat sink design similar to that specified for use inpile. After the electrical tests were completed, the same device was fueled, sealed, outgassed, and installed in the inpile configuration. The device was then operated continuously for more than 300 hours using nuclear heat in the Lynchburg Pool Reactor. During this period the converter produced a maximum electrical output of 155 watts (2.58 watts/cm²) at a computed efficiency of 10.3%.

While some of the converter characteristics were evaluated during the 300-hour life test, additional experiments are required to more thoroughly investigate the thermionic converter performance in a nuclear reactor environment.

4.2. Design Description

4.2.1. Converter

The converter used for the inpile experiment, designated the RCA Developmental Converter Type A-1197A, is shown in Figure 4-1. A cross-sectional drawing is shown in Figure 4-2. The converter consists of a cylindrical emitter surrounded by a cylindrical collector. The

molybdenum emitter, containing the nuclear fuel, is supported at the bottom by a pin connected to a copper diaphragm, which in turn is connected to the side walls. The pin and diaphragm serve to support the emitter, to allow conduction of electrical energy, to minimize end conduction heat losses, and to allow for thermal expansion of the emitter. Fins on the pin reduce radiant heat losses. A cylindrical heat dam and support disc are located at the top of the emitter to perform the same function as that of the pin and diaphragm except that the support disc is rigid and allows no movement.

The cylindrical nickel collector has ceramic insulators at each end to insulate the collector from the emitter end structure. This construction results in a device which is electrically double ended. (Note the upper and lower emitter connectors of Figure 4-1.) Attached externally to the collector are stainless steel fins, which connect to a collector cooling sleeve. These fins conduct electrical energy and maintain the desired collector temperature by conduction to an external heat sink.

The copper pinch-off tube at the bottom of the device serves as the cesium reservoir and is surrounded by a heater and insulation. This arrangement allows the cesium vapor pressure to be controlled by varying the reservoir temperature. The fuel chamber cap at the top has an exhaust tube, radiative heat dams and a pinch-off cover.

The converter is designed to provide an output of 150 watts (2.5 watts/cm²) at 0.46 volts and 325 d-c amperes. This output requires an input of 1500 watts. Other design parameters are shown in the following lists.

Materials

Emitter	Molybdenum
Collector	Nickel
Nuclear fuel	UO ₂ , enriched 20% with U ²³⁵

Dimensions

Emitter	ID = 0.500 in. OD = 0.720 in. Height = 4.250 in. Active area = 60 cm ²
Fuel	OD = 0.492 in. Height = 4.100 in.

Temperatures

Emitter	1350 C
Collector	650 C
Cesium reservoir	300 C

The RCA Type A-1197A Converter contains a number of design changes from that of previous converters to permit proper operation of the device inpile. Two of the most important changes incorporated by RCA are the following:

1. Gas-cooled nickel collector fins were replaced by stainless steel collector fins. The increased thermal resistance made it possible to reduce the outer diameter as well as to maintain the desired collector temperature with a water coolant. A split-cooling-jacket heat sink similar to that used in the heat transfer experiments was used. The cooling jacket was machine fitted to the collector sleeve to minimize the contact resistance. The coolant lines served as the collector electrical leads.

2. The emitter connector fins were modified to permit the emitter connector to operate at the temperature of the water coolant and to pass the coolant lines from the collector cooling jacket. The emitter connector was bolted to the aluminum container to complete the electrical circuit and the thermal path to the heat sink for seal-temperature control. Since the connector fins were of light construction, they were not used to mechanically support the converter within the container.

4.2.1.1. Electrical Operation

Prior to the inpile operation the converter (RCA Type A-1197A, Number 36) was operated by RCA using an electrical heat source. The converter was operated at an electrical output of more than 150 watts. The collector- and emitter-connector-cooling water was on full and the cesium heater required 48 watts to maintain the proper cesium temperature. In addition to providing an operational checkout of the converter, the electrical tests provided performance data for later comparison with results obtained inpile. Following the inpile test, an additional converter (RCA Type A-1197A, Number 40) was electrically tested. In this test both the inpile and out-of-pile performances of converter 36 were duplicated. A comparison of the results of these tests is listed as follows:

Converter	Heat source	Power output, watts	Power input, watts	Converter temperatures, C*								
				1	2	3	4	5	6	7	8	9
36	Electrical	155	1460	560	495	585	370	505	525	315	300	--
36	Nuclear	155	1503	584	477	611	408	554	474	334	296	292
36	Nuclear	132	1503	599	490	617	418	564	480	354	331	327
40	Electrical	135	1269	620	540	620	385	505	520	400	325	--
40	Electrical	155.5	1344	655	570	650	410	535	550	420	315	--

* Thermocouple locations are shown in Figure 4-4.

4.2.2. Inpile Experiment Design

To simplify the description of the inpile experiment design, the assembly is divided into three sections:

1. The converter section.
2. The load section.
3. The dry pipe section.

4.2.2.1. Converter Section

The converter section consisted of the converter with cesium-heater assembly, an aluminum cooling jacket with coolant tubes, and an aluminum can. These components are shown in Figure 4-3. The converter was installed in the aluminum can by bolting the emitter connectors to two rings brazed to the can. Thus the can itself was at emitter potential. Figure 4-3 also shows the heater and thermocouple leads. Two cesium heaters were installed to insure reliable performance: Ceramic insulators were used on the heater leads; Fiberglas tubing was used to insulate the thermocouple leads.

4.2.2.2. Load Section

The load section consisted of an incore aluminum tube containing the inlet and outlet coolant lines and fittings that formed part of the electrical load. The incore tube was welded to the top of the converter-section aluminum can. Figure 4-4 is an assembly drawing of

the inpile experiment and shows the construction of the load section. Figure 4-5 shows the details of the component parts.

Part of the electrical load was placed inpile to minimize the size of the conductors brought to the top of the pool. The out-of-pile portion of the load contained a variable resistance leg so that the total load resistance could be varied externally.

The inpile load consisted of the two outlet coolant lines from the cooling jacket fastened through fittings to one-fourth-inch nickel tubes, whose length and thickness were adjusted to provide the proper resistance. The nickel tubes were then attached to two aluminum through-tubes which were welded to the incore tube. Welding the through-tubes to the incore tube completed a parallel internal electric circuit composed of the two outlet coolant lines. In addition, this arrangement provided the means for supporting the device, since it could not be supported by the emitter connector fins. Figure 4-6 is a photograph of the inpile load after the Fiberglas insulation was installed before the addition of the incore tube.

The two inlet coolant tubes from the cooling jacket formed part of the external load. These tubes were attached by fittings to copper tubes that were brazed into a heavy-wall copper pipe extending through the dry pipe to the top of the pool. Figure 4-4, the assembly drawing, shows the out-of-pool portion of the load. The variable portion of the load consisted of a length of one-fourth-inch stainless steel tubing. The effective length could be changed by shorting across the tube with a copper conductor. The dry pipe formed the return lead of the external load.

Figure B-9 in Appendix B is a diagram of the load contained within the incore tube and lists the voltage measurements used to determine the inpile load resistance. Figure B-10 in Appendix B is a diagram of the out-of-pool portion of the load and lists the voltage measurements for this configuration.

The inpile load resistance was designed to be approximately $1.5 \times 10^{-3} \Omega$ shared equally between the parallel inpile loads formed by the outlet coolant tubes. The external load was designed to be variable between $2 \times 10^{-3} \Omega$ and infinity. This gave a range of $0.86 \times 10^{-3} \Omega$ to $1.5 \times 10^{-3} \Omega$ plus the contact resistance between collector

and jacket and between emitter connector and can. Current and voltage measurements taken during converter operation indicate the load could be varied between $\approx 0.96 \times 10^{-3} \Omega$ and $1.66 \times 10^{-3} \Omega$.

To measure the current through the inpile load, voltage taps and thermocouples were placed on the two calibrated nickel load tubes. The calibration consisted of accurately determining the variation of resistance with temperature. Load 1 was calibrated for resistance versus thermocouple emf from about 28 to about 62 C. Load 2 was calibrated for resistance versus thermocouple emf at about 28 C. Figure B-8 in Appendix B is a summary of the calibration measurements. The calibrated portion of the external load was found to have a resistance of $0.0645 \times 10^{-3} \Omega$ at room temperature.

4.2.2.3. Dry-Pipe Section

Since only part of the electrical energy was brought out-of-pile, the size of the electrical conductors was minimized and a dry-pipe design was used. A 15-foot-9-inch aluminum pipe was welded to a top plate on the incore tube and extended 2 feet 8 inches above the pool. The pipe contained the inlet coolant line (a heavy-wall copper pipe), thermocouple extension cable, voltage leads, and two helium gas lines. A plastic clamp was used to support the coolant line at the top of the pipe and Fiberglas was used to insulate the coolant line from the pipe along the length. The top of the dry pipe was sealed with epoxy. Figure 4-4 is an assembly drawing showing details of the dry-pipe design.

4.2.3. Assembly

The following paragraph briefly describes the assembly of the converter experiment for inpile operation.

Figure 4-7 shows the first step in the assembly of the experiment, the addition of the nuclear fuel to the converter. The fuel-chamber end-cap assembly was then welded on and the device was outgassed at 300 C. Details of the fuel and device outgassing are included in Appendix B. The device was pinched-off from the vacuum system at a pressure of 4×10^{-6} . After the device instrumentation was added, the converter was installed in the aluminum can as shown in the sequence of Figure 4-3. The aluminum coolant tubes were cut to length and the load section was mated to the converter section. All electrical connections were made

and the three sections (the converter section, the load section, and the dry pipe section) were welded together. Figure 4-8 illustrates the remaining steps in the assembly. A square aluminum box welded to the incore tube was used to position the assembly in an empty reflector can. After connecting all coolant and helium gas lines, the assembly was leak tested and installed in pile.

4.2.4. Instrumentation

The basic on-device instrumentation consisted of nine thermocouples and two voltage taps, which were located as shown in Figure 4-4. In addition, metal-sheathed thermocouples were installed in the inlet and outlet coolant lines, and thermocouples and voltage taps were installed on each of the calibrated load tubes.

The monitoring instrumentation consisted of two L&N 12-point recorders for continuous monitoring of temperature and emf data and a Type K-3 potentiometer for precise, periodic measurements. Selector switches were arranged to allow any single emf to be disconnected from the recorder and measured on the potentiometer. Meters were also connected to display the device voltage and current through one of the inpile loads. Since one voltmeter loaded down the reading, the voltmeters were switched out of the circuit when the potentiometer was read.

The cesium heater used a 0-18 volt, 10-ampere, filtered d-c power supply. The a-c input also had variable control. Resistors were placed in the output circuit to allow the voltage and current to be continuously monitored by a 0-10 milliampere recorder.

4.2.5. Coolant Circuit

Figure 4-9 is a schematic diagram of the water coolant circuit, including flow-monitoring equipment and the loss of flow alarm. The accurate measurement of cooling-water flow was essential to determine reliable power input data. Measurements of total flow and flow from each outlet line were made. A plot of this data is found in Appendix B. Measurements during calibration and during the 300-hour run at 1000 on January 17, 1963, result in a ratio of load flow to total flow of 0.455 for Load 1 and 0.545 for Load 2. Since only total flow was measured during device operation, it was later necessary to correct for the non-uniform flow distribution.

After the power run it was found that the flow regulator was jammed in a manner which prevented good flow regulation. The power input data at low flow rates was much more accurate than at the higher flow rates.

4.2.6. Helium Circuit

A system to flow helium into the experimental assembly was used. The basic purpose was to provide an inert gas to reduce oxidation of converter parts and exclude air from the high-flux region. During the experiment the helium circuit was used on one occasion to cool the cesium reservoir. Figure 4-10 is a schematic diagram of the arrangements.

The helium flow rate was not used in any calibration. However, a measurement of flow versus pressure in the experimental thimble was considered meaningful. These flow rates and their corresponding pressures are listed as follows:

<u>Flow rate,</u> cfh	<u>Pressure,</u> psig
1	2.0
2	4.5
3	7.0
4	9.0
6	13.0
8	15.0

4.3. Inpile Experiment Operation

The actual operation of a thermionic device using a nuclear heat source met the planned experimental objectives. The device produced a maximum of 155 watts of electrical output (2.58 watts/cm²) at a computed efficiency of 10.3%. It operated for 250 hours at an average output of 132 watts. It ran for a total of more than 300 hours, although the last 50 hours were at a somewhat reduced output. During the power run, the device produced approximately 38 kWh of electrical energy.

4.3.1. Prestartup Phase

On January 14, 1963, the inpile assembly was loaded into the center hole of the Lynchburg Pool Reactor, Core 143. All water and

helium circuits were connected and checked out. The reactor was then brought critical and leveled off at 1.3 watts. From the position of the rods, it was established that the device assembly had no effect on the reactivity of the reactor. That is, the addition of fuel and the removal of water from the experimental space added enough reactivity to compensate for the reactivity loss due to the presence of poisonous materials in the device.

The excess reactivity available in Core 143 was about 1.00% $\delta k/k$. Since the xenon reactivity effect during the run was expected to be greater than this value, a partial fuel element (95 grams U^{235}) was replaced by a full fuel element (190 grams U^{235}). This configuration was designated Core 144. The reactor was brought critical again and found to have an excess reactivity of 2.69% $\delta k/k$. Figure 2-1 is a cross section of Core 143.

4.3.2. Summary of Operation, Startup and Shutdown

The inpile converter experiment began at 1113 on January 15, 1963. The reactor reached a power level of 1 KW but was scrammed during an instrumentation adjustment. The reactor was then restarted, and the power level increased in steps to 1 KW, 10 KW, 80 KW, and 120 KW. Data were taken at each power level. The reactor power was then slowly raised (in 1 hour) to 225 KW. As may be seen in Figure 4-11, there was a small electrical output at this reactor power as the cesium temperature was raised. The reactor power was raised to 285 KW and a sharp rise in electrical output power was noted. The reactor power was then increased in successive steps to 430 KW by 2016. Figure 4-12 contains a plot of reactor power, device input, and device output versus time for the complete run. The reactor power was eventually increased to 520 KW for most of the run. The average device output power during the 520-KW operation was 132 watts.

A special experiment showed that the device output could have been 155 watts or higher for the entire run had the means been available for continuously cooling the cesium reservoir. After 250 hours the device power output began falling slowly. The reactor power was lowered to 500 KW after 275 hours and remained there until just before shutdown, when the power was adjusted to a maximum of 553 KW. The reactor was

shut down in successive steps with the device output power going to zero at a reactor power level of 225 KW.

Figure 4-13 shows the positions of shim rods as a function of time. By January 19 the xenon poisoning level was about 1.75% $\delta k/k$ for an excess reactivity of 0.94% $\delta k/k$.

4.3.3. Startup Phase (Reactor Power 0-430 KW)

The most significant aspect of the startup of the thermionic device with nuclear heat was the extremely smooth starting characteristics.

Figure 4-11 gives the reactor power, output emf, and cesium reservoir temperature versus time. There was a low level peak in output voltage at about 1805 while the reactor power was 225 KW and the cesium reservoir temperature was 228 C. This peak was probably the result of residual cesium in the device. As the cesium reservoir temperature was raised, the device output fell and then rose slightly. At 1821 the reactor was again put on a positive period. At 1828, with the reactor on period at 280 KW and a cesium temperature of 255 C, the device output rose smoothly in about 1.5 minutes to about 34 watts. As the reactor power rose to 285 KW, the electrical output remained at approximately 34 watts with irregularities. At 1912 the reactor power was raised to 355 KW. The cesium temperature increased to 295 C and the electrical output rose to about 69 watts. The reactor power was then increased to 430 KW. The cesium temperature rose to 335 C and the device electrical power increased to 104 watts. From the curve (Figure 4-11) it may be observed that the power was actually a little higher before the cesium temperature reached a maximum. The fact that the cesium temperature was not optimized is discussed in Section 4.3.6.

4.3.4. Intermediate Phase

By 2015 on January 15 it was apparent that the device was running well and responding properly to changes. The startup phase was therefore over, and the device was ready for optimizing. The first experiments to optimize the device output were performed at a reactor power level of 430 KW. This intermediate phase lasted from 2015 on January 15 until 0530 on January 16, when the reactor power was 520 KW. The experiments performed in the intermediate phase involved the changing of cesium temperature, load resistance, and reactor power. Section 4.3.6 describes

each experiment along with similar experiments during other phases. Figures 4-14 through 4-16 illustrate these changes. The reactor power was then raised to 470 KW and the cesium heater was turned off. Under these conditions the device was producing about 127 watts with a cesium temperature of 334 C. The reactor power was then increased to 500 KW and a cesium temperature change was made. The intermediate phase ended with the device producing an electrical output of about 134 watts at a cesium reservoir temperature of 343 C.

4.3.5. Steady-State Phase

The steady-state phase from 0530 on January 16 to 1630 on January 26 covered most of the 300-hour operation. During this period the reactor power was raised to 520 KW (Figure 4-17), the cesium temperature was varied, and an experiment was performed (Section 4.3.6.2) by cooling the cesium reservoir with helium. The 155 watts obtained for a cesium temperature of 294 C was the maximum electrical power output from the device. This maximum output required no increase in input power. The average output power for this phase was 132 watts.

4.3.6. Device Parameters

The proper representation of device performance would include a family of curves involving the available variables. After the need for additional helium to cool the cesium reservoir became apparent, it was decided to wait until the end of the 300-hour run to develop these curves. The lowering of output, which defined the end of the steady-state phase, made the value of such a study much less important than a post-irradiation examination. It was therefore decided to eliminate additional tests rather than to compromise the examination.

However, a number of tests were performed during the power run. They were performed over a long period of time, which makes the separation of variables more difficult. The results of these tests are described in the following paragraphs.

4.3.6.1. Device Power Output and Input

The converter electrical output power is the current times the output voltage. As discussed in the description of the inpile load (Section 4.2.2.2) the current values were obtained from voltage measurements of the calibrated nickel load tubes. The emitter-to-collector voltage was measured directly.

The device input, however, could not be measured directly. The power sharing and heat transfer experiments supply some information about the power input to the device as a function of reactor power, but the converter assembly was sufficiently different from the original mock-ups to prevent an accurate power determination from these measurements. Therefore it was necessary to depend on calorimetric measurements, calculations, and electrical test data to determine the nuclear heat input. These calculations provide a power balance of:

$$\begin{aligned} \text{Input} &= \text{Output} \\ &= P_c + P_e + P_o - P_\gamma \end{aligned}$$

where

P_c = power dissipated in the collector cooling water by the collector and inpile loads, determined calorimetrically = 3.15 watts/KW reactor power

P_e = power lost out of the ends of the emitter and dissipated through the emitter connectors to the pool water

$$= \frac{(T_{\text{Top}} - 18 \text{ C})}{462 \text{ C}} \times 150 \text{ watts}$$

The basis for this correction is included in Appendix B.

P_o = electrical power dissipated in the out-of-pile load = $V_{ca} \times I_o$

P_γ = power added to the collector and cooling circuit by γ heating = 0.53 watts/KW of reactor power. This heating rate is based upon the measured weight of the collector and heat sink components between the points at which temperature measurements were made. An effective weight of 1065 grams was used, which reflects a correction for the gamma heating distribution. The maximum heating rate at the midplane is 0.5 watts/gm per MW of reactor power.

The fact that the actual input power is the result of several calculations has led to the use of the term, computed efficiency, for the ratio of electrical power output over thermal power input (Figure 4-18).

4.3.6.2. Cesium Vapor Pressure Variations

One of the most important parameters affecting device performance was cesium vapor pressure. This was controlled by keeping the reservoir at the proper temperature to give the desired vapor pressure. Figure 4-19 shows the variation of vapor pressure with temperature.

The most important observation about cesium during the experiment was that gamma heating and insulation kept the cesium temperature almost always too high. There are several notable examples of this. It is quite apparent in Figure 4-12 at 2000 on January 18 and in Figure 4-11 at 1922 and 2007 on January 15. The first example shows a very marked improvement in output from a deliberate experimental cooling of the reservoir. The next examples show declines in output as the cesium temperature increases following reactor-power increases in the startup phase.

Data taken from the charts and log book at different times during the startup and intermediate phases show that the optimum cesium temperature was always less than 320 C. At maximum electrical power output, the optimum cesium temperature was very close to 294 C as shown in Figure 4-22.

During the device-power reduction phase described in Section 4.3.7, the optimum cesium temperature changed with time. Figure 4-32 reflects this change. At about 1100 on January 27 the optimum cesium temperature was approximately 326 C. At 0330 on January 28 it had progressed to 337 C. By 0800 on January 28 it had increased to about 350 C.

4.3.6.3. Variation of Output With Load Changes

During the intermediate and steady-state phases the load was varied from 1.25 to 1.45 milliohms. From the information available (Figures 4-14, 4-15, 4-16, 4-25) the optimum load appears to be about 1.41 milliohms. Figure 4-26 represents data taken during the power-reduction phase. A definite power reduction occurred while the data was taken. The optimum at that time was about 1.45 milliohms.

4.3.6.4. Device Temperatures

For all phases of the operation from startup to shutdown, Table B-5 in Appendix B lists the temperatures from the nine thermocouples located as shown in Figure 4-4.

The steady-state phase produced the following temperatures (centigrade) at the indicated locations:

	<u>No cooling</u>	<u>Maximum helium cooling</u>
Upper emitter	480	474
Upper seal	490	477
Collector (maximum)	617	611
Lower seal	418	408
Lower emitter	354	334
Cesium reservoir	329	294

4.3.7. Device-Power Reduction Phase

Soon after 1630 on January 26, which represented 250 hours of operation, the output of the device became slightly irregular. This irregularity progressed with time so that by 0213 on the 27th the power was down to less than 120 watts (Figure 4-27). This continued in small reductions until 0915. The electric power then fell from 118 watts to 100 watts (Figure 4-28) in 4.5 minutes. The reactor power was then reduced to 500 KW bringing the device output down to 84 watts.

The following symptoms were noted.

1. The electric power reductions took place quickly at apparently random intervals.
2. All power reductions seemed to be preceded by slight, slow power gains.
3. Most power reductions were followed by a slow partial recovery.
4. Early power reductions showed no accompanying temperature changes.
5. During later power reductions the collector temperatures tended to rise slightly and the emitter end temperatures tended to fall slightly.
6. The optimum cesium vapor pressure increased as the power output of the tube decreased.

7. The electric power output continued to respond to changes in reactor power.
8. Emitter end temperatures did not rise as the output fell, implying that the emitter temperature did not rise.

4.3.8. Shutdown Phase

The shutdown and device-power reduction phases were similar since the power reductions continued through the shutdown phase. This phase started at about 0720 on January 28. The first action was to lower the reactor power to match the device-output response (Figure 4-29). After establishing that the device output followed reactor power, it was decided to optimize total output prior to the end of the experiment.

It is interesting to note that, when the reactor power was increased to 528 KW at 0742 on January 28, the output power was 100 watts, just as it was prior to reducing reactor power from 520 to 500 KW at 0920 on January 27. The difference was that the cesium temperature was 327 C on January 27 compared to 350 C on January 28.

The reactor power was increased to as high as 553 KW bringing the device-power maximum for that day to 109 watts. Figure 4-30 gives the response as the reactor was shut down, with all electrical output ceasing when the reactor reached 225 KW at 1307 on January 28.

4.4. Postoperation Analysis

The operation in the nuclear environment was extremely smooth for more than 250 hours. Although the average steady-state power was 132 watts, the device would have operated as well at an output of over 150 watts with cesium reservoir cooling.

A complete analysis of the power reduction is impossible without having the results of a hot-cell examination of the converter. Such an examination is planned.

Figure 4-1. The RCA Converter, Type A-1197A, With Cesium Heater Assembly

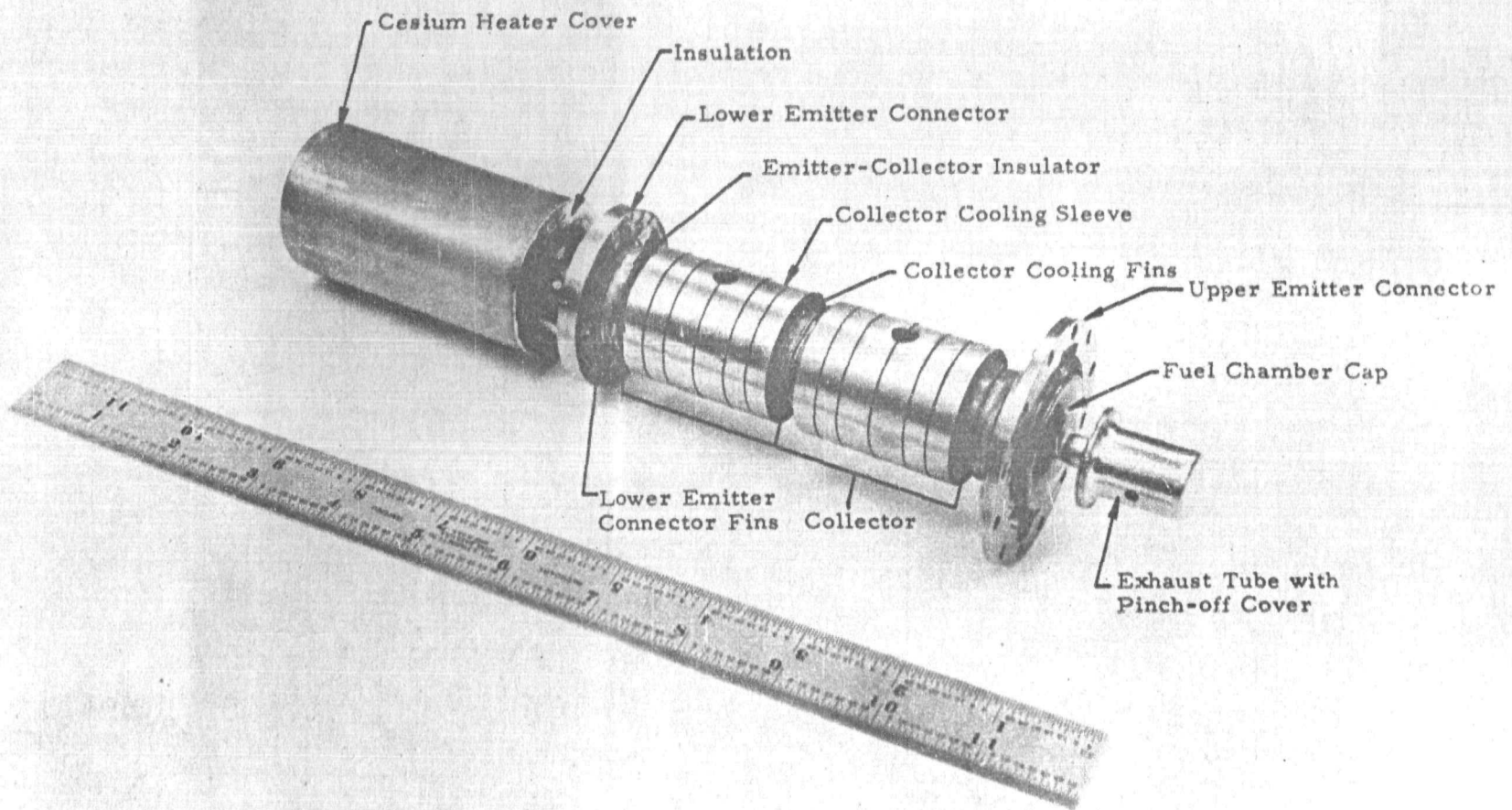


Figure 4-2. Sectional View of the Type A-1197A Converter

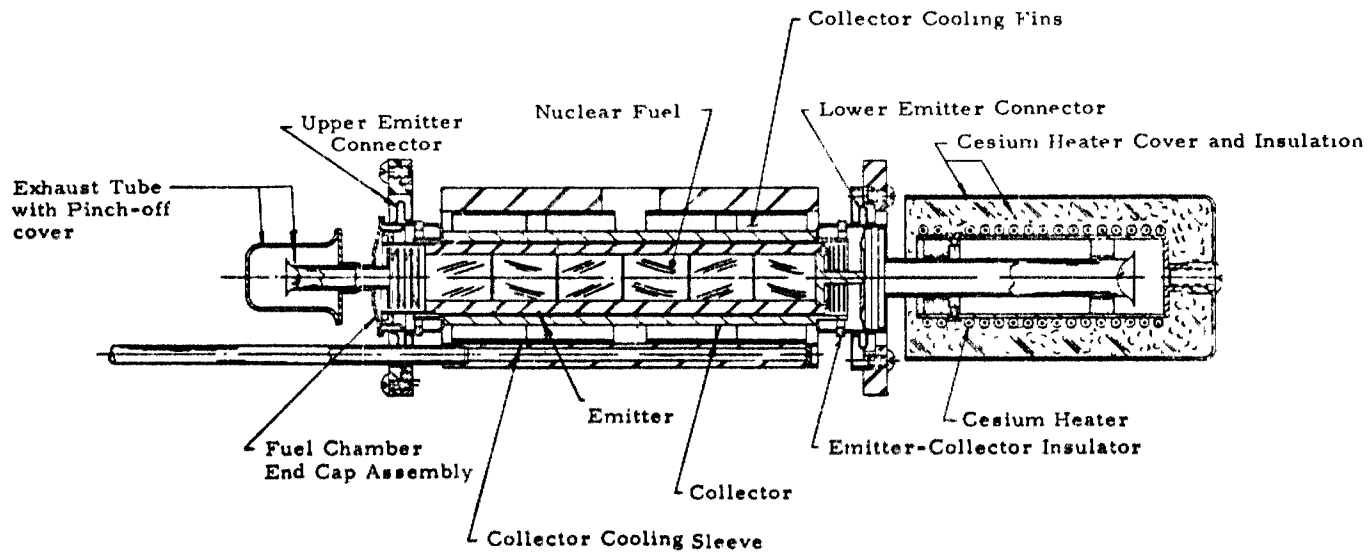
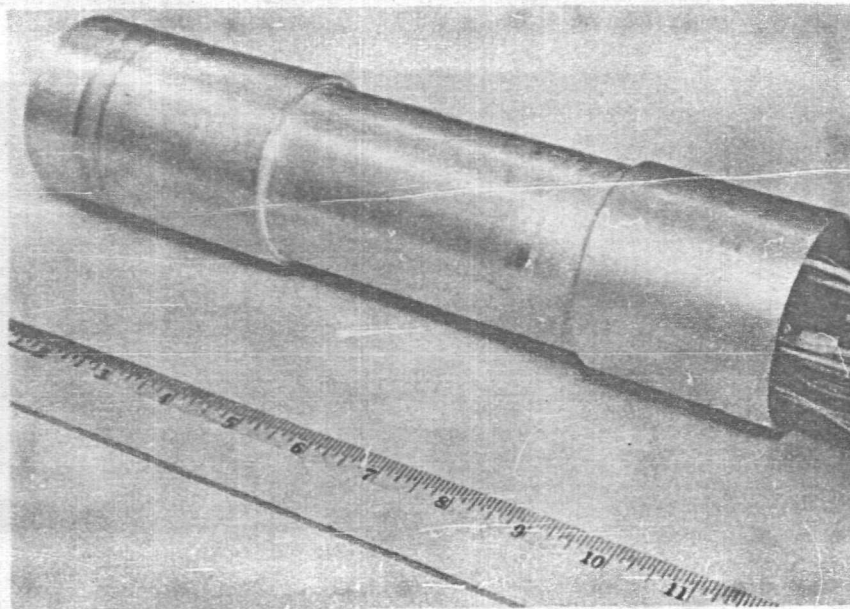
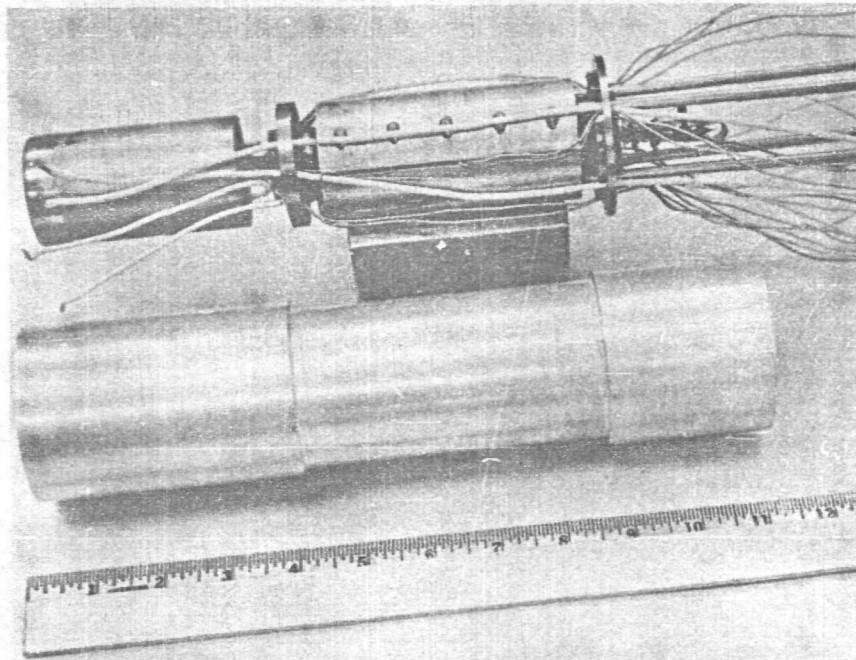


Figure 4-3. Converter Section Assembly



1

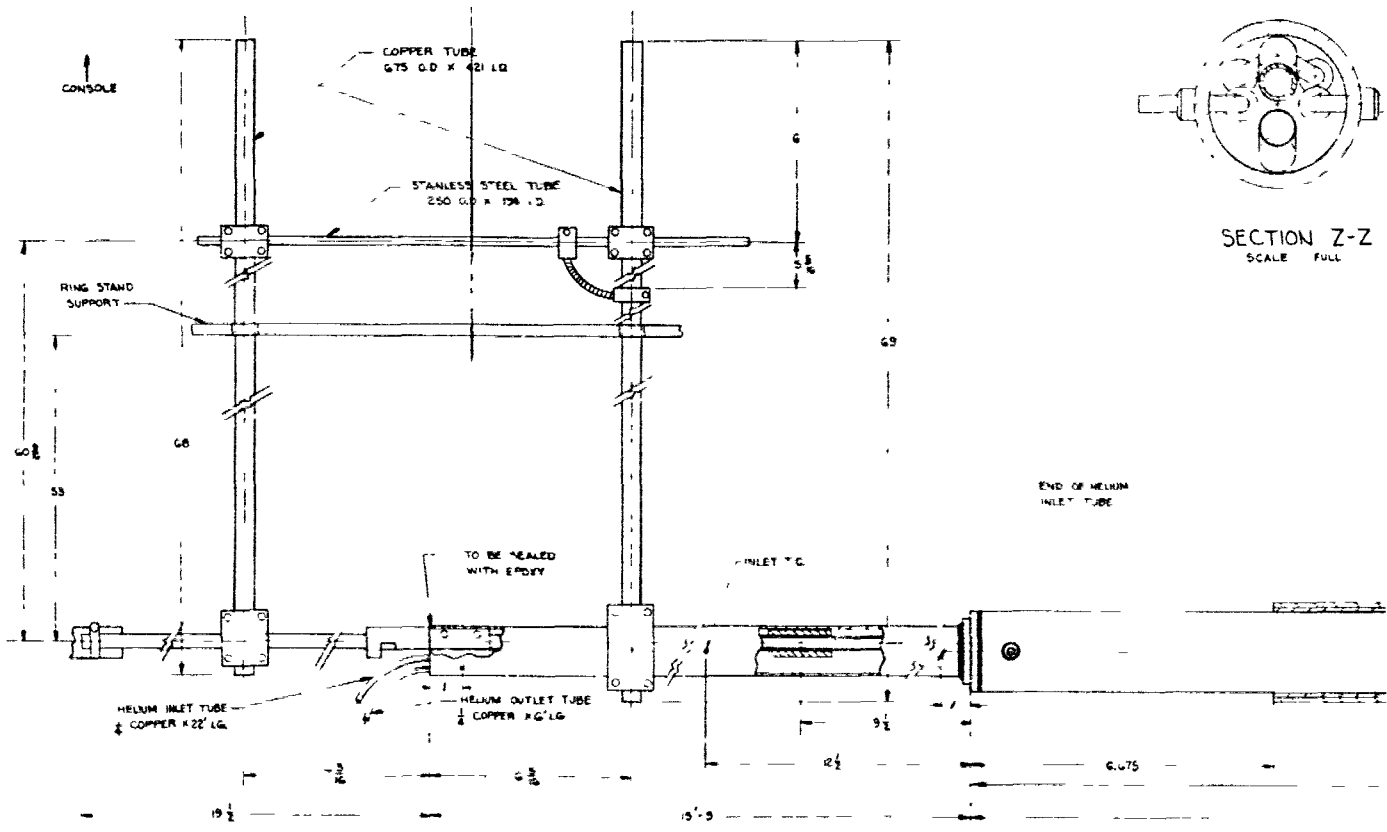
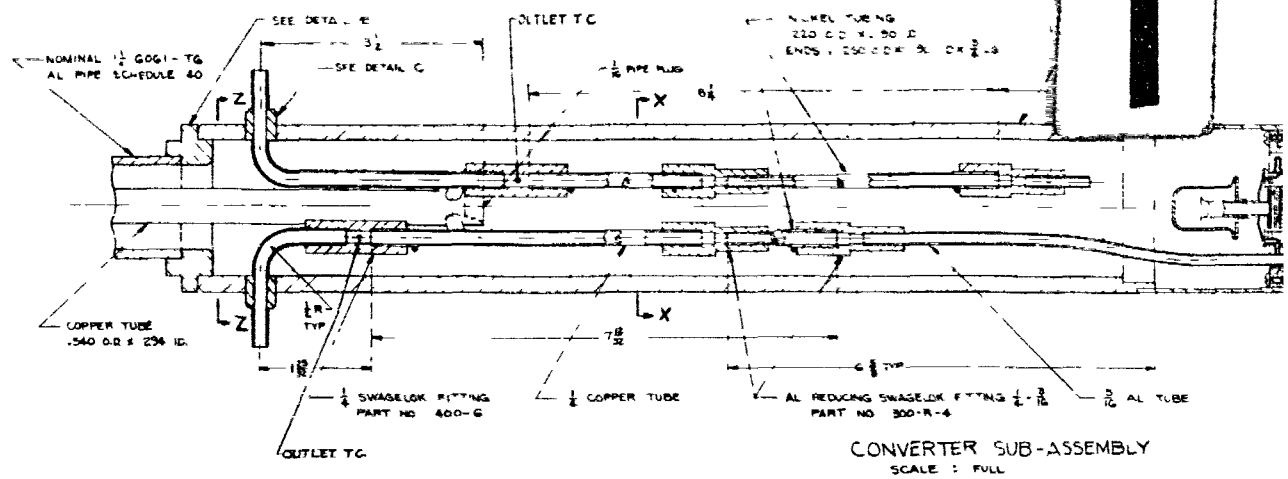
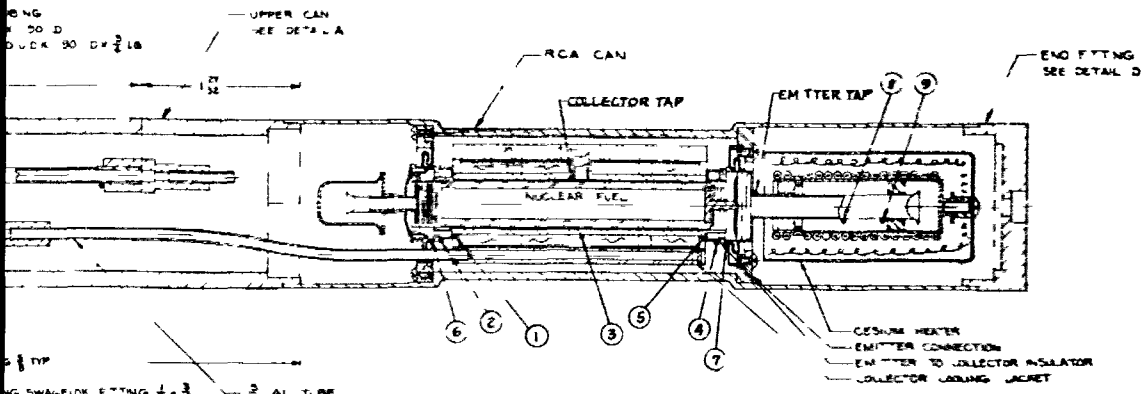
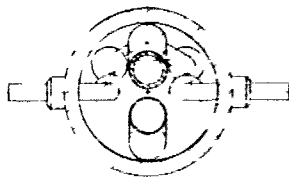


Figure 4-4. Thermionic Converter Experiment Assembly

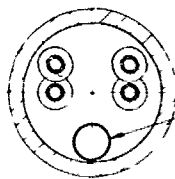


2

CONVERTER SUB-ASSEMBLY
SCALE FULL



SECTION Z-Z
SCALE FULL



SECTION X-X
SCALE FULL

500 THERMOCOUPLE LEAD

NOTES

1. TOLERANCES UNLESS OTHERWISE SPECIFIED -
 DECIMALS - $\pm .005$
 FRACTIONS - $\pm \frac{1}{32}$
2. SEE REF DRAWING DM-259 FOR DETAILS.

- THERMOCOUPLE LOCATIONS
- ◆ VOLTAGE TAP LOCATIONS

END OF HELIUM
IN TUBE

HELIUM OUTLET TOP OF SAW PLATE

0.75

0.7

12.075

1

HERMIONIC CONVERTER ASSEMBLY
SCALE 6"=10"

Figure 4-5. Component Parts of Inpile Experiment

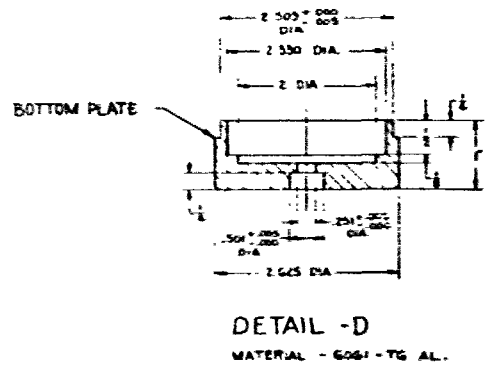
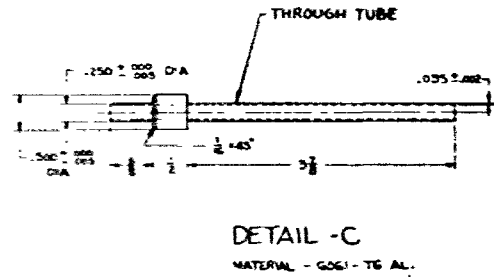
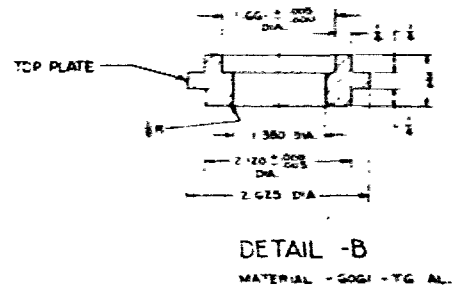
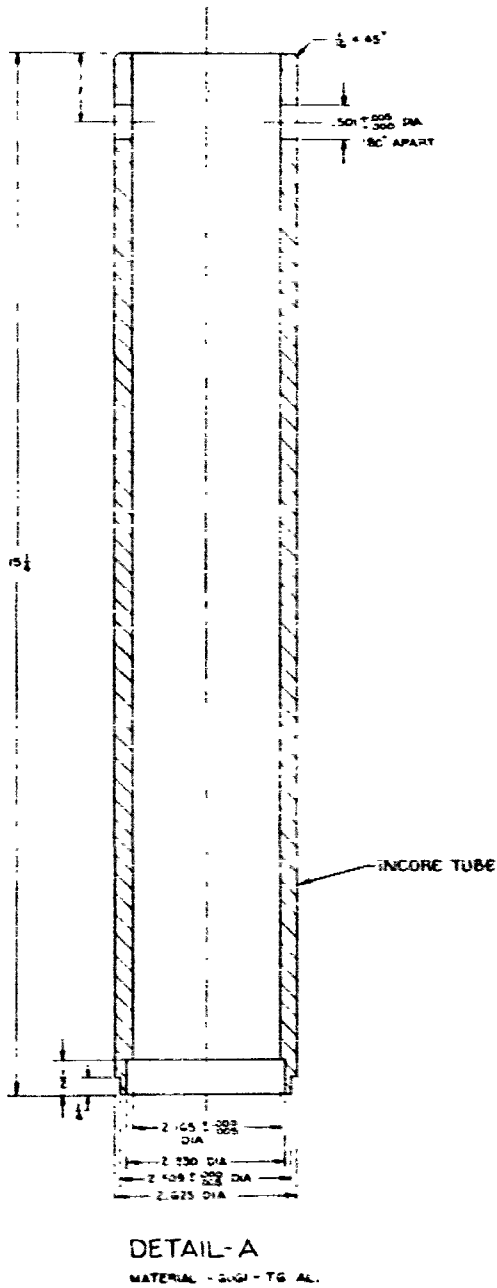


Figure 4-6. Inpile Load With Fiberglas Insulation

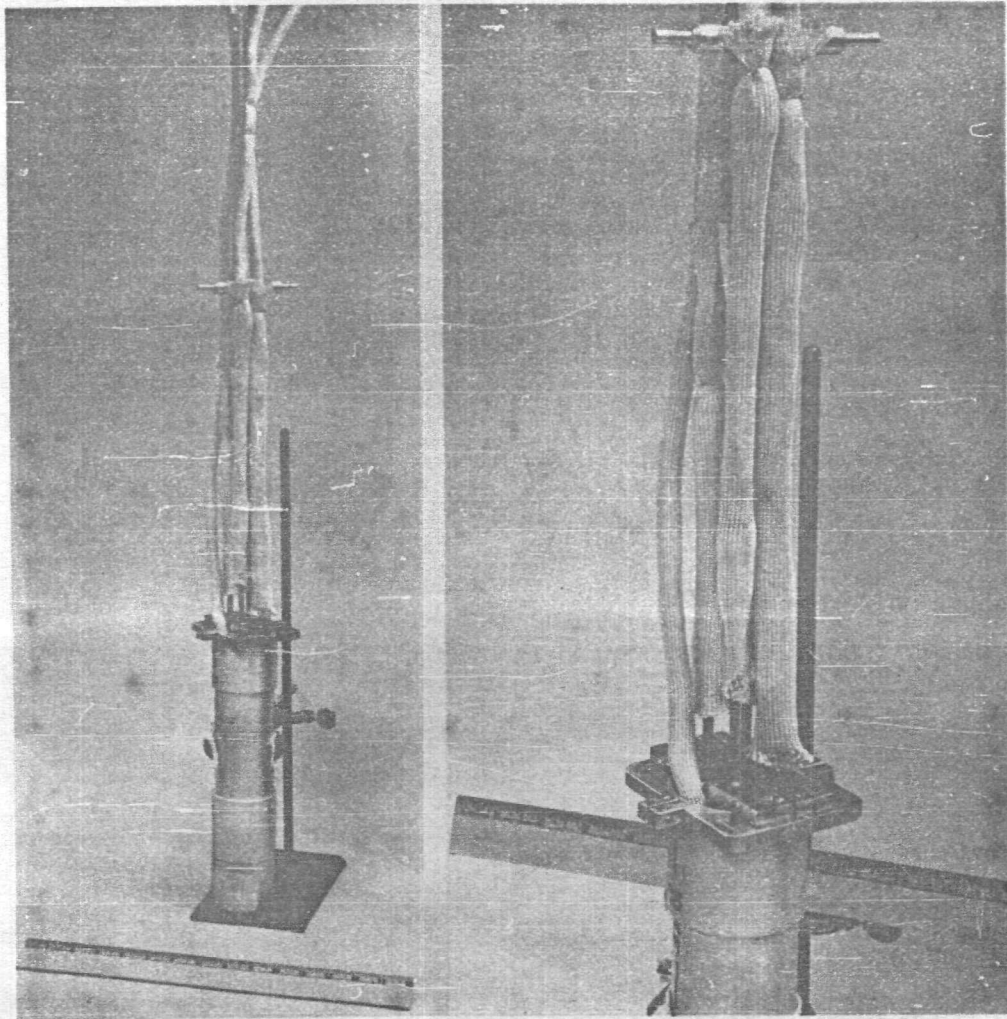


Figure 4-7. Fueling the Converter

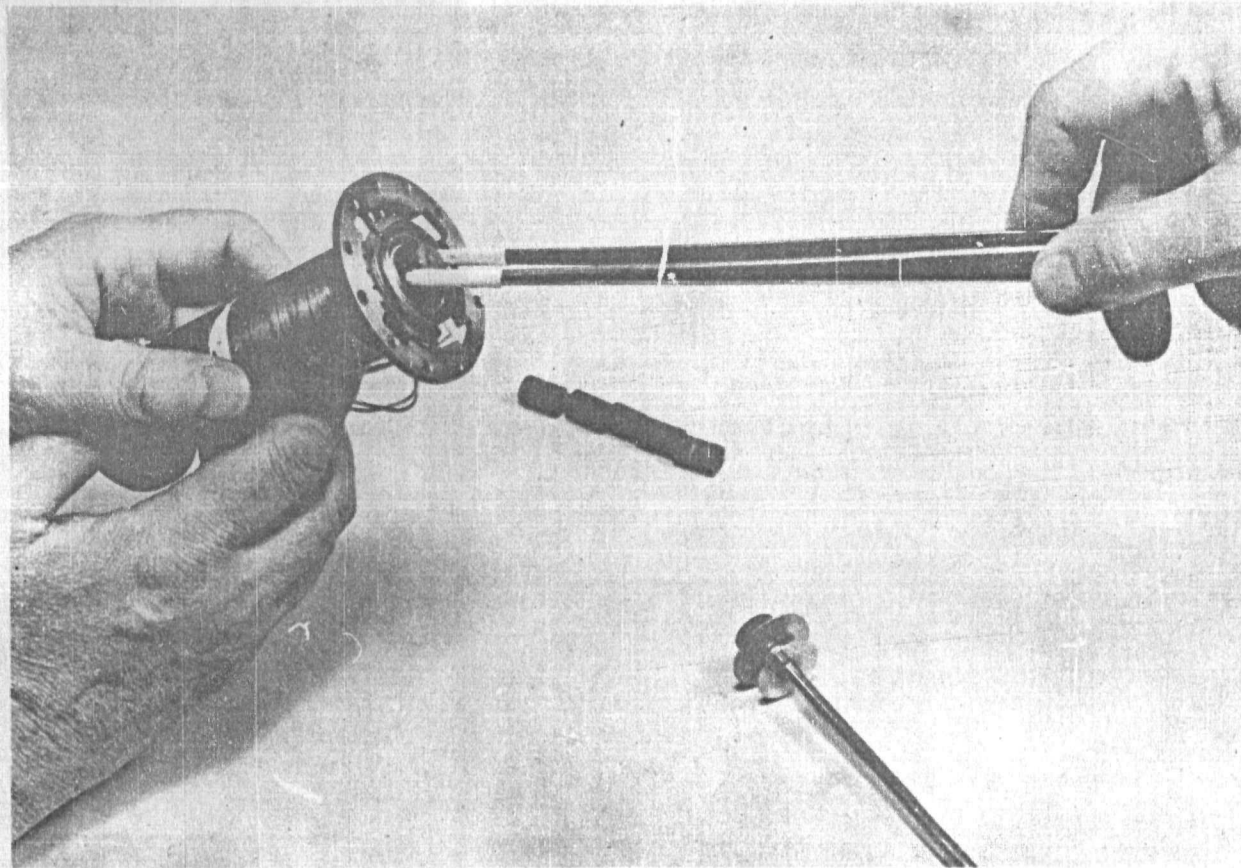


Figure 4-8. Converter Inpile Assembly

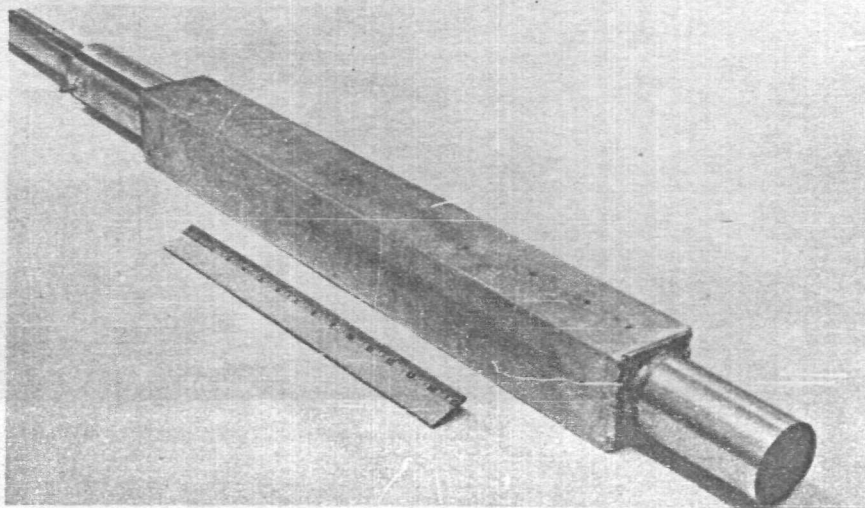
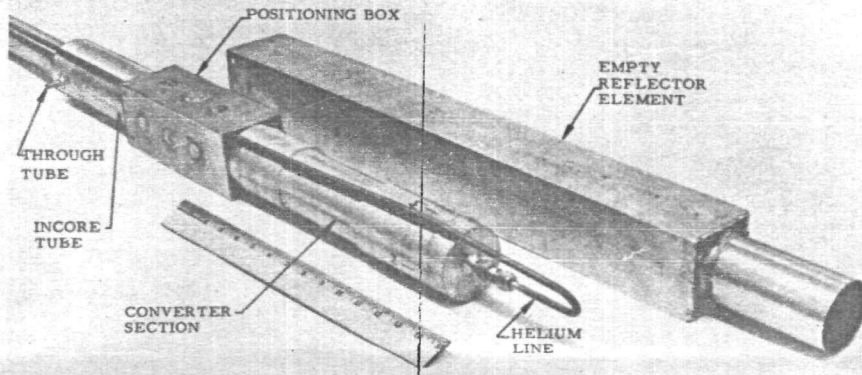
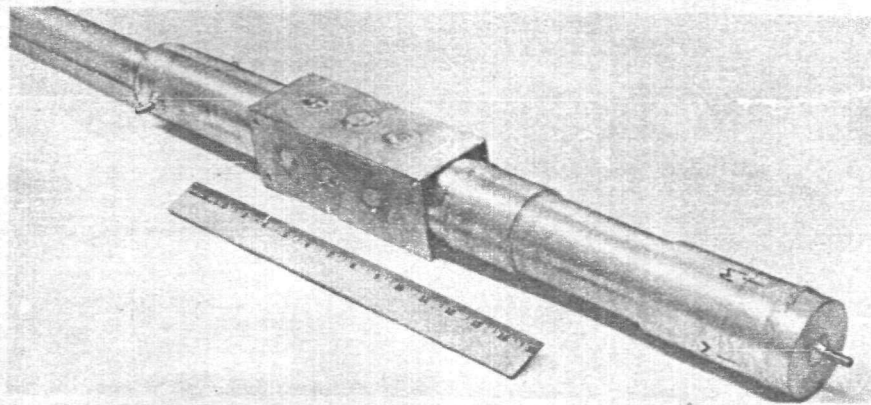


Figure 4-9. Cooling-Water Circuit

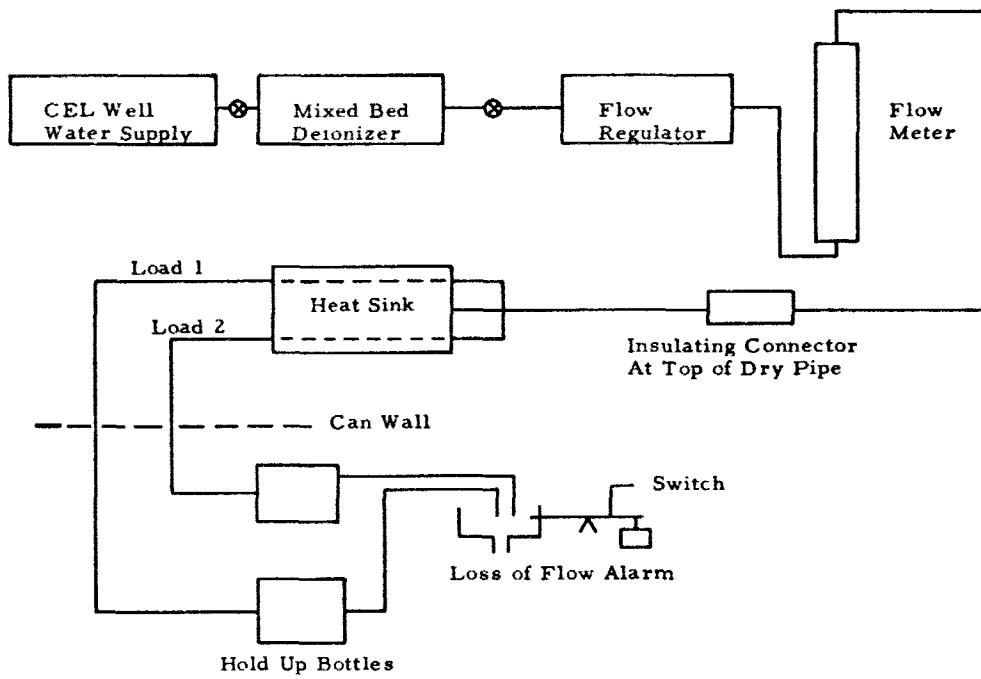


Figure 4-10. Helium Flow Circuits

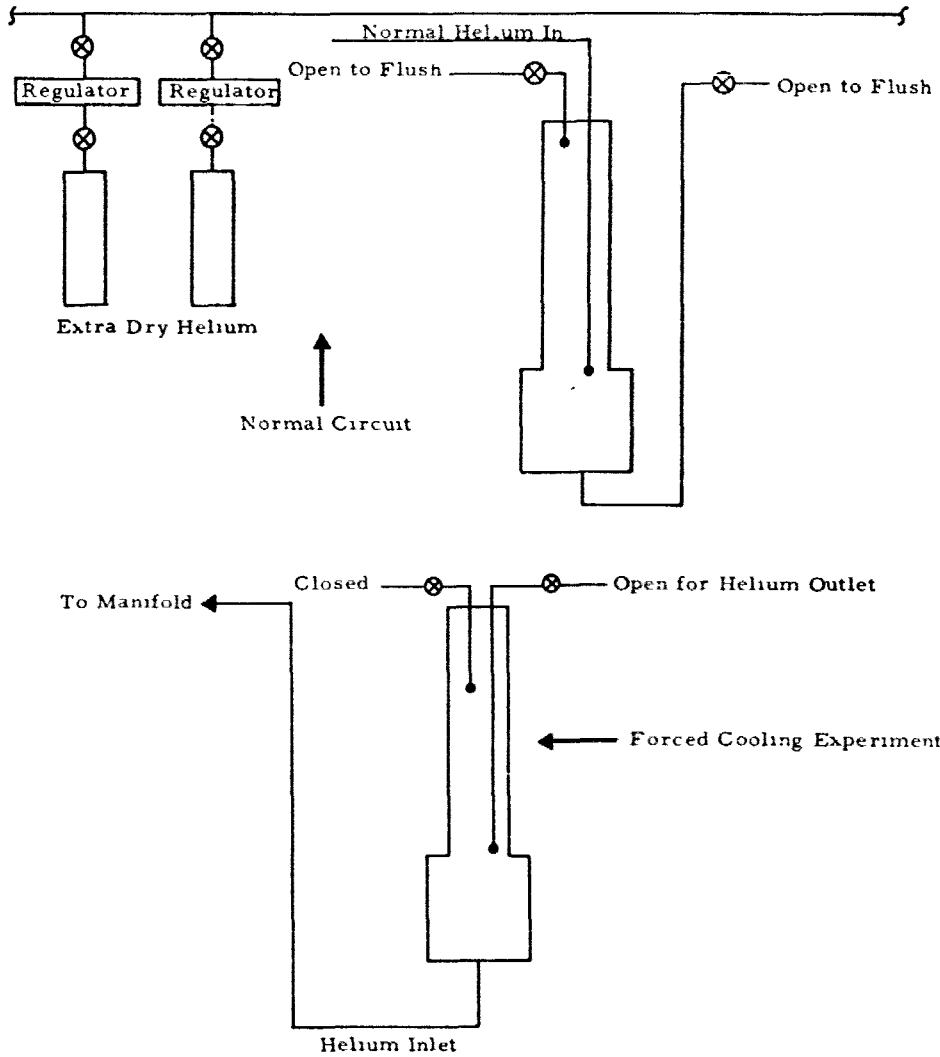


Figure 4-11. Startup Phase

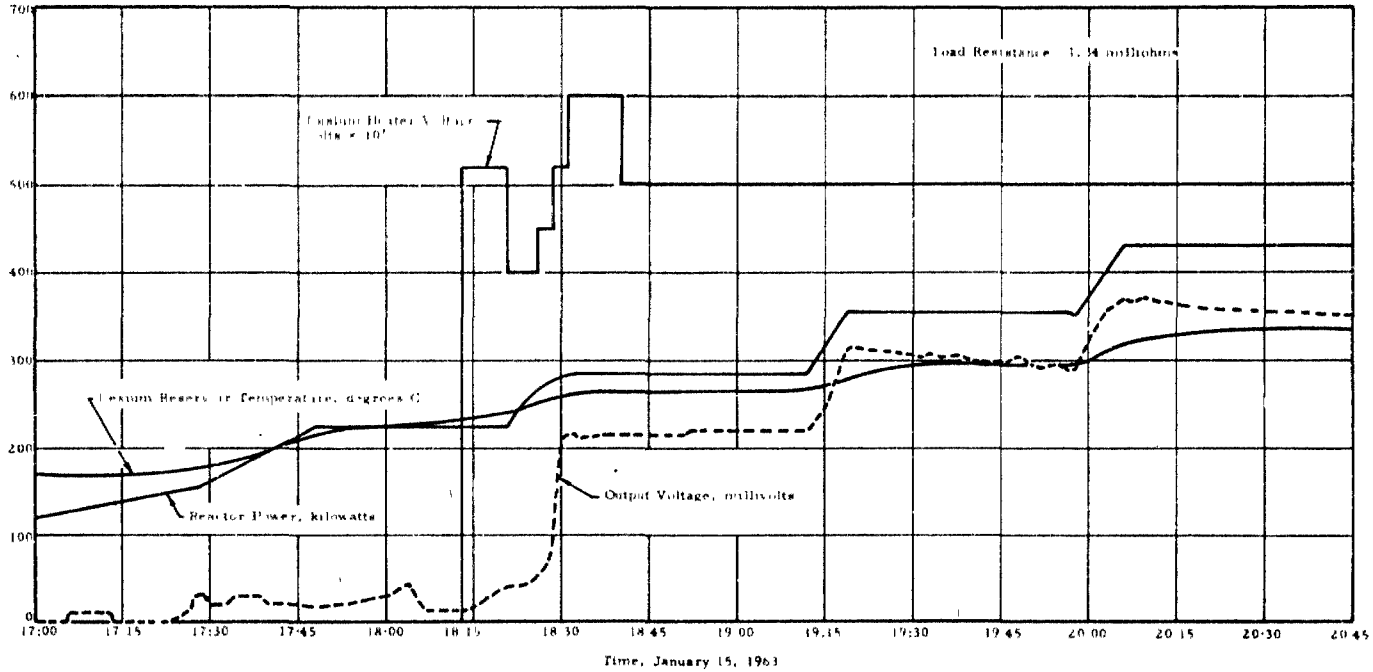


Figure 4-12. Output Power and Input Power Vs Time

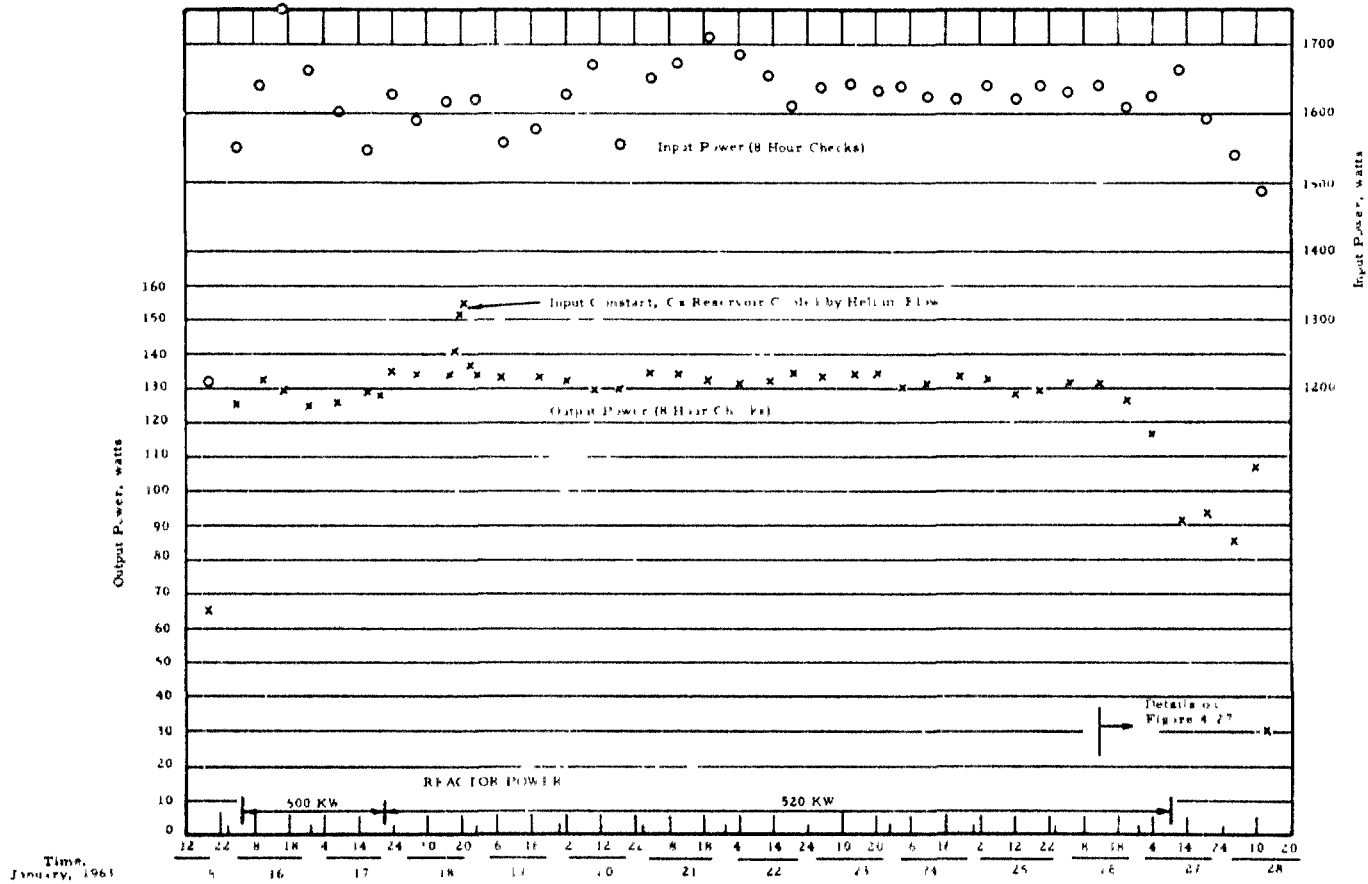


Figure 4-13. Reactor Power and Position of Shim Rods Versus Time

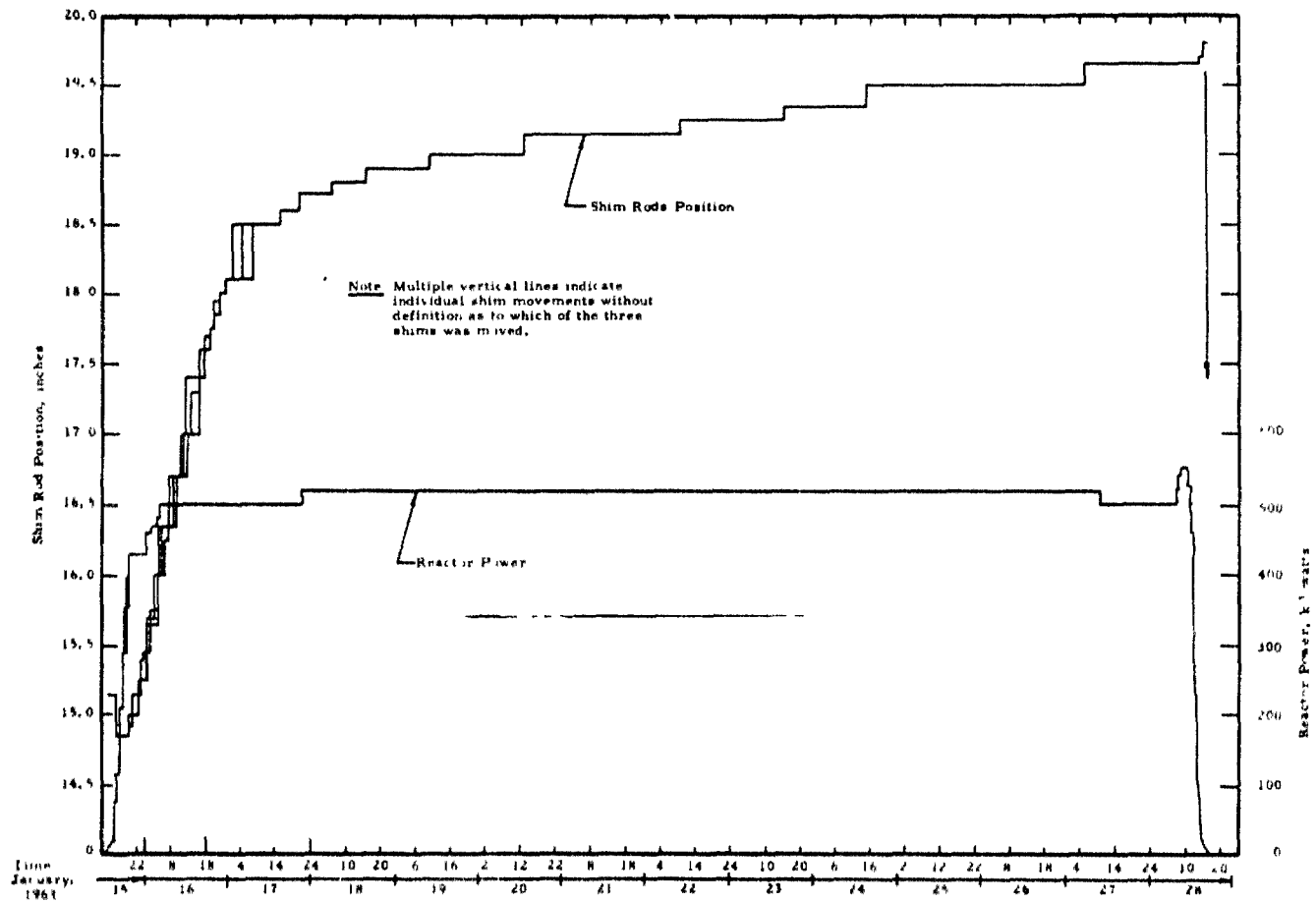


Figure 4-14. Intermediate Phase

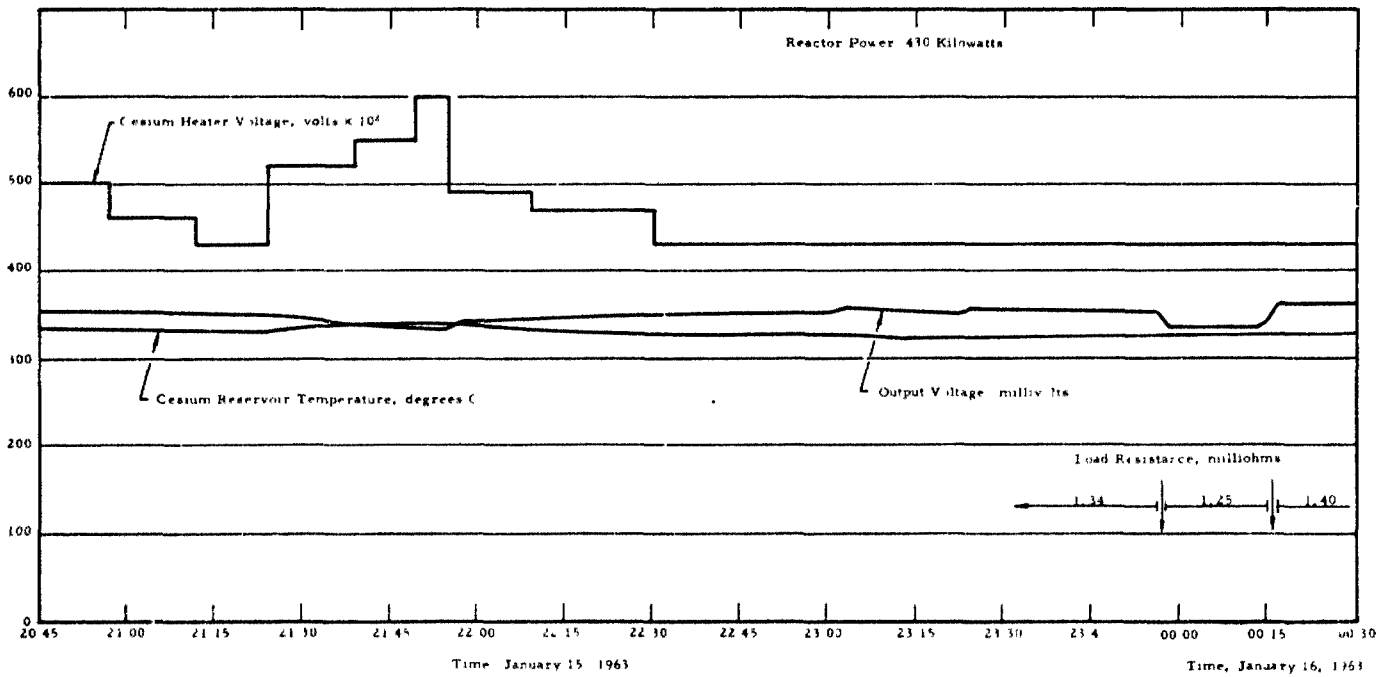


Figure 4-15. Intermediate Phase

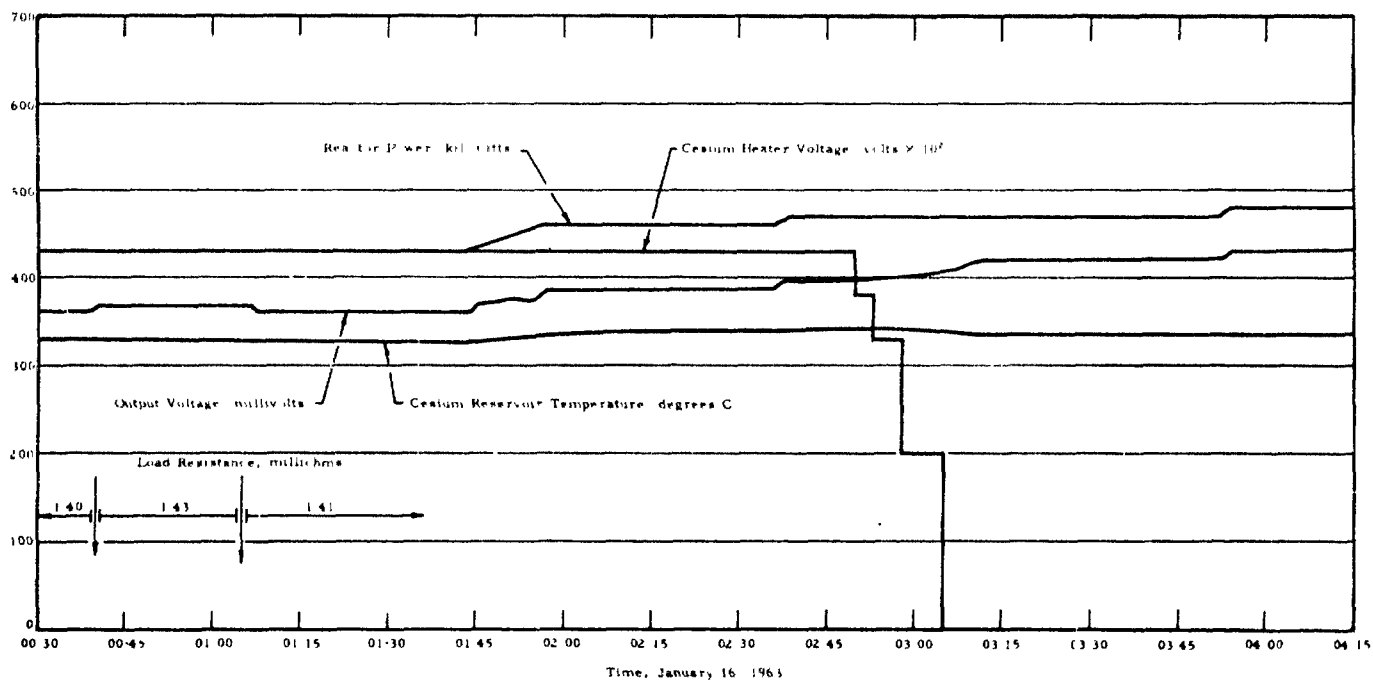


Figure 4-16. Intermediate and Steady-State Phases

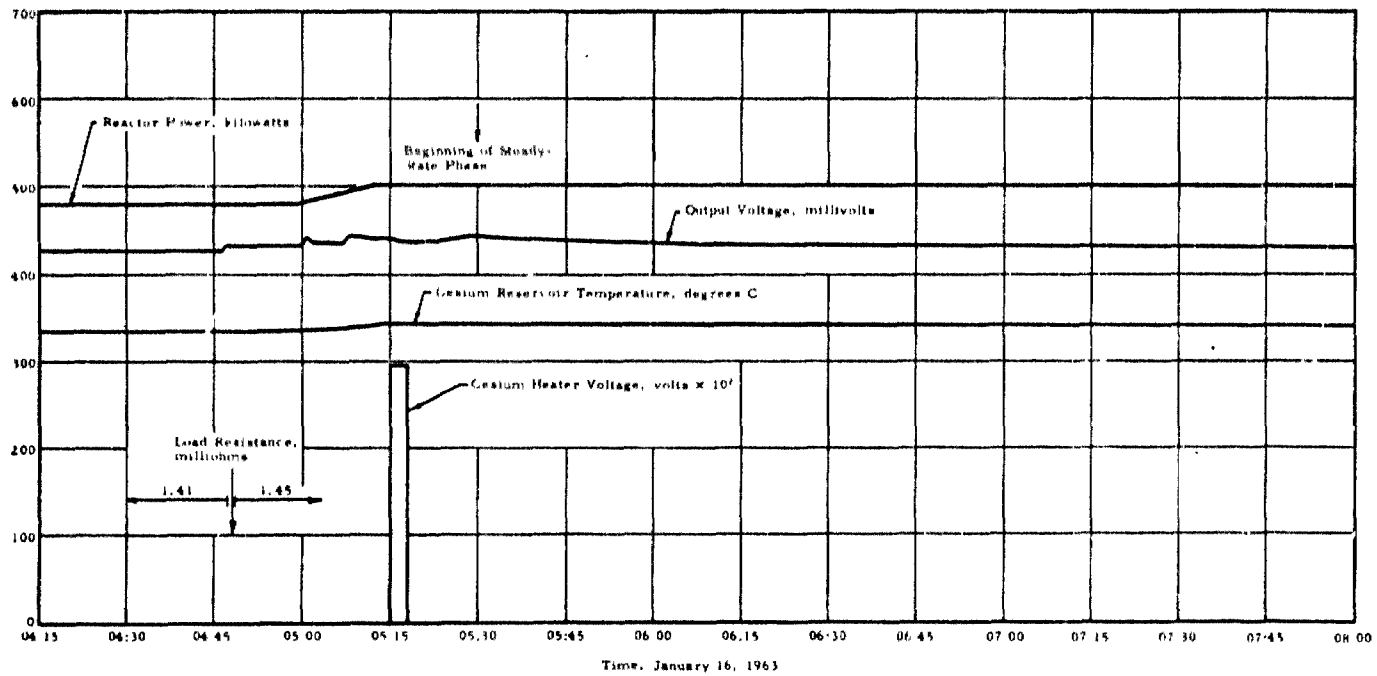


Figure 4-17. Steady-State Phase

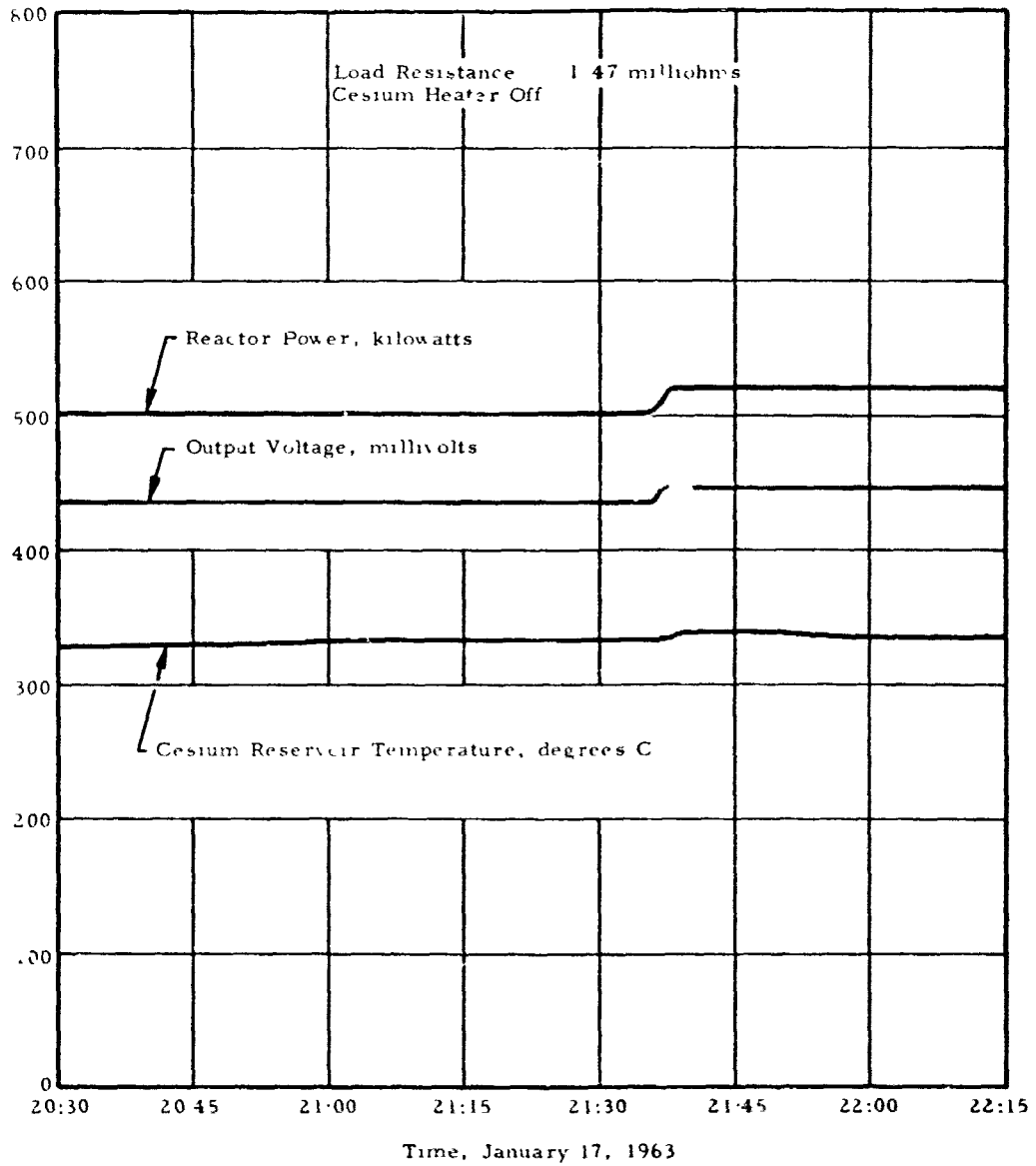


Figure 4-18. Computed Efficiency Vs Input Power

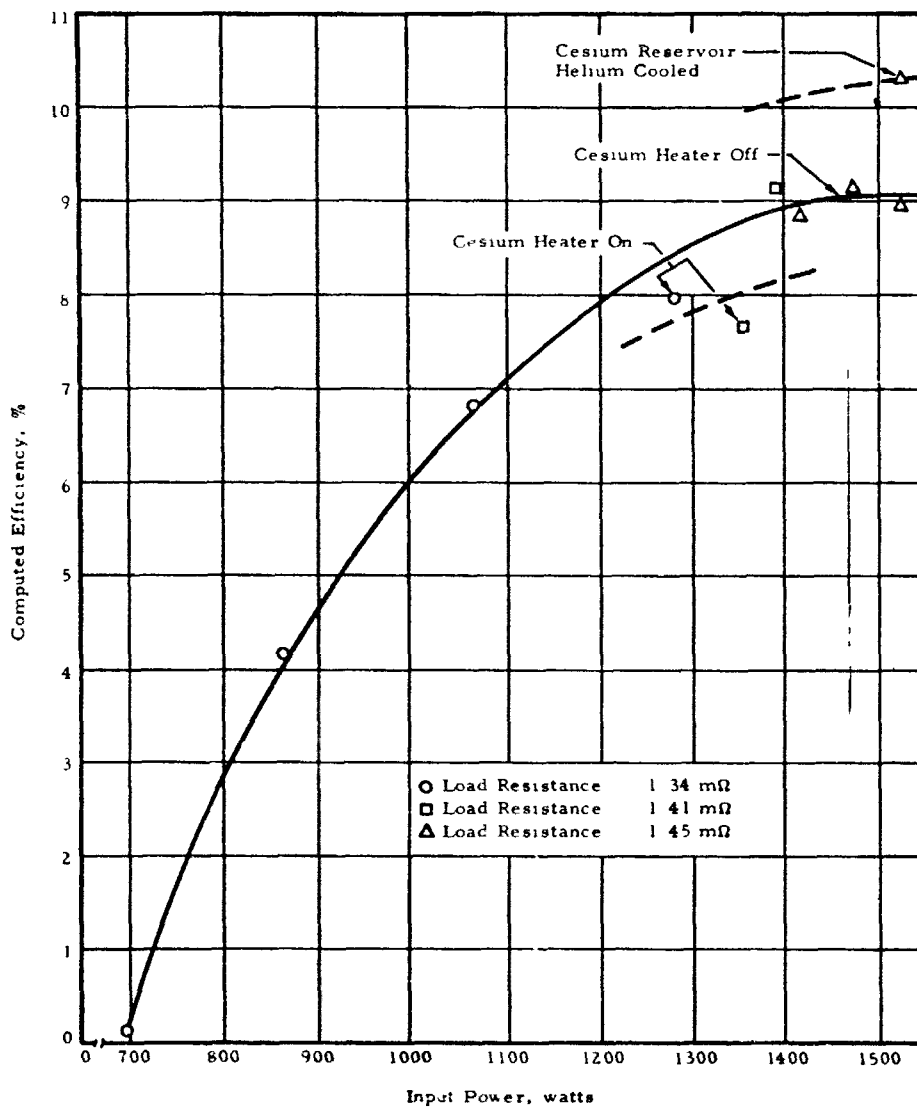


Figure 4-19. Cesium Vapor Pressure Vs Temperature

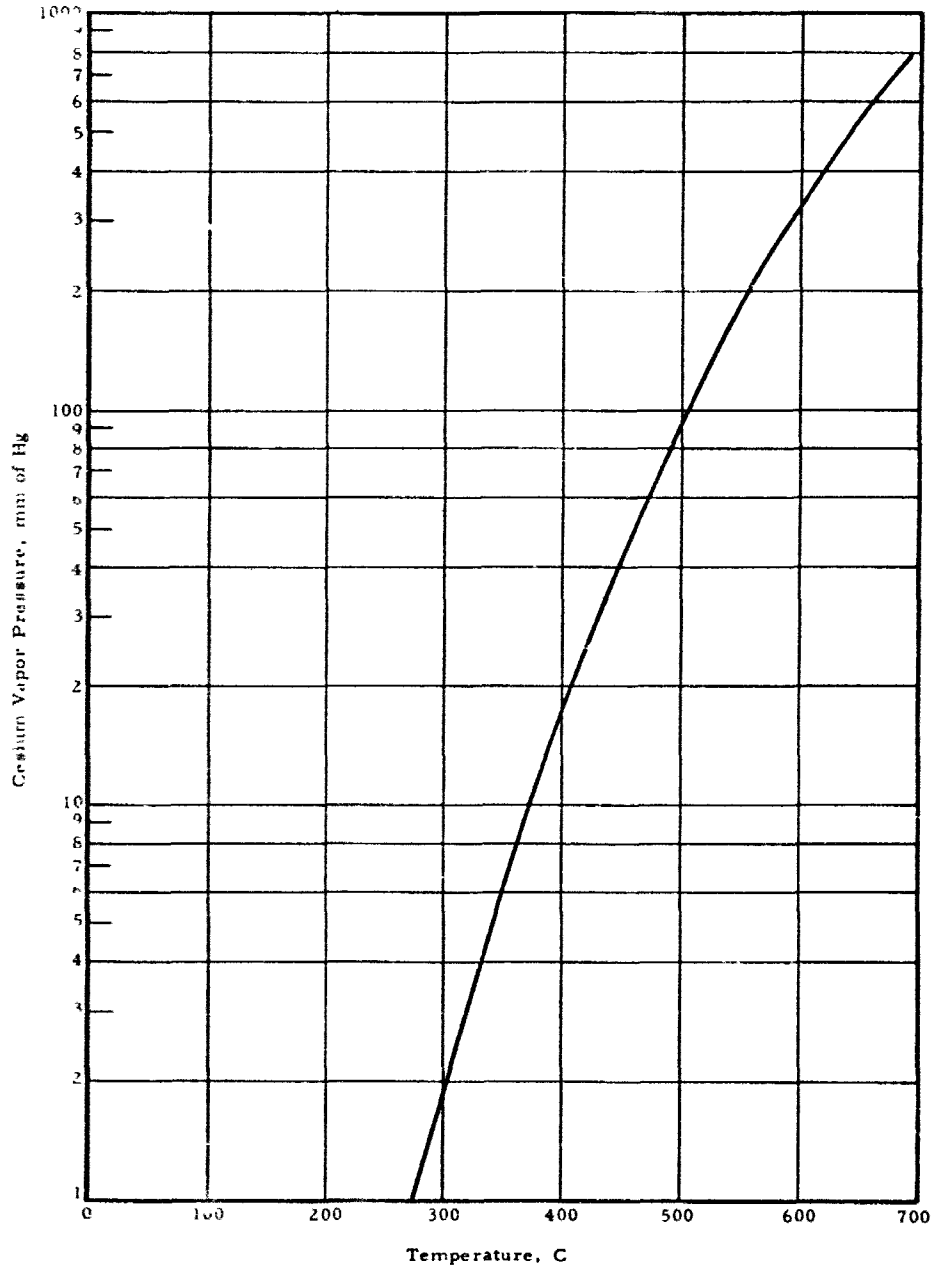


Figure 4-20. Cesium Heating Experiment, Steady-State Phase

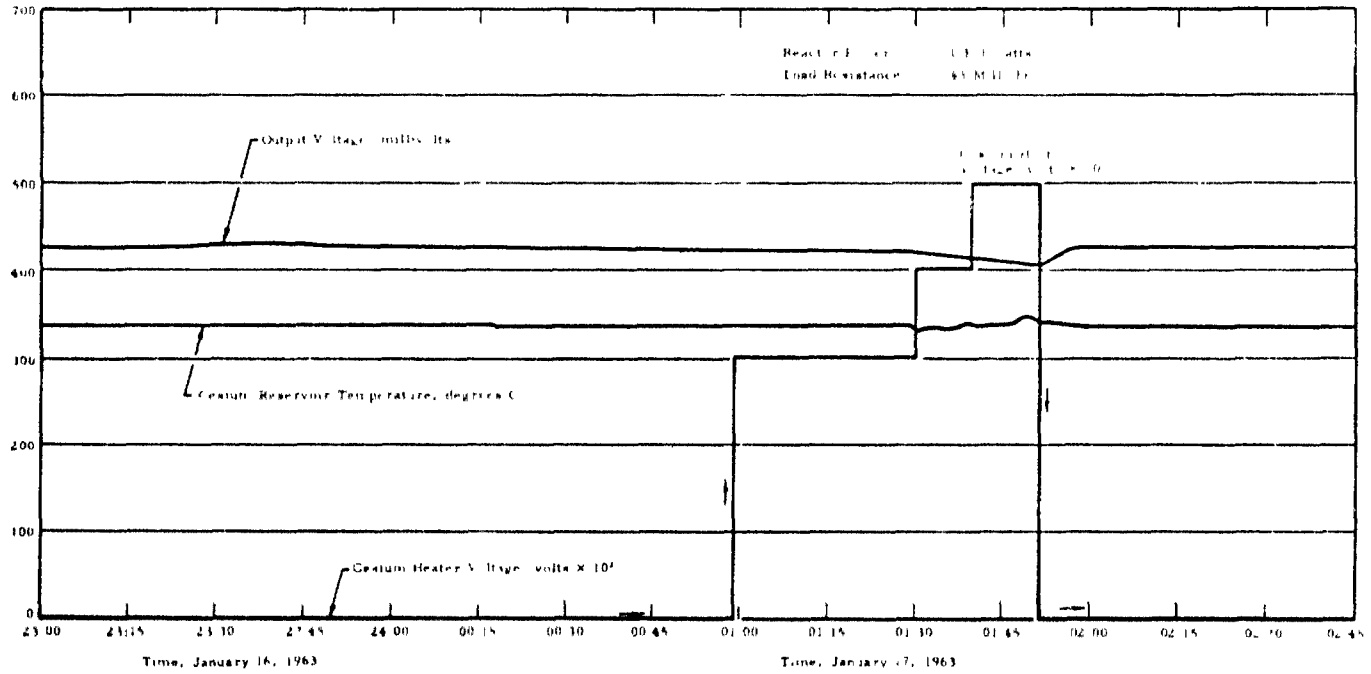


Figure 4-21. Helium Flow Experiment, Steady-State Phase

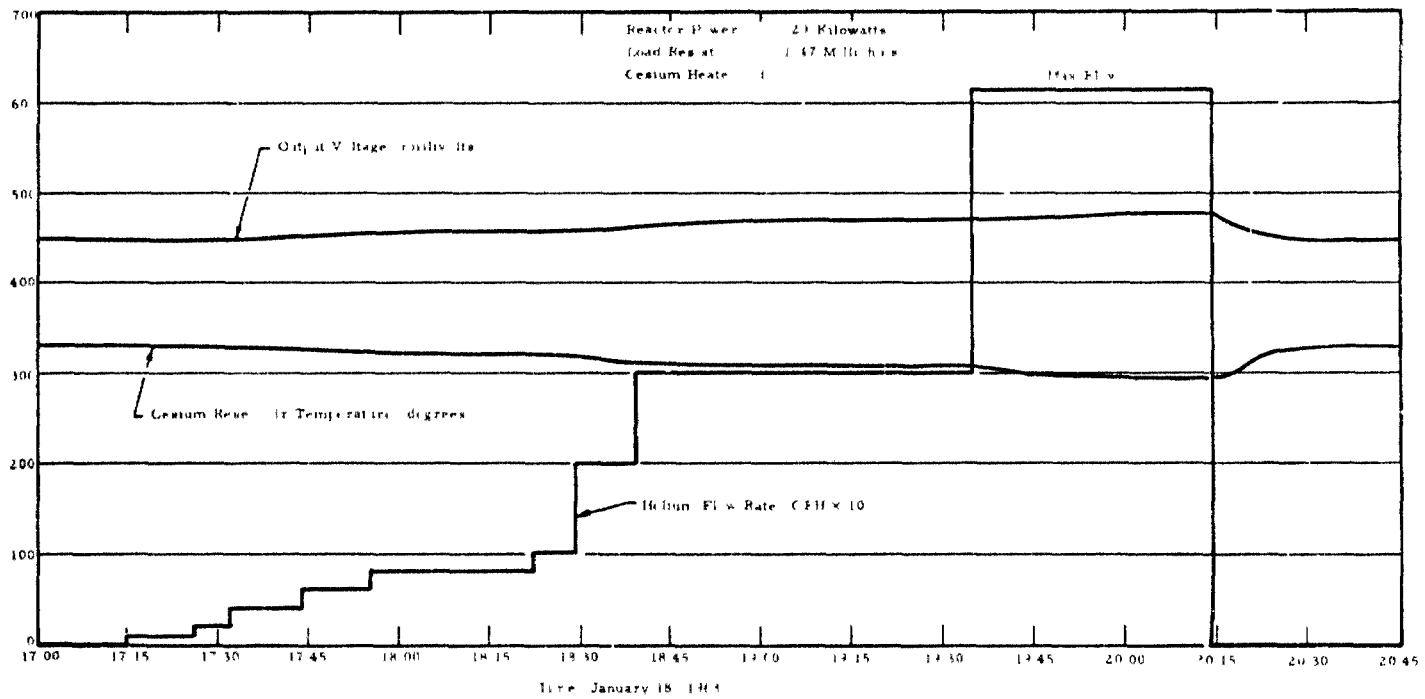


Figure 4-22. Output Voltage Vs Cesium Reservoir Temperature

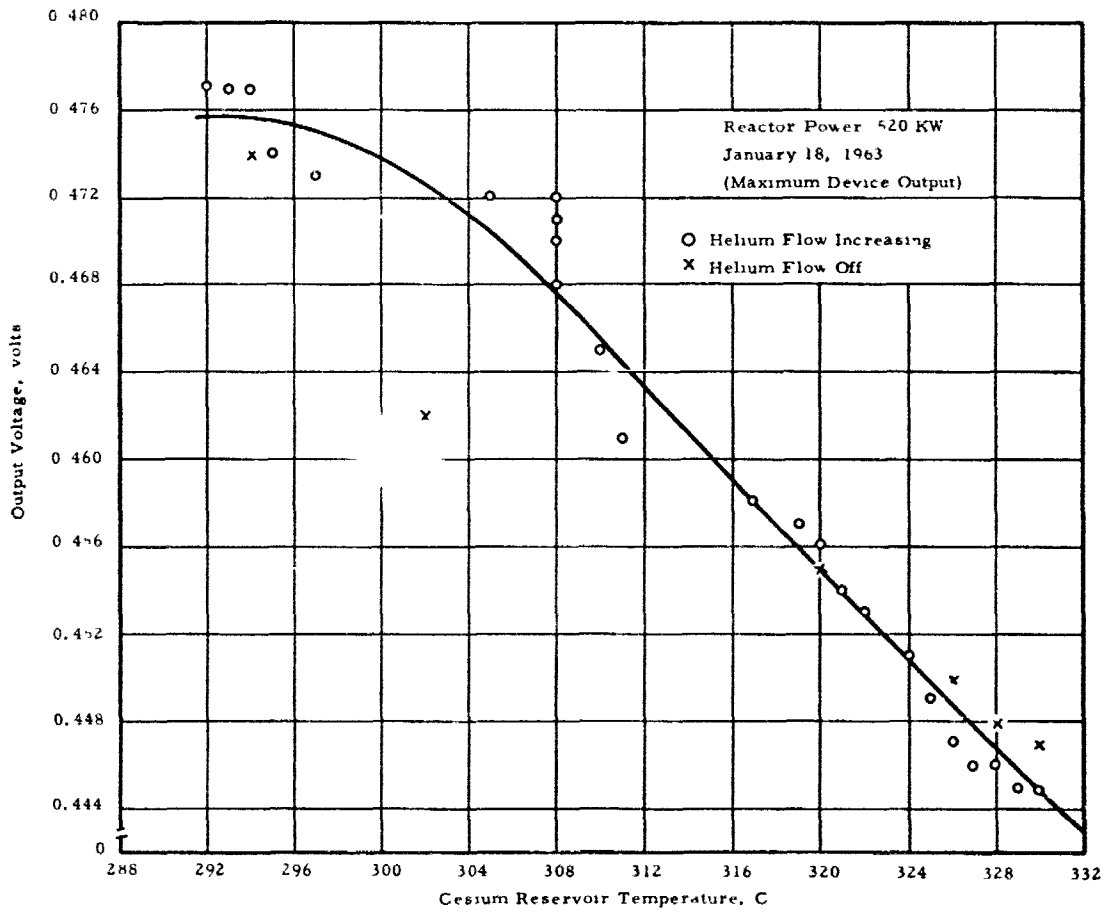


Figure 4-23. Output Voltage Vs Cesium Reservoir Temperature

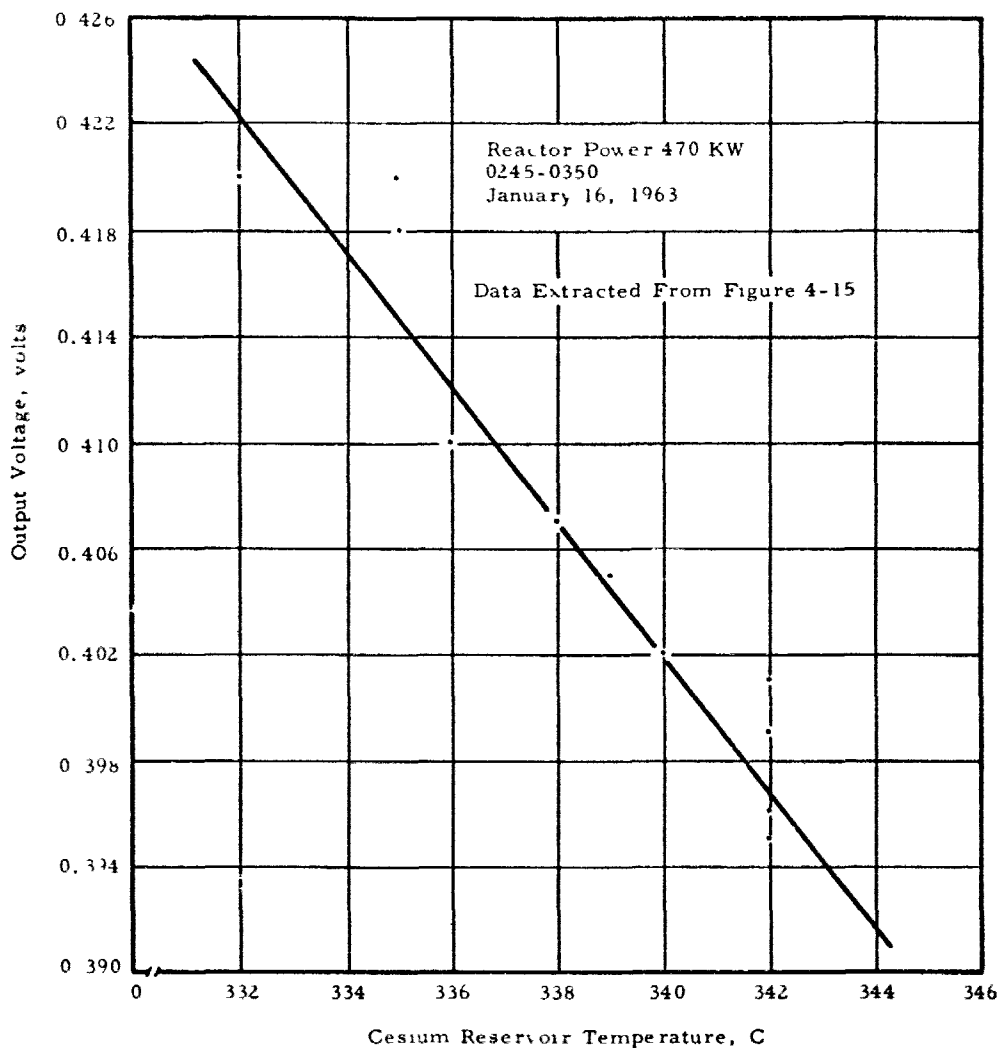


Figure 4-24. Output Power Vs Load Resistance

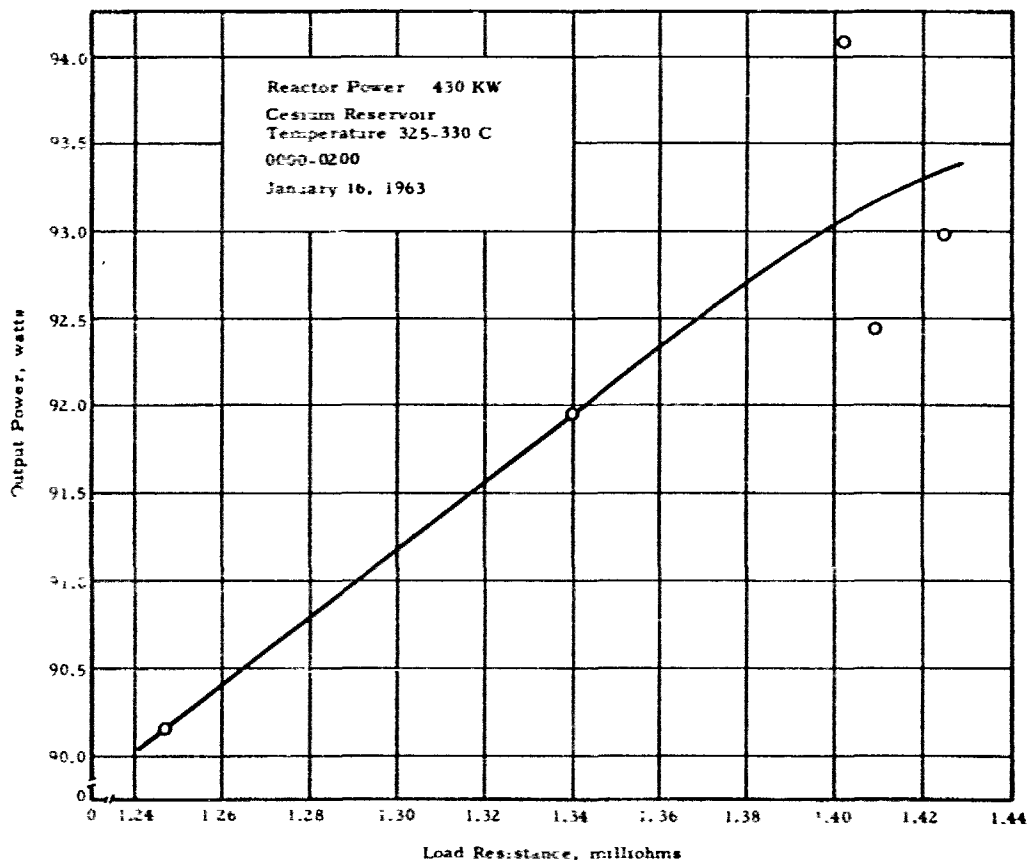


Figure 4-25. Output Power Versus Load Resistance

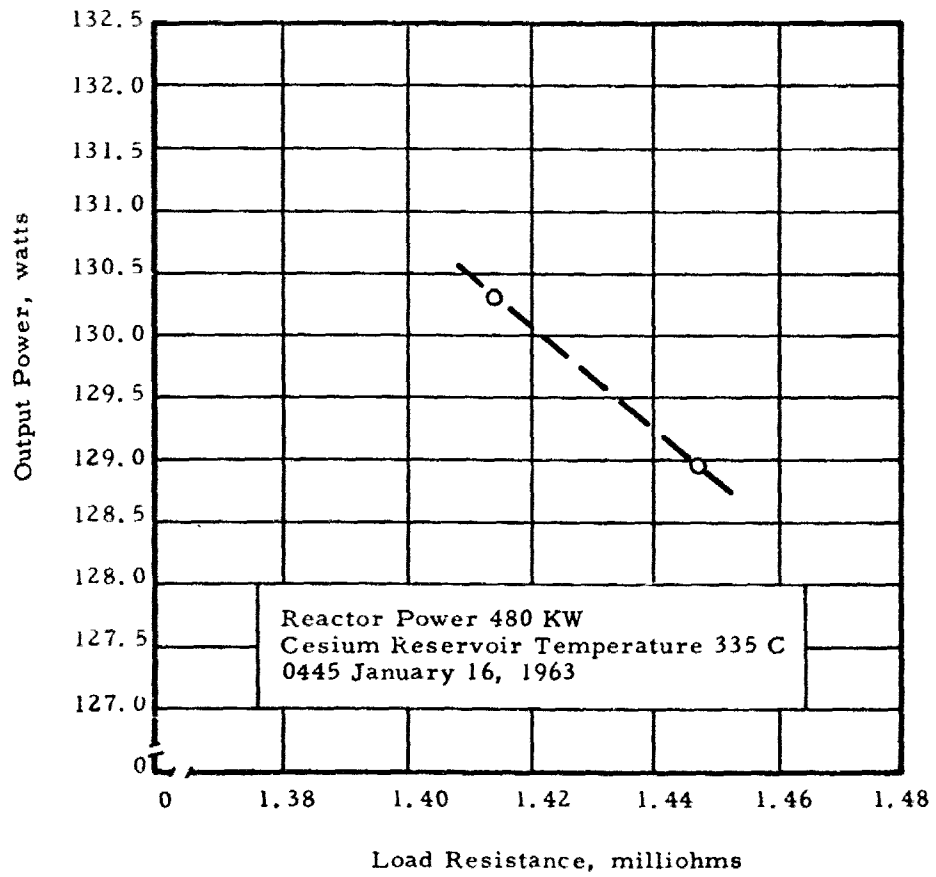


Figure 4-26. Output Power Vs Load Resistance

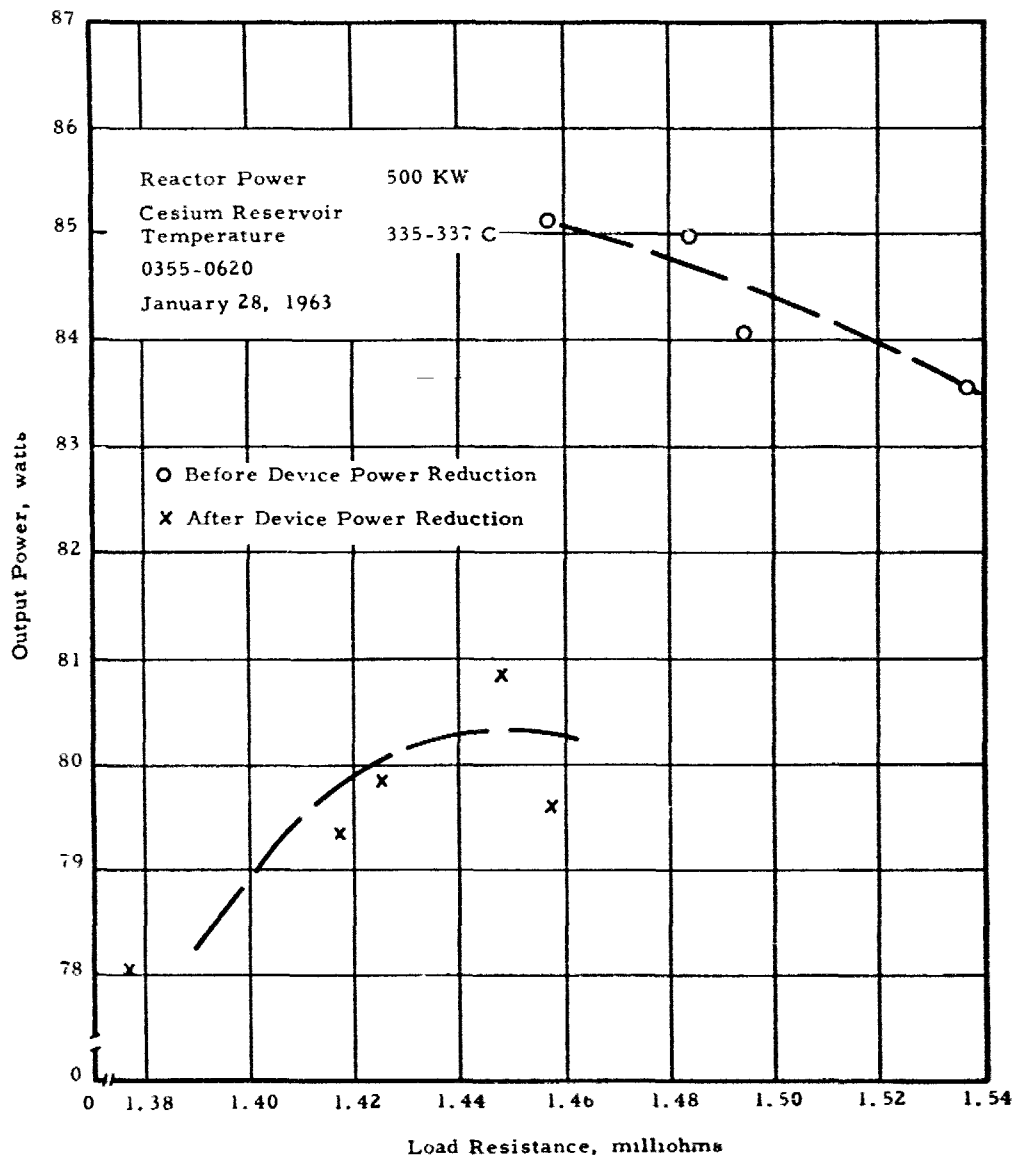


Figure 4-27 Power Reduction Phase

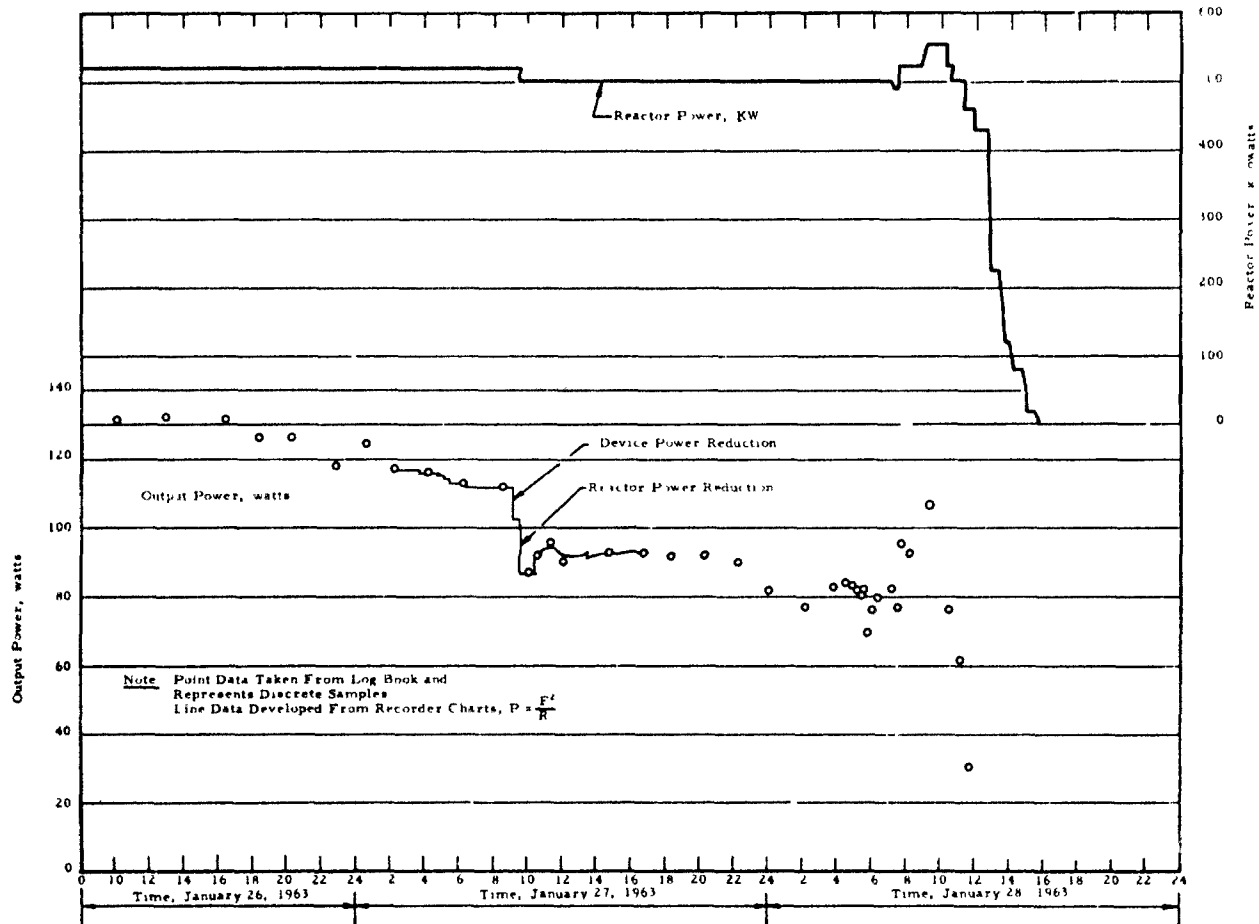


Figure 4-28. Power Reduction Phase

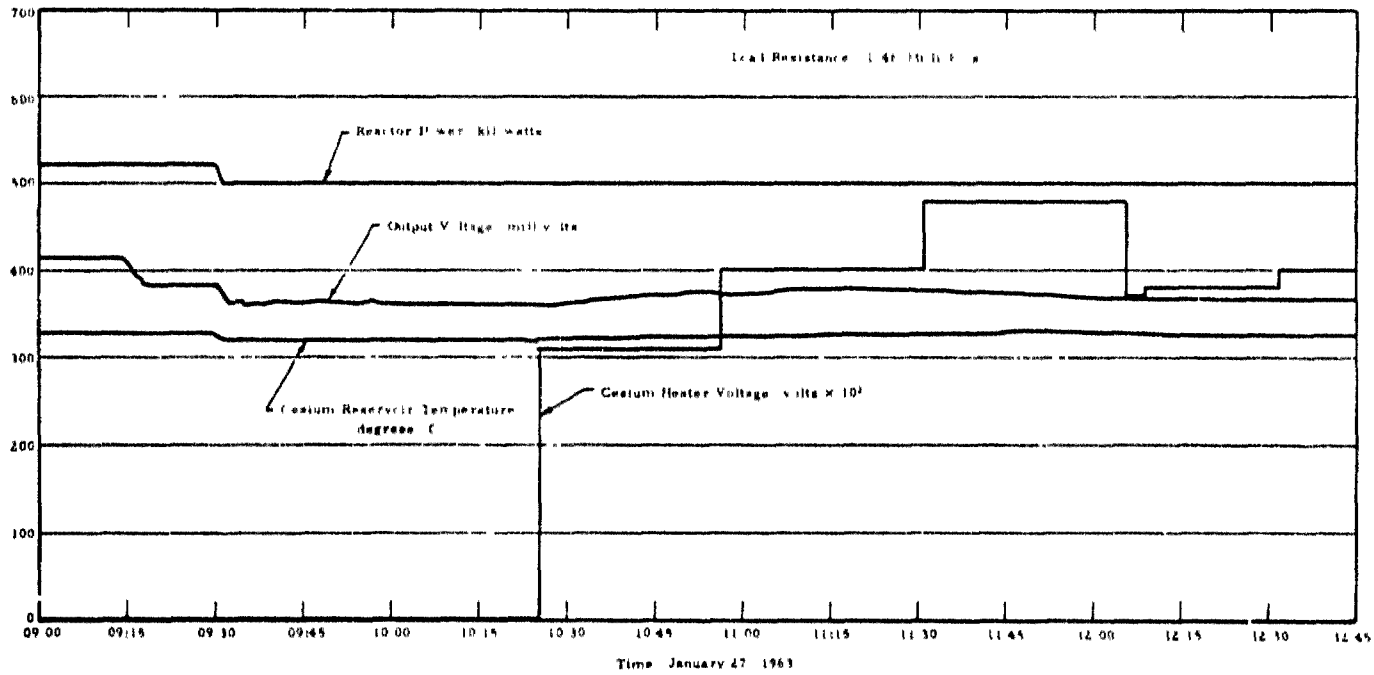


Figure 4-29. Device-Power Reduction Phase

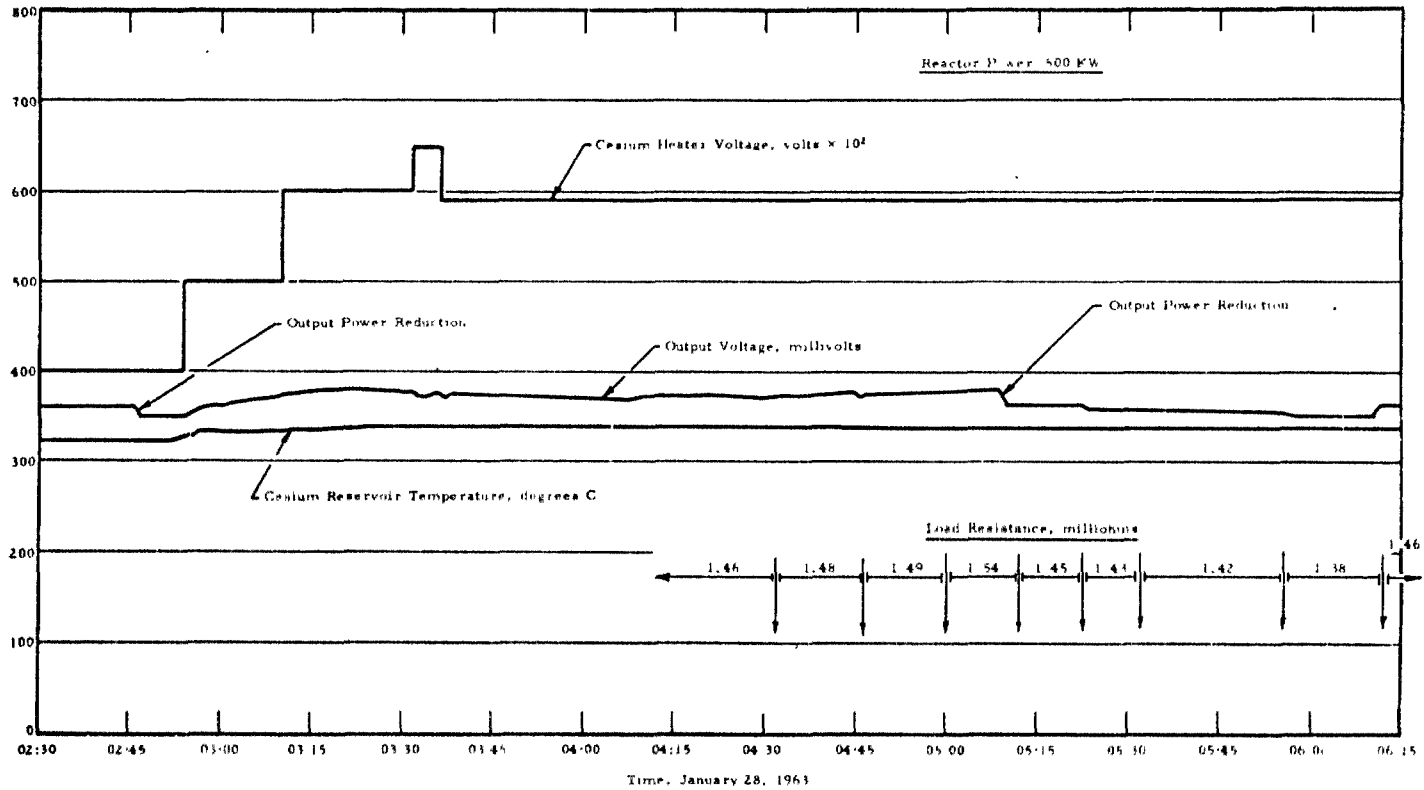


Figure 4-30. Shutdown Phase

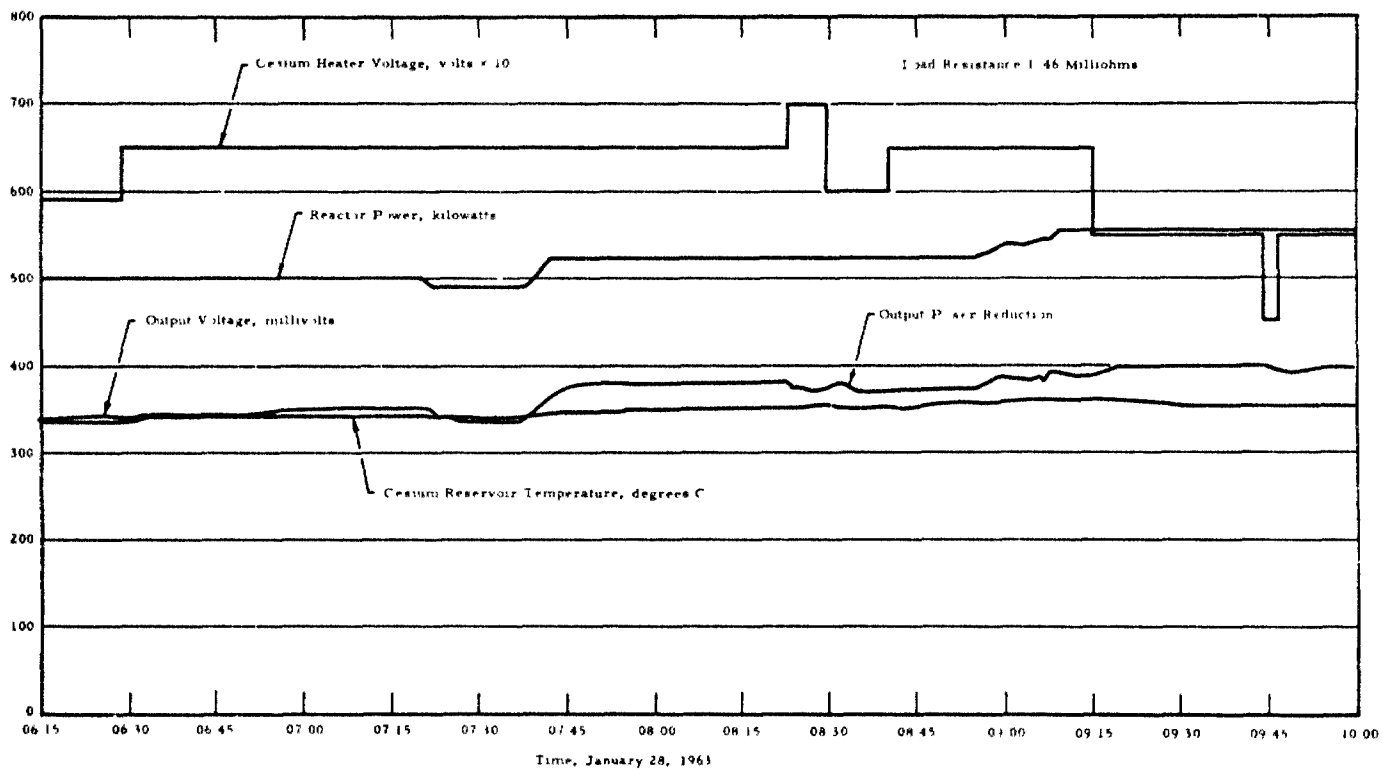


Figure 4-30. Shutdown Phase

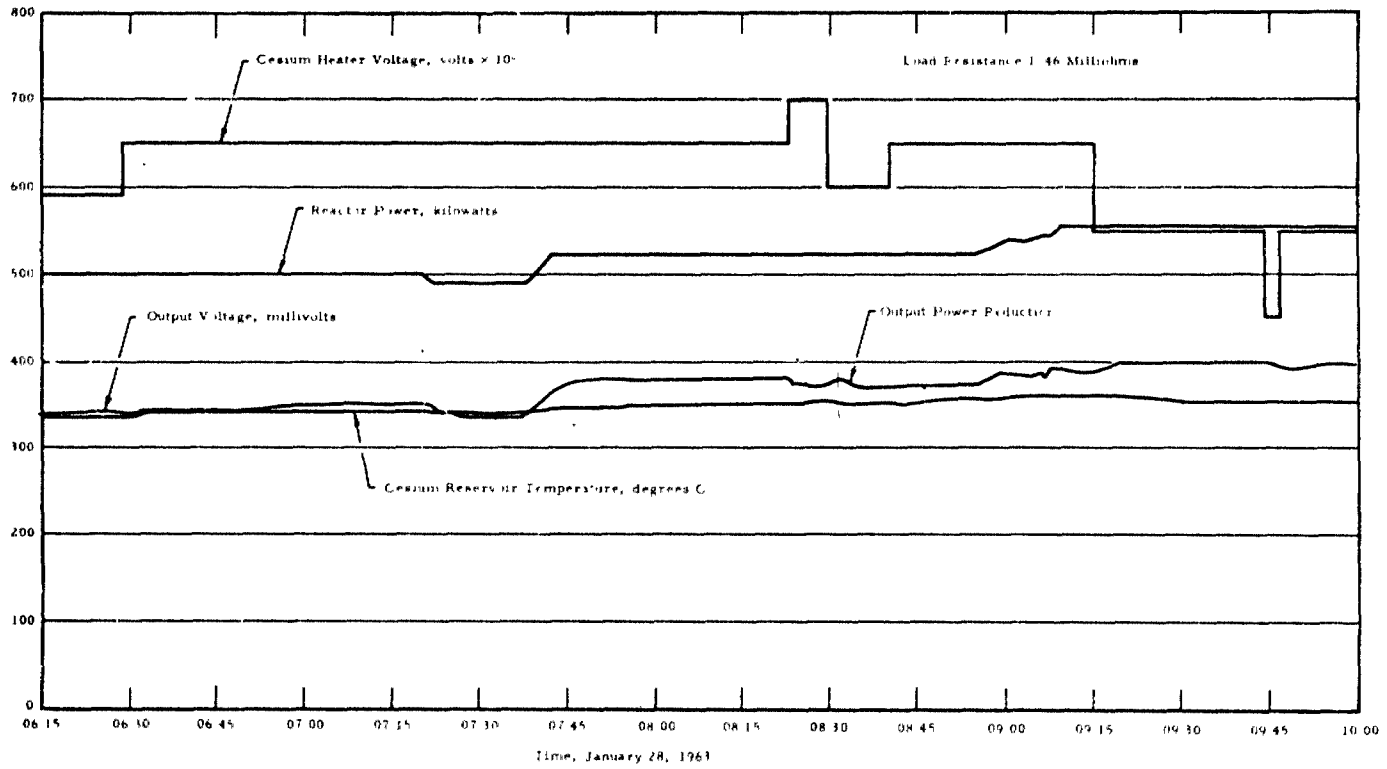


Figure 4-31. Shutdown Phase

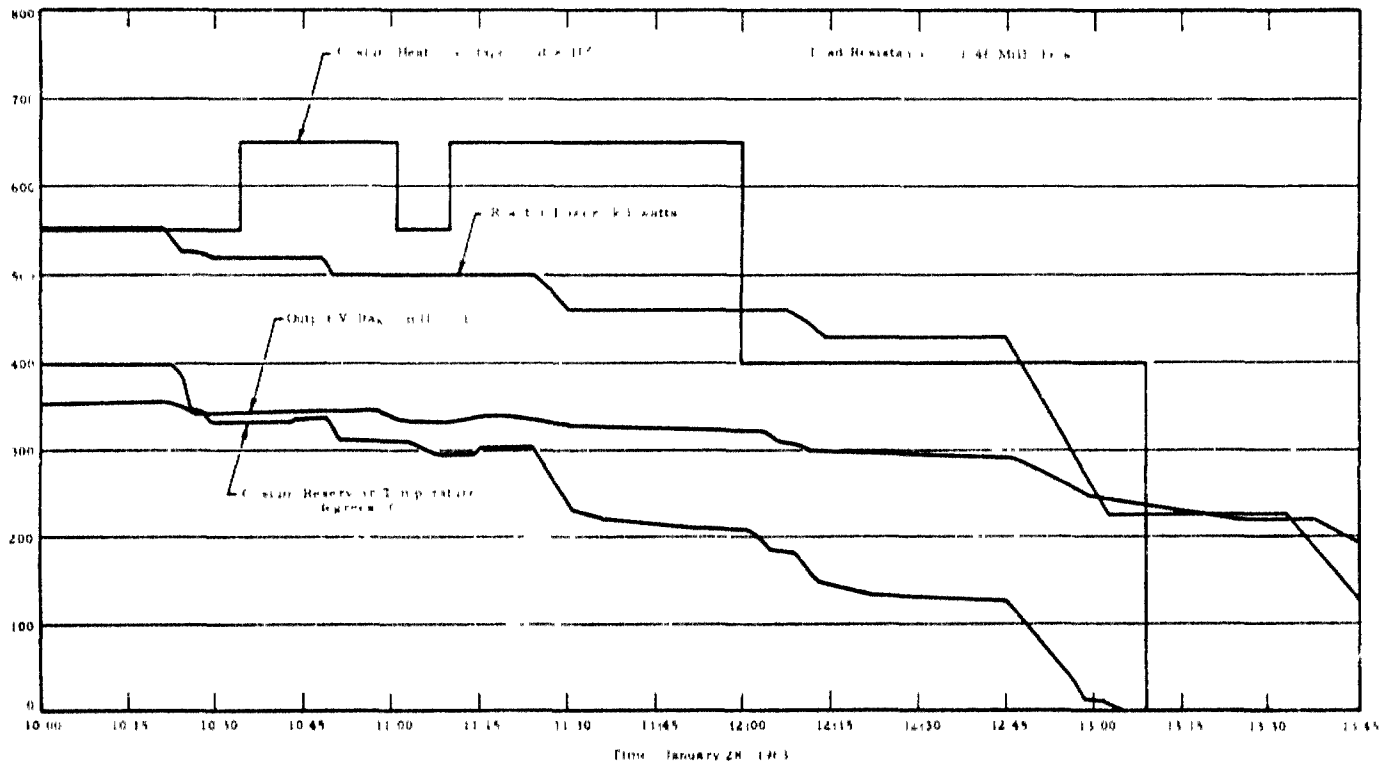
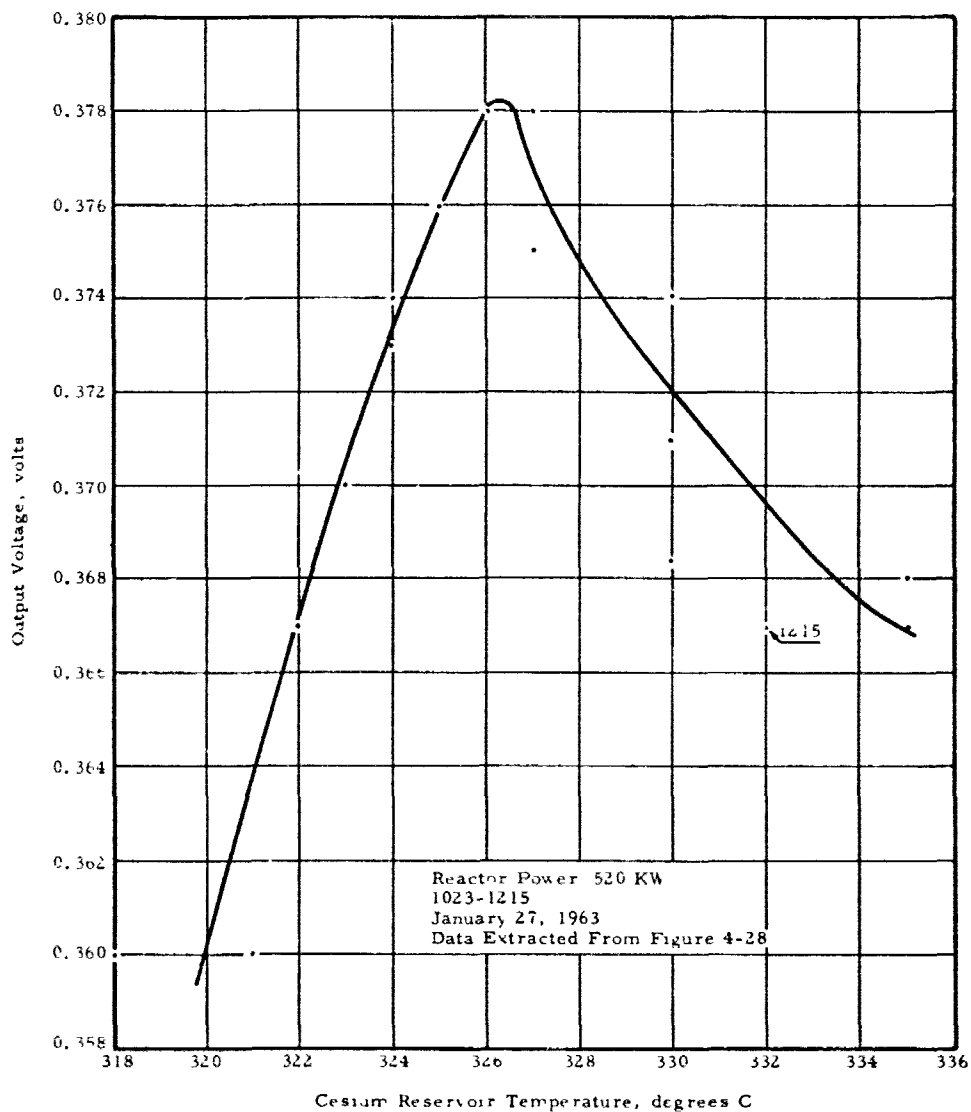


Figure 4-32. Output Voltage Versus Cesium Reservoir Temperature



APPENDIX A
Heat Transfer Experiment

APPENDIX A
Heat Transfer Experiment

1 Experiment Components and Assembly

The component parts that make up the heat transfer assembly are shown in the photographs and drawings of Figures A-1 to A-13. The device was assembled by carrying out the following steps:

1. Drill holes in the base plate for Stupakoff dual-lead insulators. Holes are drilled as shown in Drawing No. 28924 C-2, Figure A-5.

2. Drill and tap six No. 0-80 holes in the base-plate ring. Tack-weld the ring to the base plate.

3. Lead-solder Stupakoff insulators to the base plate. Remove excess solder, particularly near the edge of the base plate. Clean with acetone and alcohol.

4. File slots in the copper diaphragm corresponding to the hole pattern of the base-plate ring.

5. Attach the emitter to the base plate by clamping the copper diaphragm to the base-plate ring with the split clamp and No. 0-80 screws.

6. Measure the resistance and length of the thermocouple leads. Clean the emitter surface.

7. Run the thermocouple leads through the thermocouple leadout holes in the split sleeve. Join the halves of the split sleeve with screws and clamp in an inverted position. Attach dual-lead ceramic insulators to the thermocouple wires. Run the wires through the insulator terminals according to the specified pattern. Measure resistance.

8. Apply Sauriezen cement where needed to prevent shorting of the thermocouple leads.

9. Lead-solder thermocouple leads through the terminals. Check resistance.

10. Clean the split sleeve and slide into the outer can. Tack-weld the edge of the base plate to the bottom edge of the outer can.

11. Weld the upper Kovar support ring to the outer can. Complete the edge weld of the base plate to the outer can. Helium leak-test the assembly.

12. Attach a temporary thermocouple protective plate to the bottom pinch-off tube to prevent damage to the thermocouple leads.

13. Fuel the device and edge-weld the top plate to the outer can.

14. Connect the device to the vacuum system and bake at an emitter temperature of 300 C. Limit the base-plate temperature to 150 C. When cooled and pumped down, pinch-off and remove the device from the vacuum system.

15. Install the assembled experiment within the split coolant jacket and attach the top and bottom heat sinks to the jacket. Wrap several layers of teflon tape in bands around the coolant jacket to insulate the assembly from the external can.

16. Attach the coolant-tube assemblies containing previously calibrated metal-sheathed Cr-Al thermocouples to the tubes from the coolant jacket. These are the inlet and outlet thermocouples. Leak-test each successive operation using a static-pressure test at 50 psi.

17. Attach the thermocouple support by set screws to the bottom heat sink. Pass the thermocouple extension wire through the bottom external tube and plate and splice to the leads from the Stupakoff terminals. Clamp the extension wire to the support to prevent stressing the spliced joint.

18. Fit the external can and the top external plate to the assembly. Partially fill the bottom external tube by adding epoxy around the thermocouple extension wires and coolant tubes. Allow the

epoxy to dry and apply a second layer of epoxy

19. Weld the external can to the top and bottom external plates. Leak-test the welds and epoxy-seal using a copper tube installed through the epoxy. Pinch off this test tube

20. Position the completed assembly within an aluminum reflector can so that the center of the fuel in the device corresponds to the centerline of the core. Connect coolant tubes to the water supply and thermocouple leads to the instrumentation

The same assembly procedure was followed for both inpile heat transfer experiments with the following exceptions:

1. In the first inpile heat transfer assembly, the top external plate provided a one-quarter inch clearance space above the top of the external can (Drawing No. 36135 C-0, Figure A-10). In the second inpile heat transfer assembly, a longer pinch-off tube was left on the device to permit making a second pinch-off after irradiation. The purpose of the longer tube was to provide a region for the collection of fuel chamber gases for later gas analysis if warranted by the experimental results. Figure A-4 shows the revised top external plate and the aluminum extension tube that was added to accommodate the longer pinch-off tube.

2. It was necessary to modify the aluminum coolant jacket for the second inpile heat transfer assembly because a satisfactory leak-tight joint could not be made between the jacket and the coolant tubes. The drilled coolant channels shown in Figure A-9 were milled out and replaced by thin-walled, aluminum tubing soldered into the resulting passages. The four aluminum tubes from the jacket extended through the bottom external tube and terminated in four 3/16-inch fittings installed in two stainless-steel mixing chambers as shown in Figure A-4. The mixing chambers served as a means for connecting the parallel flow paths through the jacket to a single inlet or outlet 1/4-inch tube. The inlet and outlet thermocouples were installed in the required 1/4-inch fittings.

2. Inpile Experiment Synopsis

The inpile heat transfer experimental program was divided into two separate parts. The first series of three power runs was carried out prior to upgrading the LPR to a one-megawatt capability. Consequently for each run the experiment time available was limited to one hour at a reactor power level above 200 KW. Tables A-1, A-2, and A-3 summarize the results of the first heat transfer experiments.

The second series of heat transfer experiments was carried out after the LPR upgrading. Consequently the length of time available at power was limited only by the objective of the particular experiment. Tables A-4 and A-5 summarize the first two power runs in this series. The remaining four power runs, in which the dynamic characteristics of the system were investigated, are summarized in Table A-6.

3. Thermocouple Pattern

The thermocouple patterns used in the heat transfer experiments are shown in Figure A-14.

4. Fuel and Device Outgassing

For the first series of inpile heat transfer experiments, the fuel was outgassed for nine days at a range of temperatures from 500 to 1100 C. The time at the maximum temperature of 1100 C was approximately 8 hours at a pressure of 2×10^{-4} mm Hg. The device was then fueled, sealed and connected to the vacuum system. The device was outgassed at an outer can temperature of 312 C for about 3-1/2 hours. During this period the lower base plate temperature was maintained at approximately 100 C with air cooling. The device was pinched off from the vacuum system at a pressure of 1.5×10^{-6} mm Hg.

The fuel for the second series of heat transfer experiments was outgassed according to the schedule listed in Table A-8. The device was then fueled, sealed and outgassed. On two occasions difficulties were experienced in pinching off the device from the vacuum system due to an improperly annealed exhaust tube. In addition the device was deliberately opened to atmospheric pressure when an inspection of the base plate showed a cut in a wire solder joint. After each of these events it was necessary to re-outgas the device. The final outgassing was carried out at an outer jacket temperature exceeding 400 C for

approximately 2 hours. The device was pinched off from the vacuum system at a pressure of 1×10^{-8} mm Hg.

I
I
I
I
I
I
I
I
I
I

Table A-1. Synopsis, Experiment 73-19

Date: September 12, 1967

Description of Assembly. The heat transfer assembly for this experiment is described in Section A-1. The same device was also used in the electrical calibration experiment of Section 3. During the inlet experiment, six operable Pt - Pt, 13% Rh thermocouples were attached to the emitter in accordance with Thermocouple Pattern 2 shown in Figure A-14. Two additional Pt - Pt, 13% Rh thermocouples were attached to the structure, one at the base of the molybdenum support pin and the other on the tantalum cylinder at the inner boundary of the upper Kovar support ring. Two copper-constantan thermocouples were attached to the base and top plates and two chromel-alumel thermocouples were installed in the inlet and outlet coolant lines. Thermocouple measurements were made using a Type K-1 potentiometer (Leeds & Northrup Co.). The coolant flow was measured by a flowmeter and by timed volume measurements.

Experimental Results:

Time	Reactor power, KW	Device temperatures, C										Inlet H ₂ O, MV	Outlet H ₂ O, MV	ΔT, C	Flow, cc/sec	Device power, watts	Structure heating, watts	Emitter power, watts
		1	2	3	4	5	6	7	8	9	10							
1812	20	36.7	36.2	35.6	38.6	20.5	144	37.7	37	40	30	0.86-10	0.8760	0.37	17 RR	58	8	50
1810	40	51.8	52.6	50.9	54.7	24.4	181	52.2	51.7	--	--	--	--	--	--	--	--	--
1848	62	70.1	67.5	66.7	71.7	33.7	262	69.0	67.3	67	50	0.8897	0.9789	2.18	17 RR	145	31	312
1915	130	86.7	82.2	82.2	89.1	40.1	322	85.4	83.3	79	60	0.9324	1.0078	1.84	17 RR	292	52	-
1942	199	104.0	100.7	98.9	109.5	48.5	386	102.7	101.2	102	70	0.9895	1.1964	5.04	17 RR	800	80	770
2006	260	123.9	115.5	112.6	127.5	58.3	435	117.3	116.3	122	83	1.0596	1.3403	6.84	17 RR	1085	94	991
2021	300	129.0	121.2	118.3	135.8	57.6	448	123.1	121.9	98	91	1.1087	1.4194	7.58	17 RR	1203	120	1083
2043	350	135.5	126.5	124.5	143.3	59.1	420	130.1	127.0	77	98	1.1726	1.5304	8.72	17 RR	1383	140	1243

Operating Summary:

1710 Critical, 1 KW rod position, shim rods at 19.7 in regulator rod at 8.4 in
 1802 Power level at 20 KW, regulator rod at 8.57 in
 1820 Increased power
 1822 Power level at 40 KW, regulator rod at 8.65 in
 1837 Increased power
 1842 Power level at 80 KW, regulator rod at 8.81 in
 1858 Increased power
 1905 Power level at 130 KW, regulator rod at 9.01 in
 1912 Power level at 200 KW, regulator rod at 9.16 in
 1956 Increased power
 1958 Power level at 260 KW, regulator rod at 9.65 in
 2015 Increased power
 2016 Power level at 300 KW, regulator rod at 9.77 in
 2035 Increased power
 2043 Power level at 350 KW, regulator rod at 10.12 in
 2049 Decreased power
 2056 Power level at 200 KW
 2140 At 1 KW, power decreased on ~ 400 second period
 2145 Shutdown

Table A-2. Synopsis, Experiment 73-20

Date: September 19, 1962

Description of Assembly. Same as that for Experiment 73-19 Thermocouple pattern 2 shows the thermocouple locations (Figure A-14)

Purposes of the Experiment:

- 1 To investigate the effect on emitter temperatures of variations in rod position
- 2 To determine whether the results were reproducible after a thermal cycle and after a shutdown of one week

Experimental Results:

Time	Reactor power, KW	Emitter temperatures, C								Inlet H ₂ O, MV	Outlet H ₂ O, MV	Δ T C	Flow cc/sec	Device power, watts	Structure y heating, watts	Emitter power, watts
		1	2	3	4	5	6	7	8							
1430	80	707	676	688	727	108	--	710	674	--	--	--	--	--	--	--
1511	200	924	869	836	953	380	--	920	873	1.0418	1 2489	5.05	37.02	783	80	700
1533	80	610	575	593	620	256	--	616	576	--	--	--	--	--	--	--

Operating Summary:

- 1110 Critical, 1-KW rod position, shim rods at 19.7 in., regulator rod at 8.8 in
- 1340 Power level at 20 KW regulator rod at 8.8 in
- 1409 Increased power
- 1413 Power level at 80 KW, regulator rod at 9.08 in
- 1440 Increased power
- 1445 Power level at 200 KW, regulator rod at 9.53 in
- 1519 Decreased power
- 1525 Power level at 80 KW regulator rod at 9.0 in
- 1552 Decreased power
- 1613 Shutdown

Table A-3. Synopsis, Experiment 73-21

Date: September 20, 1962

Description of Assembly: Same as that for Experiment 73-19. A single channel recorder with a suitable switching arrangement was added to the instrumentation to monitor temperatures with time. Thermocouple Pattern 2 shows the thermocouple locations (Figure A-14).

Purpose of the Experiment: To investigate the change in heat transfer characteristics evident in Experiment 73-20.

Experimental Results:

Time	Reactor power, KW	Device temperatures, C										Inlet H ₂ O, MV	Outlet H ₂ O, MV	Δ I, C	Flow, cc/sec	Device power, watts	Structure y heating, watts	Emitter power, watts	
		1	2	3	4	5	6	7	8	9	10								
1048	20	109	290	307	310	--	--	317	290	27	29	--	--	--	--	--	--	--	--
1112	80	684	646	670	699	291	--	693	650	46	47	0.9904	1.0084	1.97	39.38	324	32	792	
1155	130	815	769	790	837	342	--	818	770	58	57	1.0114	1.0920	3.49	40.50	592	52	140	
1225	150	848	797	821	872	355	--	850	801	63	60	1.0134	1.1566	3.97	40.50	673	60	413	
1255	200	920	851	886	949	379	--	918	865	74	68	1.0376	1.2002	5.43	39.23	891	80	811	
1321	260	1002	934	958	1036	410	--	997	940	87	79	1.0935	1.3159	7.02	39.23	1153	94	1359	
1346	300	--	--	--	--	--	--	--	--	--	--	--	1.5175	8.02	39.23	1317	120	1197	
1352	400	1156	1069	1098	1196	467	--	1145	1076	114	97	1.1509	1.4386	10.71	39.07	1753	160	1793	
1417	200	876	812	834	896	360	--	874	821	79	74	1.2557	1.4935	5.80	39.23	952	80	872	
1430	130	729	683	704	746	306	--	736	686	64	64	1.2509	1.3988	3.61	39.23	592	52	840	
1445	80	587	556	571	596	251	--	596	554	53	55	1.2552	1.3464	2.23	39.07	364	32	332	

Operating Summary:

- 1000 Critical
- 1011 Power level at 20 KW, shim rods at 19.7 in., regulator rod at 9.98 in.
- 1045 Increased power
- 1108 Power level at 80 KW, regulator rod at 10.26 in.
- 1133 Increased power
- 1136 Power level at 130 KW, regulator rod at 10.42 in.
- 1205 Increased power
- 1207 Power level at 150 KW, regulator rod at 10.55 in.
- 1239 Increased power
- 1241 Power level at 200 KW, regulator rod at 10.85 in.
- 1306 Increased power
- 1310 Power level at 260 KW, regulator rod at 11.24 in.
- 1331 Increased power
- 1333 Power level at 300 KW, regulator rod at 11.60 in.
- 1343 Increased power
- 1348 Power level at 400 KW, regulator rod at 12.17 in.
- 1357 Decreased power
- 1405 Power level at 200 KW, regulator rod at 11.79 in.
- 1421 Decreased power
- 1425 Power level at 130 KW
- 1436 Decreased power
- 1440 Power level at 80 KW
- 1451 Decreased power
- 1507 Shutdown

8-V

Table A-4. Synopsis, Experiment 73-23

Date: December 14-15, 1962

Description of Assembly The heat transfer device used for this experiment was the same as that used in the first series of inpile tests with the following changes:

- 1 The fuel was outgassed at a higher temperature
- 1 There was an improved vacuum in the device at pinch-off
- 1 The center of the fuel was located one inch below the centerline of the core
- 1 A longer pinch-off tube was left on the device requiring a change in the top external plate
- 1 The aluminum coolant jacket was modified by replacing the drilled coolant channels with aluminum tubing. This modification required a change in the method of connecting the parallel flow paths through the jacket to the single inlet and outlet lines. See Figure A-4

Ten Pt-Pt, 13% R1 thermocouples were installed on the emitter in accordance with Thermocouple Pattern 3 shown in Figure A-14. Two copper-constantan thermocouples were placed on the base plate. Two chromel-alumel thermocouples were installed in the 1/4-inch fittings in the inlet and outlet water lines. Temperatures were monitored throughout the experiment using a multi-point recorder. More precise measurements were made with a Type K-3 potentiometer (Leeds & Northrup Company) at equilibrium conditions at each power level. The coolant flow rate was determined from timed volume measurements.

Experimental Results:

Time	Reactor power KW	Emitter temperatures, C								Base plate temp, C	Inlet H ₂ O, MV	Outlet H ₂ O, MV	ΔT, C	Flow cc/sec	Device power, watts	Structure heating, watts	Emitter power, watts	
		1	2	3	4	5	6	7	8									10
Dec 14,																		
1628	10	238	242	251	250	253	278	239	251	250	29	0.5269	0.5410	0.34	32.26	46	5	41
1715	20	376	384	399	396	399	364	376	400	396	31	0.5216	0.5616	0.98	33.80	138	10	128
1812	80	766	785	810	793	818	760	765	819	813	6	0.5222	0.5861	1.56	46.52	303	38	215
1923	120	910	932	968	945	980	911	915	945	998	76	0.4882	0.6190	3.19	38.17	510	58	412
2044	200	1101	1127	1169	1145	1198	1121	1113	1198	1224	98	0.5718	0.7989	5.54	37.32	866	96	770
2148	262	1215	1245	1286	1263	1374	1242	1248	1327	1358	113	0.6100	0.9071	7.25	43.10	1313	126	1187
2304	264	1211	1241	1278	1253	1315	1236	1246	1317	1352	113	0.6465	0.9374	7.09	42.74	1268	127	1141
Dec 15,																		
0015	270	1191	1220	1258	1234	1300	1219	1225	1299	1335	110	0.644	0.934	7.07	46.72	1383	130	1253
0043	290	1205	1233	1274	1247	1316	1233	1236	1316	1361	115	0.645	0.971	7.95	46.72	1554	139	1415
0112	290	1169	1195	1235	1210	1279	1200	1202	1277	1315	116	0.710	1.110	9.75	35.46	1446	139	1307
0137	340	1196	1220	1261	1234	1310	1226	1225	1308	1346	125	0.720	1.171	11.0	35.72	1645	163	1482
0205	340	1161	1183	1224	1197	1270	1191	1191	1268	1308	122	0.715	1.169	11.1	35.96	1670	163	1507
0220	390	1209	1231	1270	1244	1310	1236	1232	1313	1357	131	0.720	1.234	12.5	35.95	1888	187	1699
0305	200	903	911	938	911	967	912	924	966	994	84	0.636	0.916	6.83	36.23	1036	96	940
0354	130	761	763	785	759	807	761	774	805	826	64	0.657	0.820	3.98	36.23	602	62	540
0447	80	608	604	620	600	636	600	614	636	651	47	0.619	0.708	2.17	36.23	329	38	291
0545	20	274	270	275	265	278	261	269	278	284	24	0.542	0.588	1.12	35.47	167	10	157
0631	10	173	171	173	167	175	164	169	175	178	17	0.514	0.555	1.00	35.47	148	5	143

Table A-4. (Cont'd)

Operating Summary:

1540 Power level at 1 KW Shim Rods 1 and 2 at 18.45 in , Shim Rod 3 at 18.49 in , regulator rod at 34.5 cm
1551 Increased power
1758 Power level at 10 KW, regulator rod at 34.8 cm
1642 Increased power
1645 Power level at 20 KW regulator rod at 34.84 in
1735 Increased power
1750 Power level at 80 KW, all shims at 18.45 in , regulator rod at 34.2 cm
1852 Increased power
1910 Power level = 123 KW regulator rod at 34.8 cm
2002 Increased power
2039 Power level at 200 KW
2112 Increased power
2130 Power level = 262 KW, regulator rod at 35.5 cm
2311 Power level = 264 KW, regulator rod at 37.2 cm
2317 Increased power to 268 KW
0029 Increased power to 290 KW
0100 Power level at 290 KW, regulator rod at 40.1 cm
0122 Increased power
0132 Power level at 340 KW
0158 Power level at 340 KW, regulator rod at 42 cm
0214 Increased power
0219 Power level at 390 KW
0240 Power level at 390 KW, regulator rod at 44 cm
0240 Decreased power
0255 Power level at 200 KW
0257 Power level at 200 KW, regulator rod at 45 cm
0318 Decreased power
0329 Power level at 130 KW, regulator rod at 47 cm
0410 Decreased power
0422 Power level at 80 KW, regulator rod at 57 cm
0430 Shims raised to 18.75 in , regulator rod at 42 cm
0458 Decreased power
0520 Power level at 20 KW, regulator rod at 44.5 cm
0557 Decreased power to 10 KW, regulator rod at 47 cm

Table A-5. Synopsis, Experiment 73-24

Date: December 17 1962

Description of Assembly. Same as that of Experiment 73-23. Outlet water temperature (9) and reactor power level (12) were recorded on the multi-point recorder in place of the two device thermocouples that were inoperable during Experiment 73-23.

Experimental Results.

Time	Reactor power KW	Device temperatures, C										Inlet H ₂ O, MV	Outlet H ₂ O, MV	ΔT, C	Flow, cc/sec	Device power, watts	Structure heating, watts	Emitter power, watts	
		1	2	3	4	5	6	7	8	10	11								
1132	1	--	--	--	--	--	--	--	--	--	--	--	--	--	--	--	--	--	--
1233	10	175	170	173	167	173	163	176	174	175	18	--	--	--	--	--	--	--	--
1304	20	276	271	276	266	278	261	276	278	282	21	--	--	--	--	--	--	--	--
1339	80	631	632	646	626	658	620	631	661	675	41	--	--	--	--	--	--	--	--
1502	130	791	794	811	792	830	781	793	825	850	63	0 5861	0 7246	3 38	43 48	615	72	553	
1551	200	911	913	931	911	951	896	904	945	980	78	0 6305	0 8498	5 35	42 75	957	96	861	
1618	290	1053	1058	1075	1059	1100	1035	1038	1083	1135	100	0 6631	0 9812	7 78	42 39	1380	139	1241	
1645	340	1170	1122	1117	1124	1165	1093	1093	1139	1204	108	0 709	1 022	7 63	52 10	1665	163	1502	
1719	340	1114	1114	1117	1116	1155	1084	1084	1128	1196	108	0 757	1 042	6 93	54 95	1594	163	1431	

Operating Summary:

1117 Power level at 1 KW, shim rods at 14 25, regulator rod 38 7 cm
 1154 Increased power
 1206 Power level at 10 KW
 1233 Increased power
 1246 Power level at 20 KW
 1255 Regulator rod at 38 4 cm
 1311 Increased power
 1330 Power level at 80 KW
 1345 Regulator rod at 38 8 cm
 1410 Increased power
 1424 Power level at 130 KW
 1455 Regulator rod at 38 8 cm
 1510 Increased power
 1523 Power level at 200 KW
 1537 Regulator rod 39 1 cm
 1558 Increased power
 1608 Power level at 290 KW
 1620 Regulator rod at 39 2 cm
 1634 Increased power
 1637 Regulator rod at 39.9 cm
 1728 Reduced power
 1749 Rods in

Table A-6. Synopsis, Experiments 73-25, 73-26, 73-27, 73-28

Dates: 73-25, December 18, 1962
 73-26, 73-27, December 19, 1962
 73-28, December 31, 1962

Description of Assembly: Same as that of Experiment 73-23. Thermocouple Pattern 3 applies. For Experiments 73-26, 73-27, 73-28 a Keithley high speed recorder was used to monitor a mid-plane thermocouple during the rapid shutdown of these experiments

Purpose of the Experiments: Experiment 73-25 was a continuation of Experiments 73-23 and 73-24 to investigate the heat transfer characteristics of the assembly. The remaining three experiments were to investigate the dynamic characteristics of the assembly

Experimental Results:

Experiment	Time	Reactor power, KW	Device temperatures, C										Inlet H ₂ O, MV	Outlet H ₂ O, MV	ΔT, C	Flow, cc/sec	Device power, watts	Structure heating, watts	Emitter power, watts
			1	2	3	4	5	6	7	8	10	11							
73-25	1140	330	--	--	--	--	--	--	--	--	--	--	0.7750	1.0560	6.85	45.9	1317	158	1159
73-25	1312	330	1091	1091	1100	1104	1127	1056	1054	1086	1174	102	0.6647	0.9503	6.97	48.5	1417	158	1259
73-26	1229	80	557	550	554	555	564	528	535	561	581	41	0.6229	0.6690	1.12	46.7	220	38	182
73-27	1648	200	900	896	904	916	926	867	870	913	955	75	0.6690	0.8830	5.22	57.5	827	96	731
73-28	1520	200	854	851	868	761	876	820	888	876	903	70	0.683	0.908	5.49	43.2	985	96	889
73-28	1555	100	589	580	585	587	594	555	561	593	611	47	0.607	0.732	3.05	36.0	415	48	367
73-28	1605	200	855	849	859	870	879	823	826	885	908	70	0.610	0.880	6.79	33.0	968	96	872
73-28	1625	300	1048	1043	1054	1072	1079	1008	1006	1045	1115	93	0.624	0.976	8.59	39.2	1410	144	1266
73-28	1645	350	1120	1123	1136	1151	1157	1074	1066	1113	1399	104	0.656	1.064	9.90	39.7	1648	168	1480

Operating Summary (73-25)

1003 Critical
 1020 Level at 6 KW
 1024 Increased power
 1058 Level at 300 KW
 1103 Shims at 18.2 in., regulator rod at 45.5 cm
 1110 Increased power
 1113 Level at 330 KW
 1120 Shims at 18.2 in., regulator rod at 45.5 cm
 1325 Scram

Operating Summary (73-26)

1104 Critical
 1113 Level at 1 KW
 1119 Shims at 18.2 in., regulator rod at 44.8 cm
 1150 Increased power
 1223 Level at 80 KW
 1231 Shims at 18.2 in., regulator rod at 44.7 cm
 1246 Decreased power by running in regulator rod
 1248 Decreased power by running in shim rods

Operating Summary (73-27)

1609 Critical
 1632 Level at 200 KW
 1635 Shims at 18.2 in., regulator rod at 43.5 cm
 1659 Reactor shutdown by dropping shims

Operating Summary (73-28)

1439 Critical shims at 18.2 in., regulator rod at 40 cm
 1511 Level at 200 KW
 1517 Shims at 18.2, regulator rod at 36.5 cm
 1545 Reduced power to 100 KW
 1548 Level at 100 KW, shims at 18.2 in., regulator rod at 36.5 cm
 1601 Increased power to 200 KW
 1619 Increased power to 300 KW
 1621 Level at 300 KW, shims at 18.2 in., regulator rod at 37 cm
 1637 Increased power to 350 KW
 1638 Level at 350 KW
 1648 Shutdown by manual scram

Table A-7. Synopsis, Electrical Calibration Experiment 4

Date: September 3, 1962

Description of Assembly: The heat transfer device for this experiment is described in Section 3.2.2.1 (The same device was used in Experiments 73-19, 73-20, and 73-21.) Ten operable Pt-Pt, 13% Rd thermocouples were installed on the emitter and support structure in accordance with Thermocouple Pattern 1 shown in Figure A-14. Inlet and outlet cooling water temperatures were measured with thermometers for three flow paths, through the main cooling jacket installed around the device outer can, through the electric heater, and through a series circuit consisting of a heat sink on the top flange of the outer can and a heat sink attached to the copper pinch-off tube or the lower base plate. Electric power input to the heater was measured.

Summary on Experimental Results:

Time	Emitter input, watts	Device temperatures, C										Vacuum, mm Hg
		1	2	3	4	5	6	8	9	10	12	
1947	307	745	744	799	726	837	842	773	785	371	311	3.2×10^{-4}
2040	679	997	994	1056	977	1018	1103	984	996	447	465	7×10^{-4}
2125	1173	1258	1236	1337	1013	1372	1394	1215	1226	566	655	3.5×10^{-4}
2207	1285	1314	1294	1393	1049	1427	1450	1262	1268	620	692	4×10^{-4}
2254	1285	1339	1318	1433	1080	1420	1493	1300	1306	676	--	1.3×10^{-4}
0303	1561	1165	1099	1179	--	1173	1180	988	993	--	--	Helium, 7 microns

Table A-8. Heating Schedule for Outgassing Pellets

	<u>Stack No. 6</u>	
	<u>A</u>	<u>B</u>
Temperature after 1 hour		
Observed, C	1600	1570
Corrected, C.	1930	1820
Time above this temperature, hours	2	1.5
Maximum temperature		
Observed, C	1700	1600
Corrected, C	1970	1930
Time at maximum, hours	0.5	0.4
Minimum pressure, microns	0.025	0.020
Cooling rate, time to 950 C, hours	0.5	0.5

Figure A-1. Base Plate Components

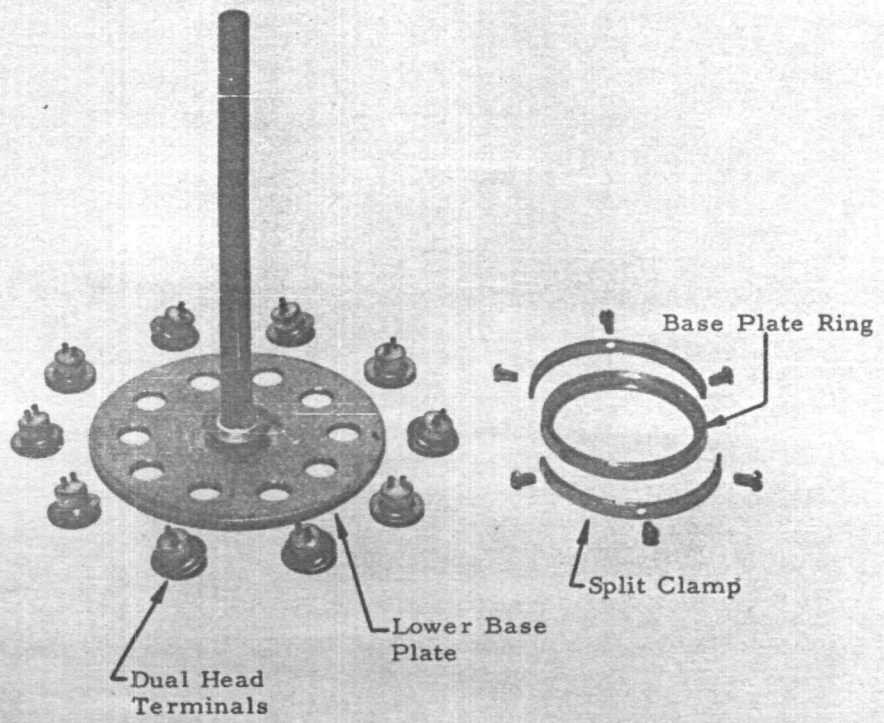


Figure A-2. Emitter Assembly and Base Plate Components

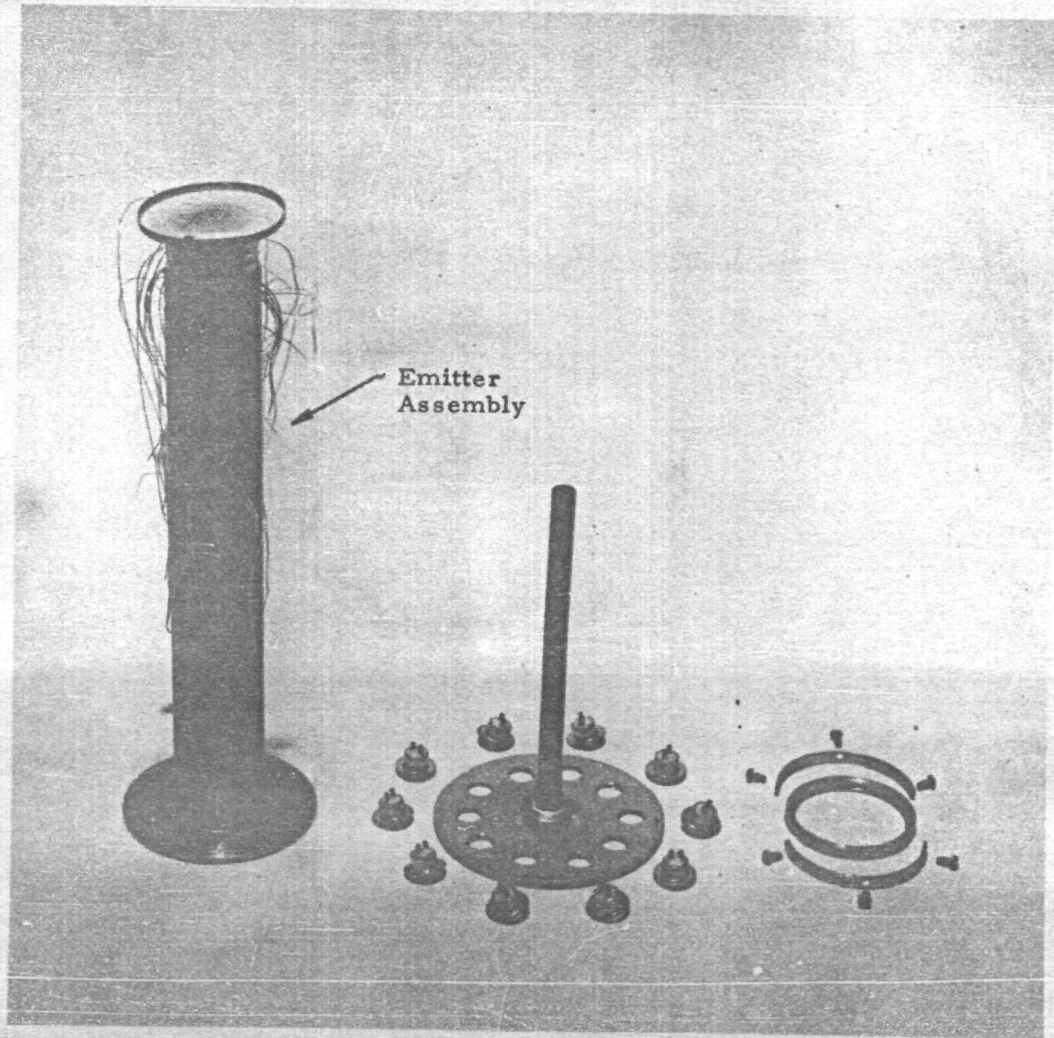


Figure A-3. Components of Heat Transfer Device

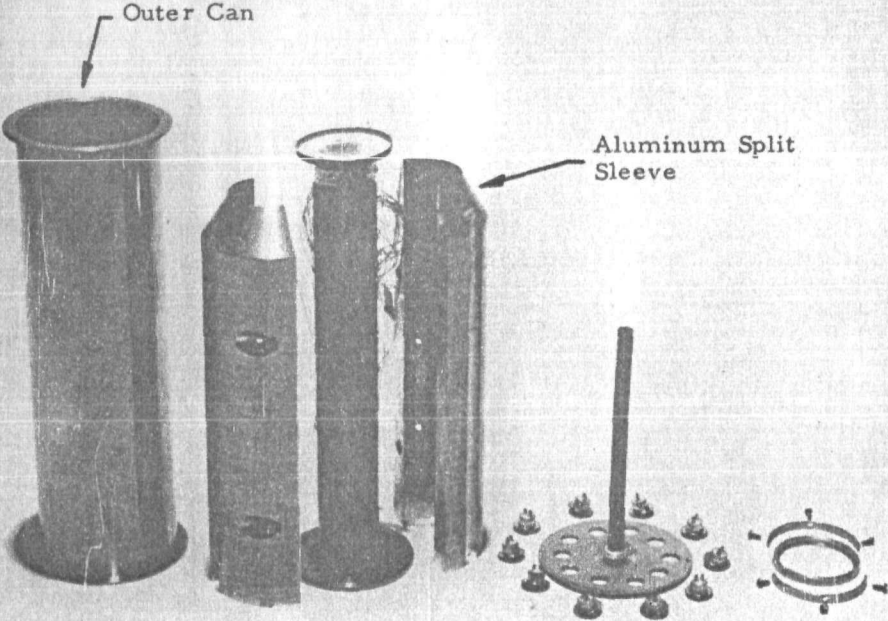


Figure A-4. Heat Transfer Assembly With Extension Tube

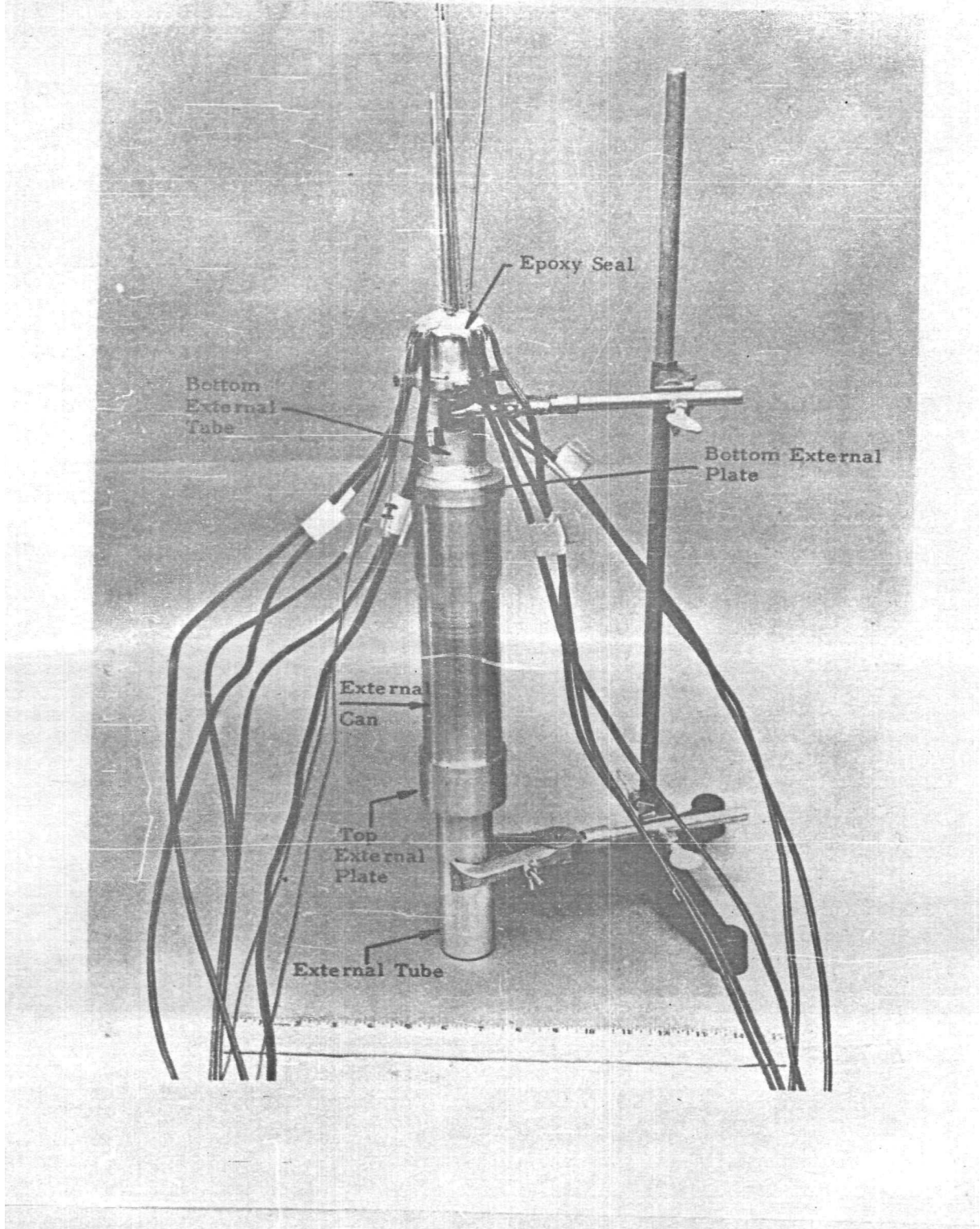
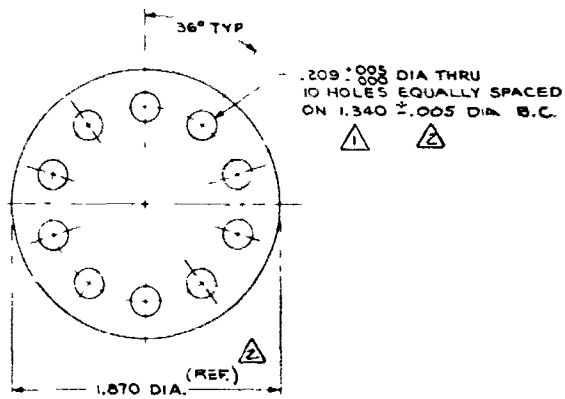
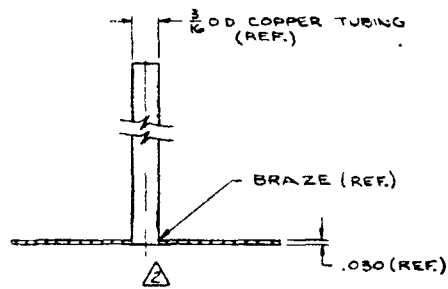
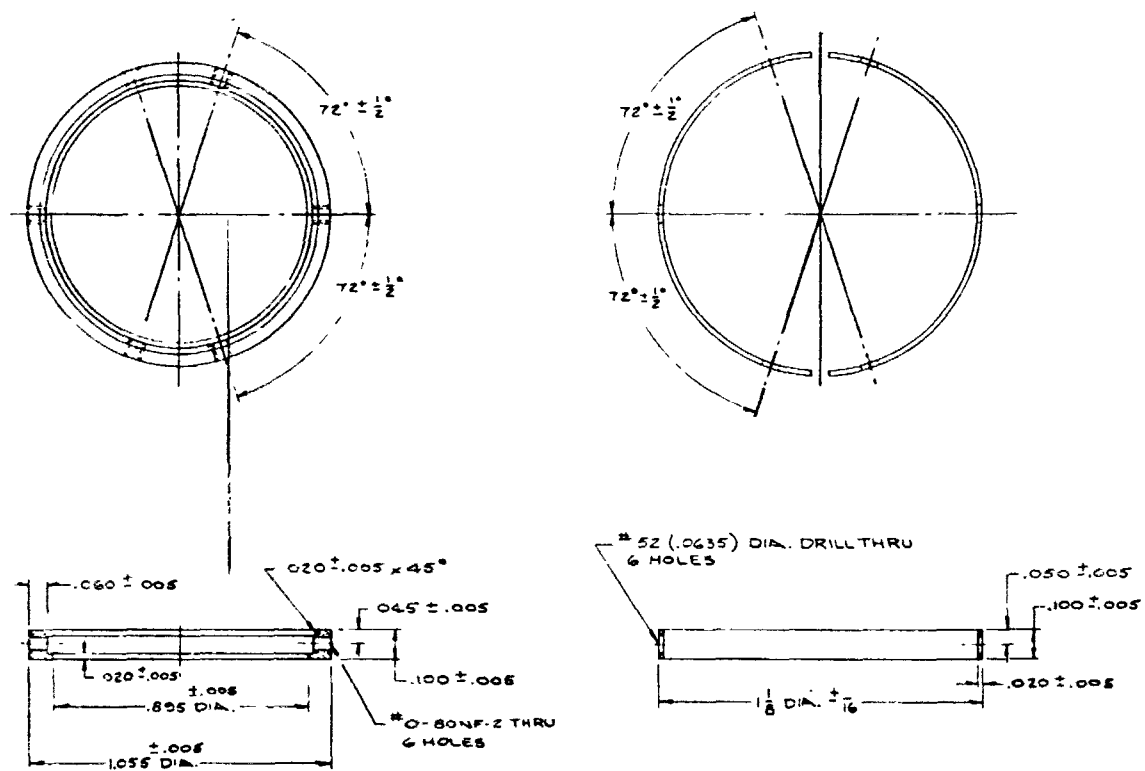


Figure A-5. Lower Base Plate



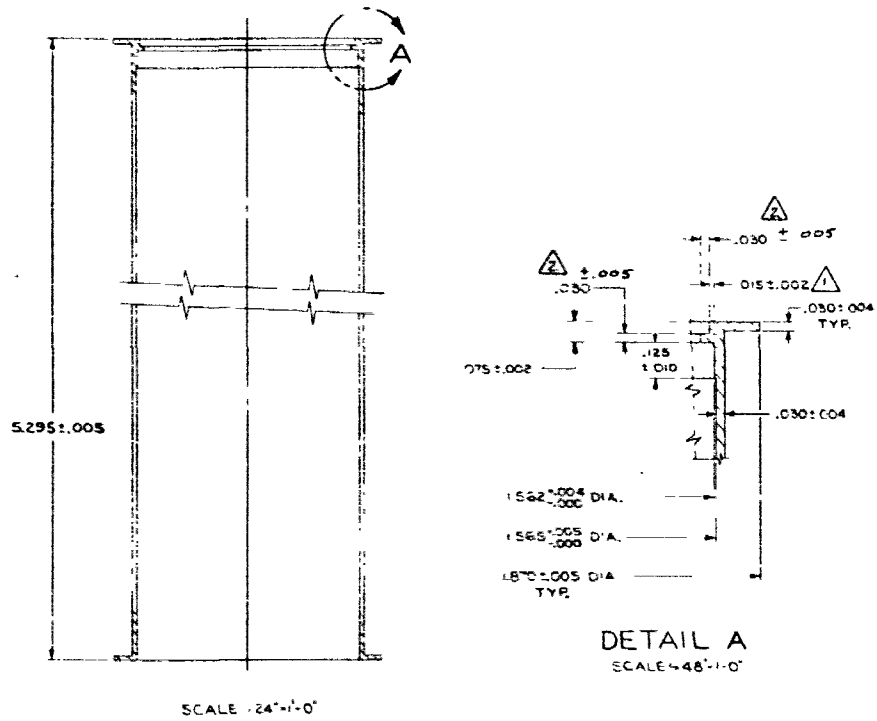
NOTES
1-MATERIAL KOVAR

Figure A-6. Base Plate Ring and Split Clamp



NOTES:
1. MATERIAL - TYPE 304 STAINLESS
STEEL.

Figure A-7. Outer Can



NOTES:

1-MATERIAL-TYPE 304 STAINLESS STEEL

Figure A-8. Split Sleeve

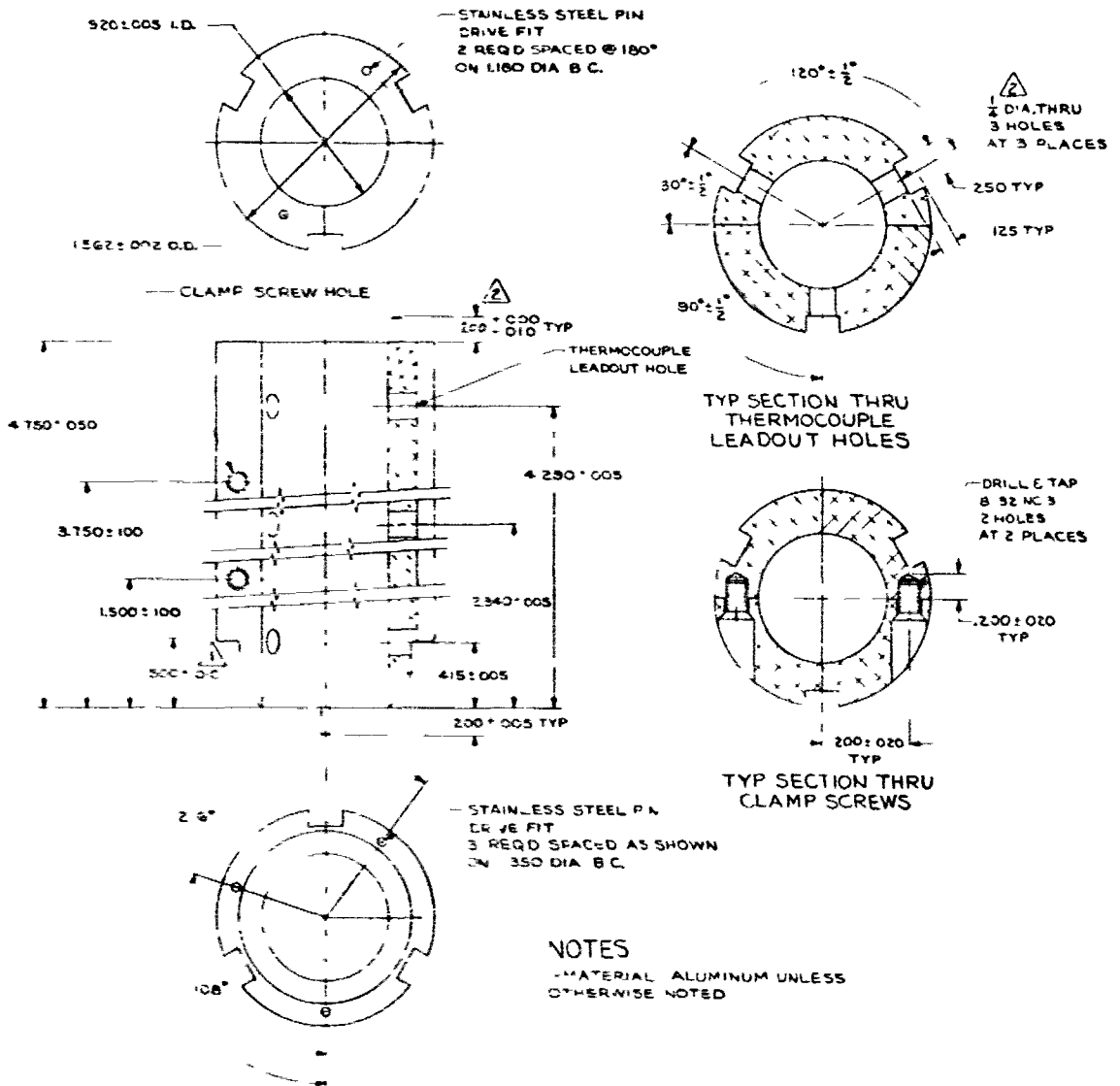


Figure A-9. Cooling Jacket

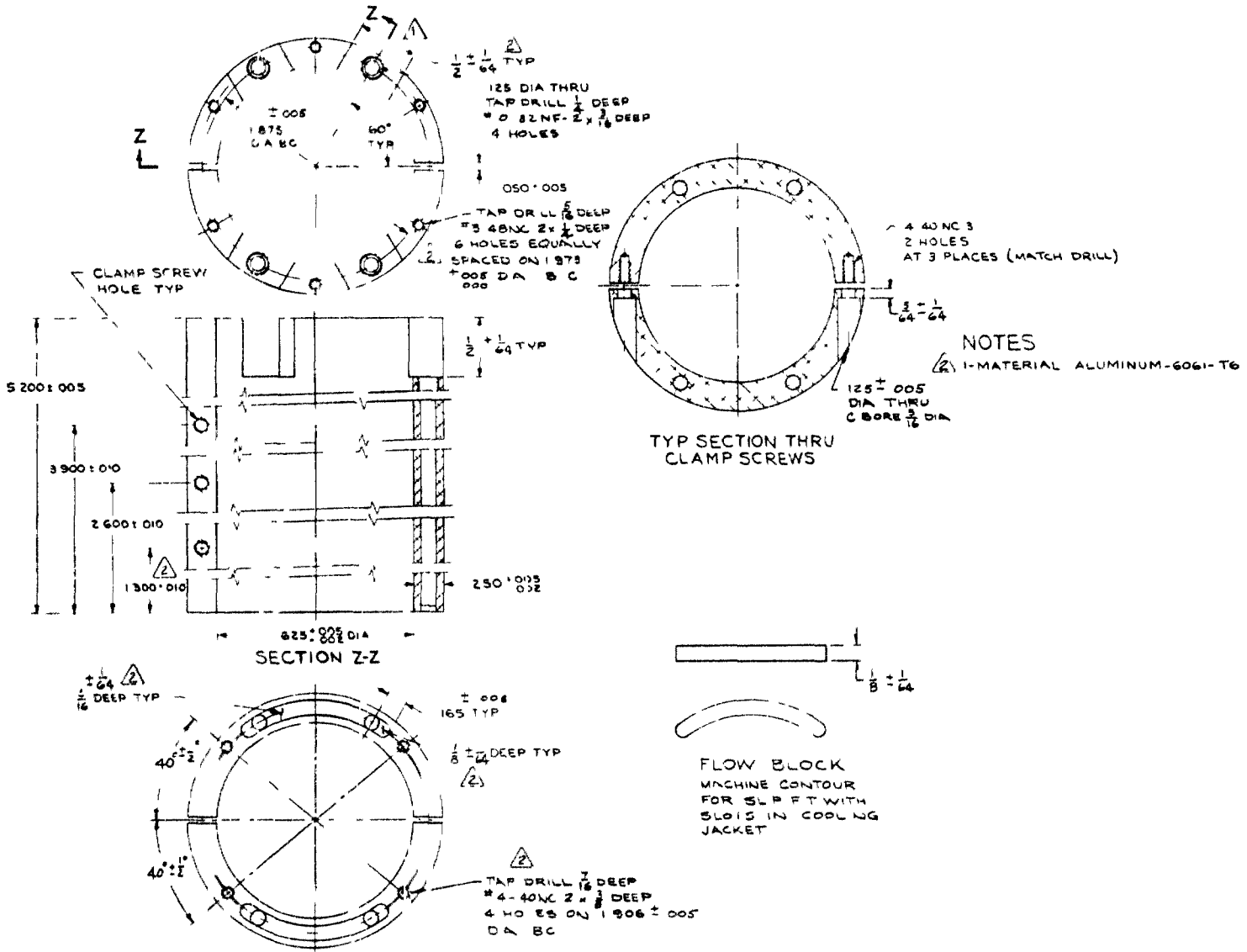
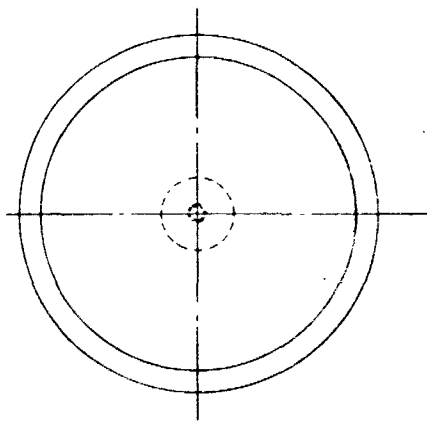
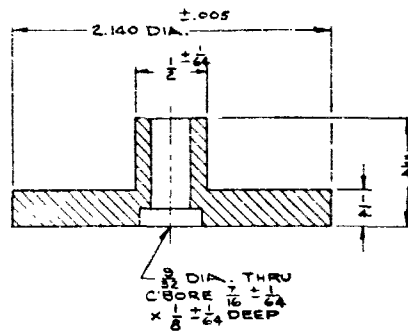
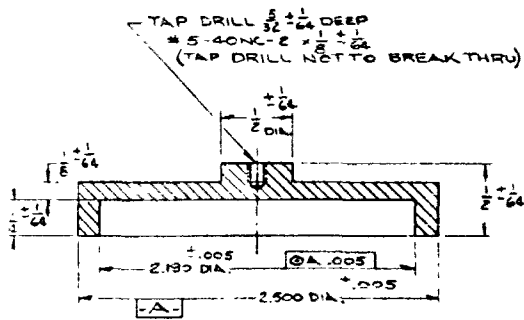
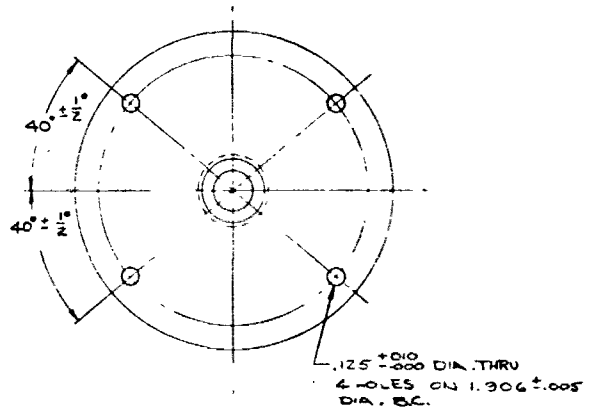


Figure A-10. Top External Plate and Top Heat Sink



TOP EXTERNAL
 PLATE

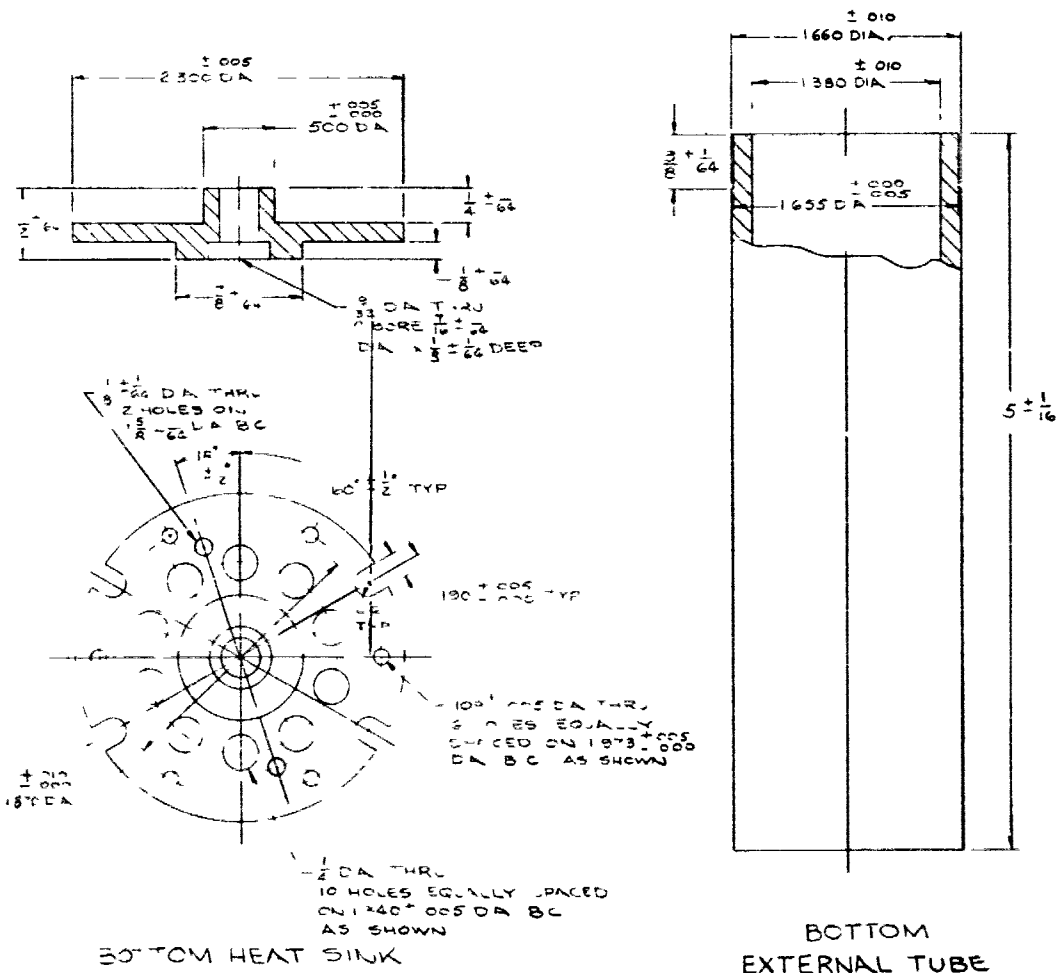


TOP HEAT SINK

NOTES

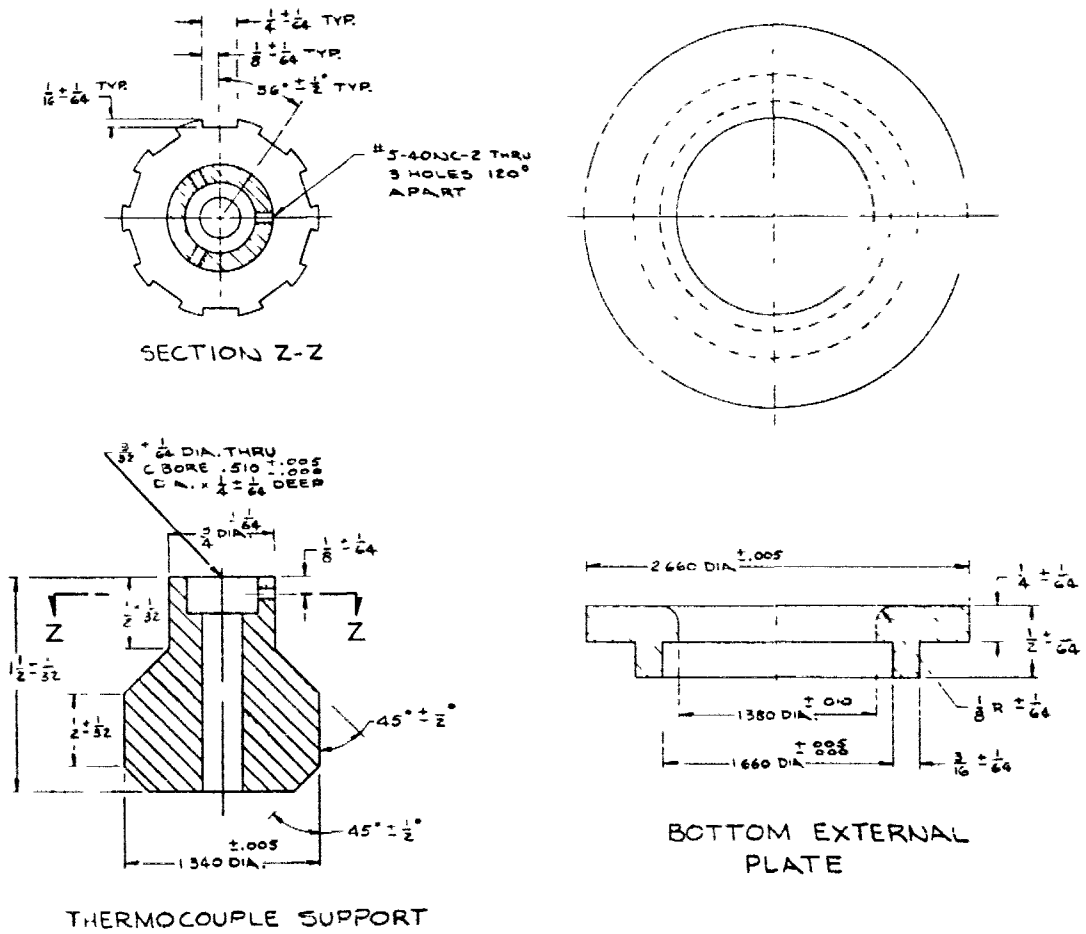
1. MATERIAL - ALUMINUM 6061-T6

Figure A-11. Bottom External Tube and Bottom Heat Sink



NOTES
MATERIAL-ALUM NUM-6061-T6

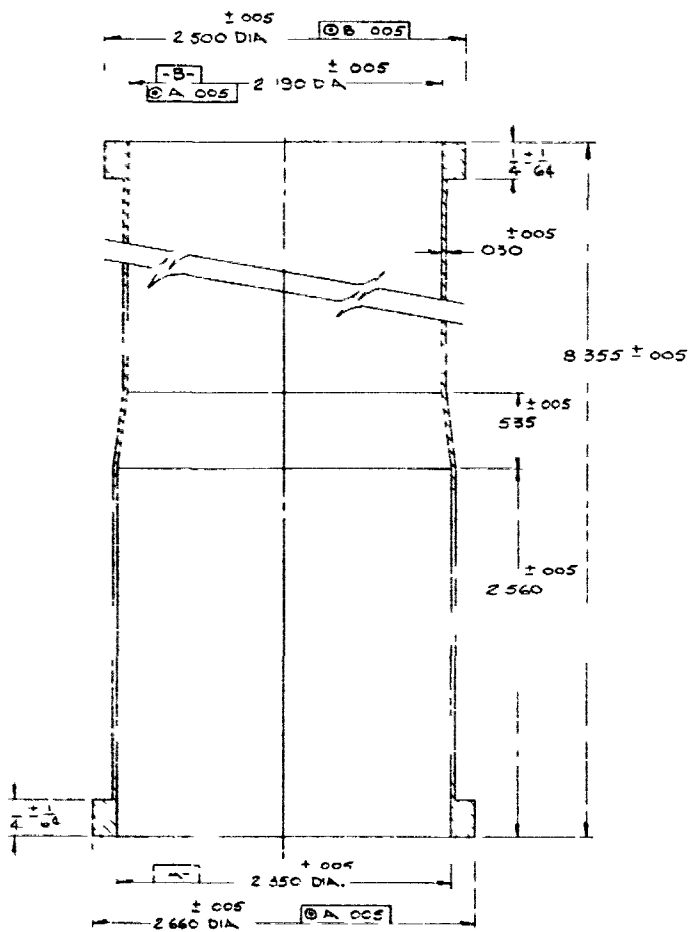
Figure A-12. Bottom External Plate and Thermocouple Support



NOTES

1. MATERIAL-ALUMINUM-6061-T6

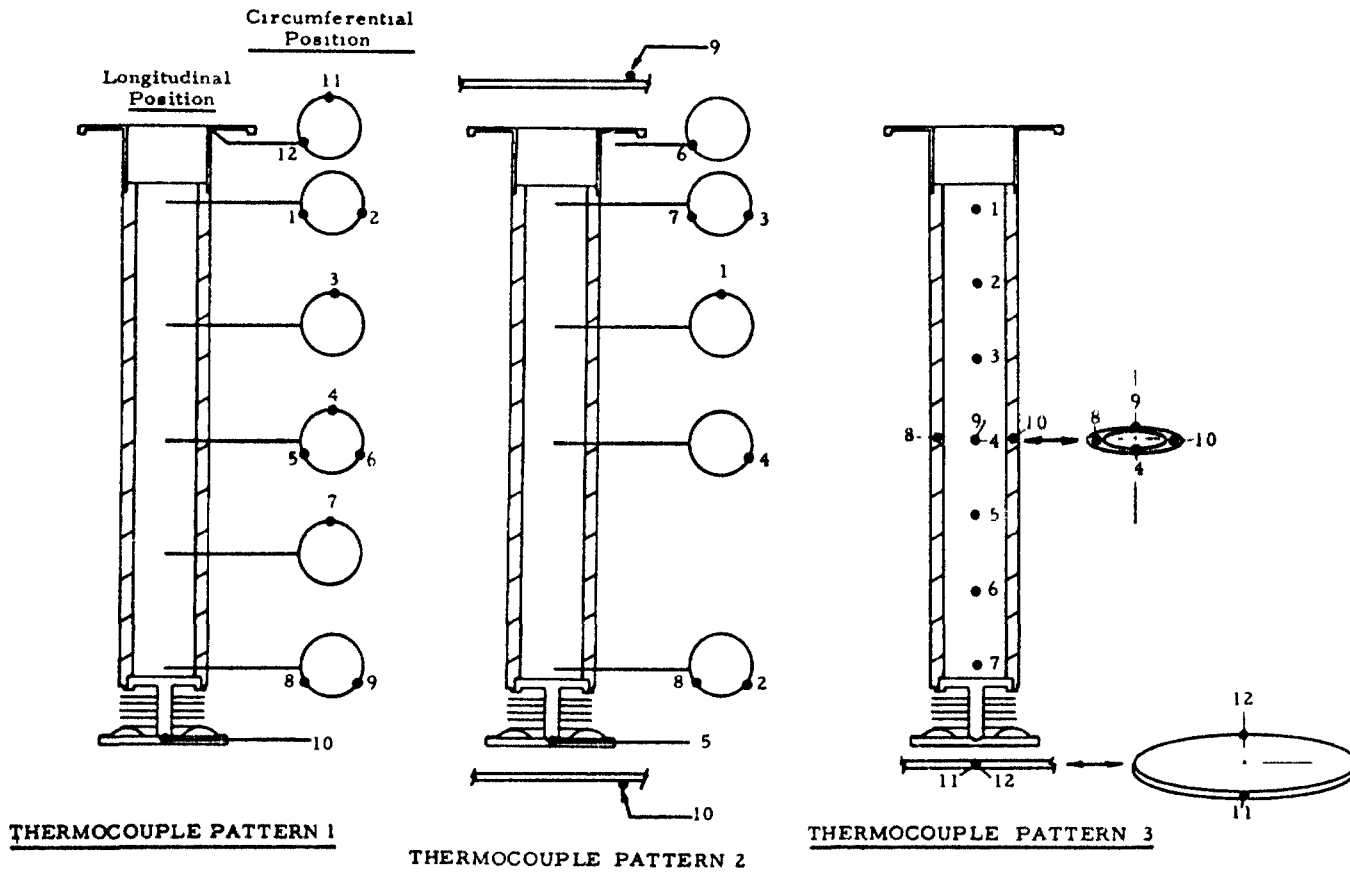
Figure A-13. External Can



NOTES

1. MATERIAL - ALUMINUM - 6061-T6

Figure A-14. Heat Transfer Experiment Thermocouple Patterns



1
1
1
1

APPENDIX B
Thermionic Converter Experiment

L
E
1
1
E
E

APPENDIX B
Thermionic Converter Experiment

1. Converter Materials and Fabrication

To aid in a postirradiation examination of the converter, details of materials and fabrication are included in Figure B-1. The following list identifies the materials in the figure.

16	Kovar	30	Copper, nickel plated
17	Kovar	31	Kovar
18	Tantalum	32	Nickel
19	Kovar	33	Molybdenum
20	OFHC copper, nickel plated	34	Nickel
21	Nickel	35	Molybdenum
24	Stainless steel	36	Nickel
25	Molybdenum	38	Ceramic, metalized and nickel plated
26	Niobium	45	Nickel
28	Kovar, nickel plated		
29	Copper, nickel plated		

2. Fuel Preparation

The fuel consisted of six UO_2 -fuel pellets enriched to 20% by weight of U^{235} . The total weight of the fuel stack was 133 grams. The pellets were sintered in hydrogen at 1790 C for 6 hours.

All fuel was outgassed prior to use. This outgassing was performed in a vacuum furnace in two units of three pellets each. An additional pellet was outgassed to determine the quantity of gas evolved over four temperature intervals and to determine the constituents of the gas collected. Table B-1 gives the heating schedule; Table B-2 gives dimensions before and after outgassing; Table B-3 gives the quantity of gas evolved from a single pellet; and Table B-4 gives the analyses of the evolved gas.

At the highest temperature interval, 1730-2000 C, the volume of gas collected was less than that collected with no sample in the apparatus.

It is possible that the recorded blank correction was not reliable; therefore it cannot be stated positively that there was or was not any gas evolved from the pellet in this temperature interval. However, it is fairly certain that any amount evolved would be smaller than the amount evolved in the next lower temperature interval. In the analyses there were small amounts of nitrogen. It was assumed that the nitrogen represents atmospheric contamination; therefore the amount of nitrogen and the atmospherically proportional amount of oxygen have been subtracted from the observed amounts. The volume percentages reported are therefore adjusted to the air-free basis. The fairly high percentages of carbon-containing constituents may reflect the possibility of contamination from the vacuum grease and wax used to seal the furnace compartment. These joints were cooled with air blowers and all due precautions were taken to avoid contamination, but the possibility of contamination remains, especially at the highest operating temperatures.

A shiny substance was observed on the fuel surface after outgassing. This substance was certainly molybdenum from the molybdenum boat, which supported the pellets during outgassing. Since the pellets were to be used in a molybdenum emitter structure, no attempt was made to clean the pellets.

Table B-1. Heating Schedule for Outgassing Pellets

	<u>Stack No. 4</u>	
	<u>A</u>	<u>B</u>
Temperature after 1 hour		
Observed, C	1700	1850
Corrected, C	2020	2160
Time above this		
temperature, hours	6	1.5
Maximum temperature		
Observed, C	1865	1855
Corrected, C	2180	2170
Time at maximum, hours	1	0.5
Minimum pressure,		
microns	3	0.8
Cooling rate, time to		
950 C, hours	1	0.5

Table B-2. Dimension Changes During Outgassing Treatment

	Diameter in mils ^(a)			Length in mils ^(b)		
	<u>Before</u>	<u>After</u>	<u>Change</u>	<u>Before</u>	<u>After</u>	<u>Change</u>
Stack No. 4, Set A						
Top	492.5	491.2	-1.3	708.5	708.8	+0.3
Bottom	492.4	490.6	-1.8	703.9	707.6	+3.7
Stack No. 4, Set B						
Top	492.3	490.7	-1.6	707.0	707.1	+0.1
Middle	492.2	492.7	+0.5	708.0	712.2	+4.2
Bottom	492.3	494.1	+1.8	710.8	714.3	+3.5
Single pellet	492.0	492.7	+0.7	715.0	715.8	+0.8

(a) All diameters \pm 0.2 mil.

(b) All lengths \pm 0.5 mil.

Table B-3. Quantity of Gas Evolved From a Single Pellet

<u>Temperature interval, C(a)</u>	<u>Time at temperature</u>	<u>Volume collected, ml STP</u>	<u>Blank correction, ml STP</u>	<u>Corrected volume, ml STP</u>	<u>Volume per gram of UO₂, ml^(b)</u>
25-1300	2 hr 30 min	7.76	0.13	7.63	0.330
1300-1550	1 hr 45 min	0.63	0.13	0.50	0.0216
1550-1730	1 hr 40 min	0.53	0.33	0.20	0.0086
1730-2000	1 hr 20 min	0.68	0.77	--	--

(a) Temperatures corrected for window losses and emissivity.

(b) Pellet weight = 23.133 gm.

Table B-4. Analyses of Evolved Gas

Temperature interval, C	Volume percentage				
	H ₂	O ₂	CH ₄	CO	CO ₂
25-1300	77.7	0.1	--	7.4	14.8
1300-1550	72.1	0.8	--	18.0	9.0
1550-1730	65.0	7.2	--	18.5	9.3
1730-2000	61.4	1.2	1.5	30.7	5.1

3. Device Outgassing

After the device was fueled, the fuel-chamber end-cap assembly was welded on and the assembly was helium leak tested. The exhaust tube was connected to the vacuum system, evacuated, and placed in a steel container in the bake-out oven. The container was flushed with helium during the bake-out at 300 C. Figures B-2 through B-7 illustrate this sequence.

After bake-out a faulty pinch-off occurred because of improper annealing of the exhaust tube. A tube was torch brazed to the exhaust tube using B-T solder without flux. The bake-out was repeated and a pinch-off was made at a pressure of 4×10^{-8} mm Hg.

4. Evaluation of End Losses

Data received from additional electrical tests after inpile operation (RCA Type A1197, Device 40) indicated that, at an electrical power output of 135 watts and a cesium reservoir temperature of 325 C, the calorimetric measurements were the following:

1. Heater input - 1909 watts.
2. Cs heater input - 70 watts.
3. Electrical output - 135 watts.
4. Emitter cooling - 217 watts.
5. Collector cooling - 990 watts.
6. Heater cooling - 640 watts

A heat balance ignoring the cesium heater input yields

$$\text{Input} = \text{Output}$$

$$1909 + x = 135 w + 217 w + 990 w + 640 w$$

or

$$1909 + x = 1982 \text{ watts.}$$

But x equals 73 watts, almost exactly the 70-watt cesium-heater input.

Since the heater is quite well insulated, it is reasonable to assume that the heat is lost into the lower-emitter cooling water. The end losses would therefore be $217 - 70 = 147$ watts for both ends, or about 74 watts for each end. This value is consistent with the design end-loss value.

Since no measurements of end losses were possible during the inpile tests, it is concluded that the end losses were a total of 150 watts at an output of 135 watts inpile. This loss should be proportional to emitter end temperatures. The pool water which was the heat sink was at about 18 C.

It is necessary to derive a relationship of end loss versus emitter temperature. It may be assumed that these losses are proportional to the temperature difference between the upper emitter end temperature and the cooling water temperature. However, the lower end is heated by the cesium heater as well as the emitter. The pool water temperature was about 18 C. Assuming that the total loss is proportional to the upper emitter end temperature, the relationship is

$$P_e = \left(\frac{T_{\text{top}} - 18 \text{ C}}{462 \text{ C}} \right) 150 \text{ watts.}$$

5. Resistance and Cooling Water Calibrations

Figure B-8 is the calibration curve of the inpile nickel load tubes as a function of thermocouple emf. Figure B-9 summarizes the resistance measurements of all segments of the inpile load. The resistance measurements of the out-of-pool load are summarized in Figure B-10. The cooling-water flow-meter calibration measurements are summarized in Figure B-11.

6. Converter Experiment Data

The instrumentation for taking data has been described. In general, data was read on the Type K-3 potentiometer every two hours during the entire run. Data was also taken continuously on two multipoint recorders. This data was always corrected by comparison to the potentiometer before presentation.

To determine the input power from the calorimetric measurements, it was necessary to correct for the flow distribution between the loads as shown in the following formula:

$$P_{in} = \frac{T_1 - T_{in}}{0.041} \times F_1 \times 4.187 + \frac{T_2 - T_{in}}{0.041} \times F_2 \times 4.187$$

where

T_1 = outlet water temperature, Load 1, millivolts

T_{in} = inlet water temperature, millivolts

F_1 = flow in Load 1 = total flow \times 0.455

T_2 = outlet water temperature, Load 2, millivolts

F_2 = flow in Load 2 = total flow \times 0.545

0.041 = mv/C for chromel-alumel.

To determine the electrical output power, it was necessary to establish the resistance of each of the three loads. The outer load resistance was that of the room temperature measurement. Load 1 resistance was read from the emf vs resistance calibration curve (Figure E-8). The thermocouple on Load 2 failed. Therefore the emf (E_2) was determined with the following relationship:

$$E_2 = E_1 + (E_{01} - E_{02})$$

where

E_1 = Load 1 emf

E_2 = Load 2 emf

E_{01} = Load 1 outlet water temperature, millivolts

E_{02} = Load 2 outlet water temperature, millivolts

The voltage drop across each load and the resistances were then used to determine the current in each load. The three currents were then added

and multiplied by the emitter-to-collector voltage to obtain electrical power.

Table B-5 lists the temperature measurements made throughout the run; Table B-6 lists the calorimetric and voltage measurements.

Table B-5. Converter Temperatures During 300-Hour Run

Date	Time	Thermocouple locations									
		Top collector 1	Top seal 2	Center collector 3	Bottom seal 4	Bottom collector 5	Top emitter 6	Bottom emitter 7	C# 1 8	C# 2 9	
<u>1/15/63</u>	1114	13.5 C	14 C	13.5 C	14 C	13 C	14 C	14 C	14 C	14 C	
	1135	14.5	15	15.5	16	--	15.5	12	15.5	15.5	
	1340	14	15	15	15	16	15	12	15	15	
	1437	24	29	33.5	33.5	34.5	31	49	25	25	
	1513	35	43	51	53	72	48	63	37	36	
	1611	160	199	128	145	136	237	164	136	135	
	1650	227	249	188	189	196	274	198	169	159	
	1756	356	338	360	280	330	334	257	224	216	
	1845	402	390	398	325	425	350	260	251	264	
	1941	463	403	481	356	471	391	304	298	295	
	2040	543	456	599	400	531	448	336	335	313	
	2254	547	456	567	407	543	442	336	328	326	
	<u>1/16/63</u>	0205	568	471	596	415	557	453	344	338	336
		0318	576	477	596	414	555	462	347	332	328
1045		608	494	621	422	567	474	448	349	330	
1656		597	490	613	422	567	470	358	335	331	
1940		594	488	611	420	564	469	356	333	328	
2125		589	485	607	418	560	468	354	332	327	
<u>1/17/63</u>	0009	587	484	606	417	559	469	353	330	326	
	0216	585	475	603	415	556	466	351	330	326	
	0413	585	482	603	415	556	468	351	329	324	
	0608	585	471	603	415	556	467	351	329	324	
	0830	585	483	603	414	557	466	352	329	324	
	1049	587 C	484 C	604 C	415 C	557 C	466 C	355 C	329 C	324 C	

B-9

Table B-5. (Cont'd)

Date	Time	Thermocouple locations								
		Top collector 1	Top seal 2	Center collector 3	Bottom seal 4	Bottom collector 5	Top emitter 6	Bottom emitter 7	Ca 1 8	Ca 2 9
	1335	592 C	485 C	607 C	414 C	559 C	475 C	358 C	328 C	323 C
	1710	593	485	608	414	560	477	353	327	322
	2006	592	485	608	413	558	477	354	327	322
	2235	602	493	617	421	566	480	352	327	328
<u>1/18/63</u>	0048	602	493	617	421	567	481	352	314	328
	0300	603	493	617	421	567	491	354	333	328
	0515	603	492	616	421	567	481	354	333	328
	0730	601	491	614	420	567	478	348	332	327
	0950	601	492	615	420	566	480	352	332	327
	1208	601	491	614	419	565	478	350	331	327
	1427	601	491	615	420	566	480	355	331	327
	1635	601	491	615	420	565	480	354	331	327
	1804	595	485	613	419	565	476	347	321	315
	1910	588	482	613	415	561	477	340	306	302
	2006	584	477	611	408	554	474	334	296	292
	2220	599	490	617	418	564	480	354	331	326
<u>1/19/63</u>	0040	599	490	617	419	566	480	355	332	327
	0245	599	490	617	420	566	480	355	331	327
	0445	599	490	616	419	565	479	355	331	327
	0645	596	488	614	418	563	476	354	331	326
	0845	597	490	616	419	565	479	354	331	326
	1104	601	491	617	419	566	481	358	331	327
	1303	600	490	616	419	566	482	357	331	327
	1501	600	490	616	419	566	481	356	331	327
	1730	600	490	617	419	566	480	356	331	326
	2016	601	491	618	419	567	481	356	331	327
	2200	599 C	490 C	616 C	418 C	565 C	480 C	355 C	331 C	327 C

Table B-5. (Cont'd)

Date	Time	Thermocouple locations									
		Top collector 1	Top seal 2	Center collector 3	Bottom seal 4	Bottom collector 5	Top emitter 6	Bottom emitter 7	Cs 1 R	Cs 2 9	
<u>1/20/61</u>	0030	599 C	490 C	616 C	419 C	565 C	480 C	356 C	331 C	327 C	
	0215	599	490	616	418	565	480	355	331	327	
	0415	598	489	615	418	564	480	356	331	327	
	0600	598	489	615	418	564	480	354	331	327	
	0700	599	490	617	419	566	480	352	331	327	
	0820	597	489	615	418	564	479	358	331	328	
	1020	594	487	612	416	561	477	350	329	326	
	1240	592	487	612	416	561	472	346	330	326	
	1423	588	485	610	416	599	469	346	330	325	
	1645	590	486	612	417	561	470	351	331	327	
	1840	593	489	615	419	563	472	350	331	32	
	2042	595	490	615	419	563	473	352	332	327	
	2222	595	490	616	418	563	474	351	331	327	
	<u>1/21/61</u>	0010	598	491	618	420	514	477	354	332	328
		0215	599	492	621	421	517	485	357	332	328
0406		605	492	620	420	517	485	340	332	328	
0630		605	492	621	420	517	485	340	332	328	
0815		603	490	619	420	517	485	351	332	328	
1029		605	493	623	420	517	485	358	332	328	
1205		603	492	619	420	517	484	354	332	328	
1405		601	491	618	417	515	482	352	332	328	
1715		601	492	619	418	517	484	358	332	328	
1905		600	491	619	417	516	483	356	332	328	
2037		604	490	618	416	516	482	355	332	327	
2230		602	493	621	420	518	485	355	333	329	
<u>1/22/61</u>		0015	599	492	620	418	517	484	354	332	328
		0200	601	488	619	417	513	482	301	331	327
		0430	598	490	619	417	514	483	302	332	327
	0630	598 C	489 C	619 C	417 C	513 C	482 C	448 C	332 C	327 C	

B-11

Table B-5. (Cont'd)

Date	Time	Thermocouple locations								
		Top collector 1	Top seal 2	Center collector 3	Bottom seal 4	Bottom collector 5	Top emitter 6	Bottom emitter 7	Cs 1 8	Cs 2 9
	0820	598 C	488 C	617 C	416 C	513 C	483 C	351 C	331 C	325 C
	1052	597	490	619	417	515	483	355	330	327
	1305	599	490	620	417	515	483	354	332	327
	1450	599	491	621	417	516	485	357	330	327
	1630	601	491	620	417	514	483	356	331	327
	1815	600	491	621	416	516	484	358	331	326
	2030	600	491	621	416	516	485	363	331	327
	2237	600	491	619	416	515	484	359	332	328
	2315	600	489	617	416	513	483	360	332	328
	2330	601	493	620	417	516	483	356	332	328
<u>1/23/63</u>	0000	598	493	620	418	516	478	351	332	328
	0230	601	494	624	418	518	485	357	331	326
	0430	600	493	623	418	517	485	352	331	326
	0630	600	493	624	419	518	485	355	330	327
	0838	600	493	624	418	517	485	356	331	327
	1026	598	491	621	418	514	484	351	331	327
	1255	600	491	619	417	565	443	351	330	326
	1425	601	491	620	416	565	443	352	330	326
	1640	597	490	619	420	563	487	352	331	325
	1825	599	491	620	420	563	481	352	331	325
	2025	600	492	620	421	563	481	350	331	325
	2215	600	490	620	420	563	482	346	331	325
<u>1/24/63</u>	0030	600	490	620	418	563	482	343	331	325
	0210	598	490	619	417	562	481	345	331	325
	0415	596	488	619	418	562	480	344	331	325
	0630	600	488	620	419	563	483	346	331	325
	0815	598	490	619	419	562	482	344	331	325
	1125	596	490	615	417	562	480	345	331	325
	1400	596 C	489 C	617 C	417 C	562 C	480 C	345 C	331 C	325 C

Table B-5. (Cont'd)

Date	Time	Thermocouple locations								
		Top collector	Top seal	Center collector	Bottom seal	Bottom collector	Top emitter	Bottom emitter	Cs 1	Cs 2
		1	2	3	4	5	6	7	8	9
	1620	597 C	488 C	618 C	418 C	563 C	482 C	345 C	331 C	325 C
	1910	597	489	619	418	563	484	349	331	325
	2015	598	490	619	418	563	484	349	331	325
	2215	598	489	619	418	563	484	347	331	325
<u>1/25/63</u>	0010	597	490	618	418	563	483	347	331	325
	0230	596	488	616	417	562	484	346	331	325
	0420	598	487	619	418	563	481	347	329	323
	0615	598	488	617	417	562	481	345	330	324
	0815	594	488	616	416	561	478	345	331	325
	1106	594	486	614	416	561	478	345	329	323
	1242	596	486	617	417	562	470	350	331	325
	1440	596	487	617	417	562	472	349	331	325
	1630	596	487	618	417	562	472	352	331	325
	1810	596	487	618	417	562	470	350	331	325
	2010	596	487	618	417	562	474	350	331	325
	2208	596	490	618	417	562	474	350	331	325
<u>1/26/63</u>	0020	597	490	618	417	563	475	350	331	325
	0208	602	490	621	418	565	480	354	331	325
	0405	600	491	620	418	564	480	354	331	325
	0615	604	490	622	418	565	484	354	331	325
	0807	600	491	620	417	563	482	348	331	325
	1007	599	490	619	420	563	480	350	328	325
	1300	600	490	619	420	563	480	350	328	325
	1625	601	490	623	418	566	482	343	328	324
	1820	598	489	618	418	562	476	346	329	323
	2020	601	489	623	416	567	478	346	327	322
	2215	596 C	486 C	621 C	416 C	563 C	473 C	345 C	327 C	323 C

Table B-5. (Cont'd)

Date	Time	Thermocouple locations									
		Top collector 1	Top seal 2	Center collector 3	Bottom seal 4	Bottom collector 5	Top emitter 6	Bottom emitter 7	Ca 1 8	Ca 2 9	
<u>1/27/63</u>	0035	600 C	489 C	624 C	416 C	564 C	478 C	350 C	327 C	327 C	
	0213	599	487	625	416	564	473	348	326	321	
	0407	599	488	625	416	564	473	347	327	322	
	0612	598	487	626	416	565	475	360	327	322	
	0844	598	487	625	415	565	474	348	327	322	
	1005	584	473	623	408	557	458	342	317	314	
	1046	585	474	619	408	556	461	343	324	321	
	1122	585	477	618	408	555	464	347	327	325	
	1200	585	475	617	408	553	464	340	329	328	
	1447	585	475	617	407	554	463	338	326	324	
	1650	585	475	617	407	554	463	337	326	324	
	1818	585	473	615	407	553	462	337	325	323	
	2020	585	474	615	407	553	462	341	325	323	
	2215	584	473	614	407	553	461	341	326	323	
	<u>1/28/63</u>	0012	588	473	623	407	559	460	345	325	322
		0206	589	472	623	407	557	459	337	325	322
0356		585	474	612	407	550	464	338	335	335	
0487		585	475	615	407	550	463	339	337	337	
0620		585	473	615	407	545	457	339	336	336	
0703		588	477	618	409	554	465	345	344	344	
0730		582	472	613	403	551	460	340	340	340	
0753		621	493	610	422	570	480	350	351	354	
0923		628	507	650	433	586	486	357	354	354	
1038		595	485	630	418	561	467	345	349	350	
1115		586	474	625	407	554	455	340	341	340	
1150		555	447	607	370	530	425	325	325	326	
1234		528	474	619	370	515	398	310	292	290	
1321		335	330	334	267	320	368	254	224	220	
1355		190	224	190	177	180	275	192	162	154	
1435		130	166	137	134	126	222	159	131	12	
1518	50 C	79 C	55 C	63 C	53 C	106 C	85 C	70 C	66 C		

B-14

Table B-6. Calorimetric and Voltage Measurements

Date	Time	Inlet H ₂ O, mv	Outlet H ₂ O, position 2, mv	Outlet H ₂ O, position 3, mv	V _{Bar 1'} v	V _{Bar 2'} v	V _{C - A'} v	Reactor power, KW	V _{outer'} mv	T _{Bar 1'} mv	Flow, %
<u>1/15/63</u>	1114	0.5400	0.5429	0.5437	0.0021 mv	0.0000 mv	0.0106 mv	--	0.0001	0.5390	73
	1135	--	--	--	--	--	--	--	--	--	--
	1340	0.5125	0.5369	0.5172	-0.0034 mv	0.0062 mv	0.0044 mv	1	-0.0022	0.5490	74.7
	1437	0.5175	0.5247	0.5281	-0.0641 mv	0.0806 mv	0.0384 mv	--	0.0011	0.5342	64.3
	1513	0.5203	0.5394	0.5376	-0.1064 mv	0.1342 mv	0.0102 mv	20	0.0000	0.5384	64.3
	1611	0.5340	0.5838	0.5764	0.3240 mv	-0.3750 mv	3.5932 mv	80	0.0044	0.5816	72.3
	1650	0.5276	0.6037	0.5911	2.9429 mv	-3.8851 mv	10.6384 mv	120	0.0488	0.6154	73.9
	1756	0.5366	0.7106	0.6800	24. + mv	7.223 mv	47 mv	225	0.3083	0.7145	60.8
	1845	0.5341	0.7514	0.7082	0.12764	0.14625	0.21636 v	285	1.414 mv	1.0476	--
	1941	0.5357	0.8065	0.7516	0.178	0.202	0.296 v	355	2.230	1.2210	60.8
	2040	0.5334	0.8516	0.8006	0.2073	0.23699	0.3508	--	2.86	1.36	72
	2254	0.5070	0.7686	0.7211	0.20745	0.23717	0.35096	430	2.8506	1.29	86
	<u>1/16/63</u>	0205	0.5029	0.8345	0.7765	0.2292	0.2617	0.3862	460	2.2986	1.4050
0318		0.4941	0.7760	0.7280	0.2490	0.28478	0.42012	470	2.5014	1.400	80.3
1045		0.4960	0.8651	0.7994	0.25708	0.29278	0.4300	500	2.1658	1.5105	70.5
1656		0.548	0.850	0.831	0.258	0.295	0.434	500	2.192	1.541	86.5
1940		0.5599	0.9197	0.8504	0.25736	0.29426	0.43229	--	2.1845	1.5707	-
2125		0.5391	0.8495	0.7928	0.25294	0.28917	0.42566	--	2.1419	1.4633	87.2
<u>1/17/63</u>	0216	0.51350	0.8180	0.7655	0.25292	0.28900	0.42509	500	2.1425	1.4477	87.1
	0413	0.5096	0.8749	0.8132	0.25377	0.29038	0.42615	500	2.1482	1.5110	72.3
	0608	0.4975	0.8532	0.7876	0.25376	0.29080	0.42754	500	2.1460	1.5004	72.6
	0830	0.4931	0.7902	0.7394	0.25186	0.28835	0.42740	500	2.1515	1.4229	85.3
	1049	0.4916	0.7911	0.7384	0.25304	0.29035	0.42723	500	2.1554	1.4525	60.3
	1335	0.5154	0.8574	0.7876	0.2589	0.29616	0.440	500	2.1950	1.507	62.3
	1710	0.5316	0.8752	0.8096	0.25966	0.29634	0.443	500	2.1938	1.5286	72
	2006	0.5480	0.8835	0.8249	0.2582	0.29486	0.440	500	2.1807	1.5424	72
	2235	0.5360	0.8885	0.8218	0.26193	0.29975	0.4460	520	2.2259	1.5545	72.5

Table B-6. (Cont'd)

Date	Time	Inlet H ₂ O, mv	Outlet H ₂ O, position 2, mv	Outlet H ₂ O, position 3, mv	V _{Bar 1'} v	V _{Bar 2'} v	V _{C - A'} v	Reactor power, KW	V _{outer'} mv	T _{Bar 1'} mv	Flow, %	
<u>1/18/63</u>	0048	0.5418	0.9012	0.8351	0.26138	0.29918	0.4459	520	2.2180	1.5665		
	0300	0.5365	0.8833	0.8152	0.26236	0.29980	0.44595	520	2.2236	1.5380	75.5	
	0515	0.5346	0.8960	0.8280	0.26240	0.29984	0.44602	520	2.2194	1.5550	72.3	
	0730	0.5446	0.9167	0.8404	0.26150	0.29840	0.44446	520	2.212	1.559	69.9	
	0950	0.5331	0.8985	0.8232	0.2616	0.2989	0.44501	520	2.2133	1.5584	71.6	
	1208	0.5203	0.8500	0.7819	0.2616	0.2988	0.44527	520	2.2093	1.5045	74.8	
	1427	0.5319	0.8850	0.8180	0.2612	0.2986	0.44461	520	2.2188	1.5447	73.8	
	1633	0.5450	0.8823	0.8203	0.26101	0.29816	0.44490	520	2.1986	1.5290	76.5	
	1804	0.5310	0.8931	0.8281	0.26804	0.30653	0.45545	520	2.2417	1.5640	72.0	
	1910	0.5345	0.8926	0.8224	0.27637	0.31572	0.47036	520	2.3110	1.5918	72.0	
	2006	0.5400	0.9031	0.8338	0.28055	0.32054	0.47795	520	2.3505	1.6114	71.5	
	2220	0.5259	0.8891	0.82150	0.26170	0.29890	0.4453	520	2.1920	1.5362	73.0	
	<u>1/19/63</u>	0040	0.5231	0.8683	0.8090	0.26057	0.29735	0.4439	520	2.1855	1.5237	74.2
		0245	0.5138	0.8610	0.8000	0.26023	0.29724	0.44424	520	2.1806	1.5168	73.0
		0445	0.5056	0.8626	0.7975	0.25964	0.29658	0.44265	520	2.1766	1.5177	73.0
0645		0.5130	0.8402	0.7829	0.25769	0.29440	0.44001	520	2.1630	1.5046	78.7	
0845		0.5182	0.8550	0.7861	0.25941	0.29609	0.44178	522	2.1741	1.4961	74.7	
1104		0.5023	0.8458	0.7830	0.26022	0.29743	0.44304	520	2.1830	1.4902	75.8	
1303		0.5110	0.8472	0.7824	0.25930	0.29655	0.44230	520	2.1827	1.4857	77.4	
1501		0.5137	0.8660	0.7977	0.25950	0.29689	0.44258	520	2.1713	1.5128	73.3	
1730		0.5264	0.8784	0.8056	0.2599	0.2971	0.44236	520	2.1800	1.5250	72.5	
2016		0.5280	0.9629	0.8870	0.26181	0.29884	0.44450	520	2.1900	1.6374	60.5	
2200		0.5354	0.8642	0.8014	0.25900	0.29664	0.44156	520	2.1764	1.5051	74.7	
<u>1/20/63</u>		0030	0.5205	0.8740	0.8132	0.25920	0.29620	0.44125	520	2.1775	1.5320	72.2
		0215	0.5210	0.8866	0.8200	0.2588	0.2957	0.44130	520	2.1725	1.540	71.1
	0415	0.5266	0.8498	0.8144	0.2585	0.29495	0.44070	520	2.1640	1.4951	74.5	
	0600	0.5190	0.8660	0.8082	0.25774	0.29469	0.44010	520	2.1564	1.5119	75.5	
	0700	0.5325	0.9821	0.8980	0.2505	0.2970	0.44230	520	2.1806	1.6350	58.2	
	0820	0.5210	0.8758	0.8134	0.2574	0.2943	0.4384	520	2.164	1.522	73.0	

B-16

Table B-6. (Cont'd)

Date	Time	Inlet H ₂ O, mv	Outlet H ₂ O, position 2, mv	Outlet H ₂ O, position 3, mv	V _{Bar 1'} v	V _{Bar 2'} v	V _{C = A'} v	Reactor power, KW	V _{outer'} mv	T _{Bar 1'} mv	Flow, %	
<u>1/20/63</u>	1020	0.5228	0.8150	0.7620	0.2448	0.2920	0.4345	520	2.144	1.449	89.5	
	1240	0.5355	0.9080	0.8304	0.2553	0.2916	0.43472	520	2.143	1.565	68.7	
	1423	0.5769	0.9090	0.8455	0.2576	0.2900	0.43170	520	2.133	1.545	73.8	
	1648	0.5671	0.8728	0.8141	0.25409	0.29062	0.43292	520	2.1440	1.4874	87.7	
	1840	0.5602	0.9180	0.8400	0.25682	0.29300	0.43676	520	2.1479	1.5640	71.5	
	2042	0.5567	0.9136	0.8474	0.25697	0.29397	0.43745	520	2.1529	1.5490	71.5	
	2222	0.5383	0.9050	0.8393	0.25706	0.29401	0.43750	520	2.1582	1.5612	70.7	
	<u>1/21/63</u>	0030	0.5278	0.8801	0.8166	0.25715	0.29420	0.4385	520	2.1552	1.5009	75.2
0215		0.5263	0.8932	0.8308	0.2615	0.2986	0.4450	520	2.164	1.583	71.8	
0406		0.5056	0.8686	0.8024	0.2615	0.2990	0.4451	520	2.148	1.529	72.9	
0630		0.5012	0.8643	0.7973	0.2611	0.2988	0.4440	520	2.142	1.519	72.9	
0815		0.4943	0.8290	0.7678	0.25323	0.29693	0.44194	520	2.1515	1.4680	79.3	
1029		0.4900	0.8505	0.7825	0.2611	0.29860	0.44564	520	2.1690	1.5045	74.0	
1205		0.4945	0.8575	0.7867	0.29660	0.29660	0.44333	520	2.166	1.5050	74.2	
1405		0.5010	0.8230	0.7637	0.29375	0.29375	0.43816	520	2.1480	1.4508	82.5	
1715		0.4944	0.8611	0.7932	0.29774	0.29774	0.44351	520	2.1757	1.5182	71.7	
1905		0.4859	0.8721	0.7984	0.29574	0.29574	0.44026	520	2.1588	1.5177	71.0	
2037		0.4893	0.8440	0.7765	0.29420	0.29420	0.43858	520	2.1515	1.4940	74.3	
2230		0.4792	0.8630	0.7890	0.29578	0.29578	0.44096	520	2.2408	1.5960	69.0	
<u>1/22/63</u>		0015	0.4679	0.8555	0.7848	0.2962	0.2962	0.4423	520	2.165	1.515	69.1
		0200	0.4663	0.7843	0.7230	0.2931	0.2931	0.4370	520	2.133	1.425	81.9
		0430	0.4520	0.8250	0.7551	0.2915	0.2935	0.4385	520	2.145	1.470	72.1
	0630	0.4532	0.8316	0.7600	0.2930	0.2930	0.4371	520	2.133	1.478	71.5	
	0820	0.4500	0.7721	0.7068	0.29315	0.29315	0.43735	520	2.1330	1.4035	83.0	
	1052	0.4542	0.8075	0.7387	0.29385	0.29385	0.43967	520	2.1545	1.4538	76.7	
	1305	0.4920	0.8796	0.8023	0.29579	0.29579	0.44078	520	2.1633	1.5273	68.6	
	1450	0.5049	0.8627	0.7493	0.29656	0.29656	0.44200	520	2.1779	1.5099	74.8	
	1630	0.5215	0.8764	0.8125	0.29566	0.29566	0.44075	520	2.1681	1.5149	74.0	
	1815	0.5164	0.8966	0.8243	0.29782	0.29782	0.44360	520	2.1950	1.5454	70.5	

Table B-6. (Cont'd)

Date	Time	Inlet H ₂ O, mv	Outlet H ₂ O, position 2, mv	Outlet H ₂ O, position 3, mv	V Bar 1' v	V Bar 2' v	V C - A' v	Reactor power, KW	V outer' mv	T Bar 1' mv	Flow, %	
<u>1/22/63</u>	2030	0.5148	0.8696	0.7880	0.26057	0.29815	0.44412	520	2.1633	1.5118	75.3	
	2237	0.4870	0.8260	0.7410	0.25849	0.29570	0.44065	520	2.1641	1.4784	78.3	
	2315	0.4677	0.8460	0.7398	0.25724	0.29420	0.43819	520	2.1540	1.4922	71.0	
	2330	0.4840	1.0054	0.9070	0.26075	0.29732	0.44186	520	2.1724	1.6850	51.0	
<u>1/23/63</u>	0000	0.4850	1.0797	0.9677	0.26163	0.29814	0.44184	520	2.1814	1.7790	44.8	
	0230	0.5245	1.0925	0.9700	0.2647	0.3021	0.44770	520	2.210	1.8818	48.3	
	0430	0.5630	1.1600	1.0435	0.2637	0.3009	0.4461	520	2.194	1.653	45.0	
	0630	0.5340	1.089	0.9880	0.2639	0.3013	0.4464	520	2.193	1.802	49.3	
	0838	0.5415	1.1125	1.0035	0.2647	0.30175	0.44701	520	2.197	1.8060	47.9	
	1026	0.5420	1.1091	0.9990	0.26245	0.29885	0.44345	520	2.1837	1.800	47.5	
	1255	0.5585	1.0960	0.9721	0.26255	0.2991	0.4487	520	2.1950	1.766	51.1	
	1425	0.5610	1.1158	1.010	0.26302	0.30078	0.44495	520	2.1950	1.7948	49.5	
	1440	0.5460	1.0222	0.9202	0.2605	0.2978	0.4418	520	2.1801	1.6712	59.4	
	1825	0.5791	1.1130	1.0082	0.2629	0.3000	0.4445	520	2.1865	1.7865	50.8	
	2025	0.5660	1.1084	0.9978	0.2642	0.3015	0.4470	520	2.1772	1.7890	49.2	
	2215	0.5627	1.1677	0.9576	0.2620	0.2990	0.4433	520	2.1520	1.7450	53.5	
	<u>1/24/63</u>	0030	0.5440	1.0805	0.9785	0.2621	0.2993	0.4446	520	2.145	1.757	50.6
		0210	0.5370	1.0050	0.9140	0.2597	0.2963	0.4410	520	2.155	1.650	57.3
0415		0.5245	1.0570	0.9525	0.2591	0.2958	0.4388	520	2.143	1.725	50.0	
0630		0.4910	1.0240	0.9370	0.2620	0.2988	0.4440	520	2.158	1.716	49.4	
0815		0.5075	1.0750	0.9630	0.2611	0.2982	0.4425	520	2.143	1.759	48.0	
1125		0.5169	1.078	0.9680	0.2606	0.2980	0.4420	520	2.156	1.771	47.3	
1400		0.5050	1.0476	0.9430	0.2600	0.2960	0.44015	520	2.159	1.715	49.1	
1620		0.5402	1.0788	0.9648	0.2618	0.2987	0.4435	520	2.180	1.770	50.1	
1810		0.5290	1.0682	0.9484	0.2627	0.2996	0.4440	520	2.1825	1.7385	50.0	
2015		0.5261	1.0644	0.9534	0.2629	0.3000	0.4446	520	2.1860	1.7384	50.1	
2215		0.5264	1.0602	0.9430	0.2615	0.2985	0.4430	520	2.1795	1.730	50.1	

Table B-6. (Cont'd)

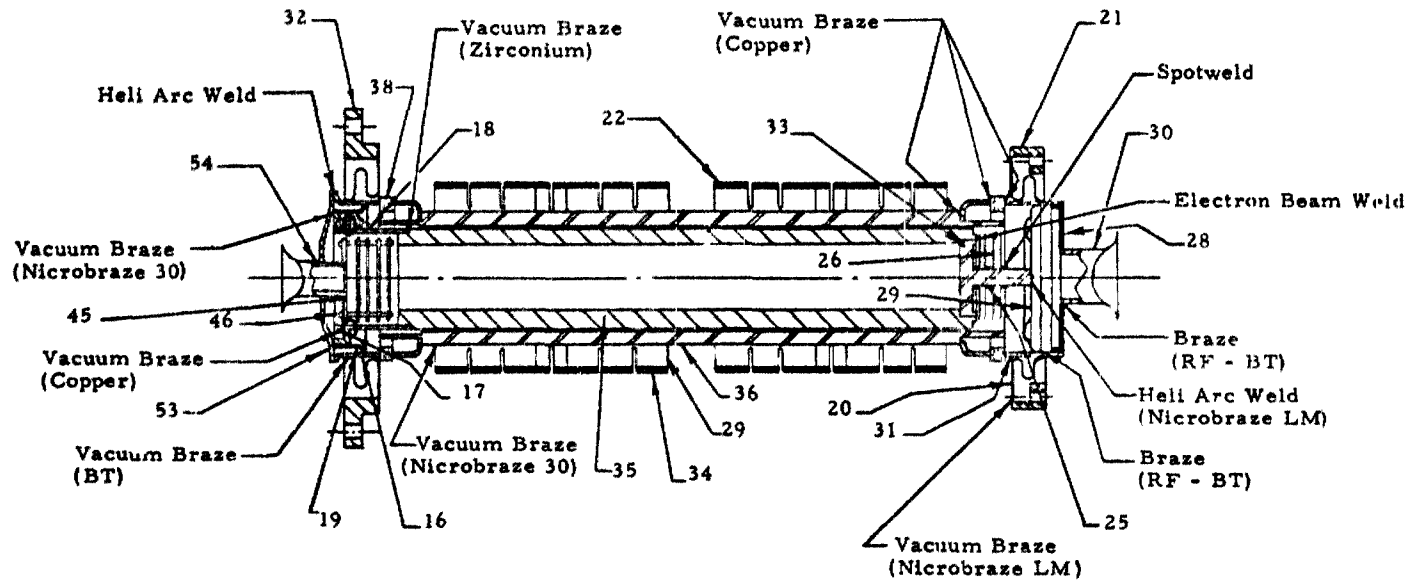
Date	Time	Inlet H ₂ O, mv	Outlet H ₂ O, position 2, mv	Outlet H ₂ O, position 3, mv	V _{Bar 1'} v	V _{Bar 2'} v	V _{C - A'} v	Reactor power, KW	V _{outer'} mv	V _{Bar 1'} mv	Flow, %	
<u>1/25/63</u>	0010	0.5070	1.0450	0.9325	0.2610	0.2979	0.4425	520	2.1665	1.720	50.0	
	0230	0.4878	0.9947	0.8866	0.2582	0.2940	0.4382	520	2.1485	1.666	53.3	
	0420	0.4802	1.0519	0.9255	0.2616	0.2985	0.4433	520	2.1822	1.738	42.7	
	0615	0.4780	1.0340	0.9260	0.2609	0.2976	0.4418	520	2.1610	1.7225	48.0	
	0835	0.4846	1.0306	0.9263	0.25804	0.2942	0.4366	520	2.1393	1.6819	49.0	
	1106	0.5042	1.0980	0.9877	0.25665	0.2923	0.4334	518	2.1310	1.7457	45.7	
	1242	0.5193	1.0732	0.9803	0.25855	0.2952	0.4385	520	2.1595	1.8348	47.0	
	1440	0.5187	1.0559	0.9581	0.25745	0.29424	0.4371	520	2.1545	1.7243	51.5	
	1630	0.5425	1.0750	0.9462	0.25787	0.29436	0.4367	520	2.1575	1.7946	50.7	
	1810	0.5294	1.0816	0.9640	0.2585	0.29536	0.43768	520	2.1530	1.7834	47.5	
	2010	0.5573	1.1226	1.0153	0.25946	0.29641	0.43876	520	2.1590	1.8015	47.2	
	2208	0.5646	1.1059	0.9936	0.25923	0.29562	0.43874	520	2.1606	1.7750	49.0	
	<u>1/26/63</u>	0020	0.5525	1.1310	1.0127	0.26034	0.29655	0.43950	520	2.1671	1.8119	46.5
		0208	0.5292	1.1100	0.9912	0.26358	0.30065	0.44546	520	2.1945	1.7992	47.1
0405		0.5311	1.1081	0.9863	0.26197	0.29856	0.44258	520	2.1785	1.7960	46.7	
0615		0.5282	1.1120	0.9940	0.26573	0.30306	0.44949	520	2.2050	1.8058	46.8	
0807		0.5244	1.0718	0.9600	0.26086	0.29798	0.44182	520	2.1767	1.7613	47.4	
1007		0.5328	1.1443	1.0283	0.26170	0.29875	0.44192	520	2.1764	1.8343	45.0	
1300		0.5609	1.1606	1.0420	0.26250	0.29968	0.44341	520	2.1829	1.8491	45.0	
1625		0.5670	1.1690	1.0488	0.26130	0.29809	0.44160	520	2.1665	1.8539	45.0	
1820		0.5422	1.1429	1.0230	0.25680	0.29272	0.43300	520	2.1200	1.8052	45.0	
2020		0.5250	1.1184	0.9950	0.25648	0.29280	0.43410	520	2.1295	1.7870	44.8	
2215		0.5530	1.0310	0.9400	0.24790	0.28300	0.41940	520	2.0566	1.6593	55.4	
<u>1/27/63</u>		0035	0.5416	1.1360	1.0140	0.2596	0.28840	0.42824	520	2.1011	1.7982	44.0
		0213	0.5017	1.0912	0.9737	0.24606	0.28116	0.41748	520	2.0466	1.7275	45.5
	0407	0.5507	1.1365	1.0280	0.24531	0.28020	0.41580	520	2.0363	1.7794	45.2	
	0612	0.5236	1.0084	0.9207	0.24170	0.27605	0.41050	520	2.0113	1.6322	44.1	
	0844	0.5447	1.1037	0.9970	0.24182	0.27492	0.40842	520	2.0133	1.7265	47.5	
	1005	0.5426	1.0894	0.9847	0.23307	0.24300	0.36000	500	1.723	1.6336	47.5	
	1046	0.5600	1.1053	1.0010	0.21884	0.24939	0.36991	500	1.8172	1.640	47.0	

Table B-6. (Cont'd)

Date	Time	Inlet H ₂ O, mv	Outlet H ₂ O, position 2, mv	Outlet H ₂ O, position 3, mv	V _{Bar 1'} v	V _{Bar 2'} v	V _{C - A'} v	Reactor power, KW	V _{outer'} mv	T _{Bar 1'} mv	Flow, %
<u>1/27/63</u>	1122	0.5626	1.1134	1.0066	0.22245	0.25347	0.37561	500	1.8350	1.6836	47.1
	1200	0.5431	1.0431	0.9989	0.21614	0.24689	0.36795	500	1.7838	1.5754	53.5
	1447	0.5786	1.1243	1.0190	0.21985	0.25156	0.37174	500	1.8175	1.6848	47.1
	1650	0.5730	1.1233	1.0215	0.22016	0.25112	0.37195	500	1.8182	1.6900	46.6
	1818	0.5681	1.0756	0.9855	0.2184	0.2493	0.36896	500	1.8102	1.6512	50.5
	2020	0.5601	1.0817	0.9814	0.21865	0.2501	0.37054	500	1.8154	1.6410	49.5
	2215	0.5415	1.0406	0.9506	0.2165	0.2475	0.3665	500	1.8000	1.5995	51.7
<u>1/28/63</u>	0012	0.5123	1.0431	0.9382	0.20638	0.23527	0.34910	500	1.7158	1.5645	50.4
	0206	0.4950	1.0035	0.9126	0.19952	0.22825	0.33817	500	1.6616	1.5215	50.0
	0356	0.4924	0.9431	0.8662	0.20750	0.23682	0.35215	500	1.7177	1.4536	55.8
	0437	0.4959	1.0098	0.9087	0.20968	0.23925	0.35414	500	1.5432	1.5598	48.8
	0620	0.5003	1.0512	0.9434	0.20161	0.23000	0.34128	500	1.6882	1.5650	47.0
	0703	0.4800	1.0599	0.9430	0.20590	0.23551	0.34892	500	1.7243	1.5848	46.0
	0730	0.4779	1.0376	0.9239	0.19632	0.22415	0.33265	490	1.6446	1.5232	46.2
	0753	0.4740	1.2755	0.9469	0.22050	0.25250	0.37445	520	1.8469	1.6567	46.3
	0923	0.4919	1.0046	0.8989	0.23220	0.26540	0.39468	553	1.9503	1.6072	56.5
	1038	0.5071	0.9906	0.8888	0.1965	0.2245	0.3335	519	1.660	1.479	56.0
	1115	0.5241	1.0881	0.9750	0.1771	0.2021	0.2994	500	1.4905	1.5354	46.3
	1150	0.5296	1.0575	0.9460	0.1229	0.1406	0.2080	460	1.041	1.3486	46.5
	1234	0.5200	1.0048	0.9145	0.07769	0.08937	0.13237	430	0.6598	1.1964	46.3
	1321	0.5230	0.7849	0.7285	0.8450 mv	0.9940 mv	5.488 mv	225	0.0090	0.7970	45.8
	1355	0.5184	0.6429	0.6176	-1.084 mv	-1.2124 mv	2.088 mv	120	-0.0087	0.6437	50.3
	1435	0.5180	0.5948	0.5800	-1.0739 mv	-1.2033 mv	1.5469 mv	80	-0.0103	0.5984	56.0
	1518	0.6299	0.6112	0.7320	-1.2445 mv	-1.3904 mv	-1.0153 mv	20	-0.0109	0.8259	11.2

B-20

Figure B-1. Materials and Fabrication of RCA Type A1197-A Converter, Device 36



Note: All Copper Brazes are Nickel Plated

Figure B-2. Converter, Fuel, and End Cap Assembly

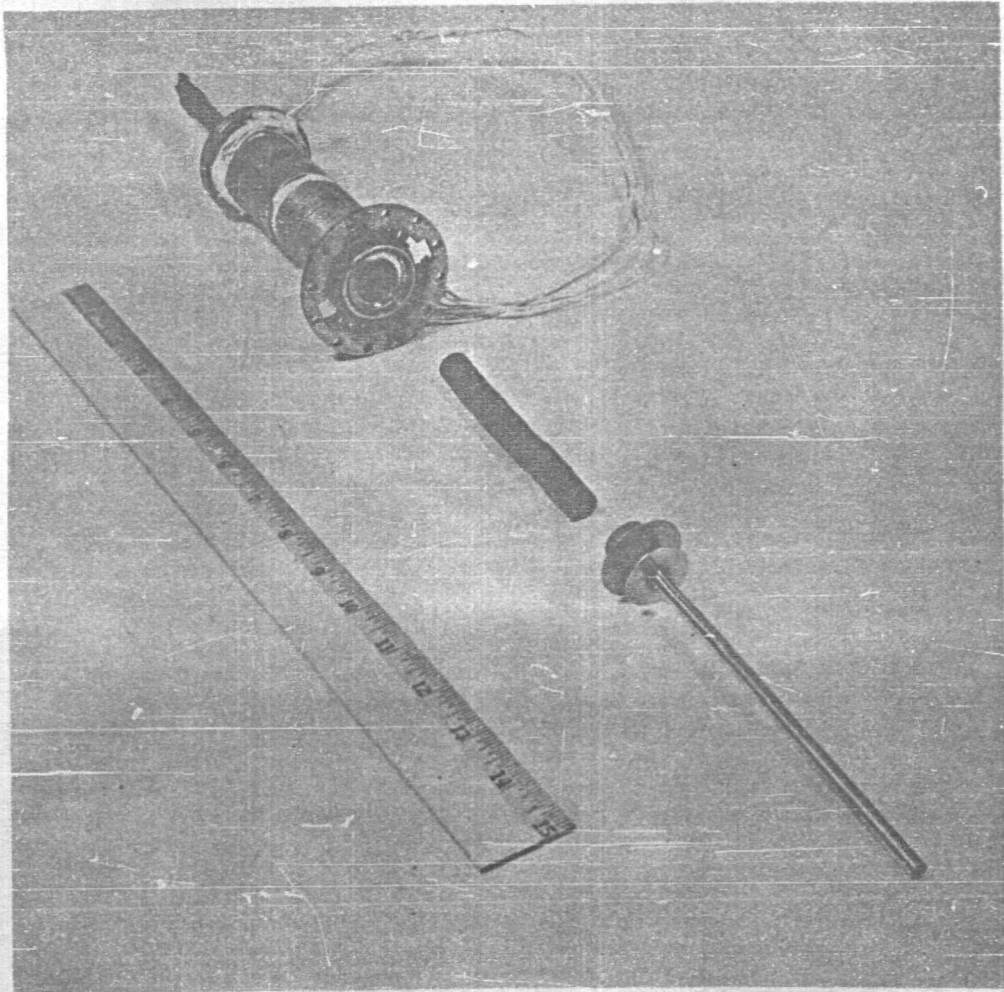


Figure B-3. View of Vacuum System and Oven

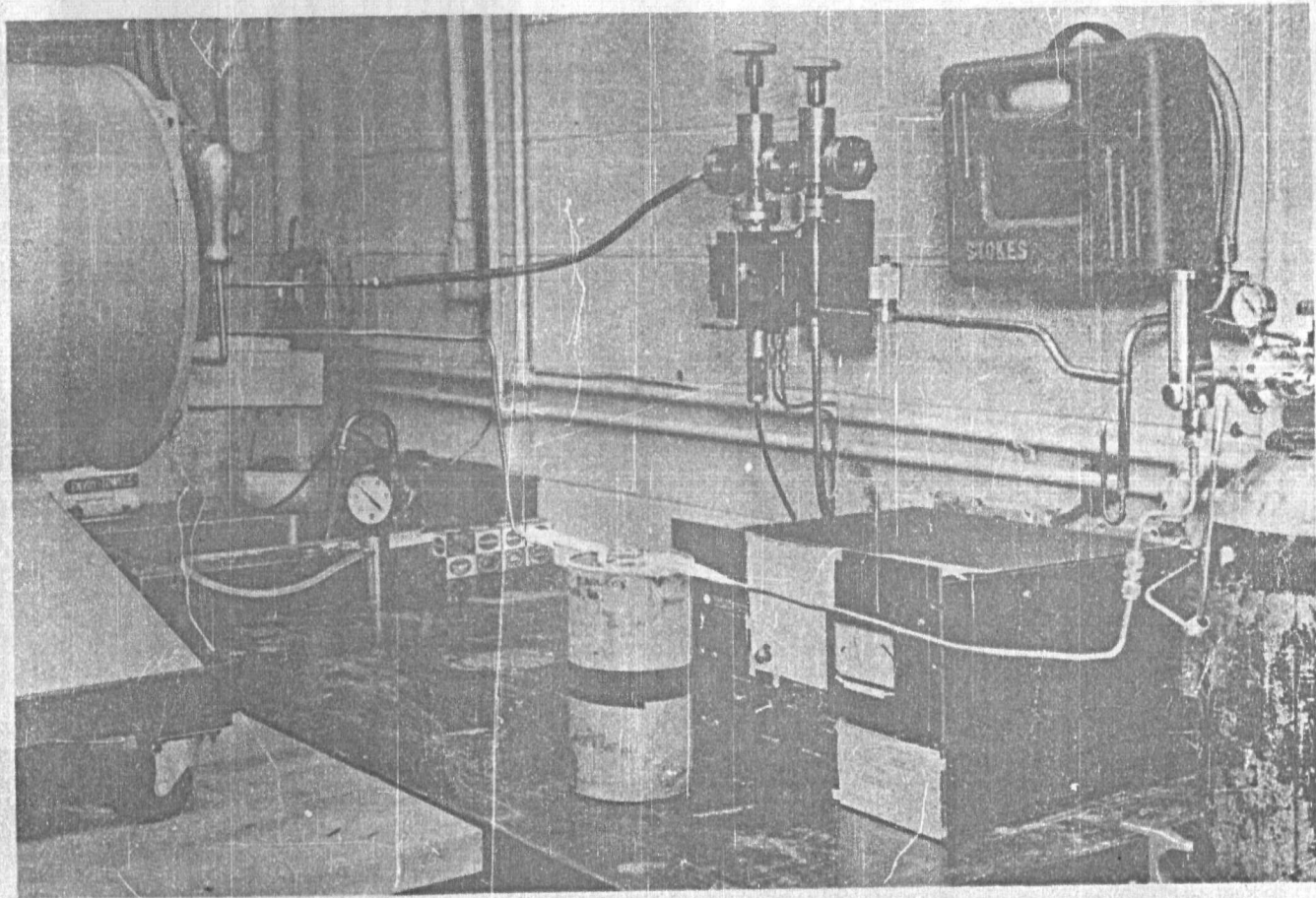


Figure B-4. Converter Connected to Vacuum System

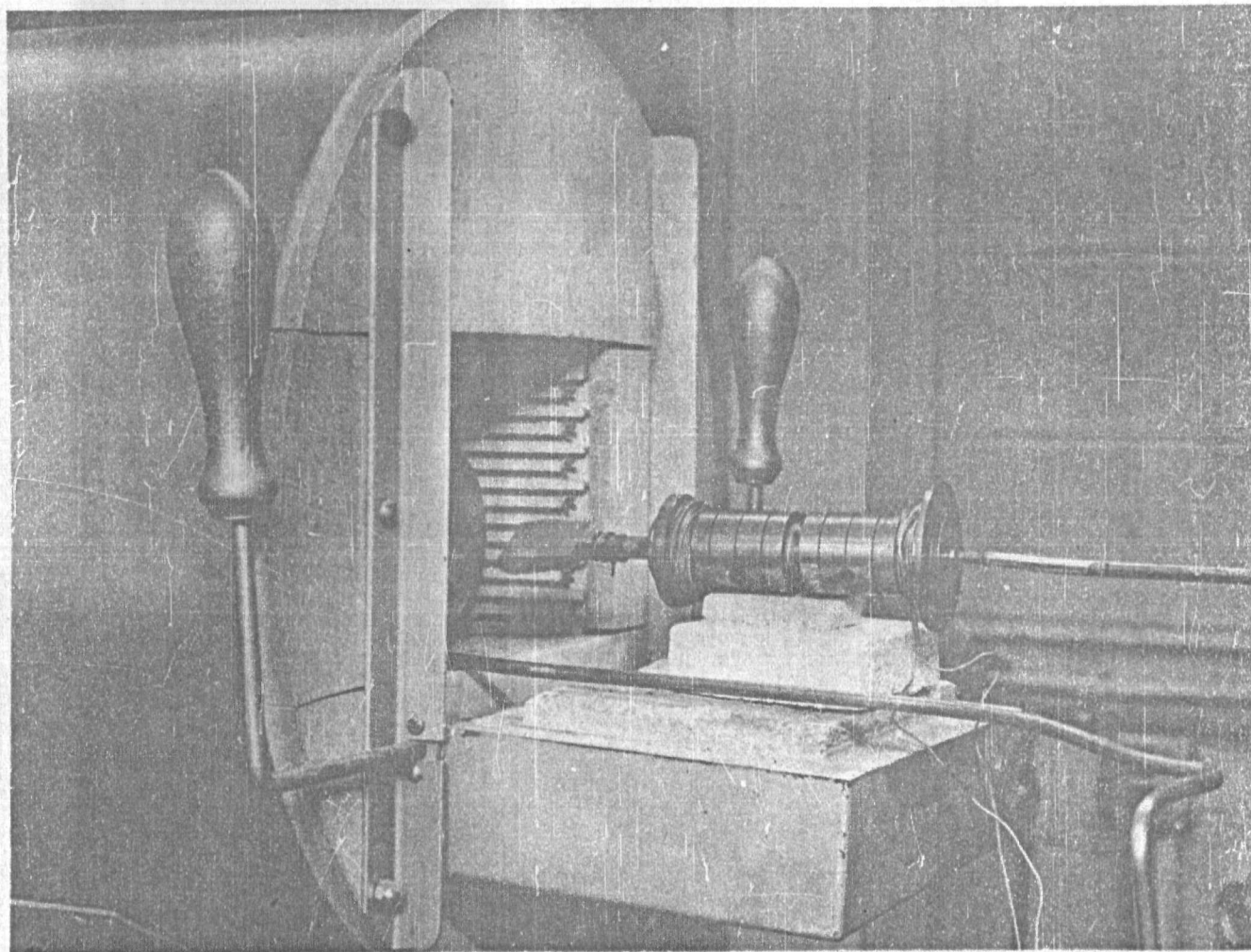


Figure B-5. Installation of Converter in Outgassing Can

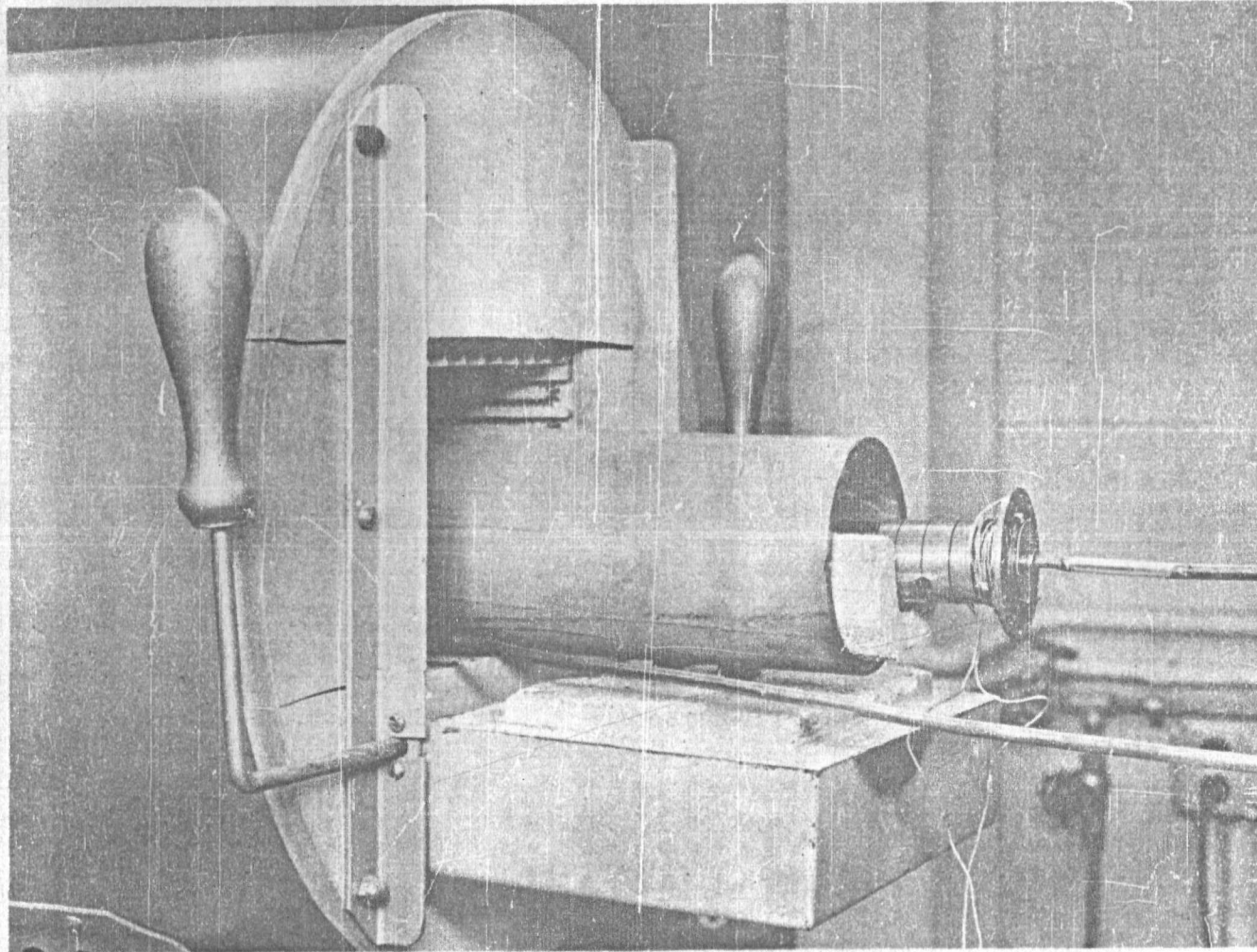


Figure B-6. Sealed Outgassing Can in Oven

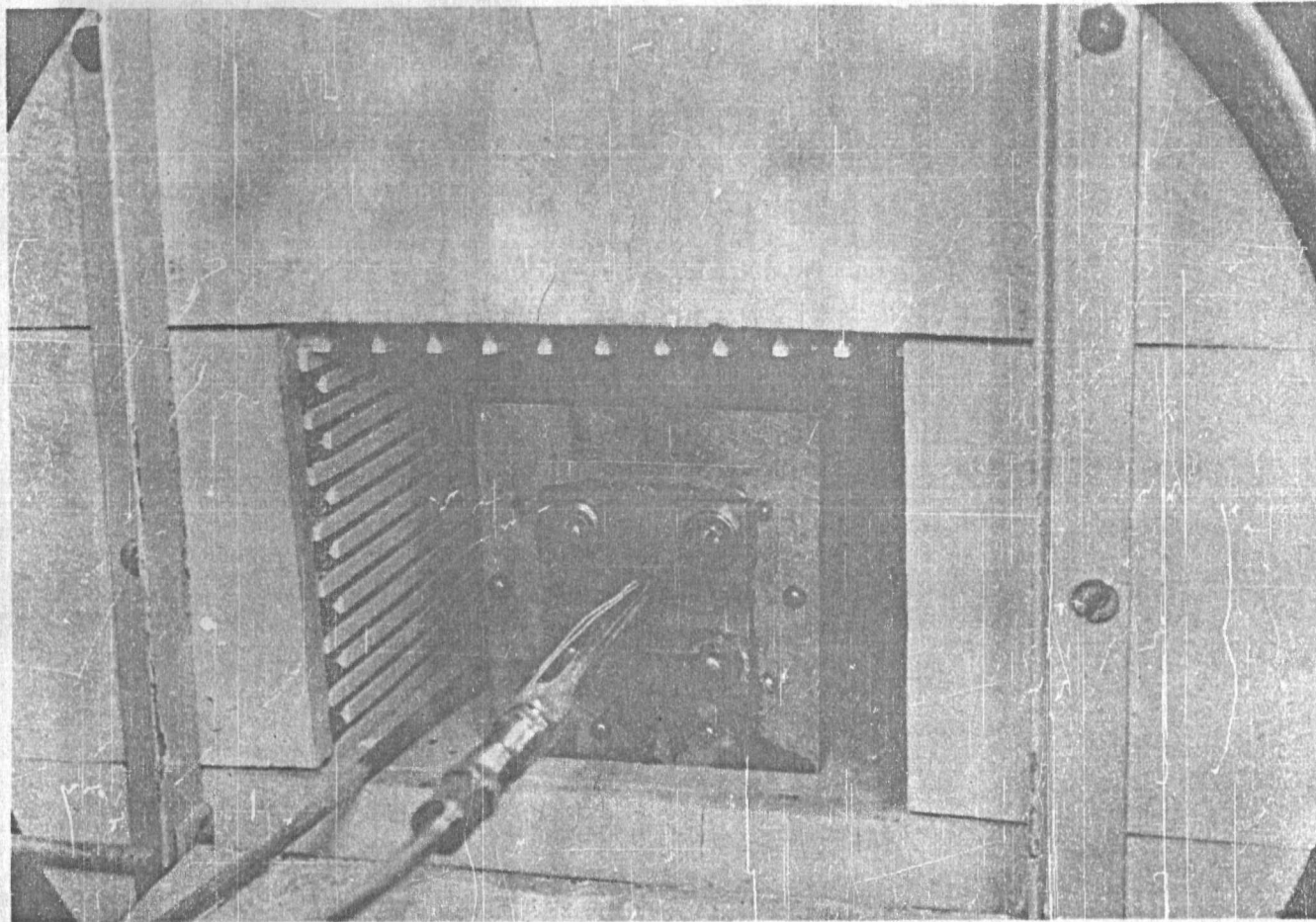


Figure B-7. Outgassing the Device in the Oven

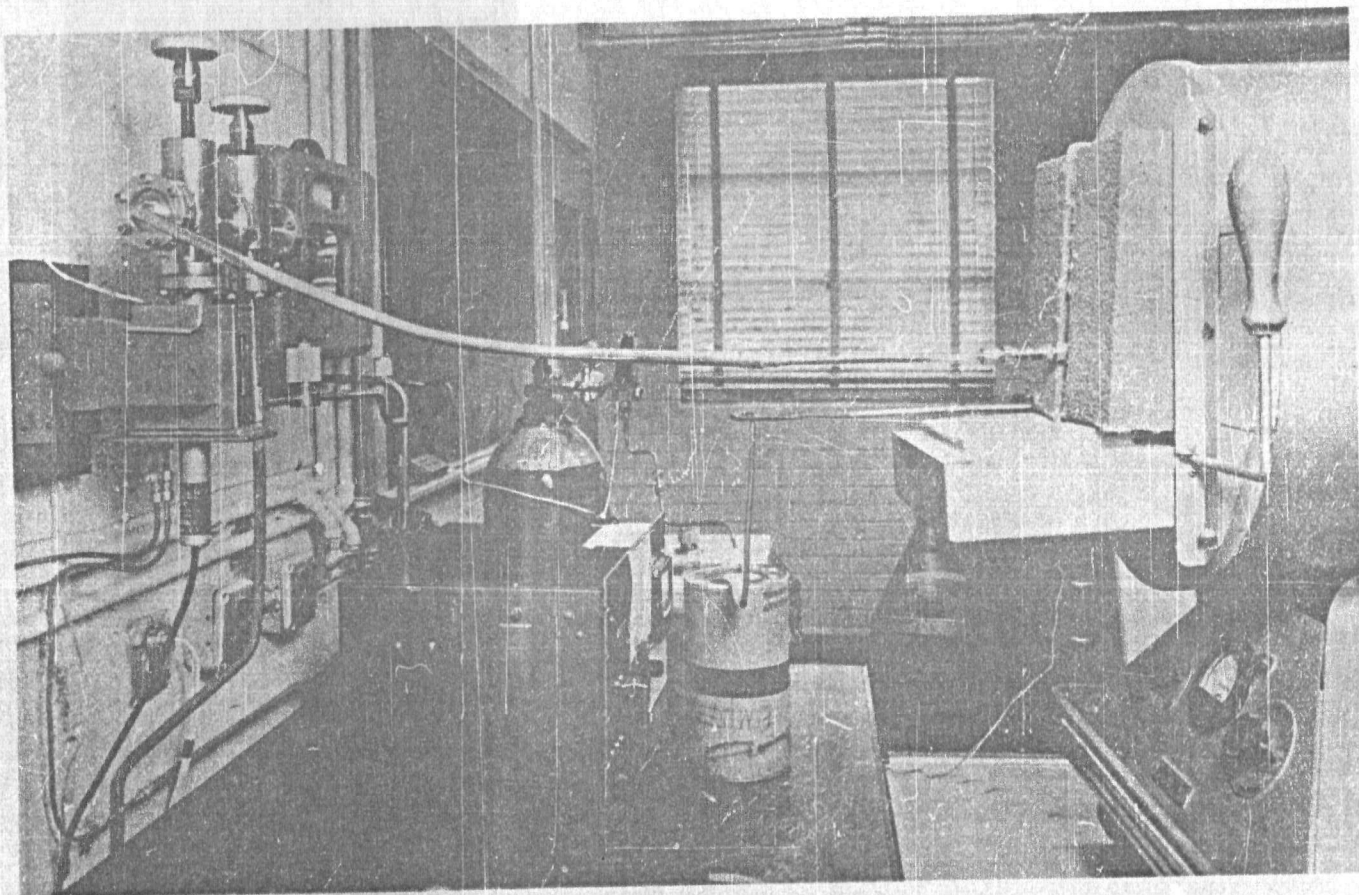


Figure B-8. Calibration of Inpile Load Bar Resistance Versus Temperature Emf

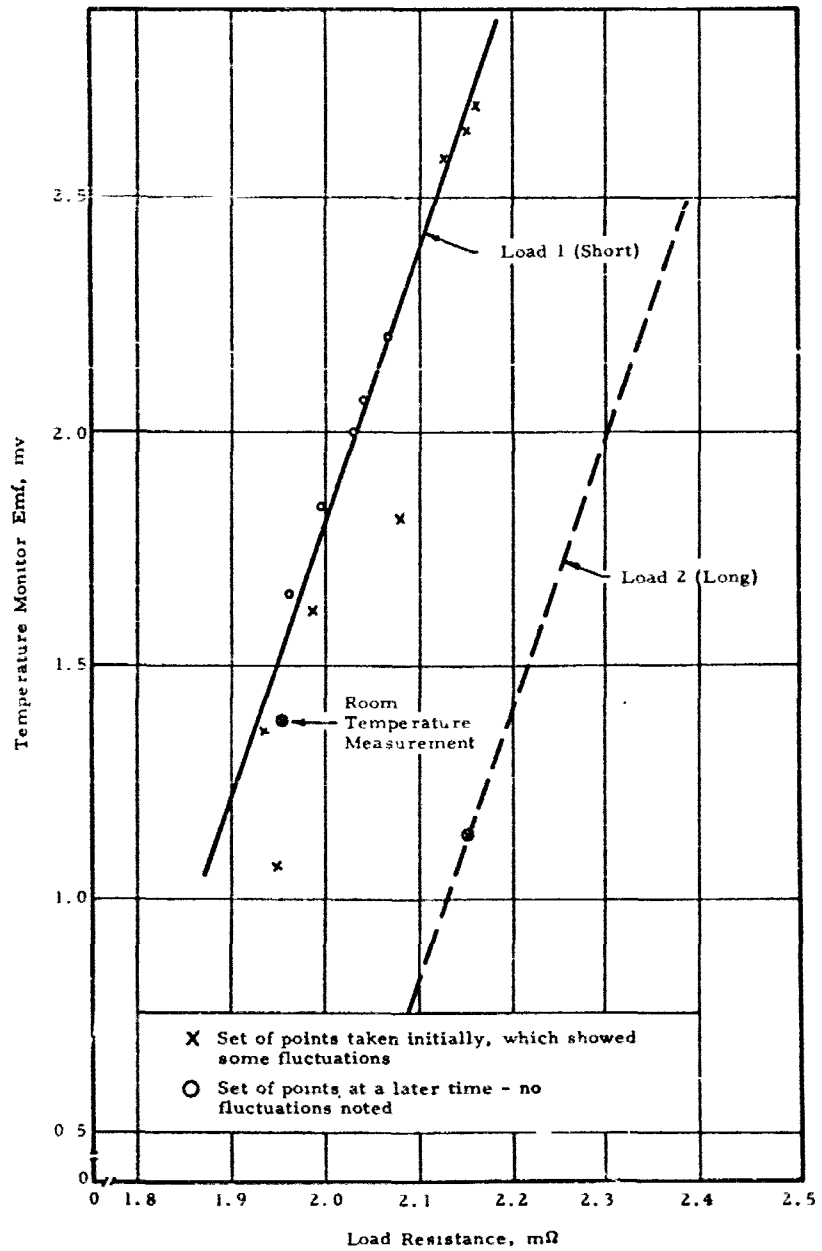


Figure B-9. Summary of Voltage Measurements of the Inpile Load

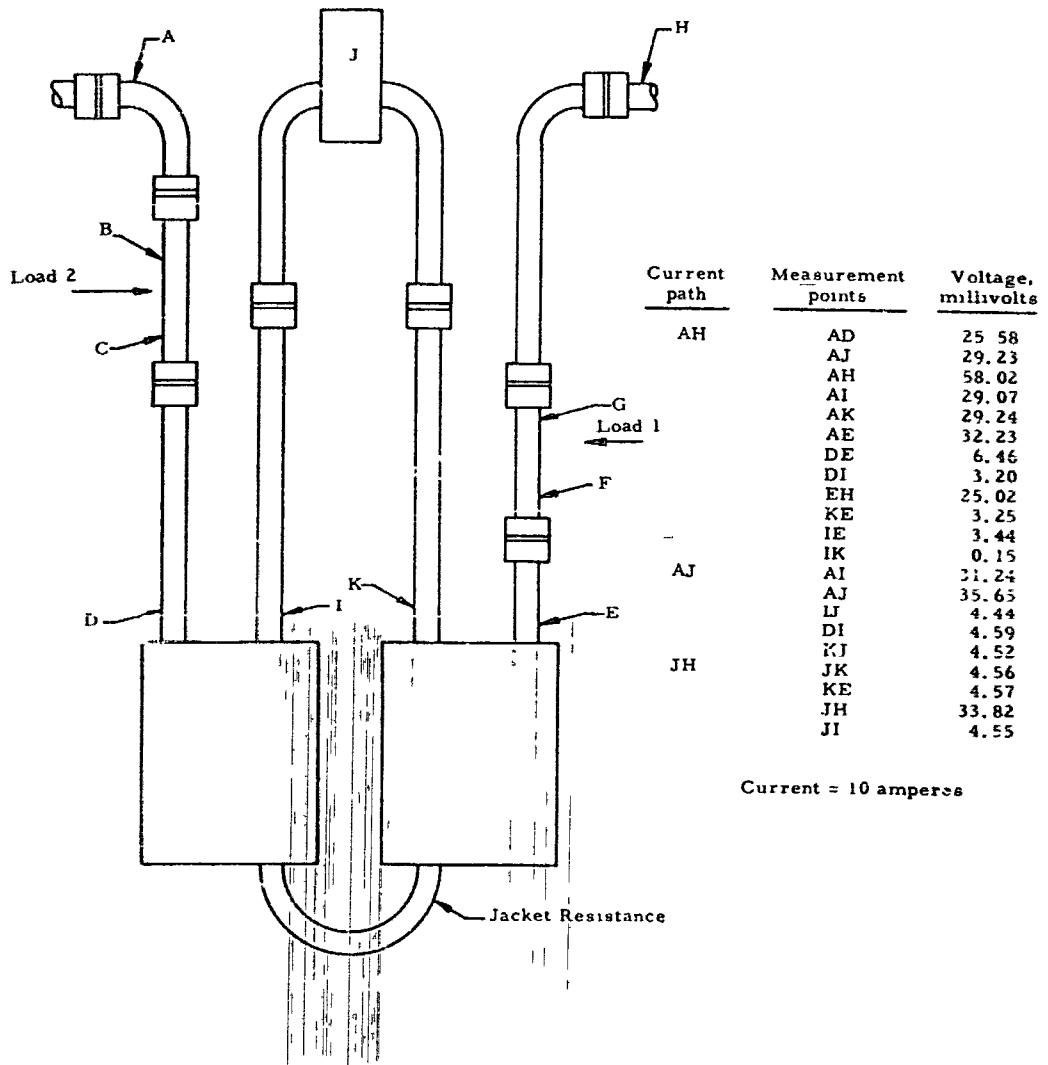
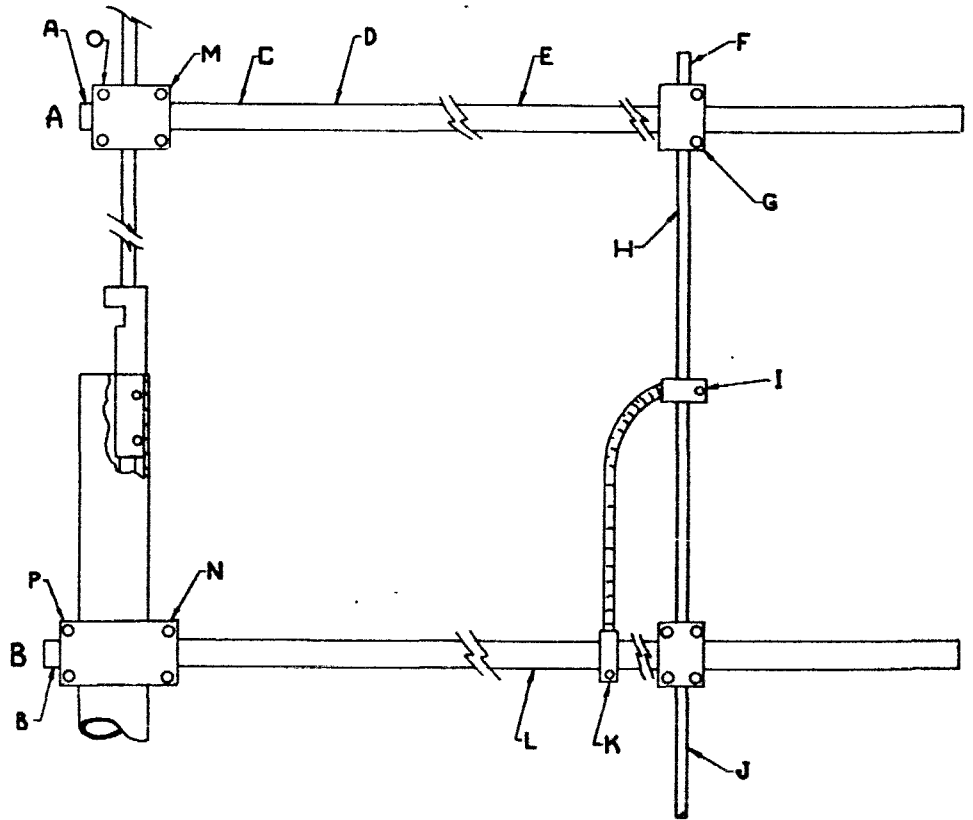


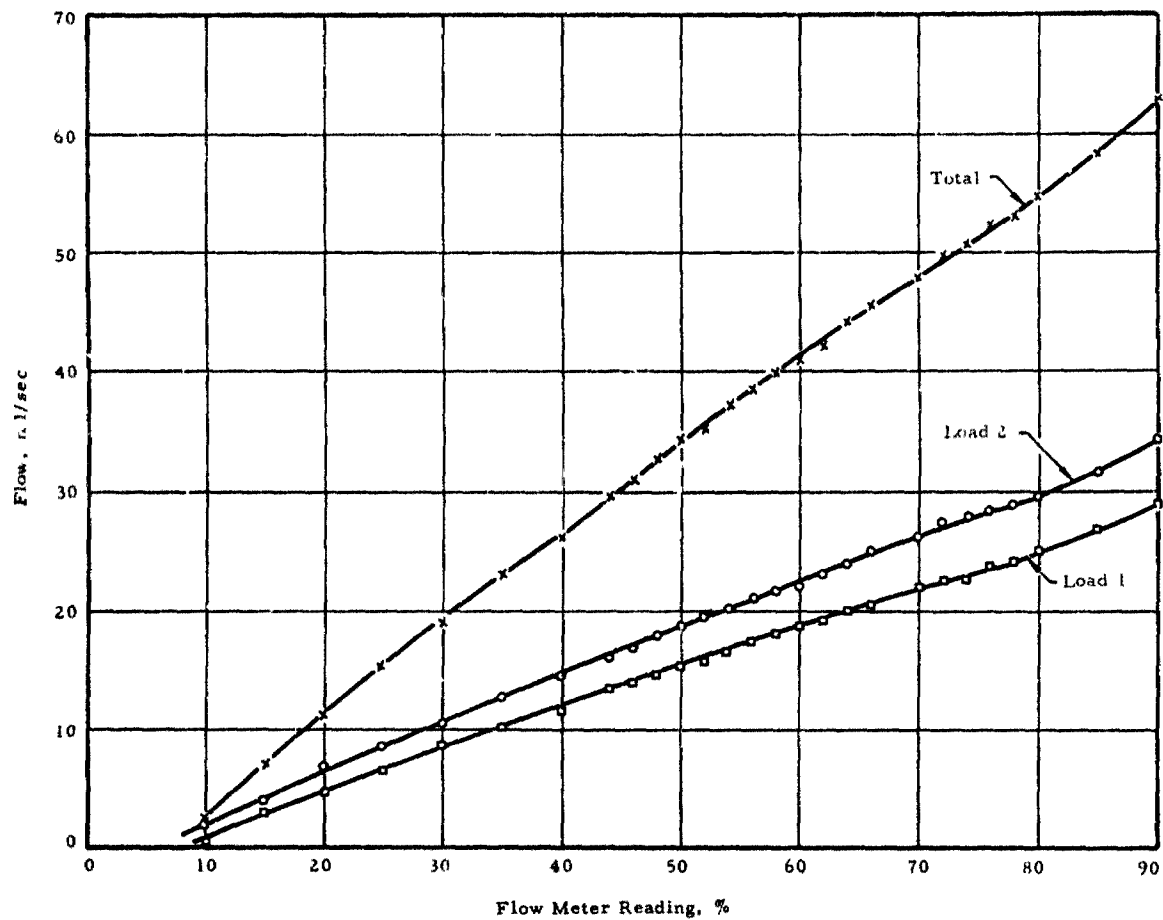
Figure B-10. Voltage Measurements of the Out-of-Pool Load



Current input	Measurement position	Voltage, millivolts
A-B	C-D	0.645
A-B	E-F	1.400
A-B	I-G	0.935
A-B	E-H	5.991
A-B	E-I	93.40
A-B	E-K	93.55
A-B	E-L	93.62
A-B	A'-B'	94.51
A-B	F-J	94.88
M-N	O-P	99.18

Current = 10 amperes

Figure B-11. Water Flow Meter Calibration Curves



REFERENCES

- 1 UO₂ Properties and Nuclear Applications, United States Atomic Energy Division, U. S. Government Printing Office, Washington, D. C., 1961, p. 190.
- 2 Handbook of Chemistry and Physics, 39th Edition, 1957-58, Chemical Rubber Publishing Company, Cleveland, Ohio, p. 2086.
- 3 Nuclear Engineering Handbook, 1st Edition, McGraw-Hill Publishing Company, New York, N. Y., 1958, Chapter 9, p. 5.

DISTRIBUTION

1. Radio Corporation of America (10)
2. The Babcock & Wilcox Company

Allen, HS	MacKinney, AL
Ball, RM	MacMillan, JH
Batch, ML	Montgomery, DW
Batten, AC	Mumm, JF
Boll, RH, Alliance	Orr, WL
Breazeale, WM	Pettus, WG
Cardwell, BB	Plunkett, DA
Carlson, RW	Roberts, DM
Central Files (10)	Sankovich, MF
Clark, RH	Sawyer, GA
Craven, JP/Barberton Library	Schutt, PF
DeBoskey, WR	Schluderberg, DC
Deuster, RW (2)	Snidow, NL
Dobel, HF	Taber, AP/Alliance Library
Edlund, MC	Technical Report Group
Embrey, NS	Thomas, CE
Engelder, TC	Travis, CC
Gibson, MD	Ward, FR
Gumprich, WC	Webb, RA
Harrison, RH	Wehmeyer, DB
Johnson, CR	Weissert, LR
Kerr, JM	Wicks, GK
Landis, JW	Williams, DVP
Lewis, RH	Wittkopf, WA
Library, AED (2)	Womack, RE
Littrell, LW (2)	Worsham, HJ